Drainage Tubes versus Sediment

Effects of vertical drainage tubes on the sedimentology and beach processes at the intertidal beach zone

Hugo H.M. Ekkelenkamp

Drainage Tubes versus Sediment

Effects of vertical drainage tubes on the sedimentology and beach processes at the intertidal beach zone

---

Author	H.H.M. (Hugo) Ekkelenkamp BSc.

Date	June 2011
Version	August 2012
University course	MSc. Civil Engineering (Hydraulic Engineering) Coastal Morphology and Protection
MSc. Committee	Prof. dr. ir. M.J.F. Stive Ir. D.J.R. Walstra Prof. dr. ir. T.N. Olsthoorn Ir. J.S. Reedijk
Accompanied by	Ir. W.D.A. van 't Zelfde Prof. dr. J. (K) Groen Dr. M.A.J. Bakker Dr. ir. A. Gerritsen Dr. ir. M. Van Ing. M. Konert Dr. L. (B) van der Valk Dr. ir. R. Spanhoff
Number of pages	222
Document status	Final version
Cover photograph	Skodbjerge, Denmark, 2009 by Ekkelenkamp Drainage tubes at the high and low water line, taken some months after installation when the top layer was removed by a storm
Commissioned by	BAM Infraconsult BV Delta Marine Consultants Delft University of Technology

bam infra BAM Infraconsult bv

Delta Marine Consultants

TU Delft Delft University of Technology

"Science uses prediction as a tool to test explanations built upon its temporary state of understanding. Engineering assumes that temporary state of understanding in proceeding directly to a useful prediction."

Baker, 1994

Acknowledgements

During the research I worked together with lots of people. It would be impossible to mention them all. There are a number of colleagues, advisors and friends which I would like to thank explicitly. Their help is very appreciated.

First I would like to thank my committee from the Technical University of Delft, ir. Dirk-Jan Walstra, Prof. dr. ir. Marcel Stive and Prof. dr. ir. T.N. Olsthoorn who were willing to judge the results objectively and advise me with their scientific knowledge of coastal engineering and sedimentology. Prof. dr. ir. Olsthoorn accompanied the committee at a later stage and reviewed this report in great detail.

From the Royal BAM Group I would like to thank ir. Ad van't Zelfde who helped me with his huge engagement and good advices. He was always up for a good discussion. Ir. Bas Reedijk often accompanied these conversations and gave interesting views. His thoughts were often constructive which gave me new ideas in solving problems. It was nice to have these men next to my office. When new developments or events concerning the drainage tube technology arose they shared it immediately with me. Other colleagues from the BAM which I would like to thank are ir. Sietsche Eppinga, Rene Binkhorst, Martin van Velzen and Bram Verdonk.

During the field research ir. Jelle-Jan Pieterse and drs. Pieter Pauw joined and helped me with the measurements. I enjoyed their cooperation and involvement. At this moment I am still working together with Jelle-Jan on some workshops and new research programmes together with the Vrije University of Amsterdam and the Technical University of Delft. We have also intentions to write some articles together with Deltares, TU Delft and BAM.

Several engineers from Deltares helped me with their expertise on coastal management and protection. Dr. Bert van der Valk, ir. Ad van der Spek, ir. Dirk-Jan Walstra, dr. ir. Ruud Spanhoff and dr. Marcel Bakker (TNO) shared their knowledge about the historical development of the geology and sedimentology of the beach near Egmond aan Zee. Dr. ir. Meindert Van was always willing to interpret and discuss the findings. Ir. Kees van Ruiten and dr. Anton Gerritsen joined me during workshops and an interesting innovation fair.

The laboratory tests and analysis would not be possible without the help of ing. Martin Konert and dr. Maarten Prins from the Vrije University of Amsterdam. Their knowledge of laboratory research, sedimentology, chemistry and physics proved very helpful. Professor Koos Groen was closely involved in the research and gave very good advice on the interpretation of the data and the structure of the report. He was always willing give reviews and feedback.

Finally I would like to thank (close) friends and family who supported me at all time. In particular Annemarie Ruitenberg, Alexandra Ekkelenkamp and Eldert Besseling for helping me finishing the report and encouraging me with their personal support.

Structure of this study

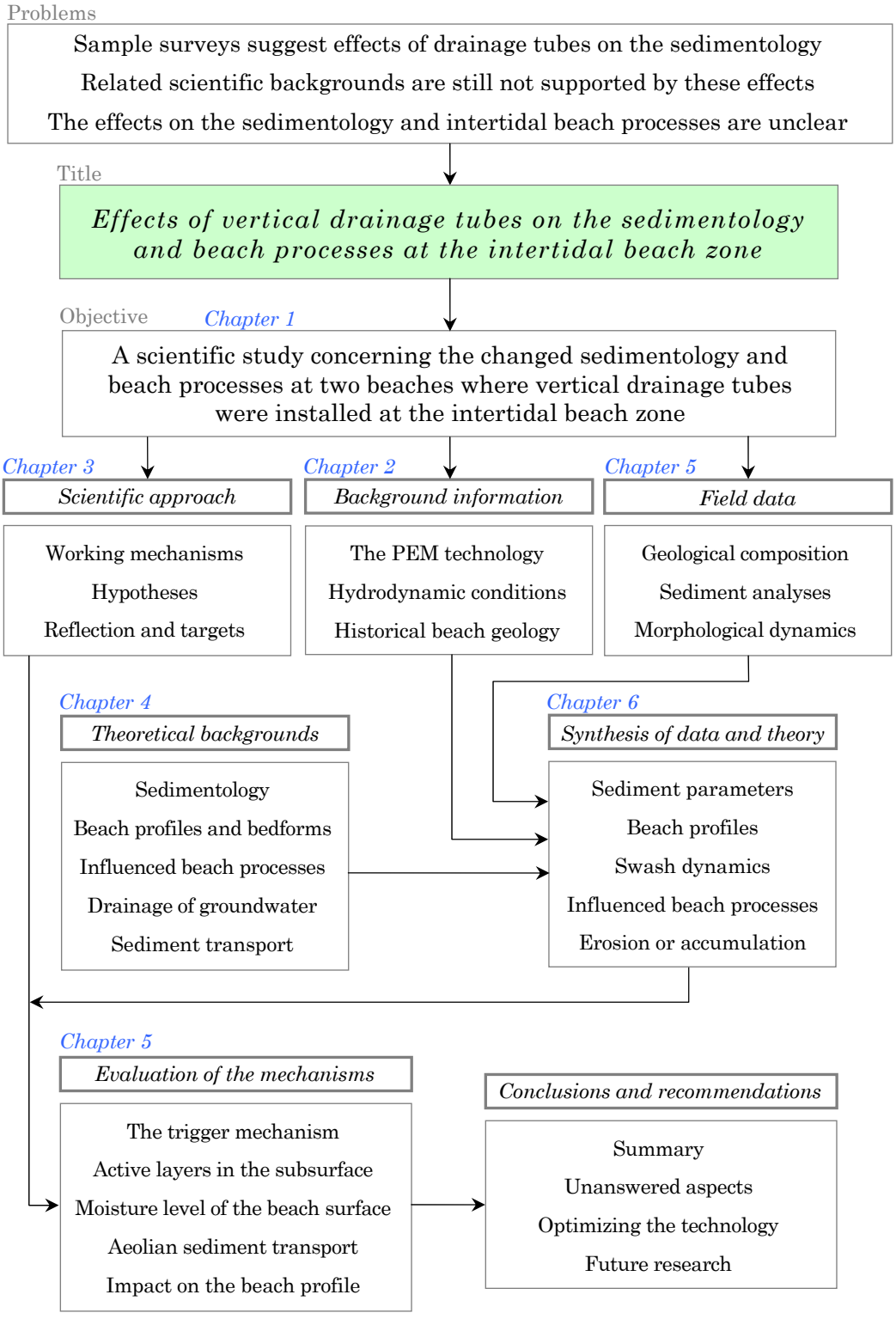

Summary

In the Netherlands almost twelve million cubic meters of sand is added to the Dutch coast every year by means of beach nourishments. A similar amount is nourished in Denmark. As people start to live near the sea, coastal protection systems become very important. The coastal area forms a safety zone against flooding. It is also a recreational area where wide beaches are desirable.

At the start of 2006 the Dutch contractor BAM started a pilot project at the Dutch coast near Egmond aan Zee. An innovative technology already used in Denmark was applied which consisted of a number of vertical drainage tubes placed at the intertidal beach area. This passive system, consisting of an array of tubes, was placed in rows on a depth of thirty centimetres below the beach surface. Deltares, a scientific engineering company, became responsible for the morphological analysis. Pieterse (2009) studied the groundwaterleverls en pressure changes near the drainage tube areas. He discoverd some minor changes of flow patterns and pressure drops. Present study elaborates on his study. One most important trigger for this study are the findings of Pieterse regarding the coarse sediments found at the drainage tube area. This time much more sediment samples are taken and analysed.

This report starts with possible working mechanisms of the tubes within the complex beach system. In addition, huge amounts of data are collected which tells us more about the sedimentology of the beach and soil structure. This data is used later on to study influenced beach processes and morphological changes.

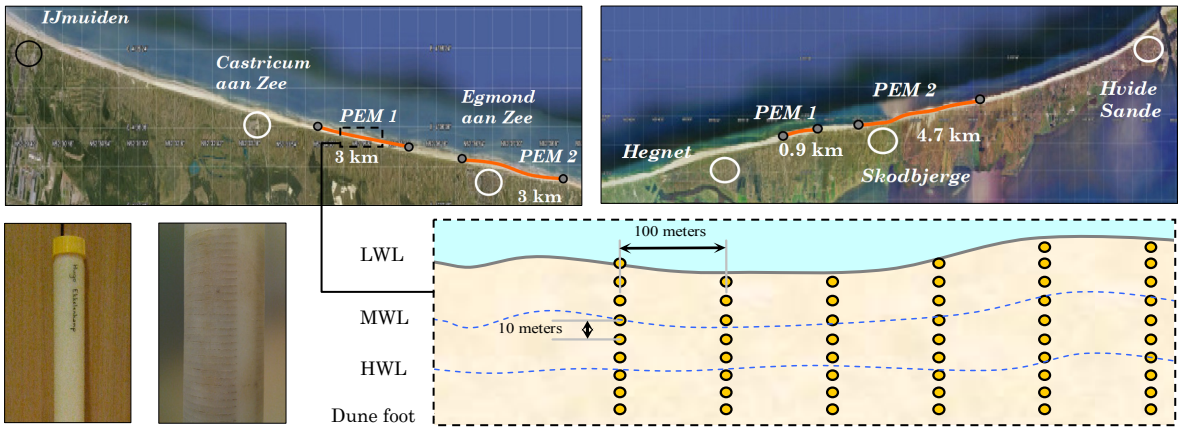

The passive vertical drainage tube system placed in rows, thirty centimetres under the beach surface

Vertical drainage tubes in practise

For this study both the beach near Egmond aan Zee as the beach near Hvide Sande are looked at. At these coastal areas several drainage tube fields are installed. At the Dutch beach a stretch of three kilometres coast was equipped with tubes. The Danish coast has two tube areas which are one and five kilometres in length. In the past a number researchers have studied these drainage systems. Engesgaard (2008) found a small influence by the tubes of the groundwater. SIC en KDI carried out diver tests (to measure the pressure differences) in 2006. They studied some physical effects which could be affected by the vertical drainage tubes near the groundwater level. At the lower part of the beach the water level gradient decreased with 64 – 70% by the tubes. Research done by Pieterse (2009) shows that below the saline groundwater a certain amount of fresh water is flowing out of the dunes. He found out that the tubes are channelling this fresh water with a higher temperature at the low water line. He also found that the sediment near the drainage tubes was coarser than outside the tube area.

Vertical drainage tubes in theory

Present study adds new results and thoughts to the work of my predecessors by studying the sedimentology of a large stretch of coastline at both beaches. A large-scale mechanism is described which describes a hypothesis for the influence of the drainage tubes on the beach sediment. This mechanism consists of five possible processes that could be categorized into three groups: pressure changes, air ventilation and vertical transport of water. Tests done by Pieterse (2009) have shown that the pressure differences between the reference and tube area can be neglected. But, at both beaches, the outflow of small air bubbles trapped in the beach surface were observed. However, the transport of water through the tubes can be deduced from the pressure measurements. It may be possible that the tubes near the low water line are transporting fresh water with a higher temperature compared to the tubes near high water.

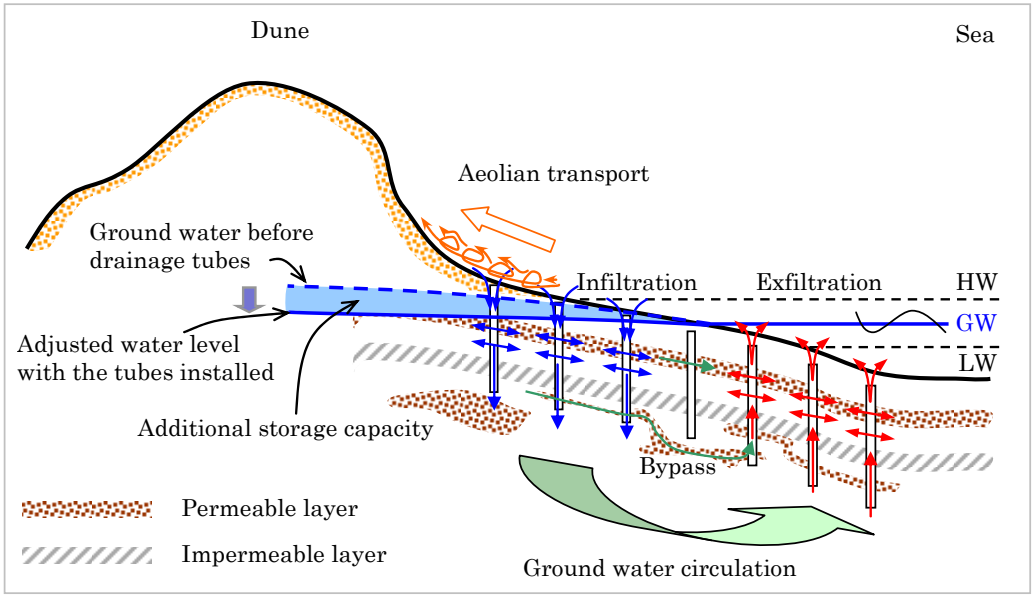

Combined large scale working mechanism in theory

Hypothesis of a theoretical large scale working mechanism

The proposed large scale working mechanism provides an example of how the system could work. It starts with the flow of water through the tubes due to a continuous variation of the sea level. A starting point or 'trigger' could be the measured outflow of groundwater by Pieterse (2009). Water stored in the beach subsoil flows from the high water line to the low water line by a groundwater gradient. The drainage capacity of the tubes is largely determined by the outflow capacity of water. As the water chooses the path of least resistance the very permeable shell layers at Egmond aan Zee or gravel layers near Hvide Sande could increase the flow through the tubes. Levelling of the groundwater gradient increases the storage capacity of water in the beach. As the moisture level of the beach lowers, the beach becomes more dry in time. Aeolian transport increases which sorts the sediment at the beach. Fine grains are blown away along the coast and into the dunes. The beach becomes more stable.

Data collected at the Dutch and Danish beach

The field measurements for this study yielded data regarding the sedimentology, geological composition, stratification of the subsoil, bottom resistance, beach bathymetry and beach envelope. The average grain diameter along the Dutch drainage tube area is 0.1 mm larger compared to the historic analysis and the reference areas. Only the active layer (defined by 2 m depth at the LWL and 1 m depth at HWL) consists of this coarse sand of approx. 0.4 mm.

With a sediment measuring device (see for detailed information Appendix B.2) the shape of every single grain was measured. The data indicates that the sediment at the drainage tube area is more asymmetrical than the sand along the reference areas. The sediment at the drainage tube area also has a more irregular shape compared to the sand of the reference areas.

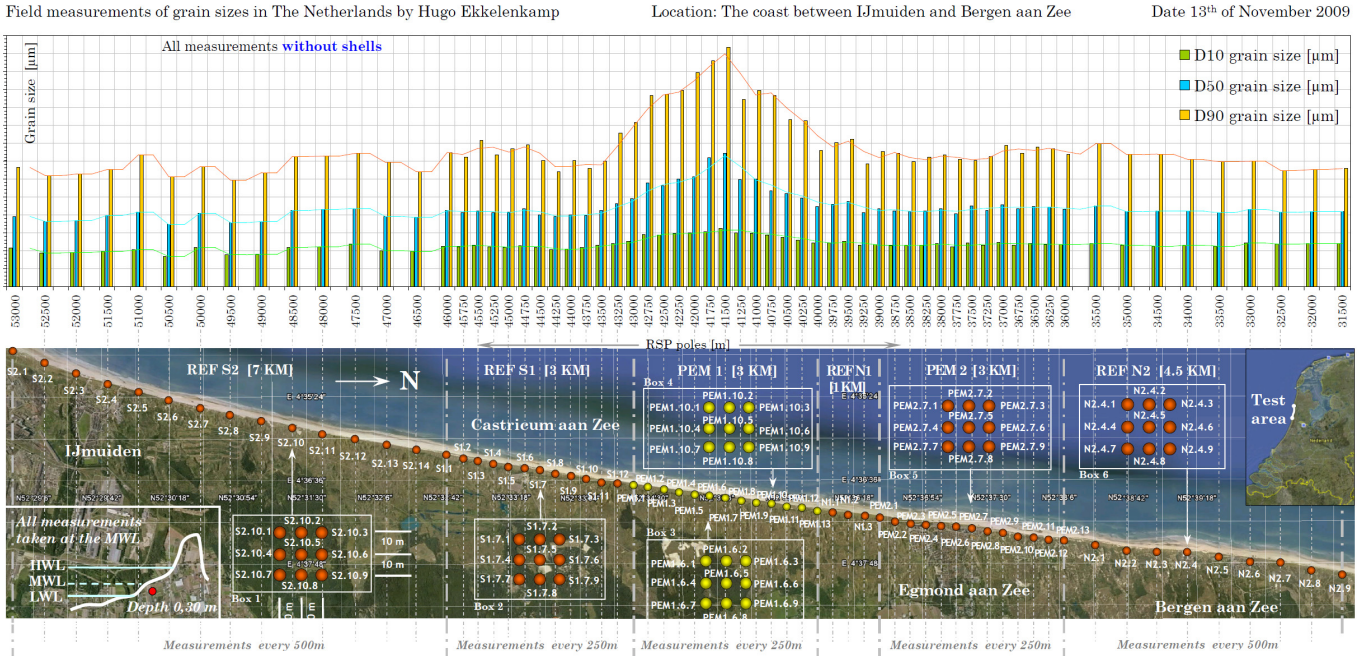

Grain size measurements at the coast between Ijmuiden and Bergen aan Zee (The Netherlands)

The Danish drainage tube areas contain coarse sediments as well. On average this sand is 0.3 mm coarser than that of the reference areas. So at both beaches the sediment at the drainage tube areas is relatively coarse.

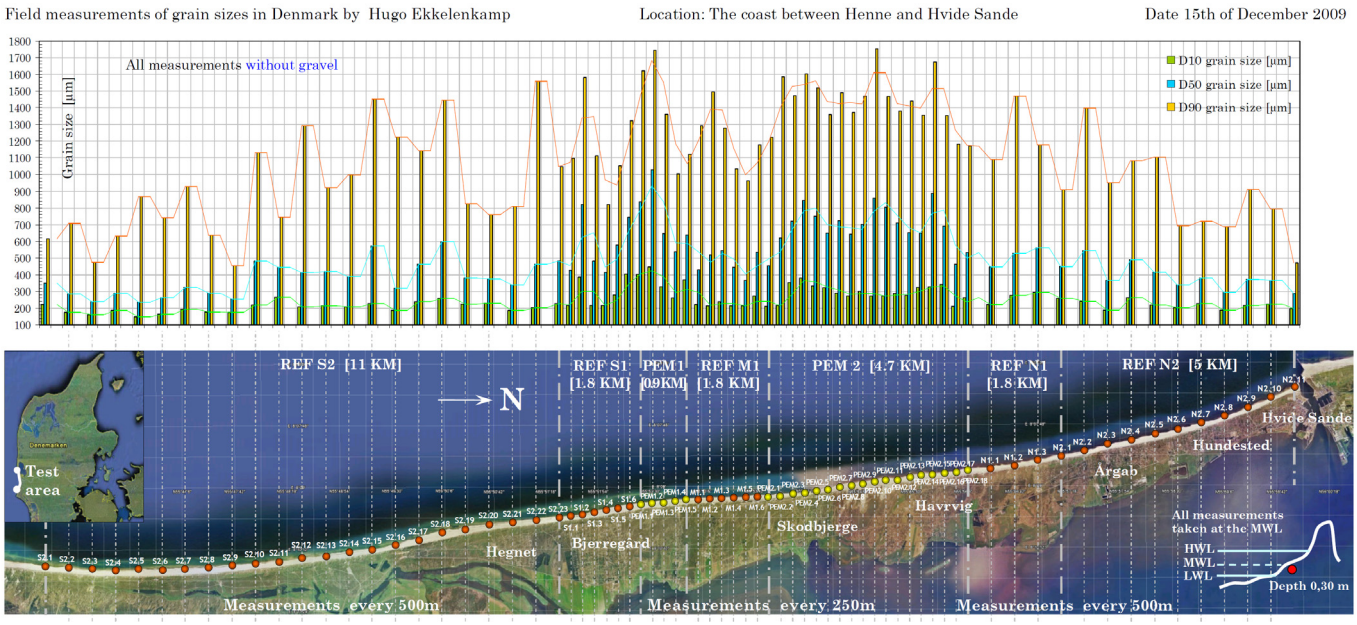

Grain size measurements at the coast between Henne and Hvide Sande (Denmark)

The subsoil of the beaches contains permeable layers. The beach near Egmond aan Zee contains shell layers while at the Danish beach gravel layers are present. The cone penetration tests indicate that the intertidal beach zone (at HWL, MWL and LWL) at the drainage tube areas consists of sand which is well packed (16 MPA). These observations were not found at the reference areas (without tubes). At these places the sand at the HWL (23 MPA) beach is well packed but near the LWL it is much weaker (10 MPA). This suggest a change of material or sediment grain size.

The beach bathymetry changed according to dGPS measurements. Over the last four years the dune foot moved offshore and the beach slope became steeper. At one point it was not longer necessary to inject the tubes anymore (Figure 5-37). They were already covered by a sand layer of 1 to 2 metre.

Effects of coarse sediment on beach processes

Coarser and less regularly shaped sediment influences some sediment parameters (like the relative size and conductivity), beach profiles, beach processes and the transport of sediment. The assumption that coarse sand accumulates and fine sand erodes seems to be the most probable. This is based on the differences between the very coarse sediment at the drainage tube areas and the very fine sand fractions at the reference areas. The sand along the tube areas is finely skewed while at the reference areas it is coarsely skewed. This indicates a more depositional environment at the beach where drainage tubes are installed.

Coarse sediment gives another hydraulic conductivity of the soil than fine sediment. In this case the reference area (fine) and drainage tube area (coarse) are compared. On average the permeability increases between 31 to 42%. The moisture level of the beach lowers. As a result of this aeolian transport increases which sorts sediment at the beach. Fine grains are blown away along the coast and into the dunes.

Due to the coarse sediment at the active surface, the beach morphology theoretically changes. At the vertical drainage tube areas the slope could increase with 32% (Dutch area) and 52% (Danish area). Beach height measurements before and after the placement of the drainage tubes (see Figure 6-5) suggest clearly a steepening of the beach and nearshore zone. In addition, the height of the beach increases in offshore direction. Accumulation of the beach combined with a steeper slope makes the beach more robust. The swash distance decreases and the beach becomes drier in time. This enhances the effect of aeolian transport. The dune foot moves in offshore direction (Figure 6-5). Future research must be done at the dunes to study the sediment on their size, shape and origin.

The swash dynamics are influenced by the changed beach profile. The wave set-up at the reference areas near Egmond aan Zee may become 0.4 m and 0.5 m along the drainage tube area. This means a theoretical set-up length of respectively 12.5 and 10.5 metre. The 'lost' beach width by the effect of wave set-up decreases. The beach gets drier and wider. The reference areas near Hvide Sande encounter a calculated wave set-up of 0.7 m. For the drainage tube areas this set-up equals 0.98 m. The expected swash length decreases from 16.1 m to 10.8 m. Again the beach width increases as the moisture level of the beach decreases. The swash length depends partly on the resistance from the beach surface. When the friction coefficient is raised the swash trajectory becomes asymmetric. If the beach gets steeper, the excursion distance of the swash motion reduces. Then the foreshore dries faster.

Groundwater flow in the beach

The beach groundwater dynamics control the foreshore sediment transport. If the phreatic level drops, the beach tends to accrete. The unsaturated zone increases when the foreshore gets steeper. If the sediment gets coarser the permeability increases and the swash motion decreases. The drainage capacity of the tubes is largely determined by the outflow capacity. This capacity is influenced by the presence of permeable layers like the Dutch shells and Danish gravel layers. These layers are present at different depths and locations along the tube areas. For both areas the water level over a tidal cycle can be lowered by centimetres if a

bypass is formed via the permeable layers. The real flow rate must be measured to check this theoretical assumptions with practice. Also the theoretical implications of the calculated change of the groundwater level on the moisture level of the beach surface must be studied by future research. Other influencing factors, which can increase the lowering of the groundwater, are the drainage capacity of the tubes and the length of the tubes. The latter is also of importance when permeable layers are deeper than two metres.

Moisture level of the beach surface

If as a consequence of sediment sorting the groundwater level is lowered, the storage capacity and moisture level of the beach change substantially. The capillary fringe defining the vandose zone depends on the sedimentology. The thickness of this fringe decreases with the larger grains measured at the drainage tube areas. Compared to the sediment from the reference areas, the coarse sediment at the drainage tube areas influence the capillary fringe. The capillary fringe is 0.27 m (REF) to 0.16 m (PEM). The same holds for the Danish drainage tube area with a difference of respectively 0.15 m to 0.08 m, again reference area compared to the tube area. An average decrease of ten centimetres of the phreatic level is considerably larger than the reduction of the water level by the drainage capacity of the tubes. Therefore bigger effects on the beach processes are more likely when the sediment at the beach becomes coarser. But it is not clear which one can be the trigger.

Infiltration, exfiltration and sediment sorting

The effects of infiltration and exfiltration influence the potential sediment transport. These two opposing effects change the balance between the uprush and backwash. The effect of infiltration is bigger for a more porous bed during backwash than uprush. The coarse sediment found along the drainage tube areas near Egmond aan Zee and Hvide Sande will influence filtration processes. These grain sizes fluctuate around the crossover point D_{q0}. Especially for the Danish case it is very likely that the crossover point is reached and the net transport is directed onshore. Also in the Dutch case the transport directions could change.

The sorting of sediment along the cross-shore profile depends on the local energy level of the wind and wave forces. The fine and coarse grain size fractions behave differently under the same hydrodynamic conditions. According to field measurements described in literature (see Appendix G) the measured grain sizes at the drainage tube areas are an exception. It's not common for the natural longshore variability of the grains sizes to vary with 33% and to remain constant over the cross-shore beach profile. Therefore it is not obvious that the large grain sizes at the drainage tube areas are completely caused by natural sorting mechanisms at the beach.

Sediment transport

The morphology at both beaches is strongly influenced by the amount of sediment transported by waves and currents. The sedimentology and beach bathymetry influence the transport rate of sediment. The longshore sediment transport (nearshore) could theoretically decrease by 20 to 30% when sediment sizes become 0.1 mm larger. Based on the Unibest-TC model it was found by a qualitative analysis that the cross-shore sediment transport rate will also be reduced. Direction changes from offshore to onshore could stimulate accumulation of sediments. The increased volume of sand on the beach and dunes was measured by yearly recordings done by the Dutch coastal authority (JARKUS data). At the drainage tube area both the dune and beach volume increased over the last three years. At the reference areas only the beach volume increased.

After four years of testing, the vertical drainage tubes at Egmond aan Zee were removed by the contractor. Although no signs of any disturbances were recorded, the project was ended because of contractual obligations. The depth at which the drainage tubes were found, varied between 1 and 3,5 metres. On average, a depth of five feet was measured. Since the installation of the tubes in 2006, they have been covered by a sand layer of 1 to 2 metres.

Contents of this study

Figures and Tables

Chapters

Appendices

1. Introduction

Almost twelve million cubic meters of sand is nourished on the Dutch beaches every year. In Denmark this figure reaches six million. Nourishments become more important than coastal revetments when longshore sediment transport can not be blocked. An unconventional system of passive vertical drainage tubes below the beach surface could add some benefits if it stabilizes the beach. At the beginning practical research was done by creating a number of test areas. Later on some theory was added to get some insight into the mechanisms. At the start of 2006 BAM and Rijkswaterstaat installed a large test site at Egmond aan Zee which is named after an ecological approach; Ecobeach. The project time span is four years. Deltares is responsible for the analysis of (D)GPS data in order to calculate any beach volume changes. Parallel to this task a more physical and theoretical study is done. Together with the report of Pieterse (2009) present study is meant to initiate the theoretical understanding of the drainage tube system and to collect data concerning the changes at the test areas. Eventually a combined report and article are published together with the Technical University of Delft and Deltares (a Dutch scientific research company).

1.1 Context of this study

In the past years many beach areas with vertical drainage tubes were created. Many theories about 'the magical tubes' were devised based on experience and practical reasoning. Until now the essential piece of theory and evidence are missing which could prove that the system should work. Related scientific backgrounds are still not associated with the effects measured by several researchers. So far some studies were done at different beaches in Denmark (Danish Governmental Coastal Authority (KDI) 2005, Fredsoe and Engesgaard 2008) and The Netherlands (Pieterse, Ekkelenkamp, Pauw 2009).

Engesgaard (2008) studied the groundwater flow. With a numerical model he described the complex flow around the beach with and without vertical drainage tubes. He focussed on a two dimensional cross-shore beach model. At high tide the flow inside the tubes reaches its maximum speed. The hydraulic gradient along the beach during mean tide is decreased by the tubes. Inflow at the dune foot and outflow at the low water line are active during high water. It has not been possible to detect a significant change of the gradient by the operation of the tubes. Changes are very small according to the scales of other beach processes. Permeable layers in the subsurface could increase the effects considerably.

SIC (Skagen Innovation Centre) and KDI carried out a test in 2006 to study the physical effects of vertical drainage on the groundwater level [SIC 2006]. The test was done in Denmark at the northern drainage tube area near Skodbjerge with divers placed between the tubes. The results show a higher water level at the drainage tubes near the low water line compared to the surrounding phreatic surface. The opposite holds for the drainage tubes installed at the high water line where the water level in the tubes is lowered. These effects suggest a downward transport at the high water line and a upward transport at the low water line. At the lower part of the beach the water level gradient decreased with 64 to 70%.

Research done by Pieterse (2009) at the beach near Egmond aan Zee shows that under the saline beach groundwater fresh water flows out from the dunes. Here the transition from

saline to fresh groundwater is situated at depths up to 7 to 9 meter. The vertical drainage tubes with an average length of two meter could not reach this boundary. They can not transport fresh water to the surface in the Dutch situation. The measurements of Pieterse show that pressure variations at one meter depth could be as large as half the wave height. In addition relative fresh groundwater near the low waterline was recorded suggesting exfiltration of groundwater.

Some data concerning the beach sedimentology shows a different situation between the reference and drainage tube area (Figure 5-23). The pressure variances and sediment transport would increase when the beach becomes coarser. The quantity of transported material depends on infiltration and exfiltration. Many other beach processes could be affected by the coarser sediment. Pieterse recommended to perform an sediment analysis on a big scale to confirm his findings of a relative short stretch of coast. The connection between the Ecobeach system and beach processes in the Netherlands and at other places in the world are yet undiscovered.

Present study continues the search for answers. Basic understanding of the transport through the tubes by Fredsoe and Engesgaard (2008) is used to qualify the impact on groundwater behaviour. These results are compared with available data. A starting point is the sediment analysis done during the summer of 2009 at the Dutch drainage tube area. The output from the Ecobeach Workshop of 2009 is used to set up a theoretical framework from which the possible working mechanisms are formulated. With the use of theoretical backgrounds and many field tests some affected beach processes are qualitatively described. Effects are predicted when the sedimentology and beach bathymetry change. At the end this study could add some new understanding of the involvement of the technology in beach systems.

1.2 Problem description

Former research done by scientists resulted in some remarkable data. Various outcomes are still unexplainable while others could be substantiated with theoretical evidence. One most extraordinary finding is the coarse sediment detected at the drainage tube area near Egmond aan Zee during field research done by Pieterse (2009) (Figure 5-23). This data is still not validated by knowledge about the geological processes at the beach.

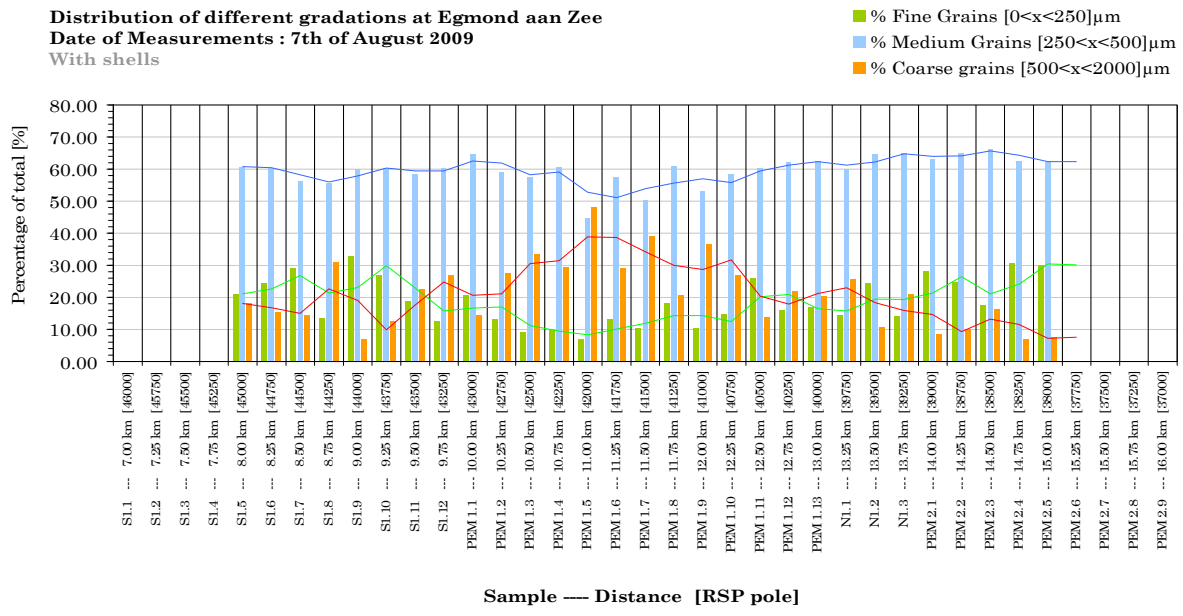

Figure 1-1 Former research of sediment samples at the drainage tube area near Egmond aan Zee

This study continues the work done by former researchers. Based on their recommendations four specific problems are formulated;

- A large scale working mechanism which suggests the relation between effects of vertical drainage tubes and affected beach processes. The sediment accumulation is not yet mentioned and validated.
- It is unclear whether the coarse sediment data from September 2009 belongs to the natural variability of the beach near Egmond aan Zee or the presence of vertical drainage tubes installed below the beach surface.
- A detailed description of the sedimentology at the drainage tube areas at Egmond aan Zee and a reference beach like Hvide Sande are not available yet.
- The related scientific backgrounds which could connect and prove the effects of the drainage tubes on the beach processes, morphology and profile development are still not associated with and applied to the data.

1.3 Objectives and methods

The purpose of this scientific research is to study the sedimentology at two beaches where vertical drainage tubes were installed and to predict the effects on the beach processes at the intertidal beach zone if the sediment becomes coarser.

This is done by;

- Analysing a large number of sediment samples at the intertidal beach zone near Egmond aan Zee and Hvide Sande by looking at their size, shape and distribution
- Measuring beach profiles and geological compositions at the subsurface
- Studying associated literature which describes the effects of the sedimentology on the intertidal beach processes and morphology
- Evaluating mechanisms when new data from the beach sediments is applied
- Validating the large scale working mechanism and suggest some recommendations

For the theoretical part of this study, there will be looked at the;

- Analysis of sediment samples
- Beach zones and profiles
- Influence of the sedimentology on the permeability, bed forms and beach profiles
- Interaction with the beach surface (friction, transport)
- Aeolian transport
- Groundwater flow in the beach
- Capillary fringe and the vandose zone
- Infiltration and exfiltration
- Capacity of the vertical drainage tubes
- Geological structures of the subsurface
- Swash dynamics
- Sediment sorting principles at the beach profile

During the fieldwork, there will be looked at the;

- (Im)permeable layers in the beach
- Sedimentology of the beach surface and subsurface (size, shape and composition)
- Coastal envelope or active beach zone
- Beach profiles and tidal levels
- Presence of shell fragments and gravel layers in the subsurface of the beaches
- Conditions of the subsurface (cone penetration tests)
- Vegetation at the dunes
- Width of the beach and swash motion

1.4 Research questions

In order to fulfil the objectives a number of central research questions are formulated;

1. Which small scale hypotheses could initiate a plausible large scale working mechanism that results in accumulation of sediment at the beach surface?
2. Are the changes in sedimentology measured at the beach near Egmond aan Zee [79] reducible by analysing the sediment at the drainage tube and reference areas near Egmond aan Zee and Hvide Sande?
3. Does the data complies with the facts and figures from the historical geological beach development?
4. Which qualitative transformations along the intertidal beach area could evolve from a changing sedimentology that would change the beach morphology and bathymetry?
5. Does the field data support the large scale working mechanism?

1.5 Readers guide

This study starts with explaining the technology of the vertical drainage tubes by describing their use in practise (Chapter 2) and giving some theoretical leads (Chapter 3). The associated literature given in Chapter 4 forms the background information which will be used to interpret changes of beach morphology. The coarse sediment found by Pieterse 2009 is evaluated by a detailed description of the sedimentology and morphology at the drainage tube areas at Egmond aan Zee and a reference beach like Hvide Sande (Chapter 5).

The synthesis of mechanisms and measurements connects the field data to the beach processes, morphology and profile development by describing the implications of the measured data (Chapter 6). These processes are compared with the observed bathymetry and morphodynamic state of the beaches.

This report concludes with the facts and findings arising from the data and the comparisons made with literature. A number of recommendations are given which could be used as a starting point for future research. Some advice is given about the possible improvements of future systems in order to optize the technology. New measurements and research programmes supported with field studies must be started to continue this work.

2. Vertical drainage tubes in practise

A decade ago in Denmark, a contractor built a large cable in the beach. He dug a trench and installed an active drainage system. After some weeks the sand around the project accumulated with more sediment. At the end of the project the contractor decided to leave the tubes in the beach for a while without the pumps. The accretion of the beach continued. He could not believe his eyes and patented the technology. At that time he heard of an abandoned church that was on the verge of collapsing into the sea. He decided to place a number of drainage tube rows into the beach (Figure 2-1). In the following weeks the beach in front of the church started to grow. The believers were delirious about this and started to use the church again. Unfortunately the tubes were installed without a legal permit. The contractor was forced to remove the tubes from the beach. After the magical tubes were removed, the beach started to erode again. Sadly the local people had lost their place of worship again to nature. One intriguing question remained: does the tube technology change the beach?

2.1 The drainage tube technology

The PVC drainage tubes (Ø 6 cm), with filter slots (0.2 mm wide) halfway, are installed in a raster of cross-shore rows, placed 20 cm below the beach surface (Figure 2-1).

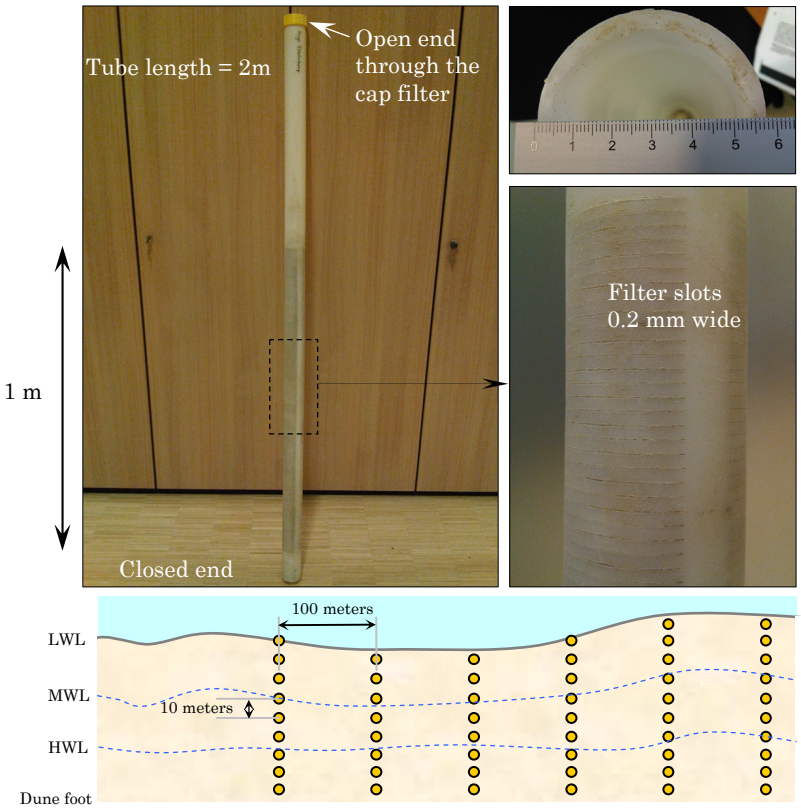

Figure 2-1 Details of the vertical drainage tube technology used at Ecobeach and Hvide Sande

2.2 The beach near Egmond aan Zee

The Holland coast is the central part of the Dutch coast between Den Helder in the north and Hoek van Holland in the south. In the middle of this 120 km stretch of coast lies the beach of Egmond aan Zee which mainly consists of a sandy beach and multiple barred nearshore zones. The beach is located between the breakwater of IJmuiden and the Hondsbossche Zeewering. The shoreline position has changed over the last centuries. Its front shifted 290 metres landwards until it stabilized some decades ago. Until then, almost one metre of coast was lost to the sea every year [86].

Figure 2-2 The village of Egmond aan Zee endured a coastal withdrawal of one metre per year

Every couple years, Rijkswaterstaat performs beach nourishments. In many cases these are nearshore nourishments. Appendix H gives an overview of beach nourishments done over the last years. The last one was performed in 2005 at the foreshore near Heemskerk (Figure 2-3). It is still unclear whether or not part of this sand volume can still be found at its initial location. It is obvious that most sediment is spread out over the beach in all directions.

Figure 2-3 Beach nourishment done at Heemskerk in the year 2005

2.2.1 Description of the drainage tube site

Near Egmond aan Zee two drainage tube areas (PEM 1 and PEM 2) were installed in the beginning of 2007 (Figure 2-4). Only the southern tube area is studied because here all necessary tubes were installed (see Appendix F).

Figure 2-4 The beach near Egmond aan Zee, study area 1 (The Netherlands)

The shoreface has a concave profile with an average beach width of 140 m and steepness of 1:35 to 1:45 [86]. The upper part of the shoreface is characterised by multiple nearshore subtidal bars. The morphology is typified by a swash bar. Over the last four years when the drainage tube project was carried out the beach volume changed substantially. At the reference area, little sand accumulated at the dunes while the beach volume increased significantly. At the tube area, the dune volume and beach volume both increased (Figure 2-5).

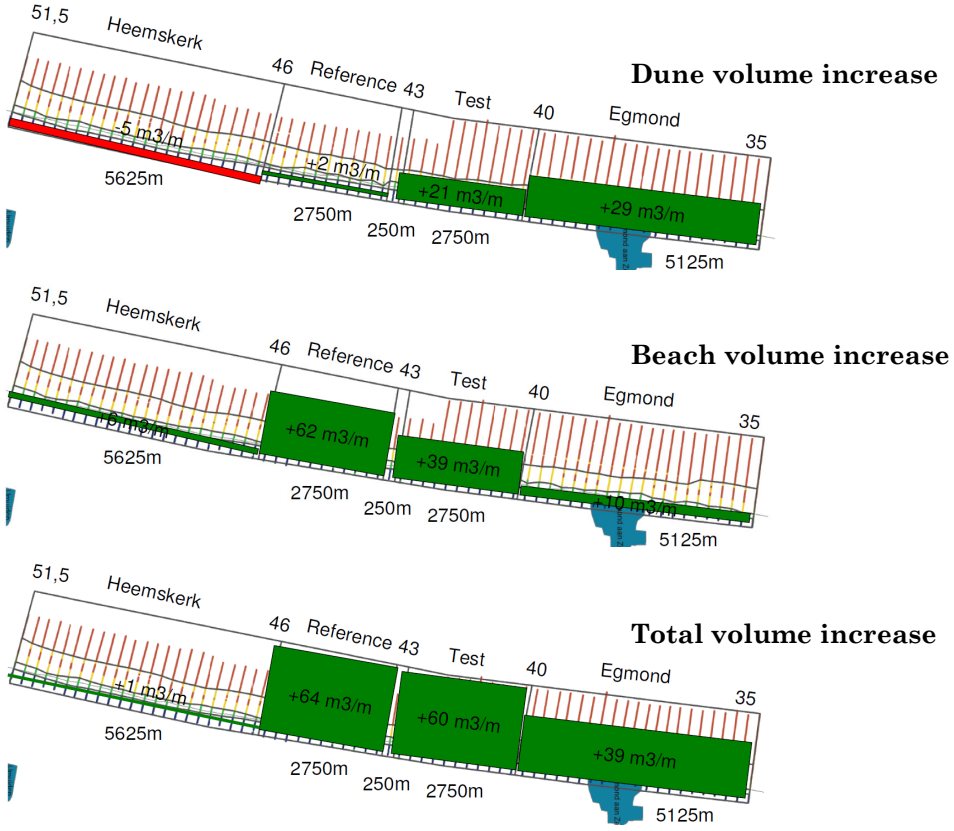

Figure 2-5 Sediment volume changes over the years 2007 to 2010 at Egmond aan Zee [B.R.]

2.2.2 Hydrological conditions

The mixed energy coast along Egmond aan Zee endures both wind waves and tides. The sandy beach structure shows morphological responses. Appendix J contains detailed information about its hydrodynamic conditions. Most winds at the beach come from the North Sea. The prevailing wind direction is southwest (23%). In addition there is wind from west (16%), east (13%) and northwest (12%). The largest wind set-up along the coast results from north-westerly winds. The extreme wave heights at the beach near Egmond aan Zee also come from the northwest (Figure 2-6). During winter, the average wave height becomes 1.65 m. Throughout the summer the waves are 0.95 m. The governing wind climate causes a yearly mean wave height of 1.20 m. The mean centroidal wave period equals 5 seconds. During fair weather conditions, the waves approach the coast most often from the northwesterly direction.

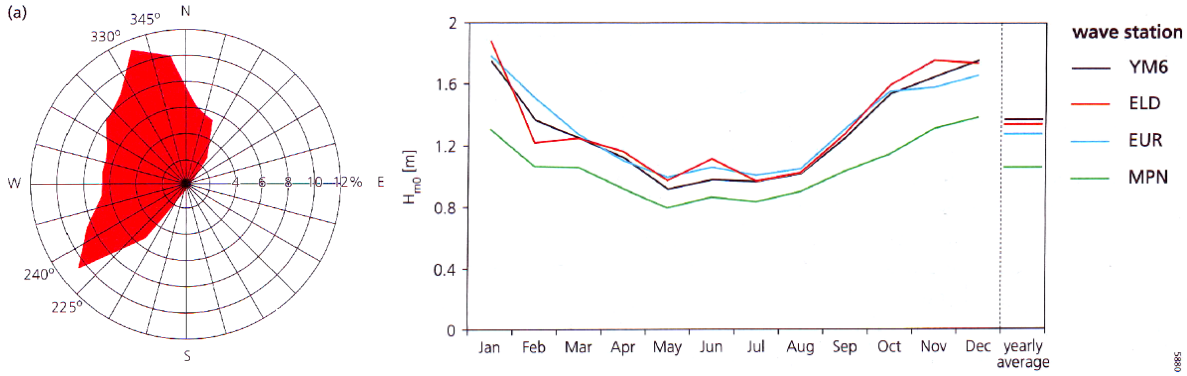

Figure 2-6 Yearly averaged wave climate at station IJmuiden [86]

The tidal currents are northwardly directed during the flood period of 4 hours and southwardly directed during the 8 hours ebb period (semi diurnal asymmetrical tide). The mean tidal range is 1.65 m. The spring and neap tidal range are about 2.0 and 1.4 m respectively.

At the intertidal beach zone, the low-tide swash bar and the high-tide swash bar migrate continuously. Breaking wave processes influence the height and location of the bars. The high-tide bar is mostly influenced by swash processes during flood. Channels may occur in between bars. It is important to observe the system at Egmond aan Zee and take its location into account in the field measurement plan.

2.2.3 Historical development of the beach geology

At the beach near Egmond aan Zee, a number of processes have initiated sediment sorting along the beach. Basically, one can distinguish four different periods in time:

1. The OerIJ period from 2500 BC to approx. 100 AD (active period 500 BC)
2. The erosive period 700 AD to 1995 (average shoreline retreat of 1 m per year)
3. Beach nourishments from 1995 to 2005 (beach and foreshore, new ones are planned)
4. Vertical drainage tubes installed at the beach near Egmond aan Zee, 2006 to 2011

During these periods, coarse sediment was supplied to and eroded from the beach system. The sorting of sediment resulted from changing energetic conditions caused by storms or streams.

The first OerIJ estuary dominated the coastal environment for a period of approx. 2600 years. This bay was situated near Beverwijk and Heemskerk. Sedimentation along the coast started from 2500 BC and filled the inlet with sediment which was trespassing the area. The inlet migrated northwards to Castricum aan Zee where a new entrance to the OerIJ was formed. Large water height differences occurred, which increased marine activity.

From 650 BC onwards, the freshwater discharges from the Flevomeer and Vecht increased significantly. The increased tidal prism enlarged the storage capacity of the hinterland. The currents became stronger which caused erosion of fine sediments along the inlet. Autoloading processes were initiated by the subsidence of clay or sand onto the peat layers and by anthropogenic drainage of the subsoil. The increase of the tidal range and volume enlarged the channel and inlet considerably. During its most active period (500 BC) large volumes of sand moved through the system. Large sediment transports supplied coarse sediments from the glacial era which accumulated at the banks and bed surface of the inlet and channels.

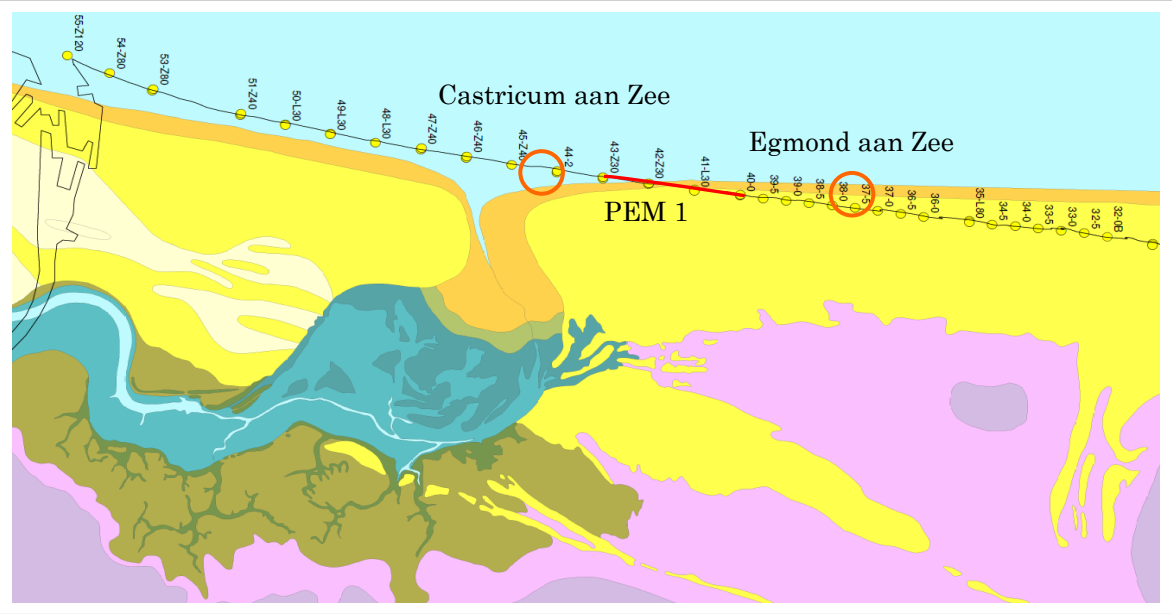

Figure 2-7 OerIJ estuary year 20 AD near Egmond aan Zee

The active marine phase lasted almost two hundred years. Around the year 400 BC, the estuary started to accrete which had negative consequences for the tidal prism volume. Together with the accumulation of fine sediments, the oligotrophic peat formation started. The estuary became separated from the sea. [100] Appendix G shows the development of the OerIJ in more detail. At this moment the upper fifty metres of sediment consist of Holocene and Pleistocene deposits. As far as we know at this moment, the interface lies around -20 NAP.

Pleistocene deposits

The Pleistocene sediment consist of clay/loam (formation of Drenthe), large river sands (formation of Kreftenheye) and cover sand (formation of Boxtel). The clay/loam sediment was formed during the penultimate glacial period and has a bluish gray colour. The Kreftenheye formation consists mainly of very coarse sediment (sands) which were carried by the river Rhine during the last glacial period, 'the Weichselien'. In this sediment very coarse particles are present with sometimes even gravel or marine shells which are remains of older 'Eem' deposits. The formation of Boxtel consists of fine aeolian sands which lie on top of the other Pleistocene deposits. These covering layers of sand were formed during the 'Late Glacial'.

Holocene deposits

The oldest Holocene deposits, the 'Layer of Velsen', lie at the transition depth of twenty metres. This sediment consists of strongly packed peat with clay on top. It is very plausible that this specific layer is found by Pauw (2009) which was observed at a depth of -18 m NAP. On top if this layer lie the 'sands of Castricum'. These medium to coarse sands were formed by large tidal channels. They are connected to the 'layer of Wormer' which lies at a depth of -16 to -20 m NAP. These are tidal deposits formed during the first half of the Holoceen period. They consist of fine marine sand particles.

The sand package from -17 m NAP to the surface is attributed to the 'Spisula sands'. These sands are named after the Spisula Subtruncata shells which are present at this layer. The beaches near Egmond aan Zee (particularly the intertidal beach area without fine dune sands) consist of this type of sediment which belongs to 'the formation of Zandvoort' [100]. Besides the shells these sands are characterized by moderately fine buff coloured sand. At deeper layers between -4 and -15m NAP, gray sand is deposited with varying amounts of shells. During the field tests which were done for this study (Chapter 5) this layer was found at depths of -5 to -6 m NAP (Figure 2-8).

Figure 2-8 Gray sand deposits found at -5m NAP

After the Oer-IJ (100 AD) the erosive period started. Old layers of Spisula sands eroded while the coastal profile shifted shorewards. Moderate to very fine sediments moved onshore with even little amounts of coarse fragments from glacial deposits. Today it's difficult to distinguish these offshore deposits from beach sands. Drills, which were done some years ago and collected into the Dutch geotechnical archive, show grain size differences within 50 μm . [100]

Grain size

In the past, a number of researchers have studied the grain size at the beach near Egmond aan Zee. Their measurement techniques differ from each other. Even their classification methods vary from median grain size to D_{63} values. The data and findings from these studies are combined and shown in Figure 2-9.

Eisma (1961) gives a description of average grain size values at the beach along the Dutch coast. A number of samples were taken from the beach at every RSP pole between the dune foot and high waterline and at the intertidal beach area.

Many researchers studied the grain sizes at Egmond aan Zee in the period between 1980 and 1988. From the Dutch Geographic Archive, data of drill samples are available. For present study these are ordered and analysed (see also Appendix G). The outcome of the analysis is shown in Figure 2-9. Data from the Dutch technical advise committee for water defences is also plotted in this graph.

Bemmelen (1982) studied the grain sizes at the intertidal beach area. He took four samples every two kilometres along the coast and five samples every twenty kilometres. The sediment northwards of IJmuiden was moderate/well sorted and more coarse than at the Wadden Zee. The kurtosis was positive. At the low water line, the sediment was coarser than the sand along the high water line. In longshore direction, Bemmelen did not find large grain size differences of the active beach layer (intertidal area). The fluctuation of the median grain sizes at the beach near Egmond aan Zee was 10% (time variation) and 4-8% (distance variation). The sediment sorting varied around 15% (Egmond 7%). Bemmelen did not find a relation between the wave conditions at sea and the grain sizes at the beach. During periods of heavy weather, the beach sediments became more uniform. High water levels eroded the dunes which moved fine dune sands to the beach and further offshore. Some measurements show coarser sediments between the high water level and dunes at Egmond aan Zee. The median size from all data sources varies between 180 and 360 µm (Figure 2-9).

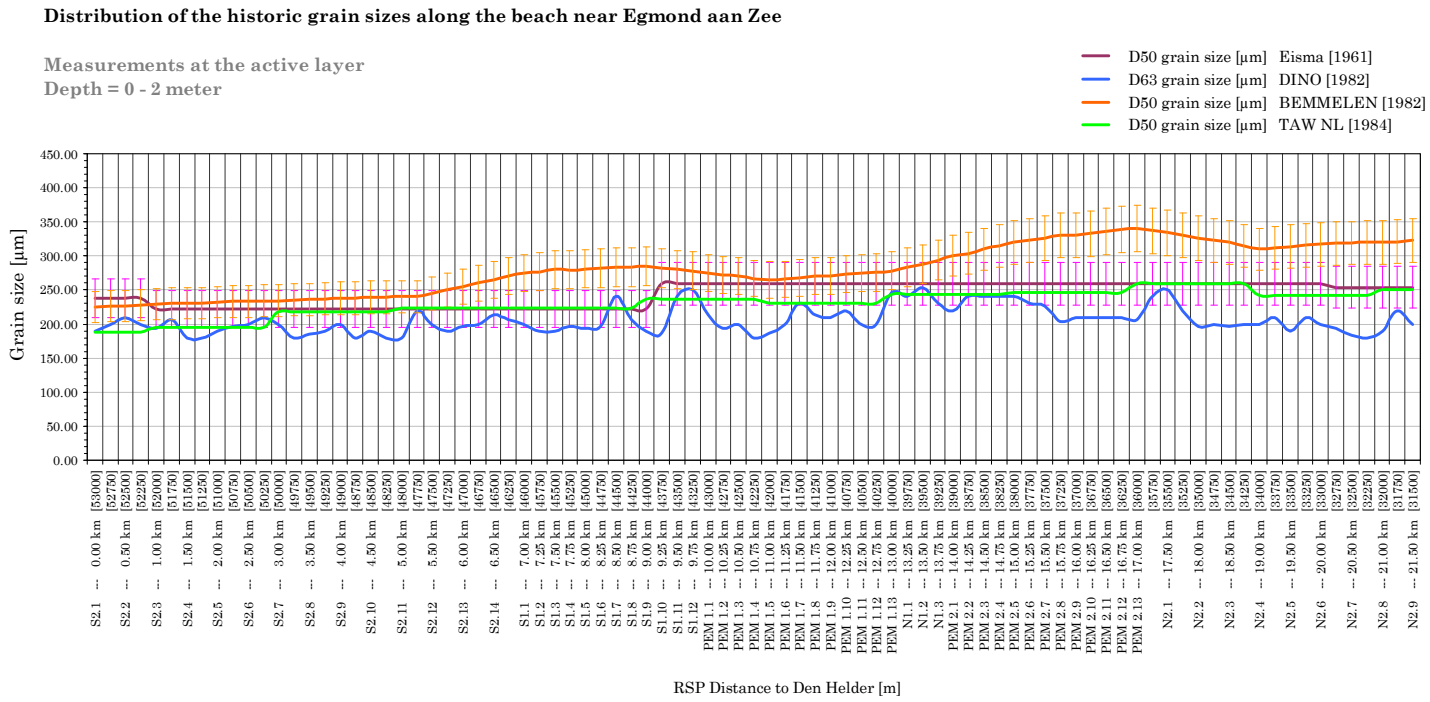

Figure 2-9 Historic grain sizes of the active beach surface at the study area [see also appendix G]

Janssen/Mulder (2004) studied the grain size (Table 2-1) and cross-shore sediment size and sorting (Figure 2-10) at the beach near Egmond aan Zee. The grain size varies around 320 µm .

Table 2-1 Average historic grain sizes along the beach from Castricum to Egmond aan Zee

Research	Year	Grain size [µm]
Janssen/Mulder	2001	303 to 332
Janssen/Mulder	2002	305 to 314

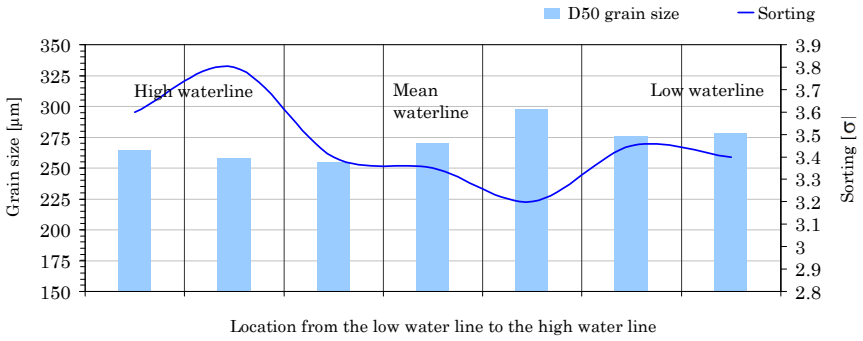

Figure 2-10 Average cross-shore grain size and sorting along the Dutch beach [56]

From Figure 2-10 it becomes clear that at this specific location the sediment gets better sorted from the low water line to further onshore. The median grain size around the mean water line is around 10-15% larger than the cross-shore average. This falls within the natural variability of the beach according to Bemmelen (1988).

Beach nourishment activities could increase the coarse fraction of the beach sediments. Research by Spanhoff et al. has shown that these new sediments will spread out after a few years. The beach nourishments done at Egmond aan Zee may increase the average grain size of a very wide area along the beach and offshore.

Figure 2-11 shows the historic grain size analysis together with the OerIJ estuary during its active marine phase. The coarse pleistocene glacial layers are not found in the beach subsoil.

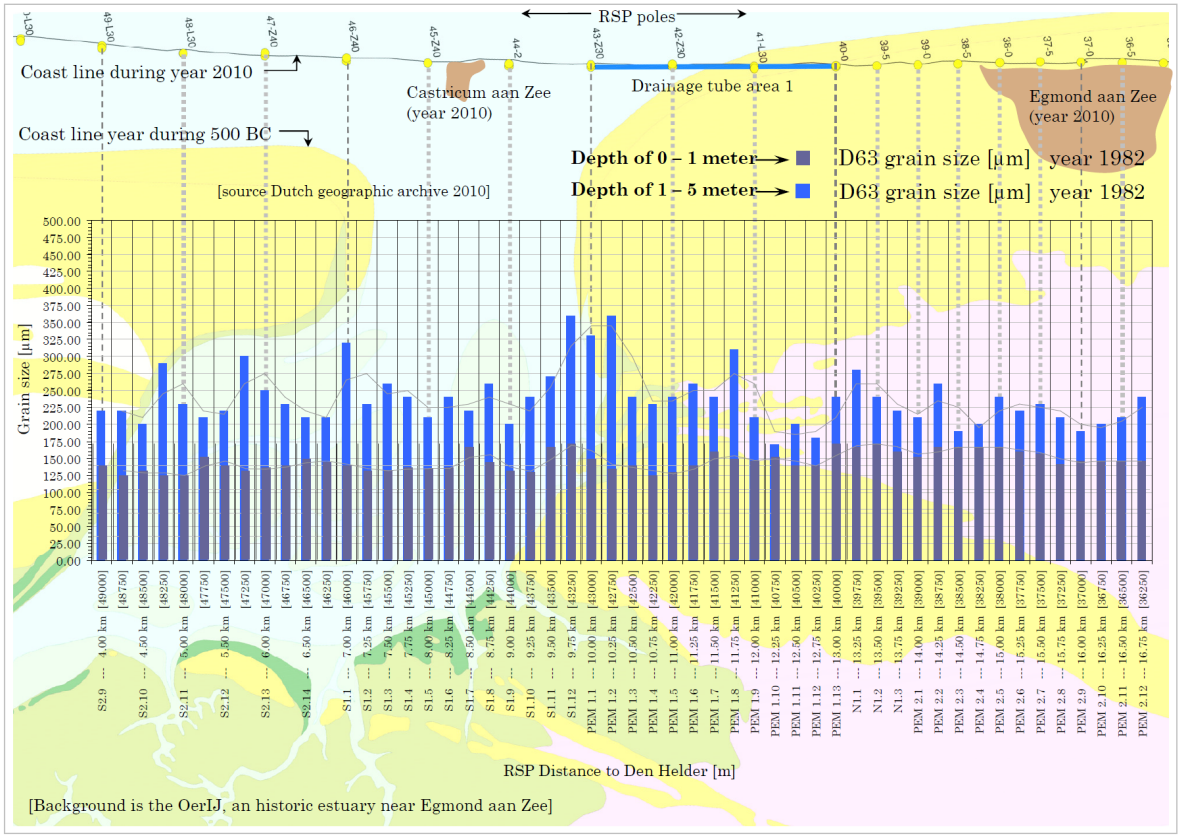

Figure 2-11 The grain sizes around the year 1982 together with the active OerIJ estuary

2.3 The beach near Hvide Sande

The Danish coast is more than seven thousand kilometres long. The highly exposed North Sea coast at the west of Denmark is a typical sandy beach in front of dune ridges. During the Pleistocene glaciations, some coarse sediments accumulated. At the southwest of Jutland Saalian glaciation sediments dominated, while Weichselien glaciations formed the surface layers in northern and eastern Denmark. The Saalian period radically formed the landscape.

Hvide Sande lies at the westcoast of Denmark (Jutland) next to a large lagoon. This is the most southern bay Ringkøbing Fjord which is 40 km long and 10 km wide. The construction of a permanent sluice and lock at Hvide Sande stopped the natural southwards transport of sediment. The entrance of the harbour is protected by jetties which extend 450m into the sea. A bypass with pipelines was made to continue the longshore sediment transport of sediment to the coast south of Hvide Sande (Figure 2-12).

Figure 2-12 The entrance of Hvide Sande harbour with the sediment bypass

The net long shore sediment transport along the coast is approx. 2.1 million cubic metres per year. This sandy coast is vulnerable to erosion. Three shore parallel bars are formed along the coast. Most of the longshore transport takes place in the bar zones. The grain size is medium to coarse (0.3 to 2.5 mm) with many remains from the glacial periods. Shingles and stones can be found on the beach. At a depth of 10 to 12 m below the surface, fine sand can be found. Underneath are layers of very fine sand or silt with in some cases even clay. [41]

2.3.1 Description of the drainage tube site

Near Hvide Sande again two drainage tube areas (PEM 1 and PEM 2) are installed with reference areas on both sides (Figure 2-13).

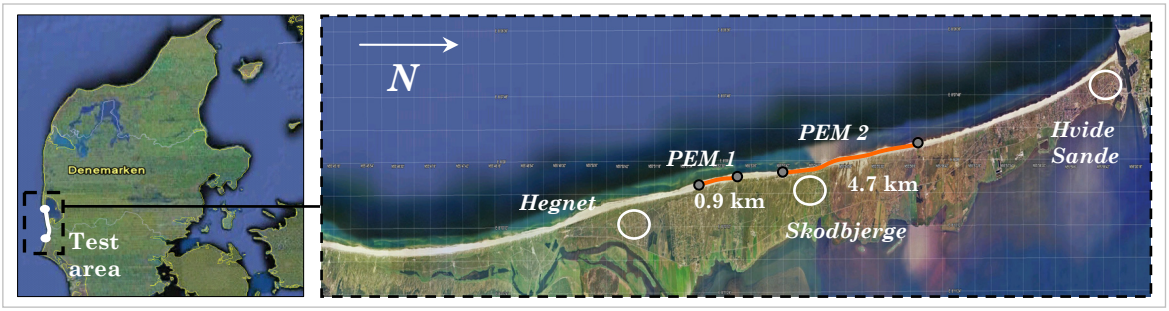

Figure 2-13 The beach near Hvide Sande, study area 2 (Denmark)

At the beginning of January 2005, most of the vertical drainage tubes were placed by drilling a hole in the beach. As with the Dutch system, the tubes were placed thirty centimetres below the beach surface. Where the beach was wide enough, additional tubes were placed.

2.3.2 Hydrological conditions

The tide is bidiurnal with an average difference between high and low water of 0.8 to 1.0 metre. The Gulf Stream comes from the Waddenzee and is directed northward at the coast of Jutland. Much higher water levels are created by storm surges. These are often caused by strong westerly winds. Water levels can be up to more than 3 m above mean sea level. During easterly winds, water levels may drop to -2 m below mean sea level. The water level within the fjord varies between -0.5 and 0.5 m.

The north-western winds have a fetch length which stretches from the coast of England to the western coast of Jutland. This causes very high waves which vary between H_s = 2 to 4 m with an average wave period of 6 - 10 seconds. During extreme events, even 6 m wave heights occur with a wave period of T_p = 12 s.

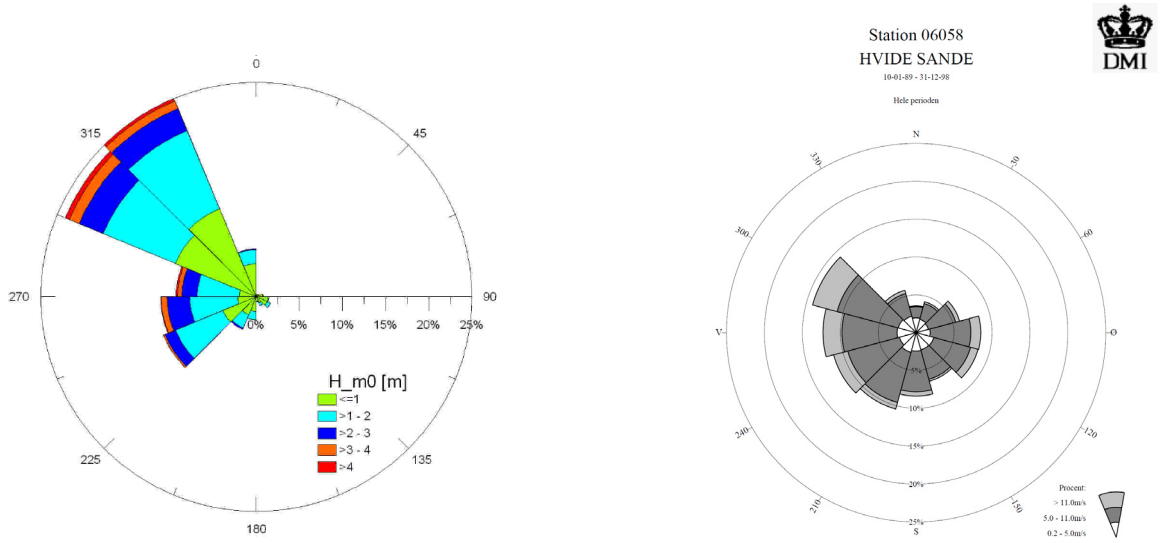

Figure 2-14 Yearly averaged wave and wind roses at Hvide Sande

The angle between the coastline and the dominating incoming waves is 45^0, which causes a net southwards sediment transport. The average natural erosion of 2 m per year is compensated by beach nourishments, which have stabilised the coast over the past ten years. Appendix H gives a detailed overview of the nourishments done at the beach near Hvide Sande.

In order to monitor the influence of the drainage system near Hvide Sande, the groundwater table was measured in 2005. The spit which separates the North Sea with the fjord, forms the transition zone between both water levels. The water level at the fjord is slightly higher than that of the sea. Precipitation will contribute to the freshwater discharge [41]. The groundwater depends strongly on the permeability of the beach.

It was found by Fredsoe (2008) that the fresh-water runoff through the beach is less than 1% of the total salt and fresh water runoff. This means that the freshwater pressure has no meaning at the beach near Hvide Sande and therefore it is not suspected that the drainage tubes will influence the fresh water runoff.

2.4 Some results from the past

Research done by several scientists resulted in data which shows some different effects measured near the drainage tubes. This section describes some of their results briefly.

2.4.1 Pressure and temperature differences

A scientific study of Ecobeach in The Netherlands was done by Pieterse (2009). Details of this study and the places where measurements were taken are given by Figure F-2 in Appendix F. This research focused on the groundwater behaviour in the vicinity of a drainage tube and its influence on the pressure guidance. It was found that the fresh water flows under the saline beach groundwater at a depth of 7 – 9 m at the HWL. This is almost the same at the beach near Hvide Sande according to some observations [41]. So the drainage tubes are not long enough to transport fresh water to the surface. Measurements show that at 1 m depth the pressure variations are as large as half the wave height.

Measurements on the groundwater table [79] were done with divers measuring pressure variances (Figure 2-15 and Figure F-1 of Appendix F). Diver 2 and 5 are at 0.5 m from a tube and at a depth of 1.40 m (LWL). A small phase shift could indicate the storage capcity of the beach surface and a better guidance of pressures through the bottom at the wave front. As Figure 2-15 shows the phase shift is negligible for both short and long waves. The divers used for this study could be to inaccurate [79]. The natural variability could also be to large.

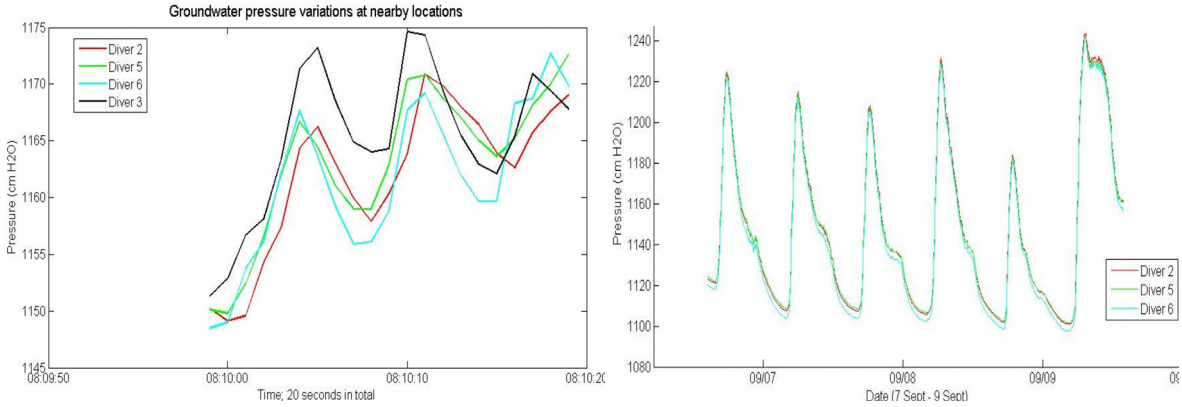

Figure 2-15 Pressure variations in the vicinity of the tubes wind (l) and tidal (r) waves [79]

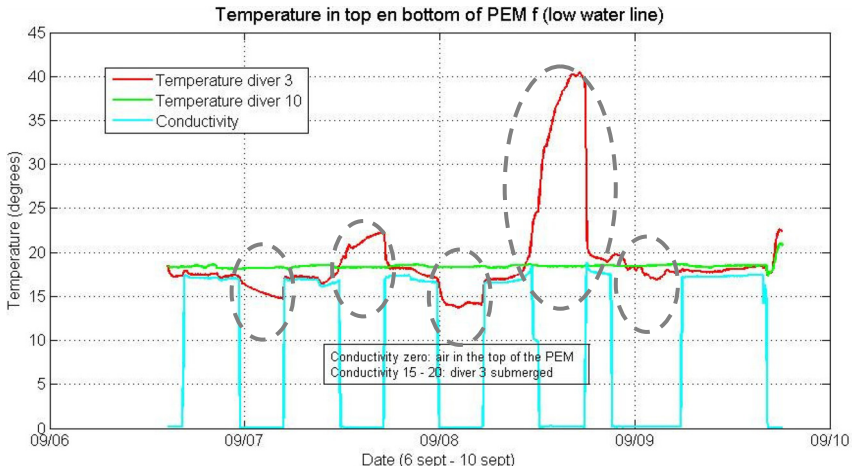

Figure 2-16 Temperature variations of the water near and away of a tube at the LWL [79]

The temperature (Figure 2-16) was measured with the use of diver 3 and 10 which were placed respectively at a distance of 10 metre and next to a drainage tube. Both divers were positioned at a depth of 1.40 m (LWL). The conductivity measurements in this graph are not representative. The surrounding sea water temperature was around 15 ºC. The temperature graph of diver 10 shows a stable temperature of 18.6 ºC originating from probably fresh water from the dunes which was warmed up during storage. At diver 3 fluctuating temperatures were measured probably indicating inflow of sea water and outflow of stored and/or fresh water. The stabilised temperature at the drainage tube could indicate an almost constant transport of stored water.

2.4.2 Conductivity measurements

Conductivity measurements also indicated vertical transport of groundwater through the tubes, especially near the low water line (Figure 2-17). Details of this study and the places where measurements were taken are given by Figure F-2 in Appendix F. Here Diver 1 is placed in the tube. Diver 2 and 5 are placed at a distance of 0,5 metre and Diver 6 is installed 4.5 m from the tube. The divers are installed at a depth of 1.40 m near the low water line. The distance to the sea waterline is constant.

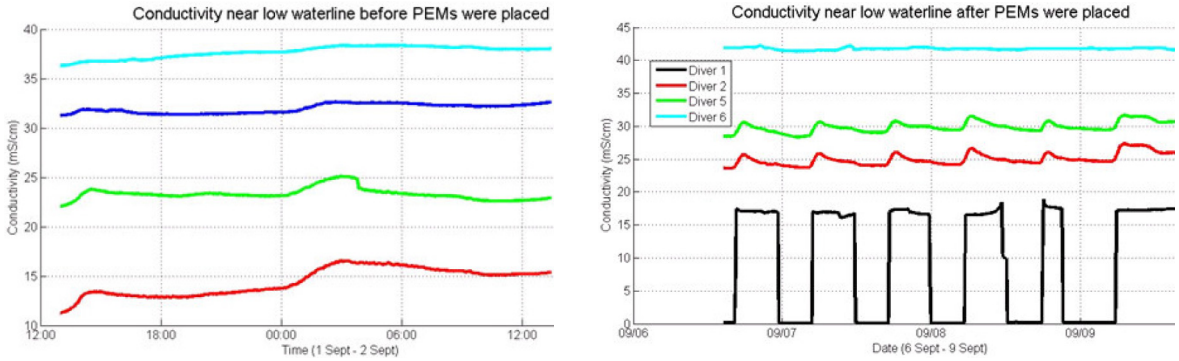

Figure 2-17 Conductivity measurements before and after placement of tubes [79]

The water flowing through and along the tube (diver 1–5) shows larger conductivity fluctuations. This could indicate that the transport of fresh water from the dunes is intentified near the low waterline. This closely resembles the previous case of the temperature fluctuations. The reference situation (before the tube was installed) shows a uniform pattern, which was also found at several other places at the beach.

2.4.3 Groundwater salinity distribution

As part of the Ecobeach research programme Pauw (2009) studied the groundwater salinity distribution at the beach near Egmond aan Zee. He found that the hydraulic gradient at the dunes is about 0.0003. It increases in offshore direction to 0.007 close to the sea. The depth of the deep fresh-salt groundwater interface at the beach lies at -70 NAP. Salt and breakish water (intertidal sea water movement) was found on top of fresh groundwater at the beach. This depth was 2 m (HWL) and 7m (LWL). At a depth of -18 m NAP, a relatively thin loam layer is present. This layer slows down the infiltration and exfiltration of water. When impermeable layers are present in the subsurface, fresh groundwater flow toward the submarine groundwater discharge zone is presumably even higher [76]. Pauw confirmed that the groundwater level at the beach is driven by the sea level. The largest salinity changes in the intertidal zone were observed near the high water line. Near the middle and low water line, the groundwater salinity is stable. This means that the measured fresh water transport through the tubes and stable surrounding areas [79] affirms the filtration mechanism of the vertical drainage tubes.

3. Vertical drainage tubes in theory

Over the years 2005 to 2009 a number studies were done which described the effects of the drainage tubes on beach processes and morphology. The founder of the technology used beach photographs [55] to prove that the shore erosion decreased. Later on, scientists got involved who approached the technology from a more theoretical point of view [41]. Their knowledge was based on conventional coastal principles like sand waves, migrating bar systems, rip currents (sometimes very deep) and dune holes. Scientist from Denmark even programmed a model which included the vertical drainage tubes as a highly permeable element in the beach. Later on, their their focus shifted from desk research to the practical functioning of the tubes. Some studies were done with tubes in real life [41]. These studies focused on the capacity of the drainage tubes in order to gain more insight in the physical capabilities of the technology. These findings were supported by a theoretical model.

Although these models are convenient, one must realise that a number of empirical relations, which are embedded in these models, are models on their own, often based on specific field data on a particular location in the world. Many models frequently turnout to be inadequate for the tasks for which they are used. [96] In coastal engineering, models must contain parameters which are based on morphodynamic processes. It is important to distinguish between models that answer quantitative questions and models that focus on qualitative questions. The latter are often answered with basic scientific models [96]. This study uses both by measuring changes at the beach and interpreting them using theoretical backgrounds. The goal is to use as few model parameters as possible. The most important controlling elements are considered.

During the last decades, different dewatering systems were applied at beaches. With pumped wells and drains, the beach groundwater was artificially lowered. Often these systems were based on horizontal tubes, connected to pump stations. Several projects have shown that beach accretion can occur in areas where groundwater is pumped below or just landward of the surf zone. The pore pressure is reduced locally, which increases the intergranular friction. This process makes erosion of sediment more difficult. The deposition of sediment passing the beach is enhanced by this effect. Several authors have investigated effluent and influent groundwater impacts in the surf zone. Their studies show that dewatering or reduction of pore pressure increases intergranular friction and shear stress. The principles may be applicable in explaining sedimentation when the vertical drainage tubes are installed.

Pressure equalizing technology could be considered as a passive system to control shore erosion. The vertical drainage tubes form a naturally functioning draining system. The large scale groundwater fluctuations, which normally take place in the beach, are forced by tidal fluctuations. The response of the aquifer is dominated by a large increase of water levels at the low water line and dampened fluctuations at the dune foot. The groundwater elevation from this lateral pressure response is influenced by the permeability of the soil. If the permeability increases, the pore pressures are reduced and shear strength at the beach becomes higher. The sediment transport is delayed. This hypothesis explains that small scale processes may cause large scale phenomena. In this respect, this effect can be compared with a weather forecast. Small atmospheric changes may result in completely different weather conditions.

This chapter focuses on the relation between the tube system en changing beach processes. Here integral mechanisms are assumed.

3.1 Hypotheses and working mechanisms

Here, five small scale hypotheses are given which concern possible working mechanisms of the vertical drainage tubes installed in the beach. These hypotheses are based on knowledge, site visits, reasoning and experiences from the past. The latter refers to knowledge gained from active drainage in beaches. Figure 3-1 shows a scheme that summarizes the five effects. These form the basis of a large scale working mechanism.

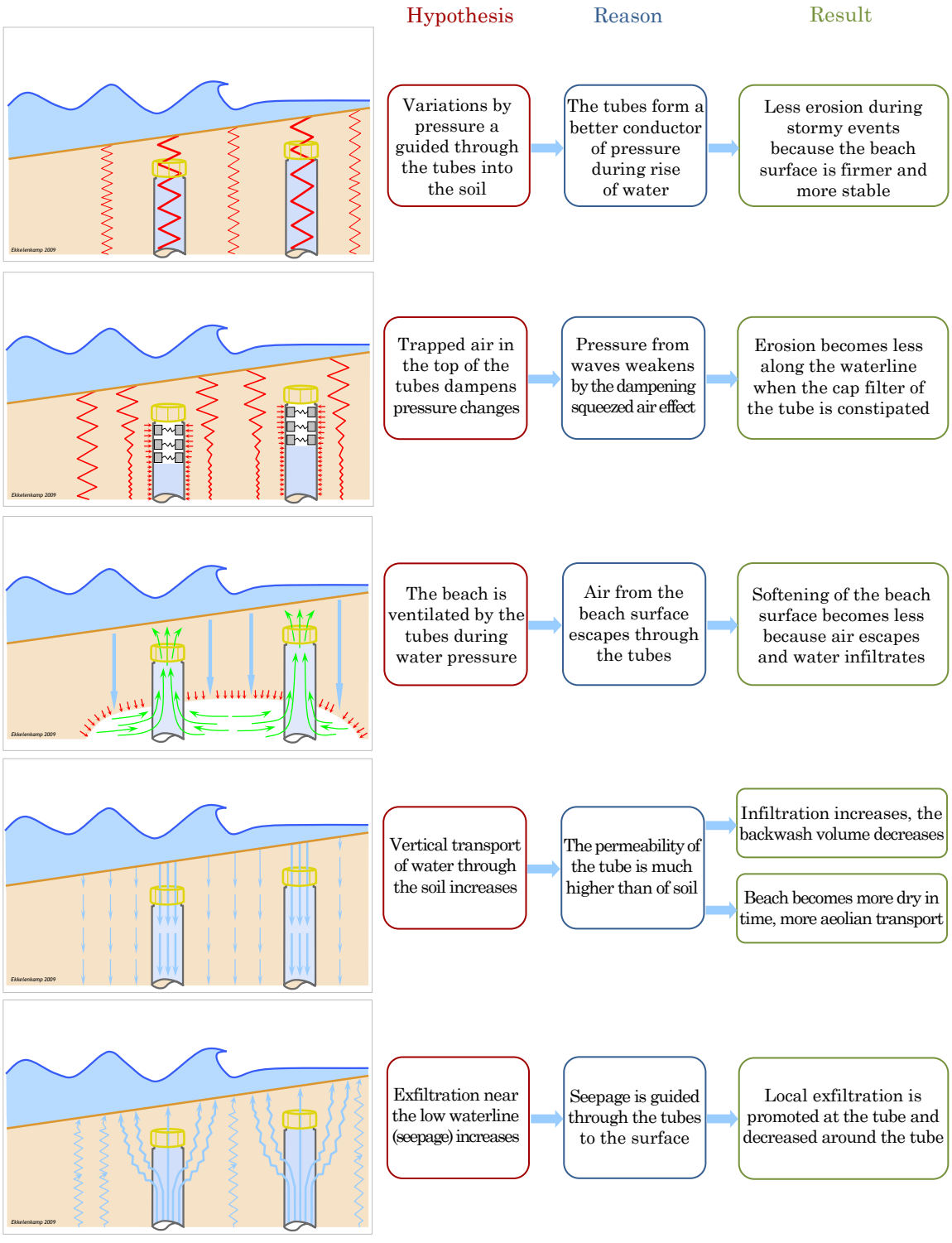

Figure 3-1 Small scale working mechanisms of the vertical drainage tubes

3.1.1 Small scale hypotheses

Basically, three different effects can be distinguished; the influence on pressure variations, guidance of air trapped in the beach and the physical transport of water.

Pressure variations

Pressure changes with a short time interval are considered here. This pressure drop or rise results from passing waves. The waves cause pressure variations in the beach surface. The pressure can be increased or decreased by the vertical drainage tubes. Tests show that the pressure from a wave of half a metre is reduced by the soil to 0.20 m at one metre depth [79]. Drainage tubes are filled with water, which forms a better conductor to transport pressures into deeper soil. This effect can only be active when tubes are less than one metre below the beach surface. Otherwise, the soil above the tubes has dampened any pressure variations. The pressure variations caused by waves have a specific frequency and amount of energy. These vary between 0.08 and 0.25 hertz [79]. This relates to short waves. Long waves give frequencies of 0.0125 to 0.05 hertz.

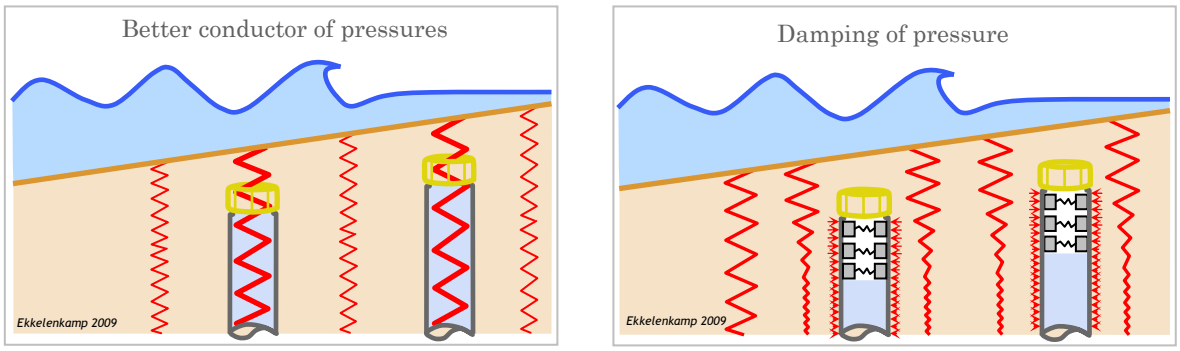

Figure 3-2 Hypothesis: Better conductor of pressures (l) and Damping of pressures (r)

The pressure variations can also be decreased by vertical drainage tubes (Figure 3-2). The filter, located at the top of the drainage tube, may be clogged. The upper seventy centimetres of the tube does not have a vertical filter. This facilitates a column of air which is trapped in the tube. The groundwater level must be below this column. The air acts like a dampening system. The spring stiffness of air is lower than water. The compressing air decreases the amount of pressure transported into the soil, after the water table increases. Field tests showed that the maximum column height of trapped air is nine centimetres under the top of the vertical drainage tube [79]. This confirms that a confined air volume can exist.

Ventilation of air

The groundwater level may rise fast when waves infiltrate the surface. This depends on the grain properties of the beach.

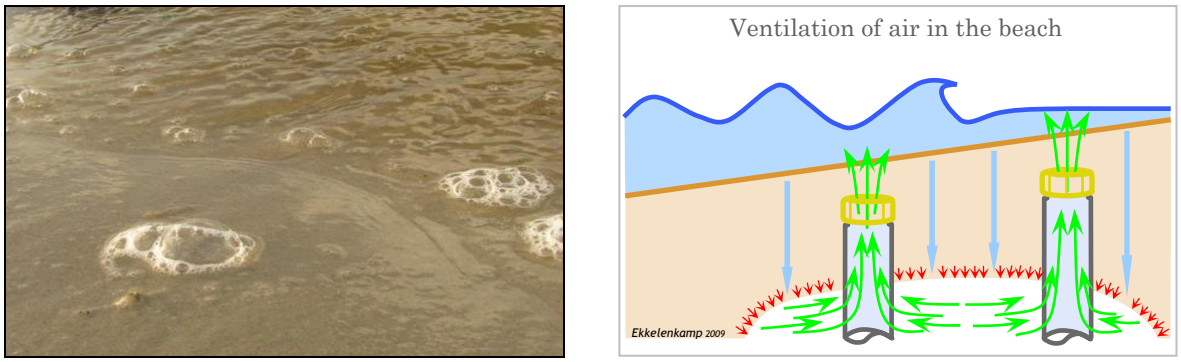

Figure 3-3 Air comes up as bubbles at the surface (l) Hypothesis: Ventilation of air in the beach (r)

From a number of beaches in the world it is known that air can be trapped in the beach surface. During rising tide this air comes up as bubbles (Figure 3-3). Vertical drainage tubes may pierce these air volumes. This way, trapped air can be released through the tubes when the water pressure increases. This outflow of trapped air can only exist if the filter at the top of the tube is not blocked by accumulated sand particles. Air fields must have a scale of several metres in order to notice any effects of the blow out. In that case, the beach might become more stable when softening of the beach surface decreases and water infiltrates more easily.

Transport of water

The groundwater table may change on a short or long scale. This change is caused by short waves or tidal oscillations. The tidal wave is asymmetrical and depends on the permeability of the beach. The wave amplitude decreases in the direction of the dunes. The rising groundwater table takes less time than the lingering falling tide. This motion has a large time scale of hours. Waves initiate a quick response of the groundwater level. This results in a propagation of a few metres into the beach subsurface. This movement is more dampened.

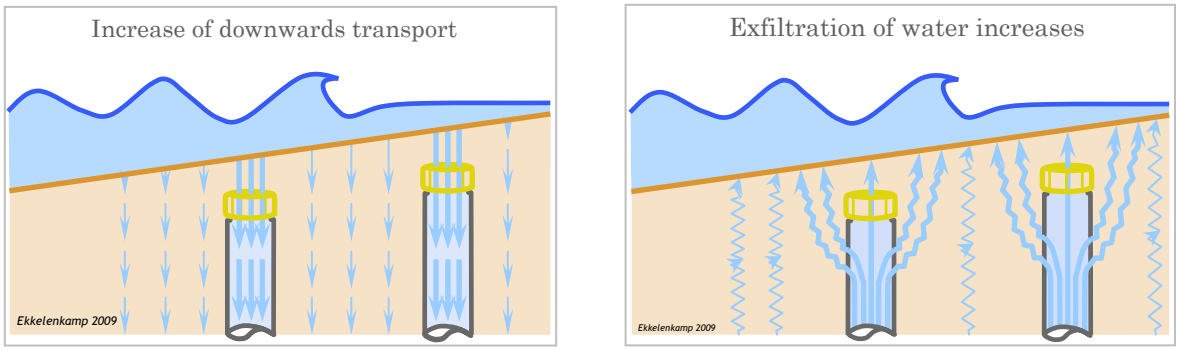

Figure 3-4 Hypothesis: transport downwards of water (l) Exfiltration of water upwards (r)

The transport of water through the vertical drainage tubes, can commence when a pressure gradient exists. This may result in a piezometric head difference between the high water and low water level (tidal scale of hours) or a pressure change by an incoming wave (small scale of seconds). During falling tide, tubes installed at the upper part of the beach transport water downwards (Figure 3-4), while tubes at the lower part transport water in an upward direction (Figure 3-4). Local water level changes, initiated by waves, cause infiltration under the wave and exfiltration at the bore front.

Water level variations can be measured by pressure differences. Field tests were done by Pieterse (2009) to investigate this effect [79]. Tidal fluctuations have a long time scale in the order of hours. The vertical drainage tubes induce a water level difference during falling tide of up to several centimetres. This difference decreases (a few centimetres) during rising tide. The physical transport of water through the drainage tubes is suggested by analysing water temperature variations related to the depth. Tests reveal that the temperature and conductivity within and near a tube are larger than that of the surrounding soil. This could indicate vertical transport of water through the drainage tubes.

Conductivity measurements show that water, transported through the drainage tubes at the low water level, has a varying conductivity level. This phenomenon is not detected in the surrounding ten metres of the tube. The tubes at the low water line could transport seepage water which is less salty than sea water. This is fresh seepage water which is canalized. Exfiltration in the surrounding area may theoretically decrease while the surface becomes more stable.

3.1.2 Large scale working mechanism

The hypotheses mentioned in Figure 3-1 concern working mechanisms on a small scale. There are several ways in which a combination of these mechanisms can form a large scale working mechanism (Figure 3-5). The promotion of local infiltration and exfiltration increases the permeability of the beach. This has a stabilizing effect on the beach surface and results in less erosion as less air is trapped. These relatively small scale processes form an effect which may influence beach processes significantly. For example the groundwater gradient could decrease.

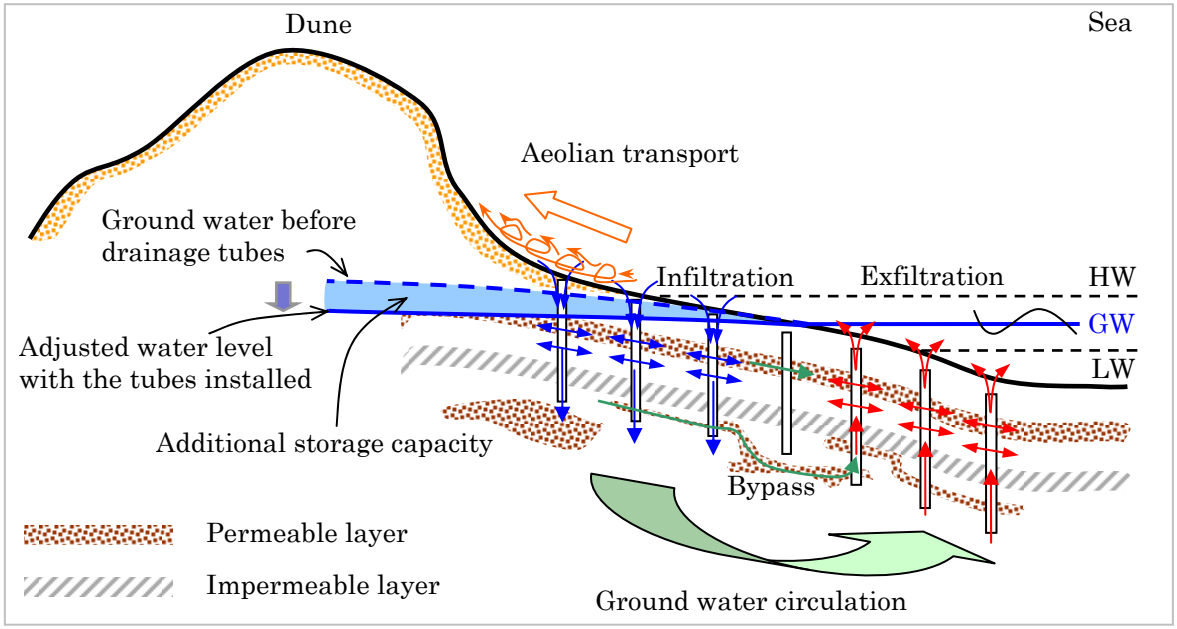

Figure 3-5 Theoretical proposed large scale working mechanism of the vertical drainage tubes

The groundwater level depends on the hydraulic conductivity of the beach surface. Above the phreatic level, a capillary fringe exists, which depends on the permeability and structure of the sand grains. [49] During falling tide the groundwater level drops. A time lag exists between the groundwater and sea level. The difference between the high and low water lines causes a piezometric level difference. This gradient induces groundwater circulation. At the high water line, the flow is directed downwards. The opposite occurs at the low water line, where there is exfiltration. Although the vertical drainage tubes have a high permeability, the water transported through the tubes must be discharged to the surrounding soil. Thus, the amount of transported water depends on the drainage capacity of the sand, i.e. its permeability.

Beaches around the world often consist of layers with different permeability. Dutch beaches, like the Egmond aan Zee beach, are known for large quantities of shells. Danish beaches were influenced by the glacial period, when granules were deposited. Permeable layers may be present in the subsurface of both beaches. If these layers exist, they can be penetrated by the vertical drainage tubes (Figure 3-5). Now, the vertical filter of the tube connects the upper soil structure (high water pressure) to the more permeable layer. The water chooses the path of least resistance. This means that water is transported through the tube via the permeable layer to the next tube. As long as a connection with the sea exists, the water will choose this path. Infiltration of water will be promoted at the high water level, while exfiltration of water will be found at the low water level. Levelling of the groundwater level lowers the phreatic level at the upper part of the beach. Surveys along the beaches of Egmond aan zee and Hvide Sande show some thin layers (centimetres) of clay. Again the circulation may change if these layers are penetrated (pressure drops).

When the groundwater level drops, the vandose zone (distance between the phreatic level and the beach surface) also drops. As the beach gets drier the aeolian transport of sand grains to the dunes and along the coast increases [102]. First, the fine grains are transported by the wind. Eventually the beach could hypothetically become coarser by this sorting mechanism. If the median grain size of the beach sediment increases, the beach surface will become more permeable. Infiltration and exfiltration may also increase. The net offshore transport can turn to a net onshore transport, i.e. accretion. This whole process may go on by repeating itself.

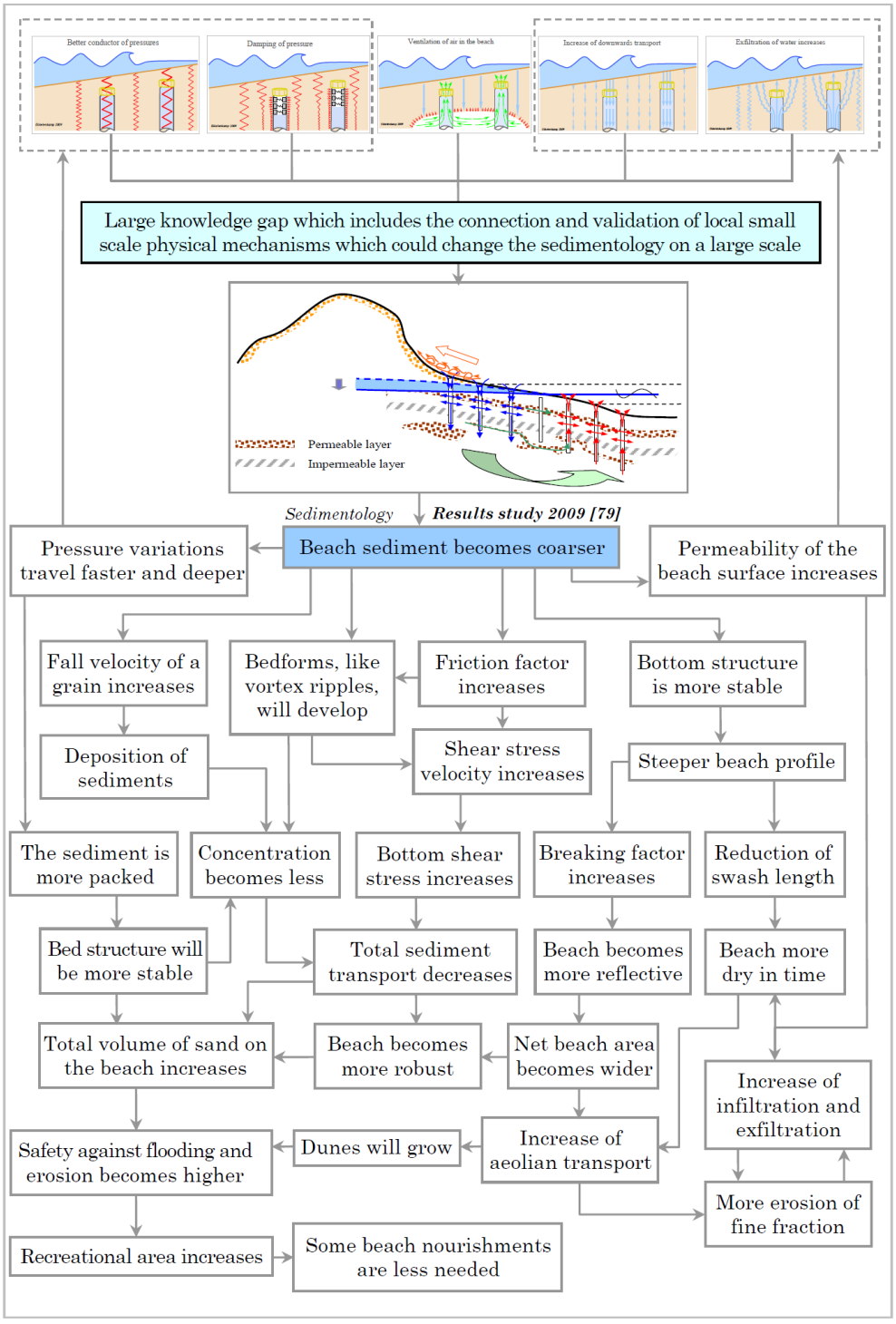

Figure 3-6 Event tree of the process from small to large effects on the beach zone

3.2 Research approach for this study

The scientific method used in this study is a hybrid of theory and practice. The basic input for theoretical concepts is formed by the field data. Simultaneously, the configuration of field tests and measurements is based on theoretical backgrounds and working mechanisms. The choice of test methods and field measurements is controlled by theoretical arguments.

Theoretical backgrounds of this research are given in chapter 4. There, the relevant scientific principles are given as tools to interpret the field data. This information is gathered from field measurements made on the beach at Egmond aan Zee (The Netherlands) and Hvide Sande (Denmark). The starting point for the scientific field research is the large scale working mechanism explained in section 3.1.2.; *Levelling of the groundwater and desiccation of the beach.*

The reflection on the assumption that the groundwater level is levelled, gave rise to some suggestions for more detailed research. The permeability, groundwater circulation, aeolian transport, storage capacity, bed friction, active layer at the beach and the vandose zone of the beach are, in one way or another, related to its sedimentology. The theoretical backgrounds describing these mechanisms depend on the grain properties of the sediment at the two different beaches. A detailed exploration of the sediment characteristics forms the basis for the data set used for this study.

3.2.1 Literature study

The sediment samples, which are collected during the field research, must be analysed. There are some basic formula available from literature which can be used. Descriptive parameters can be defined which express the grain size and shape of the distribution. Although the analysis of grain shapes is not new, an analysis of such a vast number of individual grains is certainly a novelty. Therefore, state of the art methods are presented and used.

The intertidal beach zone is dominated by the swash dynamics and beach profile. Grain properties have a major impact on these beach profiles. Many theoretical relations are available which express the steepness of the profile in terms of sediment size. Also the permeability of the beach and bed forms like ripples depend on the grain size. There are basic relations between the dimensions of ripples and flow conditions available in literature.

Groundwater behaviour forms the basic ingredient to explain the large scale working mechanism of vertical drainage tubes. Also the height of the vandose zone determines the level of saturation of the beach. Again, the grain size plays an important role. The presence of permeable layers is a requirement (in theory) for the increased horizontal flow in the beach surface. This will therefore be examined during field research.

Beach processes like infiltration and exfiltration, swash asymmetry and sediment sorting depend on the desiccation of the beach. In literature, one can find theoretical concepts which describe these processes in detail. The present study focuses on a qualitative analyses of the facts (data). Some formula are given which will be proven to be very useful.

3.2.2 Field work

Two different types of beaches at Egmond aan Zee and Hvide Sande will be examined. In theory, many beach processes are influenced by grain properties. The sedimentology of the two beaches will be studied by the analysis of many sediment samples from both areas. This is done with a Laser Diffraction Sensor (Figure 3-7). In the Egmond aan Zee case, samples are also taken at depths of one to six metre, in order to define the coarseness of the beach envelope and subsurface. All samples will be carefully analyzed in a geotechnical laboratory.

Their size, shape, roundness and weight will be determined and the gravel and shell fractions will be quantified.

Figure 3-7 Test facility to analyse the sediment samples (laser diffraction sensor)

The beach profiles are taken from the dune foot to some metres below the low water level. The measurements will be done with a theodolite and GPS. The timing of the measurements is crucial, because hydrodynamic conditions may change rapidly. Data before, during and after a storm is collected. This way, the active beach profile can be determined. The data will be compared with measurements from the past. In order to gain insight in the soil composition, a number of cone penetration tests will be done with a drill depth of twenty metres.

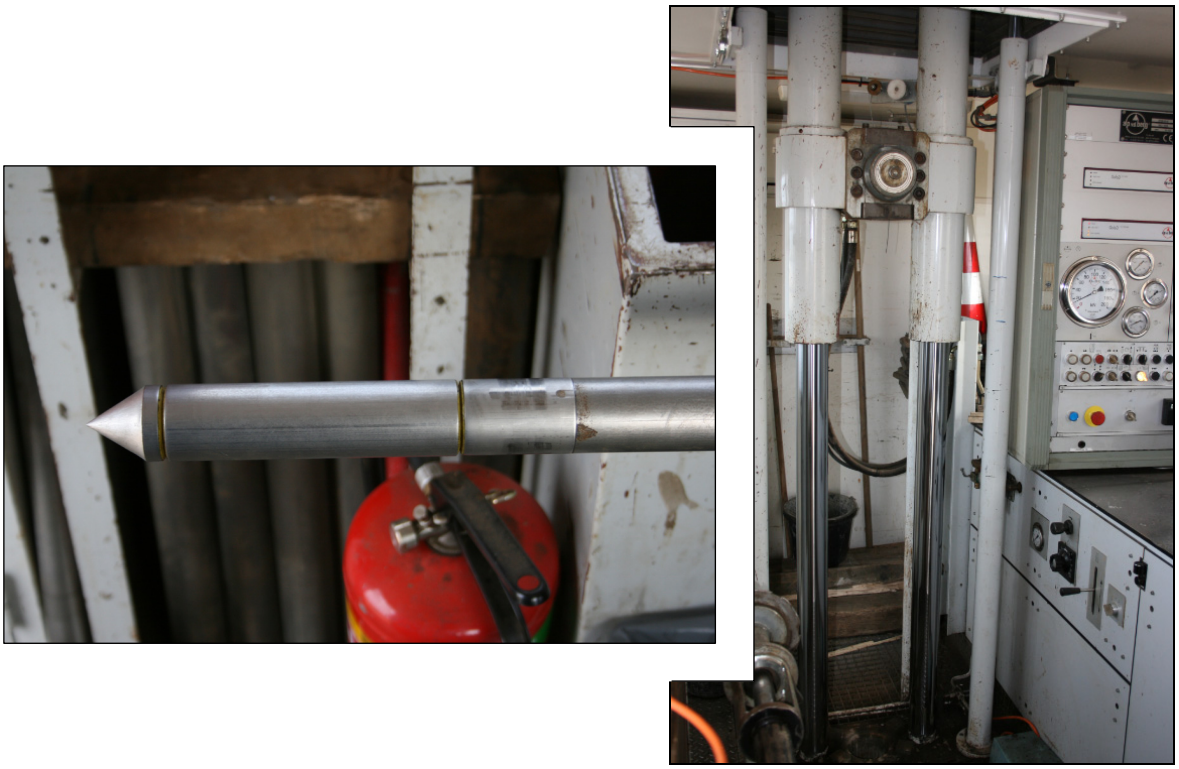

Figure 3-8 Cone penetration tests to study the conditions of the subsurface

4. Theoretical backgrounds

The purpose of this study is to investigate the effects of vertical drainage tubes on the sedimentology of two beaches and to connect any changes of grain properties with intertidal beach dynamics and processes.

Beaches around the world differ in many ways from each other. Energetic environments or a specific geological historic background can for example determine the way a coast behaves. In the past many models have been designed and built to give insight in this acting. These models are often giving answers in a qualitative manner. Theoretical backgrounds form the basic input and reasoning to questions about beach behaviour.

There are many interventions by man which affect morphological processes on the beach. The way the beach reacts on changes is difficult to predict. Some interventions are large like beach nourishments done near the study area at Egmond aan Zee and Hvide Sande. Other projects may look radical like the six hundred drainage tubes installed below the beach surface at one test site, but could change the morphology only on a minor scale. It's crucial to study the processes that may be affected by projects like the tubes. In addition to this also the time and space scale are of great importance. People often think of the beach as a solid system which soon reforms itself to its old equilibrium situation. But beaches can also be destabilized quite easily. Nourished beaches are likely to be unstable relative to natural beaches. Often lack of knowledge results from unknown initial conditions about the impacts of such projects. [96].

It's reasonably to think that the beach is sensitive to initial conditions. There are non-linear systems like sediment transport mechanisms which are very sensitive to conditions that effectively prohibit the detailed prediction of the beach evolution. [47]. Thieler et al once wrote down an interesting statement. "Beach state is certainly an initial condition on which some beaches are strongly dependent. Perhaps an even better example may be the formation of or the presence of shell and gravel lags, formed in the initial stages of a storm or present when a storm strikes a sandy shoreline. The lags will delay the response of the shoreface to storm conditions resulting in an overall storm response considerably different than would have occurred if the affected sediment body was uniform, well-sorted sand." [96]. Vertical drainage tubes installed below the beach surface may initiate different conditions. If these conditions are not well known and registered, it is deceptive to predict the effects based on experiences from the past. Therefore it's necessary to examine the changed conditions by studying the past behaviour of the system as well as the description, classification, origin, and interpretation of the beach sediments and the basic theoretic principles which could be affected. Minor changes by the drainage tubes could initiate greater processes which are not thought of when the principles of the technology are not well understood. The present studies are not aware of this fact and pretend the system could not work. This is not scientific and justified.

In order to interpret the raw data resulting from the experiments done during this study, some theoretical backgrounds help to clarify certain phenomena and findings. It is important to know the processes which form the intertidal beach zone and how the sediment properties have their influences on it. Frequently the morphological dynamics at the coastal zone are described by sediment volume changes and transport formulas. In order to get insight in the sediment transport mechanism the iterative scheme shown in Figure 4-1 is made.

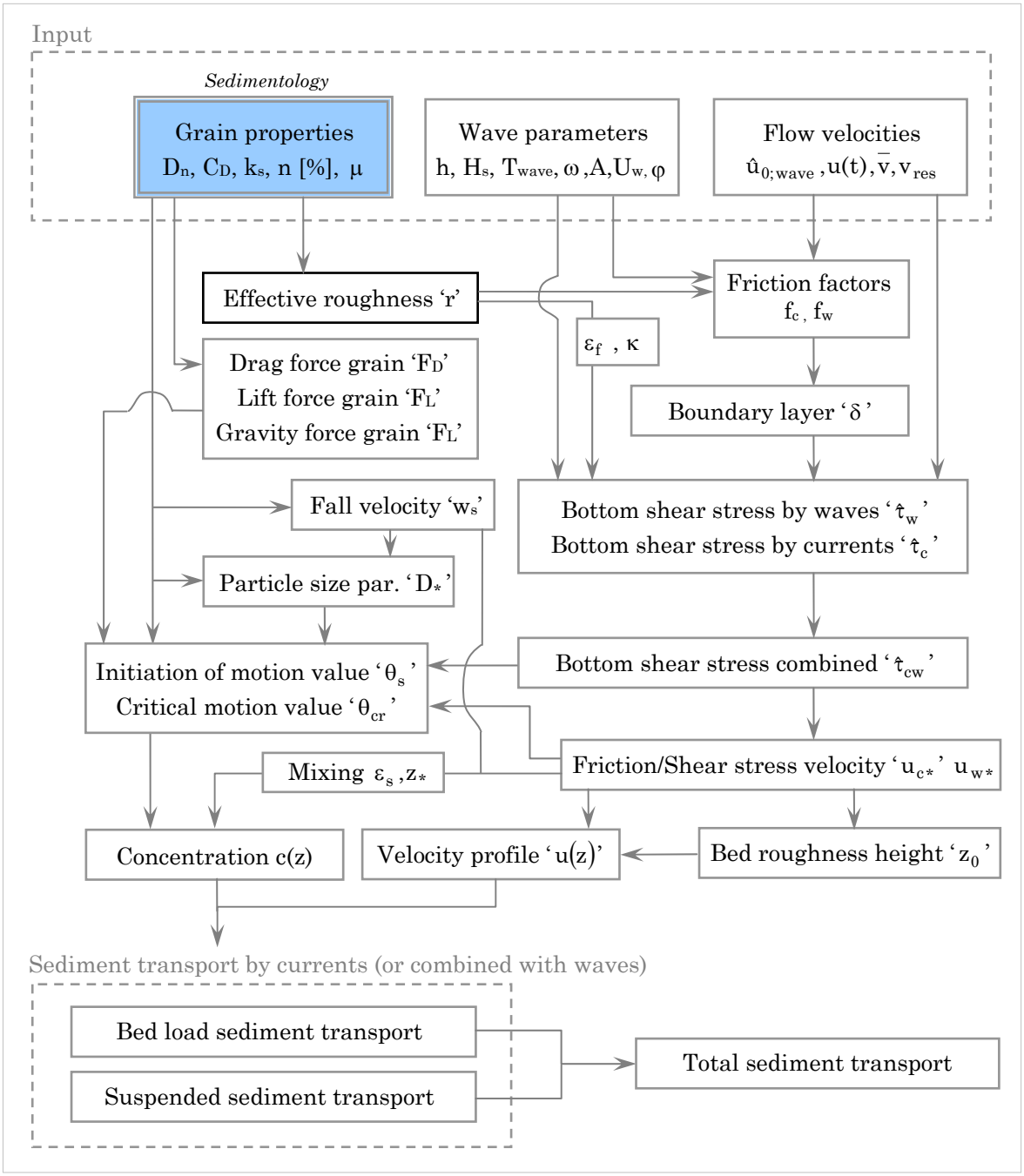

Figure 4-1 Iterative scheme to indicate the importance of know sedimentology

The scheme shows the basic steps between the input parameters and the sediment transport. It becomes clear that the transport of sediment depends on the sedimentology. The development of the bottom shear stress, which counteracts the driving force by the waves and currents, is one example. This stress determines the initiation of motion for which the grains at the beach surface start to move. Before calculating and modelling the right amounts of sediment transport volumes, the grain properties should be examined carefully. Determination of the real grain properties is often forgotten while the actual sediment transport volume may change considerable with a different beach sedimentology [75].

Predictions of the changes within the intertidal beach zone, sediment transport mechanisms and volumes cannot be modelled and studied without good understanding of the sedimentology and groundwater behaviour. There are complex fluid and sediment interactions between the surface flow and the beach groundwater. Especially perpendicular flow to the bed is of importance [49]. Many aspects like permeability and sediment grain properties may have large influences on this. Therefore the change of groundwater dynamics and altering sediment properties cannot be seen apart.

The theoretical backgrounds focus only on the essential properties which interact with the sedimentology of the beaches. This chapter starts with theoretical backgrounds of the grain properties (4.1) which determine the sedimentology of the intertidal beach zone. They form the basis on which the field tests and the sediment analyses were done. The profile and interactions with the intertidal beach zone (4.2) are ruled by these sediment characteristics. The next paragraph (4.3) treats aspects concerning the bottom surface which are affected by the grain properties at the beach. The sedimentology of the surface may change and affect the swash dynamics and the aeolian transport mechanisms. Other hydraulic processes like infiltration and exfiltration are discussed in paragraph 4.4. Next the sediment transport resulting from changed beach conditions is explained. Basic transport formulae which determine the beach morphology and development are discussed.

4.1 Sedimentology

Beaches in The Netherlands and in Denmark can be composed of a wide variety of materials of many sizes and shapes. The composition and size, however, vary in a very narrow range [29]. Most beaches are made of silica sand. The beaches along the Dutch coast contain substantial amounts of shell fragments. In Denmark, the beach is coarser with lots of gravel (layers). These two beaches, described in this study, have two different systems with different sizes of sediment and composition (Figure 4-2).

Figure 4-2 Sediment with shells from Egmond aan Zee (l) and with gravel from Hvide Sande (r)

An exact grain size range for sand's heavy minerals cannot be made because heavy minerals are found in too many different sizes. Sand is made of minerals, with silicate as the most common. The second is feldspar. These minerals are very hard and resist the abrasion of the trip from mountains to the coast. Other minerals present in sand are hornblende, garnet,

magnetite, ilmenite and tourmaline (and many others). These minerals are referred to as heavy minerals because they are denser than quartz. They can often be seen as black layers of grains at sediment samples. To quantify the difference between quartz and heavy minerals, the specific gravity is used, which is the density of the mineral divided by the density of fresh water. For heavy minerals, the specific gravity is larger than 2.87, whereas the specific gravity of quartz is 2.65. [29]

There exist some descriptive parameters which form the basis to the input of sediment transport formulae. These are based on the grain sizes of the particles. The permeability of the beach is strongly dependent on the porosity and grain size. One aspect of sedimentology is the shape of grains. During this study the shape of the sediment is analysed. The shape of the sand grains affects their behaviour in the marine environment. A flat grain would settle differently than a more spherical grain. Also, the shape is a measure of age. This study treats the aspect ratio and sphericity of the grains.

4.1.1 Descriptive parameters

The grain size is the most fundamental parameter of sediment particles, affecting their entrainment, transport and deposition. Grain sizes can provide clues to the sediment provenance, transport history and depositional conditions [16]. The sediment samples included in this study are compared by grain distributions. Here, an ideal distribution is used assuming a log-normal, Gaussian, distribution with an geometric grain size scale. This scaling method has the advantage that equal emphasis is placed on small differences in fine particles and larger differences in coarse particles. Most sedimentologists have adopted the logarithmic Udden – Wentworth grade scale (Table 4-1).

Table 4-1 Size scale of sand by Wentworth and Udden

Grain size [phi] and [mm]		Descriptive terminology
-2	4.000	Granules
-1	2.000	Very coarse sand
0	1.000	Coarse sand
1	0.500	Medium sand
2	0.250	Fine sand
3	0.125	Fine sand
4	0.063	Very fine sand

The parameters used to describe a grain size distribution fall into four principal groups [16];

- The average size
- The spread (**sorting**) of the sizes around the average
- The symmetry or preferential spread (**skewness**) to one side of the average
- The degree of concentration of the grains relative to the average (**kurtosis**)

These parameters can be obtained by mathematical of graphical methods. The mathematical 'method of moments' is the most accurate since it employs the entire sample population [16]. However, outliners (which can be caused by shell fragments [33], affect the statistics. Therefore, approximations obtained by the formula of Folk and Ward (1957), are not always outdated.

The evenness can be expressed as D_{60}/D_{10} . It expresses the uniformity of the sample. In the NEN 5104 this D_{60}/D_{10} coefficient is used to define spreading; <1.80 very small, 1.80 – 2.20 moderate small, 2.20 – 3.00 moderate large, >3 very large. The gradation is often expressed with D_{90}/D_{10} . Sediment is well sorted for values of <1.50, moderately sorted for 1.50 – 3.00 and poorly sorted for >3.00.

The sorting of the sand sample refers to the range of sizes present. A perfectly sorted sample contains sand of all the same diameter. Poorly sorted sand contains a wide range of sizes. A numerical measure of the sorting is the standard deviation, σ_G , which is defined as (F&W);

$$\sigma_G = \exp\left(\frac{\ln D_{16} - \ln D_{84}}{4} + \frac{\ln D_5 - \ln D_{95}}{6.6}\right) \qquad \text{Eq.4-1}$$

Table 4-2 Explanation of the standard deviation [NEN 5104]

Sorting σ_G	
Very well sorted	< 1.27
Well sorted	1.27 – 1.41
Moderately well sorted	1.41 – 1.62
Moderately sorted	1.62 – 2.00
Poorly sorted	2.00 – 4.00
Very poorly sorted	4.00 – 16.00
Extremely poorly sorted	> 16.00

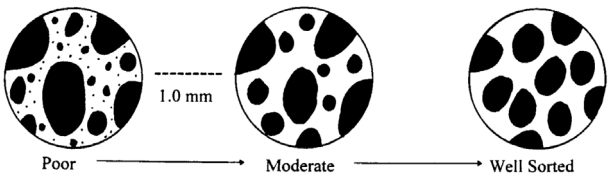

Figure 4-3 Difference between a poorly sorted and well sorted sample

A well sorted sample is a poorly graded sample. This is visualised by the sharp peak in the distribution. Distributions with a wide range of sizes are termed well graded or poorly sorted. Perfectly sorted sand would have a standard deviation of zero.

Another measure which describes the distribution is the skewness. If the grain size distribution becomes asymmetrical, the sample can be very fine or very coarse skewed. A negative skewness (in the case of geometric graphical measures) indicates that the distribution is skewed to fine grain sizes. Duane (1964) showed that a positive skewness is an indicator of an erosive environment. In that case, the finer materials have been winnowed out by the action of wind, currents and waves. A more depositional environment would likely have a negative skewness. The skewness can be obtained from the distribution by (F&W);

$$Sk_G = \frac{\ln D_{16} + \ln D_{84} - 2\cdot(\ln D_{50})}{2\cdot(\ln D_{84} - \ln D_{16})} + \frac{\ln D_5 + \ln D_{95} - 2\cdot(\ln D_{50})}{2\cdot(\ln D_{25} - \ln D_5)} \qquad \text{Eq.4-2}$$

Table 4-3 Explanation of the skewness

Skewness Sk_G	
Very fine skewed	-0.30 – -1.00
Fine skewed	-0.10 – -0.30
Symmetrical	-0.10 – 0.10
Coarse skewed	0.10 – 0.30
Very coarse skewed	0.30 – 1.00

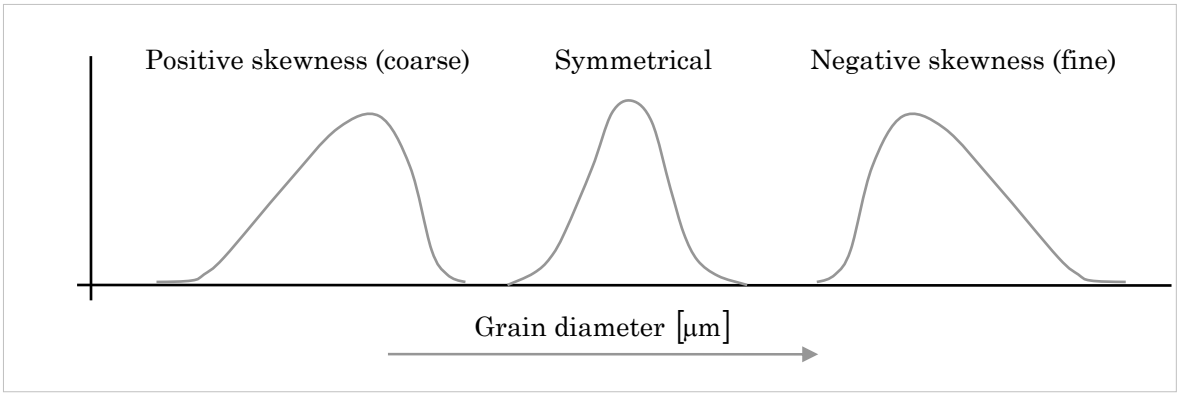

Figure 4-4 Difference between positive skewness and negative skewness

The kurtosis defines the peakedness of the grain size distribution. Kurtosis is a measure of whether the data are peaked or flat relative to a normal distribution. Data sets with high kurtosis tend to have a distinct peak near the mean. They decline rather rapidly and will have heavy tails. A grain size distribution with low kurtosis tend to have a flat top near the mean rather than a sharp peak. A uniform distribution would be the extreme case. [66].

Variations in kurtosis can largely be related to the degree of polymodality of the sediments, The grade of peakedness of a grain size distribution reveals the relation of the sorting of the central part of the curve in relation with the coarse and fine tail. When both gravel and sand populations are present in the sediment in more or less subequal proportions, the kurtosis value is low (platycurtic, Figure 4-5). With the increase of the medium sized population, the kurtosis value rises and then falls to near normal as sand approach unimodality.

$$K_G = \frac{\ln D_5 - \ln D_{95}}{2.44 \cdot (\ln D_{25} - \ln D_{75})} \qquad \text{Eq.4-3}$$

With:

K_G = kurtosis

In order to say something about the kurtosis of the distribution, some boundary's are proposed in Table 4-4.

Table 4-4 Explanation of the kurtosis

Kurtosis K_G	
Very platykurtic	<0.67
Platykurtic	0.67 – 0.90
Mesokurtic	0.90 – 1.11
Leptokurtic	1.11 – 1.50
Very leptokurtic	1.50 – 3.00
Extremely leptokurtic	> 3.00

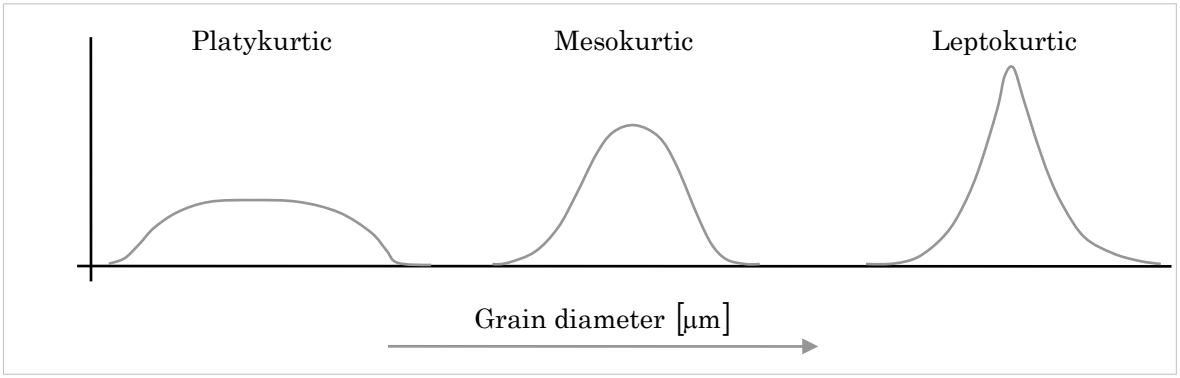

Figure 4-5 Difference between positive skewness and negative skewness

4.1.2 Hydraulic conductivity

The permeability depends on the soil type. In general, coarser material has larger pores and thus a larger permeability. Finer materials can fill up some of theses spaces. Therefore, different methods to define the permeability coefficient are available. The figures, presented in Appendix M, relate the permeability to the grain size. The permeability depends in reality on the properties of the soil and the liquid flow. One of the most comprehensive formula, quite useful in determining the beach permeability, is suggested by Kozeny-Carman (Carman 1937 en Kozeny 1927) (Appendix M). In practise other formula and curves are available, often related to a grain diameter like D_{10}. For an extensive overview some graphs are presented in Appendix N. One well known formula comes from Hazen (1892);

$$k = C \cdot D_{10}^{\,2} \qquad [m/s] \qquad \text{Eq.4-4}$$

With:

k = permeability coefficient of the soil [m/s]

C = 530-1300 (van Riel 1976) C = 410-1460 (Taylor 1948)

For coastal sands C= 1060 (Terzaghi 1925) is often used

D_{10} = 10% of the total volume is smaller than this grain diameter [m]

Experimental data confirms that for sand, like the sediments found at the beaches of Hvide Sande and Egmond aan Zee, a more practical approach seems to agree [82]. This is allowed for the condition of a porosity of 0.40 (40% relative density). This is usual for natural sand, which has porosities in the range of 0.25 to 0.50 [43].

The D_{10} value is a very important parameter in relation to the permeability coefficient. It is often assumed that also the grading D_{60}/D_{10} has major influence. Beyer (1964) did many experiments on the grading of sand. He came up with a new relation for the constant C;

$$k = \left(\frac{268}{D_{60}/D_{10}} + 55 \right) \cdot 10 \cdot D_{10}^{\,2} \qquad [m/s] \qquad \text{Eq.4-5}$$

D_{60}/D_{10} = grain diameters [m]

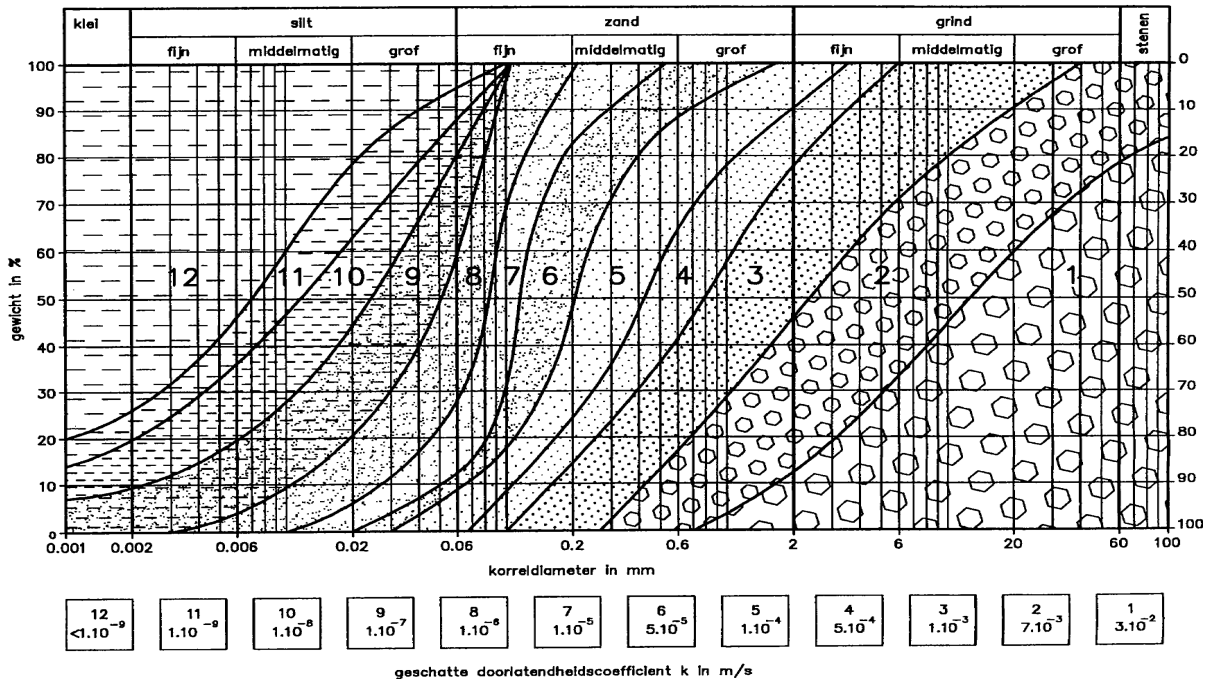

Figure 4-6 Permeability coefficient for given grain diameters and soil type by Beyer (1964)

An other commonly used formula to calculate the permeability coefficient is that of Krumbein and Monk (1943), where k is given by [51];

$$k = 760 \cdot D_{50}^{\,2} \cdot e^{-1.31 \cdot \sigma} \qquad [m/s] \qquad \text{Eq.4-6}$$

With:

σ = sediment sorting

D_{50} = median grain diameter [m]

4.1.3 Settling velocity

The settling characteristics of sediment determine whether or not sediments of a particular size experience erosion or deposition. Models capture this by accounting for the depositability of sediments by including their settling velocity (w_s) in the model. By the settling velocity, the terminal or fall velocity of a single sediment particle which settles through an extended, resting fluid is meant. The settling velocity is one of the key variables in the study of sediment transport, because mechanisms like suspension, deposition, mixing and exchange depend on it. For example, an error in the estimate of the falling velocity may be magnified by a factor of three or more in the computation of the suspended load transport [57]. Although it is not possible to predict the settling velocity very accurately, for engineering application there are some basic formulae available [108]. Beside the fluid kinematic viscosity and the drag coefficient (C_D), the grain diameter is very important.

Studies done by Schlichting (1979) show that RE<1 for a laminar Stokes flow and RE>10^5 for a turbulent flow. For both extremes the drag coefficient is approximately a constant value. If the downward force equals the upward force, the settling velocity is obtained;

$$w_s = \sqrt{\frac{4 \cdot (\rho_s - \rho) \cdot g \cdot D_{50}}{3 \cdot \rho \cdot C_D}} \qquad \text{Eq.4-7}$$

w_s = settling velocity [m/s] C_D = the drag coefficient D_{50} [m]

For natural sand particles one can not use the Stokes approximation nor the Newton range [108]. Some empirical formulae were developed which are used in practice. Cheng (1997) gives an expression for the fall velocity that utilizes the particle diameter. His formula belongs to one of the best [38]. The settling velocity can be calculated by;

$$w_s = \frac{\nu}{D_{50}} \left[\sqrt{\left(25.39842 \cdot \left(\frac{4}{3} \cdot \frac{\Delta \cdot g \cdot {D_{50}}^3}{\nu^2} \right)^{2/3} \right)} - 5.03968 \right]^{3/2} \qquad \text{Eq.4-8}$$

With:

ν = kinematic viscosity [m^2/s] $\approx 10^{-6}$

D_{50} = median grain diameter [m]

Δ = relative density ≈ 1.53 (salt water)

For natural sands of 63 μm to 1000 μm Gibbs (1971) provided an empirical formula for the settling velocity, solely depending on the median grain diameter;

$$w_s = \frac{-3 \cdot \nu + \sqrt{9 \cdot \nu^2 + g \cdot {D_{50}}^2 \cdot (s-1) \cdot (0.003869 + 0.02480 \cdot D_{50})}}{0.011607 + 0.07440 \cdot D_{50}} \qquad \text{Eq.4-9}$$

ν = kinematic viscosity [cm^2/s] D_{50} [cm]

Van Rijn (1993) gives a formula which represents the upper limit for natural sand because of their more angular shape (Figure 4-7). If many particles settle at the same time, then hindered settling may occur. More particles settle somewhat slower than single particles because the downward motion of one sediment particle will generate a compensating upward flow elsewhere.

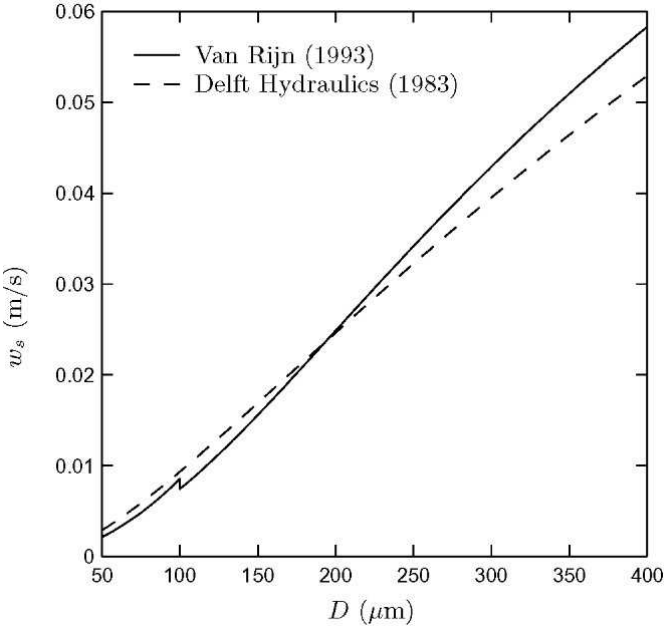

Figure 4-7 The settling velocity related to the grain diameter [85]

Natural sediments are not perfectly spherical. Another variable must be included since the fall velocity will be affected by the particle shape. The most stable orientation of irregular grains is to have their maximum projected area oriented perpendicular to the direction of fall. The fluid will be displaced around a larger surface in comparison with a sphere of the same nominal diameter [57].

The practical result is that for a natural grain (nonspherical) the settling velocity will be lower than that of a sphere with the same diameter. Dietrich (1982) developed an expression which includes the affect of shape and roundness on the settling velocity. He distinguishes mainly four different categories; spheres, well rounded particles, naturally rounded particles and crushed sediments. His analyses can be regarded as the most comprehensive to date in terms of data employed to derive the formula [57]. The three different drag coefficients are given in Appendix M.

4.1.4 Aspect ratio

The grain shape is a key factor affecting the mechanical properties of granular materials. Some interlocking features which armour the beach surface are related to the shape of the sand grains. Several grain shape parameters which describe the shape (shape factor) are available in literature. They differentiate the sand grains. Figure 4-8 shows some digital images of sand grains. Differences in shape, surface texture and roundness are clearly visible. This section describes the aspect ratio related to the ratio of the height and width of the grain.

The shear strength of granular materials like sand depends on the normal effective stress, the intergranular friction and the dilatancy [28]. The grain shape significantly defines the

structural arrangement of a granular mass. Quantification of the particle form requires the measurement of the length, breadth and thickness.

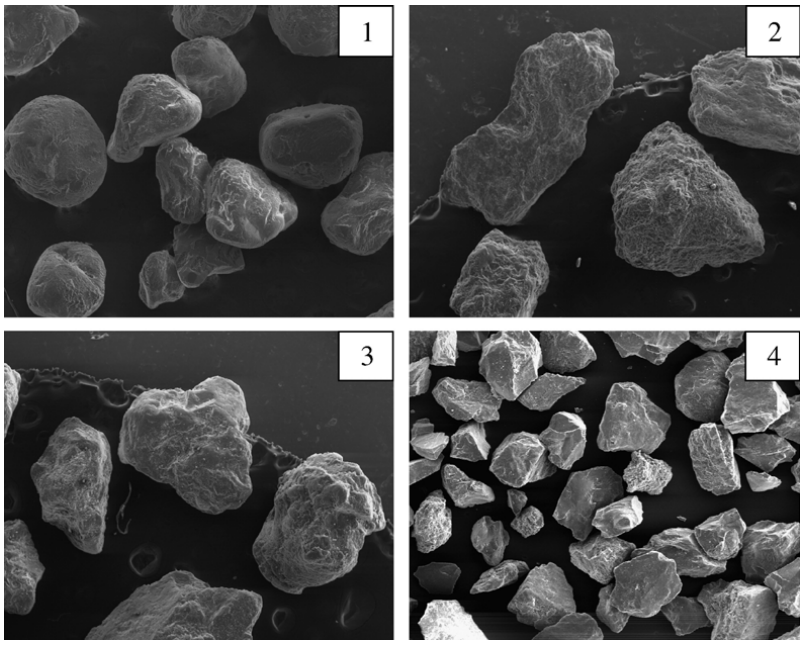

Figure 4-8 Digital images of sands with different shapes and surface textures [28]

During this study, sediment samples are analysed in order to calculate their form through their aspect ratios. The definitions from BCR (BCR-information 1980) are followed and a Sympatec QICPIC dynamic image analysis system is used. This device performs particle shape analyses of suspended particles captured on film. It allows the analysis of a large number of particles (up to 10^6), yielding statistically robust results [58]. The aspect ratio is defined as the shortest/longest diameter of a sand grain particle;

$$\text{aspect ratio} = \frac{F_{min}}{F_{max}} \qquad \text{Eq.4-10}$$

With:

F_{min} = minimum Feret's diameter

F_{max} = maximum Feret's diameter

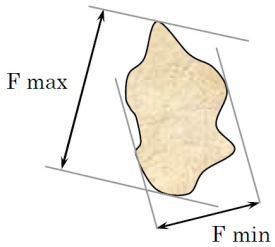

Table 4-5 Classification of the particle form, based on the aspect ratio [16]

Aspect ratio	Terminology
0.00 – 0.20	Extremely asymmetric
0.20 – 0.40	Very asymmetric
0.40 – 0.60	Moderately asymmetric
0.60 – 0.80	Slightly asymmetric
0.80 – 1.00	Symmetric

4.1.5 Sphericity

The sphericity is considered here to be a measure of the degree to which the shape of a particle approximates that of a true sphere. The parameter depends both on form and roundness, because a perfect sphere has equal length, width and thickness [16]. The degree of sphericity is quantified by comparing the surface area of a particle (by it's perimeter) to that of a perfect sphere (with the same perimeter). Here, the method of Cox (1927) is used, which defines the sphericity by the perimeter of a sphere divided by the perimeter of the real grain particle (which is measured by the QICPIC device from a dynamic image analysis). In Appendix N a table is presented which gives an overview of some commonly used circularity factors.

The sphericity is calculated as follows [58];

$$\text{sphericity} = \frac{2 \cdot \sqrt{\pi \cdot A}}{P_{real}} \qquad \text{Eq.4-11}$$

With:

A = area of the largest cross section

P_{real} = the perimeter of the grain particle

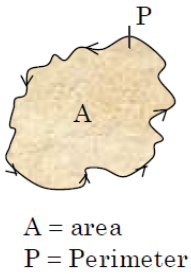

A = area
P = Perimeter

Table 4-6 Classification of the particle roundness, based on the sphericity [16]

Sphericity	Terminology
0.894 – 1.000	Very high sphericity
0.775 – 0.894	High sphericity
0.632 – 0.775	Moderate sphericity
0.447 – 0.632	Low sphericity
0.000 – 0.447	Very low sphericity

The classification scheme for the sphericity of a grain particle, defined in Table 4-6, gives five classes. The limits are defined so that ellipses are evenly distributed across the range of circularity values. The average value will provide an estimate which can be used as proxy for the particle sphericity.

4.2 The intertidal beach zone

The coastal zone is formed by many interacting processes. The element descriptions are difficult to label because various authors are defining this zone with different terminology and subdivisions. Therefore the coastal zone with the intertidal beach area is described before looking at the beach processes in detail. This ensures a clear description of the various elements. The coast forms the transition zone where land meets the sea. As a result of this land is influenced by marine and lacustrine hydrodynamic processes like waves, currents and wind.

Figure 4-9 shows the coastal zone with the terminology and subdivisions which are used throughout this report.

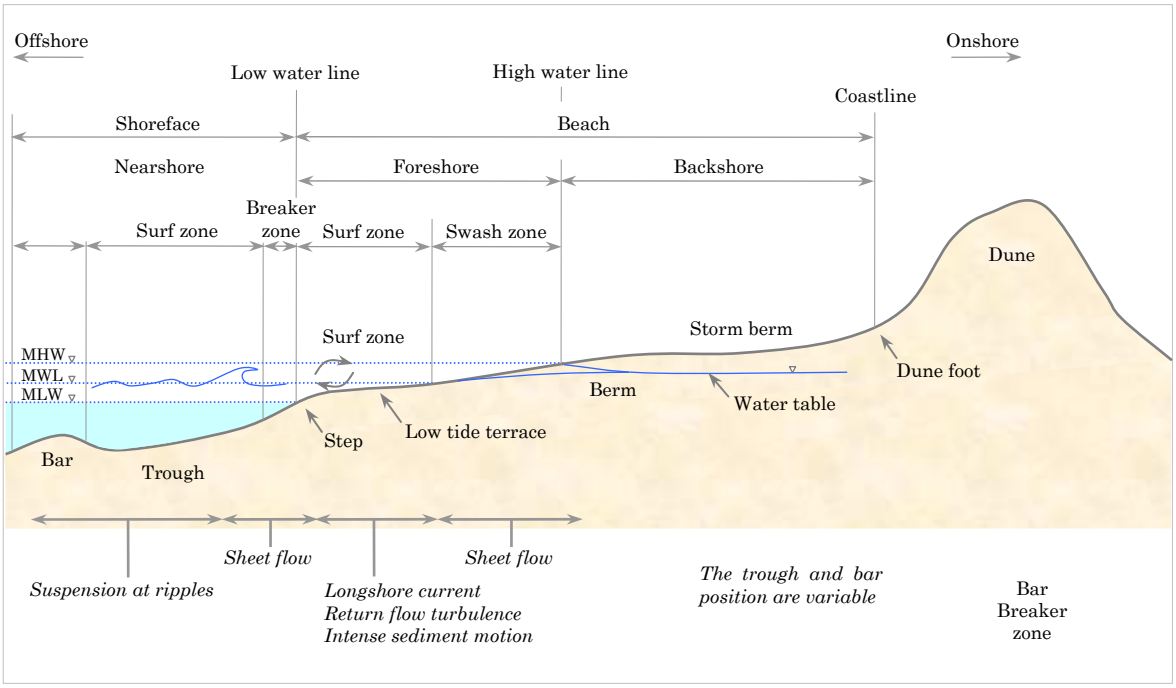

Figure 4-9 Drawing of the coastal zone with terminology and subdivisions

This paragraph deals with the intertidal beach area where the vertical drainage tubes are installed. The grain properties, as described in paragraph 4.1, determine the sedimentology of this part of the beach. They will influence the way the beach behaves and develops. Vice versa, the bathymetry determines the flow dynamics and can cause waves to plunge. Changing beach profiles also interact with sorting principles and bars. The barred beach of Egmond aan Zee has a specific profile. In order to treat the flow dynamics and sediment transport, the specific profile of this beach is looked at. Hydrodynamic properties were described in chapter 2.

4.2.1 Description of the beach area

This study focuses on the beach taken from the nearshore area to the dune foot. The reference and test areas investigated in this study (where vertical drainage tubes are installed and sediment samples were taken) focus on the intertidal beach area (Figure 4-9). The beach area is divided into two sections, the foreshore and backshore. The hypotheses, mentioned in paragraph [3.1], have their appliance mainly on these two regions. The foreshore extends from the low water line to the high tide level. The latter is limited to the wave uprush. The more energetic conditions make the foreshore steeper than the backshore [20]. The backshore is relatively horizontal which makes the distinction of these two areas. The berm or berm crest is situated at this transition. Berms are the flat areas created during times of accretionary wave conditions. During storm conditions a vertical step or scarp may form on the berm [71]. Berms or terraces are on the beach just above the uppermost swash level landward of the high water level shown in Figure 4-9. At the berm the fluidization of the surface as well as the capillary fringe are the main micro scale processes which may be affected by the vertical drainage tubes. Also groundwater flow is affected in this area [51].

The swash zone is defined as the region which starts from the surf zone, limited by the run-down, and measured to the high water line, which is based on the run-up of the waves. The swash zone shifts with the tides and natural conditions. Mainly this area will become dry in time when the water table drops. Many processes like infiltration and exfiltration, the capillary fringe and fluidization of the surface are acting in this region [49]. Their theoretical backgrounds will be described in more detail in paragraph 4.4.

Further offshore exists a moment where waves start to break at some distance offshore the beach area. This zone is called the bar breaker zone. At this moment the bore turbulence of the incoming waves begins to significantly affect the sea bed, sediment concentration and velocity profiles. These processes will determine the sediment transport fluxes [49]. The region between this initial point and the still water level, the lowest point of backwash, is called the surf zone. Here the height of the waves is controlled by the water depth as the wave 'feels' the bottom. The position of the surf zone shifts constantly back and forth because of the influence of tides and natural conditions. Under calm conditions the surf zone may be reduced to a narrow swash zone. Under storm conditions it may extend offshore to depths of 8 to 10 metres, where waves first begin to break [85]. Turbulence and aeration are produced which cause significant momentum. This results in a longshore as well as cross-shore directed current which induces sediment transport.

The breaker depth stands for the moment waves start to break. Orbital motions are affected by a decreasing water depth in upland direction. Therefore the wave height and wave steepness increase towards the breaker line. This area is called the bar breaker zone. The ratio significant wave height and breaker depth is often called the breaker index. (Boussinesq 1872);

$$\gamma = \frac{H_b}{h_b}$$ varies between 0.3 and 1.59 [Kaminsky and Kraus 1993] Eq.4-12

$$\frac{H_{max}}{h} = 0{,}78$$ (Boussinesq 1872) Eq.4-13

To describe the beach slope the Iribarren formula can be used which includes the beach slope and the incoming wave height and length.

The slope causes waves to surge, plunge, collapse or spill. The surf similarity parameter after Iribarren (1949) is described by;

$$\xi = \frac{\tan\alpha}{\sqrt{\frac{H}{\lambda_0}}}$$ Eq.4-14

With:

ξ = surf similarity parameter	[-]
H = wave height	[m]
λ_0 = deep water wave length	[m]
α = beach slope	[-]

Galvin (1968) found a relationship between the wave geometry and the breaker type. The following domains were found from Galvin's experimental data;

Spilling breakers: $\xi_H < 0.50$

Plunging breakers: $0.50 < \xi_H < 3.30$

Surging breakers: $3.30 < \xi_H$

As a consequence of piling up mass flux, which is carried by short waves, there exists a set-up added to the mean water level [85]. The water level difference between the breaker water level and the maximum water level rise (wave set-up) equals;

$$\Delta h = \frac{3}{8} \cdot \gamma \cdot H_b \qquad \text{Eq.4-15}$$

With:

Δh = maximum wave set-up [m]

γ = wave breaking index

H_b = wave height at point of breaking [m]

Just outside the breaker zone (before breaking) the total wave set-down equals;

$$h'_b = -\frac{1}{16} \cdot \gamma \cdot H_b \qquad \text{Eq.4-16}$$

With:

h'_b = water level change [m]

H_b = wave height at point of breaking [m]

h_b' = still water depth at breaking point [m]

During accretional stages small-scale features like berms, swash bars, intertidal bars and ridges are formed. These bars are common subtidal features along sandy uninterrupted coasts. The bars drawn in Figure 4-9 are nearshore. They are generally located at depths up to eight metre and oriented shore parallel. The conceptual model of bars and rip channels in between is in line with the situation at Egmond aan Zee and Hvide Sande. The position of the bars depends on the hydrodynamic conditions. Bar migration is a well registered phenomena at Egmond aan Zee [90].

In order to get the right information about the sedimentology at the beach of Egmond aan Zee and Hvide Sande, some precautions have to be taken. As these swash bars are moving all the time, their sand is repeatedly refreshed. Therefore the sediment samples are taken next to the bars. Additional samples on the swash bars are taken to compare their grain properties. The samples are taken at the outmost point in sea to deal with the set-up.

4.2.2 Beach profiles versus sand size

The transport of sand is the main steering mechanism which determines the state and morphology of the beach [29]. The combination of hydrological aspects, like wind waves and currents, the nearshore and offshore sedimentology and the orientation of the coast make the beach system behave in a certain way [85]. The beach has a dynamic equilibrium state. This beach condition is mainly controlled by the waves, water level and sediment grain sizes [71]. The shape of the beach profile has been studied extensively by Bruun and Dean [29], Bruun (1954). In their reports some basic formulations are mentioned which are based on research of many sandy coasts (and their profiles). Beside the water level and hydrological conditions, the grain size forms an important parameter in this theory. As a result of this, fine-grained beaches have gentle slopes while coarser-grained beaches are steeper. [29]

The shape of the beach profile determines the vulnerability of the coast to storms. Also the habitat and recreation area are affected. The equilibrium profile can be defined as a cross-shore profile of constant shape which is reached if it is exposed to constant wave and water level conditions. Hydraulic conditions will definitely not be constant in time. Therefore an absolute equilibrium shape will not exist, but one can speak of a dynamic equilibrium profile. Bruun (1954) developed a predictive equation for an equilibrium beach profile by studying beaches. He proposed a simple law to relate the water depth 'h' to the offshore distance y;

$$h = A \cdot y^{m} \qquad \text{Eq.4-17}$$

With:

h = water depth	[m]
A = shape parameter	[-]
y = offshore distance	[m]
m = exponent equal to $2/3$	[-]

Especially the shape parameter is important and often subject to hydrodynamic properties and sedimentology. Several methods are available in determining the shape parameter. A larger value gives a steeper nearshore bed slope. Waves may break more often. The intertidal beach area may become shorter normal to the coast. This results in a drier beach.

4.2.2.1 The beach shape

Kriebel (1991) [62] found that for sediment sizes with a fall velocity of 1 to 10 cm per second, the shape parameter could be related to the fall velocity by;

$$A = 2.25 \cdot \left(\frac{w^2}{g} \right)^{1/3} \qquad \text{Eq.4-18}$$

or by Moore (1982);

$$A = 0.508 \cdot w^{0.440} \qquad \text{Eq.4-19}$$

w = fall velocity [cm/s]

Moore (1982) [71] studied the functional dependence of the shape parameter and found it to be an increasing function of the median grain size D_{50} for a wide range of materials. Both methods (D_{50} and w_s) are presented by a graph in Appendix N. The presented figure shows that the shape parameters based on the median grain diameter differ from the values which are calculated by the settling velocity. Therefore, two methods are used.

Moore (1982) described relations which apply to varying grain sizes;

$$A = 0.410 \cdot (D_{50})^{0.94} \qquad D_{50} < 400\mu m \qquad \text{Eq.4-20}$$

$$A = 0.230 \cdot (D_{50})^{0.32} \qquad 400\mu m \le D_{50} \le 1\ mm \qquad \text{Eq.4-21}$$

$$A = 0.230 \cdot (D_{50})^{0.28} \qquad 1\ mm \le D_{50} \le 4\ mm \qquad \text{Eq.4-22}$$

$$A = 0.460 \cdot (D_{50})^{0.11} \qquad 4\ mm \le D_{50} \qquad \text{Eq.4-23}$$

Dean (1977) argued that the shape parameter should depend on a uniform dissipation per unit volume of water across the surf zone and the breaker index γ [98]. The wave-energy-flux dissipation per unit water volume across shore D(x) can be calculated from measurements of wave height and water depth at adjacent, closely spaced waves. This formula is not used in this study because the available data is not sufficient to give valuable results.

Vellinga (1986) relates the effect of the grain size on the shape of an erosion profile;

$$A = 0.39 \cdot w^{0.440} \qquad \text{Eq.4-24}$$

Or;

$$A = 0.700 \cdot \left(\frac{H_0}{\lambda_0}\right)^{0.17} \cdot w^{0.44} \qquad \text{Eq.4-25}$$

With:

H_0 = deep water wave height

λ_0 = deep water wave height

w = fall velocity

The formation of beach profiles results from the interacting process of at least three individual constructive forces. These are the net onshore shear stress at the bottom, the streaming velocity force at the bottom and the intermittent suspensions and selective transport of the particles by wave induced velocities. The third force results from the turbulence generated during the breaking of a wave. Sediment will be suspended and advected by the prevalent velocities until deposition [29]. If the fall time of a particle is less than one-half of a wave period, a net onshore sediment transport will result. If the fall time gets longer, but still less than one wave period, a net offshore sediment transport may occur [71].

Whether a beach will erode or accrete and bars move onshore or offshore can be estimated with a dimensionless parameter called the Dean number;

$$N = \frac{H}{w \cdot T} \qquad \text{Eq.4-26}$$

N = Dean number H = wave height w = fall velocity T = wave period

For N>3.20, erosion is probable [29], whereas for N<3.20 accretion is probable. Large values of N occur during storms (with large wave heights). The Dean number is often called the dimensionless sediment fall velocity parameter. It's a rather crude estimator of beach morphodynamic state. Parameters based on the slope development are better indicators [84].

4.2.2.2 The beach slope

The beach slope is reflected in the study done by Wiegel (1965). He made the following graph (Figure 4-10).

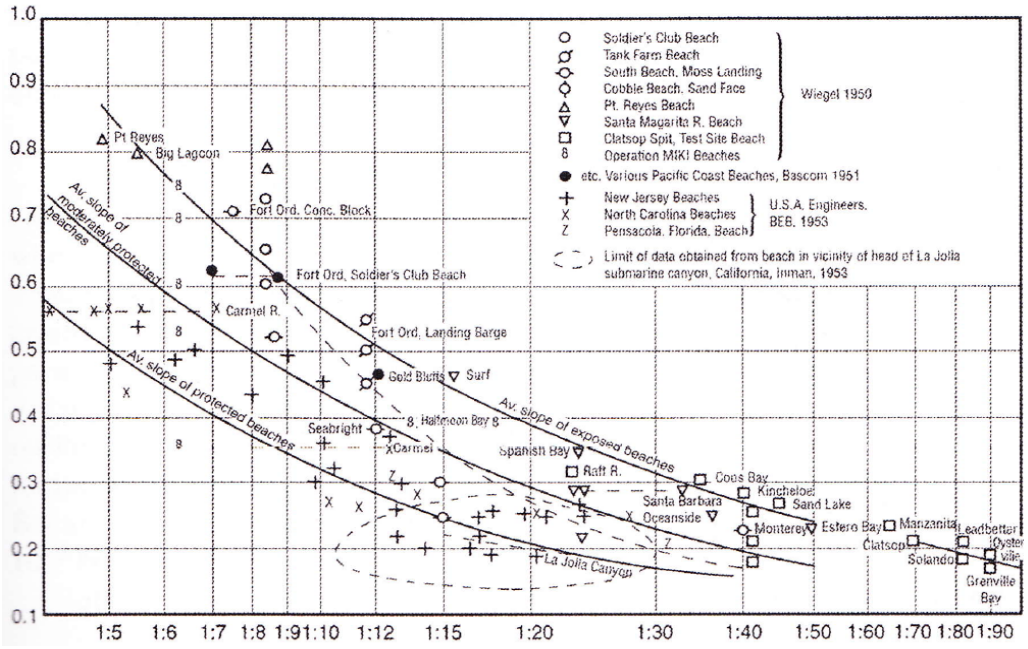

Figure 4-10 Grain size versus beach slope [105]

Many studies relate the proportionality between the beach face and the sediment size to swash infiltration and hydraulic conductivity (section 4.4.3). More infiltration during swash will lead to less water that will flow during backwash. This becomes very important for coarse sand beaches where swash infiltration is very important. The beach slope tends to increase with permeability [84]. The Manning's coefficient is used to calculate the beach profile. This number is related to the grain sizes.

$$n = 0.015 + 0.200 \cdot (D_{50} - 0.0003) \qquad \text{Eq.4-27}$$

D_{50} = median grain diameter [m]

n = Manning's coefficient

For dissipative beaches, like the Egmond aan Zee beach with spilling waves $(\xi = 0.19)$, the following relationship between the wave height and wave set-up holds;

$$h = 0.35 \cdot \xi \cdot H_0 \qquad \text{Eq.4-28}$$

With:

h = wave set-up [m]

H_0 = characteristic offshore wave height [m]

ξ = surf similarity parameter [-]

Reis (2010) suggests a relation between the grain size and the beach face slope;

$$\beta = \left(\frac{a}{2}\right)^{2/3} \cdot B^{-4/3} \cdot D_{50}^{4/3} \qquad \text{Eq.4-29}$$

With:

$$a = \frac{\xi \cdot H_0 \cdot S^2 \cdot \phi^3 \cdot g}{150 \cdot \nu \cdot \left(1 - \phi^2\right)}$$

H_0 = offshore wave height

S = average sand grain Sphericity

ϕ = porosity

ν = kinematic viscosity = 10^{-6} m^2/s (for water)

$$B = \frac{h_{flow}^{5/2}}{n}$$

h_{flow} = height of return flow

$n = 0.015 + 0.200 \cdot \left(D_{50} - 0.0003\right)$ (variation of Manning's coefficient)

D_{50} = median grain diameter [m]

4.2.3 Bedforms and ripples

The beach profiles were discussed in section 4.2.2 on a meso scale. The large sedimentary structures like bars and beach slopes modify the main flow pattern. They make the incoming waves refract, diffract or break. Small scale structures (such as ripples on micro scale) on the other hand have no immediate impact on the main flow patterns, but strongly influence the boundary layer structure and turbulence intensity near the bed [73]. Together with grain properties they determine the flow velocities near the bed. Hence, they have a great influence on the sediment transport mechanisms.

The interaction with velocities like the orbital motion will not be considered here. Depending on the hydraulic conditions, different types of bed shapes will develop. One can think of ridges, ripples, dunes and bars. If such bed forms predominate, the bed roughness needs to be related to this bed. This effect on the dynamics and geometry of the bed must be seen together with the equivalent Nikuradse roughness depending on the grain size (Table 4-7).

Figure 4-11 Asymmetrical ripples at the beach of Hvide Sande [33]

4.3 Interaction with the beach surface

The first field research at the beach of Egmond aan Zee, done during August 6th 2009, formed the trigger and basis to investigate the influence of the drainage tubes on the sediment properties. Changing grain properties will influence the morphodynamics in the tidal beach area in many ways. Lots of literature is available which describes the flow dynamics at this zone. It would be too comprehensive and unwise to describe all hydrodynamic processes which affect the state and development of the beach. Therefore, only the interaction with the beach surface is described in this paragraph. The focus is on the swash motion and dynamics.

The development of the swash zone is to a large extent dominated by the uprush and downrush flows (Figure 4-12). Part of the transporting efficiencies can be explained in terms of differences in bed shear stress for a given velocity profile [74]. The uprush has a rapidly accelerating character while the downrush is more gradually accelerated. The accelerating flow generates a stronger bed shear stress [74]. To clarify the important role of sedimentology in accordance with the transport mechanisms of sediment, a scheme (Figure 4-1) was given, which visualises involved elements. There are mainly three basic input fields which are shown in the scheme. Starting with the grain properties, the characteristics of the beach surface will determine the bed load transport and suspended transport of sediment.

Figure 4-12 Uprush and backwash flows at the drainage tube area (tube just installed)

There are some other mechanisms which influence the swash [74];

- In unsteady flows exists a lag between the instantaneous bed shear stress and sediment transport rates.
- Infiltration and exfiltration (section 4.4.3) affect the beach profile (section 4.2.2.2) and the boundary layer. Infiltration occurs usually during uprush, while exfiltration causes destabilisation of the bed during backwash [24].
- Fluidisation (section 4.4.3) plays a role in the swash zone sediment transport process. It may be caused by horizontal pressure-head gradients near the uprush front. Also upward pressure gradients (once measured by Baldock (2001)) can cause fluidisation of the bed.

4.3.1 Bed roughness

The sediment transport rate, which forms the basis of morphological changes, depends closely on estimates of the resistance to oscillatory flows. A roughness height is used to characterize this resistance. The resistance properties of the bottom are mainly determined by the roughness [26]. The roughness height is a fundamental parameter for calculating the transport. It forms an important input for the bottom shear stress. This section focuses on the determination of the bed roughness, mainly ruled by the grain properties. Different situations are mentionable, like steady flows, oscillations and ripples.

For flat beds the roughness is expected to be around the order of median grain diameter or of some larger grain size percentiles [26]. In general, the height of the flat and fixed bed is given in terms of the Nikuradse roughness k_s. This value varies considerably depending on the grains and flow boundaries. High Shields parameter values mean that the sediment moves along the bottom. The roughness increases with the presence of a sheet-flow layer [26]. This

can be several orders of magnitude larger than for a fixed bed. Like Wilson (1987) and van Rijn (1993), it is often assumed that the sheet-flow roughness height is in the order of the layer thickness.

At high rates of sediment transport, there exists a momentum transfer between the flow and the bed. Sediment particles, receiving momentum from the flow, transfer this energy when they are picked up (accelerated) and eventually deposited. The total bed roughness contains a contribution from the moving sediment (r_s), as well as the usual r-value (r_f). The index 's' stands for suspended (moving) and 'f' for fixed.

In order to quantify the bed roughness, three different situations are described;

- Roughness under steady flows
- Roughness under oscillatory flows
- Roughness under waves with ripples

Many scientists tried to formulate the roughness in terms of the grain diameter. Table 4-7 gives an overview of these relations. A larger grain diameter results in a higher bed roughness.

Table 4-7 Various relations to calculate the bottom roughness

Research	Bottom roughness (k_s or r)
Einstein (1950)	D_{65}
Engelund and Hansen (1967)	$2 \cdot D_{65}$
Mahmood (1971)	$5.10 \cdot D_{84}$
Ackers and White (1973)	$1.25 \cdot D_{35}$
Kamphuis (1975)	$2 \cdot D_{90}$
Charlton et al (1978)	$3 \cdot D_{84}$
Hey (1979)	$3.50 \cdot D_{84}$
Nielsen (1979)	$2.50 \cdot D_{50}$
van Rijn (1982)	$3 \cdot D_{90}$

Table 4-8 Relationships to predict the equivalent roughness in oscillatory flows

Research	Effective roughness ratio
Grant and Madsen (1982)	$\frac{k_s}{D_{50}} = 160 \cdot (s + 0.50) \cdot \theta_{cr} \cdot \left(\sqrt{\frac{\theta}{\theta_{cr}}} - 0.70 \right)^2$
Wilson (1989)	$\frac{k_s}{D_{50}} = 5 \cdot \theta$
Nielsen (1992)	$\frac{k_s}{D_{50}} = 70 \cdot \sqrt{\theta}$ Shields; $\theta = \frac{u_*^2}{(s-1) \cdot g \cdot D_{50}}$
Madsen (1993)	$\frac{k_s}{D_{50}} = 15$
Xu and Wright (1993)	$\frac{k_s}{D_{50}} = 15 \cdot \theta$

4.3.2 Friction factor

The bed roughness forms the basis of the friction factor. Although large uncertainties can be observed, the equivalent bed roughness influences the total sediment transport significantly [25]. The roughness height is included in sediment formulae via the friction factors. These coefficients are increasing with the grain size. But, the total roughness does not only depend on the grain properties. The hydrodynamic conditions are also very important. More detailed backgrounds about the influence of changing grain sizes onto the friction factor are included in Appendix M.

Jonsson (1966) showed that the wave friction factor depends on the Reynolds number $A^2 \cdot \omega/\nu$ and the relative bed roughness r/A. For $r/A \approx 0$ the smooth bed conditions apply. The friction term in that case becomes;

$$f_w = \frac{2}{\sqrt{A^2 \cdot \omega/\nu}} \qquad \text{Eq.4-30}$$

Or;

$$f_w = 0.024 \cdot \left(A^2 \cdot \omega/\nu \right)^{-0.123} \qquad \text{Justesen (1988)} \qquad \text{Eq.4-31}$$

One widely used relation, which assumes a fully developed rough turbulent regime, is suggested by Swart (1974) after Jonsson (1966);

$$f_w = \exp\left[5.213 \cdot \left(\frac{r}{A} \right)^{0.194} - 5.977 \right] \qquad \text{for waves} \qquad \text{Eq.4-32}$$

$$f_c = 0.24 \cdot \left[\log\left(\frac{12 \cdot h}{k_s} \right) \right]^{-2} \qquad \text{for currents} \qquad \text{Eq.4-33}$$

The swash zone, within the intertidal beach area, is dominated by the uprush and backwash motion. Sediment processes occurring in this region determine the erosion or accretion of the beach. As the bore continues landward (from the surf zone), it reaches a point near the swash zone whereupon the bore collapses on the beach face. During this uprush phase, the bore turbulence is no longer being generated [81]. After its maximum rise on the beach face (see section 4.2.1), the uprush edge reverses direction and becomes backwash. This flow acts under gravity (ballistic motion equation, not treated here). There exists energy dissipation by [81];

- Bed friction
- Vertical flow into the bed (infiltration and exfiltration, section 4.4.3)
- Pressure gradients coupled with the presence of fluid mass offshore of the leading edge
- Friction effects by entrained sediment

Infiltration during the uprush is not significant. During the backwash, it has a substantial effect on the flow. Flow into a porous bed increases the bed shear stress, while flow out of a porous bed decreases this stress [81]. This has to do with the suction during infiltration and blowing during exfiltration. A drier beach, which could be initiated by the vertical drainage tubes, may influence this process.

4.3.3 Aeolian sediment transport

From the beach further onshore towards the coastline is the backshore zone (Figure 4-9). Within this area the aeolian transport (wind-blown transport) is the basic transport mechanism of sediment. Although this area is not directly affected by water motions, the vertical drainage tubes (placed unto the dune foot) may affect the aeolian transport by lowering the water table. This mechanism is clarified by hypotheses described in chapter 3. The less moist sand at the upper part of the beach is most readily transported by wind. Aeolian sediment transport is enhanced by a low moisture content within the beach that makes the sand more transportable [29]. Aeolian transport will also selectively remove the finer fraction of the material, leaving a so-called lag layer. This surface layer contains coarser particles. To predict changes in the rate of aeolian transport, the role of fetch has to be understood. A change in grain size or sorting of sand may occur when the rate of aeolian sediment transport changes [102].

Figure 4-13 Aeolian transport along the coast at the intertidal beach area

Bagnold (1936,1943) proposes a relationship for the aeolian sediment transport rate in which the sediment flux per unit width is taken as mass unit width per unit time;

$$q = C \cdot \sqrt{\frac{D_{50}}{D_{ref}}} \cdot \rho_a \cdot u_*^3 \qquad \text{Eq.4-34}$$

With:

C = a constant ranging from 1.50 to 3.50

D_{50} = the median grain diameter of the sediment at the surface

D_{ref} = the reference sediment diameter, often taken as 0.25 mm

u_* = critical shear velocity or threshold shear velocity to cause sediment movement

Although the fine sediment fraction is more easily removed from the surface sand, the sediment transport is larger for the coarser sediments. Coarser grains form a less cohesive layer of sand. Therefore, the critical shear velocity forms an important parameter. The sediment size also enters the relationship through this velocity and smaller sediment sizes would be easily transported [5]. The soil resistance mechanism is one inter-related process which contributes to the existence of the fetch effect. This implies that the threshold entrainment velocity of sediments at the beach surface could change depending on the nature of the sedimentology.

Whether the maximum rate of transport is ever achieved depends on the character of the sand surface; the grain size, beach slope, roughness, vegetation and moisture content. The moisture content is widely acknowledged as an important factor in controlling release of sediment from the beach surface. If all other parameters are equal, the rate of sediment transport over a wet surface is less than over a dry surface [10]. The groundwater level (possibly affected by the drainage tubes, the grain size and permeability) and water level excursions (friction, bed slope) influence the moisture of the beach surface. Section 4.4.1 describes the capillary fringe in the beach surface. This additional height of water above the groundwater level depends strongly on the sediment characteristics. The moisture level of the surface may decrease when the sedimentology changes. The average shape of sediment fractions also changes by aeolian transport.

Roundness

Research done by Folk (1978), Goodie and Watson (1981) and Khalaf and Gharib (1985) conclude that the roundness of dune sediment increases as the grain size increases. The nature of aeolian transport and grain mobilization may account for this [97]. Coarser grains move as a creep load and finer grains are saltated. Grains moved by creep are probably subjected to less grain-upon-grain impacts. This creates fewer opportunities for edge abrasion. Figure 4-14 [97] shows the relation between the roundness and grain size for accumulated sediments. Large sediments (>1mm) are not easily picked up and stay more angular. The beach surface sands become more angular when less aeolian transported sand accumulates on the beach. This may suggest that locally wind erosion reduces the roundness.

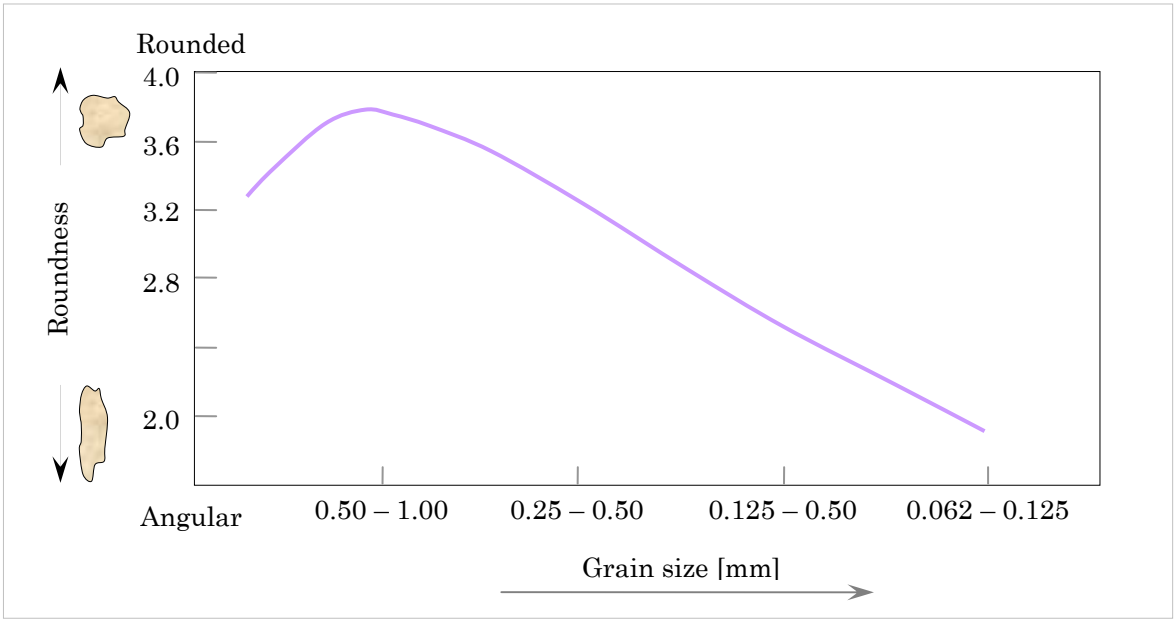

Figure 4-14 Relation between the mean roundness and the grain size for accumulated sediments

Sphericity

Studies done by Richardson (1903) and Khalaf and Gharib (1985) suggest that aeolian shape sorting occurs because round and more spherical grains are more readily transported by the wind. Sphericity, the measure of how close a particle becomes to being uniaxial, has an effect on selective aeolian transportation [97]. The mean sphericity values increase with the grain size. This is visualised by Figure 4-15 [97]. Spheroid grains are more readily mobilized by the wind, especially as the grain size increases. Accumulated coarse grains are more regular shaped. This means that irregular shaped particles stay on the surface when the beach encounters large aeolian sediment transport rates and less aeolian transported sand accumulates on the beach.

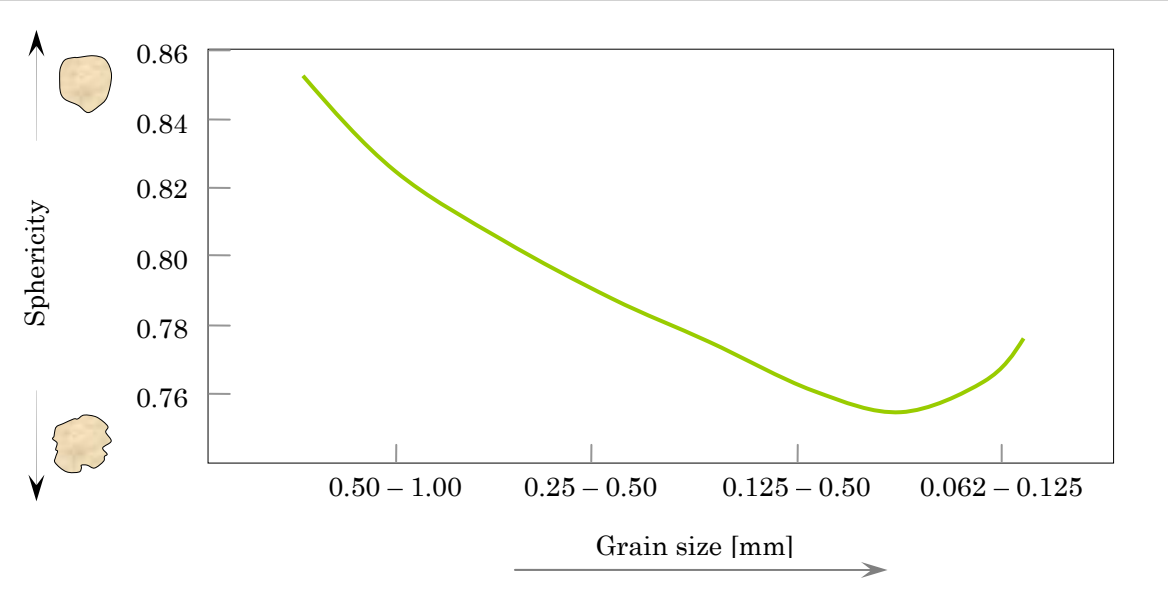

Figure 4-15 Relation between the mean sphericity and the grain size for accumulated sediments

4.4 Some influenced beach processes

Predictions of swash zone sediment transport and beach profile evolution cannot be made unless the complex fluid and sediment interactions between the surface flow and the beach groundwater are better understood. Several beach processes are acting at the intertidal beach area. Many of them are strongly influenced by the sedimentology of the beach surface. One example is the capillary fringe which depends on the hydraulic conductivity and influences the beach groundwater dynamics. The capillary fringe (section 4.4.2) can have a significant effect on the water exchange particularly in terms of storage capacity at the aquifer.

The effects of infiltration and exfiltration (section 4.4.3) are generally invoked to explain why beaches with a low water table tend to accrete. Again modelling and experimental work indicate that the hydraulic conductivity of the beach, which depends strongly on the sedimentology, remains a critical parameter.

The natural variability of the sediment is mainly steered by sorting mechanisms. The sediment sorting principles acting along the beach profile depend on the energy level of the wind and wave forces at work. Some beach processes can explain the coarsening of different parts at the beach profile. The cross-shore transport mechanisms also have a large influence on the beach state. Section 4.4.5 describes these processes.

4.4.1 Groundwater flow in the beach

Beaches with a low water table tend to accrete. Beaches with a high water table tend to erode. [49], [51]

The beach groundwater dynamics control the swash zone sediment transport. This affects the morphology of the intertidal beach. Many researches have found that the cyclic erosion and accretion of the beach face result from interaction with the groundwater table. [51] Many beach processes are affected by the groundwater. Some of these are infiltration, exfiltration, fluidization and the capillary fringe. Also interstitial fauna and the macro fauna of sandy beaches are directly affected by swash and groundwater processes [51]. The groundwater table is affected by the geology of the beach and the hydrodynamic conditions. The inundation from the dunes plays an important role. This study focuses on the interaction with the swash motion. Section 4.1 described the grain properties which will influence the interaction with the groundwater.

The beach groundwater system is an unconfined aquifer (Figure 4-16). The variation in the sea level will create flow in the beach. The vertical movement of the groundwater level is subject to a phase shift in time with an amplitude. This amplitude is smaller than the amplitude of the sea level. The delay depends on the adaptation time. Wind waves (short wave periods) give an oscillation only some metres from the waterline. Tidal flow (with much longer wave periods) causes further wave penetration in the beach. The phreatic zone is the permanently saturated zone beneath the water table. The unsaturated zone extends from the water table to the sand surface. [49]. Above that level, a capillary fringe exists which depends on the grain properties (section 4.4.2). This fringe can develop immediately above the water table as a result of the force of mutual attraction between water molecules and the molecular attraction between water and the surrounding sand [49].

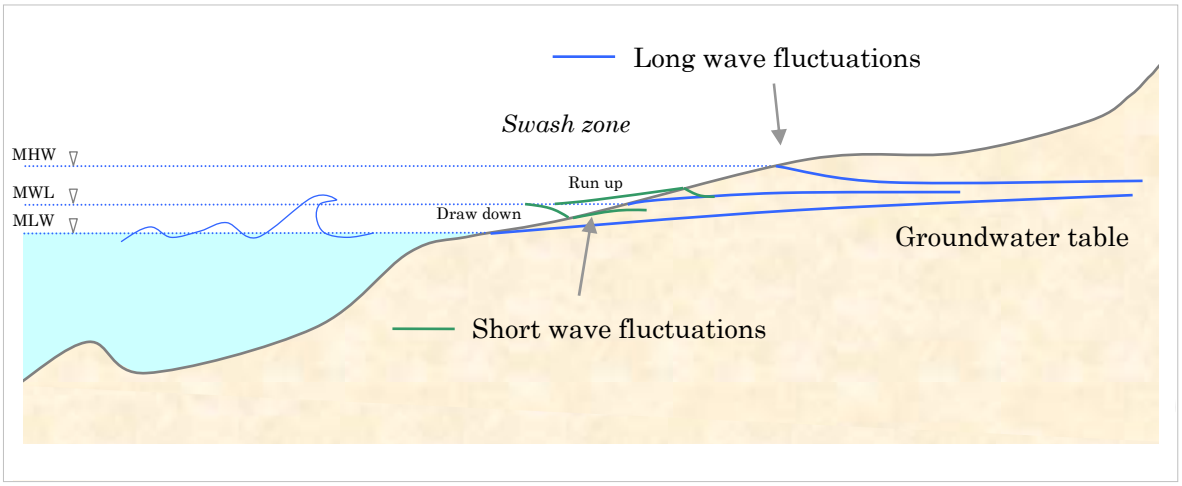

Figure 4-16 The conceptual groundwater system at the beach

The most important parameters in the groundwater system are water pressures, hydraulic conductivity, moisture content and water table elevation. The slope of the water table is seawards for a falling tide and landwards for a rising tide. On a rising tide the slope gets steeper [49]. The beach fills more easily than it can drain under gravity. The propagation of the 'groundwater waves' depends strongly on the aquifer parameters (grain properties) and capillarity [51].

The difference between the high water level and low water level causes a flow in the beach during falling tide (Figure 4-17). The flow at the landward located drainage tubes is directed

downwards, while the flow at the tubes more seaward is upward. Within the tubes there is nearly no flow resistance [41]. In the soil, an excess pressure gradient is needed, which depends on the beach permeability. The permeability coefficient 'k' follows from the grain properties (see section 4.1.2). If the vertical drainage tubes lower the groundwater a bit, the beach could become slightly drier in time. Here, a drainage effect by flow through the tube is discussed.

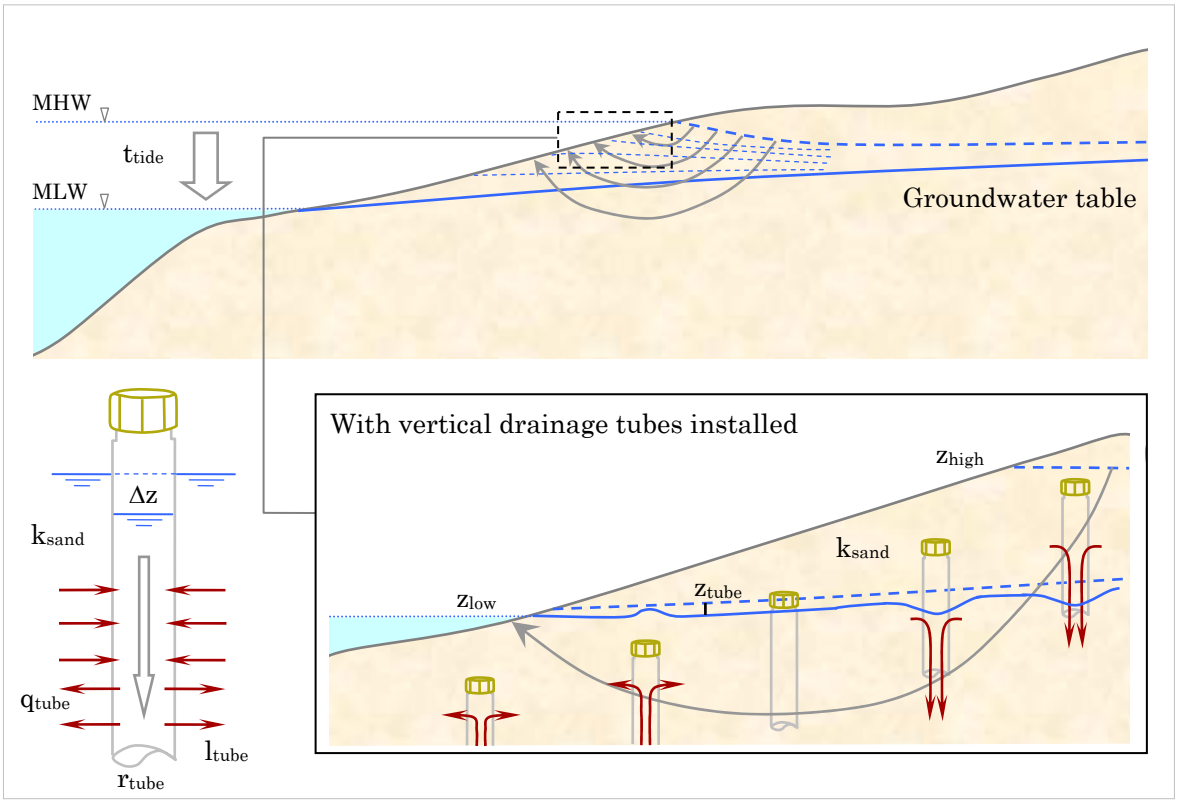

Figure 4-17 The groundwater flow pattern introduced by a falling tide

The lowering velocity for the high water level to become the low water level equals;

$$V_{tide} = \frac{z_{high} - z_{low}}{t_{tide}} \qquad \text{Eq.4-35}$$

With:

V_{tide}	= lowering velocity of the water table in the beach	[m/s]
z_{high}	= water level at high tide	[m]
z_{low}	= water level at low tide	[m]
t_{tide}	= duration drop high to low tide	[s]

The hydraulic gradient, which causes this flow, equals;

$$i = \frac{V_{tide}}{k} \qquad \text{Eq.4-36}$$

With:

i = hydraulic gradient causing the water table drop in the beach outside the tubes [-]

V_{tide} = lowering velocity of the water table in the beach [m/s]

k = permeability coefficient of the soil [m/s]

The loss in energy head becomes;

$$\Delta z = l_{tube} \cdot i \quad [m] \qquad \text{Eq.4-37}$$

With:

l_{tube} = length of the tube filter [m]

i = hydraulic gradient causing the water table drop in the beach outside the tubes [-]

In cross-shore direction the tubes are placed every 10 metre. The drained area A_{tot} around the tube is approximately a circle with a radius of 5 metre. The area occupied by the tube equals;

$$A_{tube} = \pi \cdot r^2 \qquad \text{Eq.4-38}$$

With:

A_{tube} = area of the tube [m^2]

r = radius of the tube [m]

The loss in energy head causes a flow through the tube. The flow velocity in the tube depends on the radius of the drainage tube and the outflow capacity. The velocity can be calculated with [41];

$$V_{tube} = \frac{q_{tube} \cdot \alpha}{A_{tube}} \qquad \text{Eq.4-39}$$

With:

V_{tube} = Velocity through tube [m/s]

q_{tube} = flow rate through tube, see Figure 4-18 [l/min]

A_{tube} = area of the tube [m^2]

$\alpha = 6 * 10^{-4}$ (from l/min to m^3/s) [-]

The empirical relation, presented by Figure 4-18, is limited to sand with an grain size of 0.4 mm. Therefore, new experiments must be done in order to get new relations between the head difference and flow rate. In case of smaller sediment, the flow through the tube would be smaller. For coarser sediments, the flow would increase. The drainage tubes themselves could be improved by engineering the system. One could think of larger filters or bigger tubes.

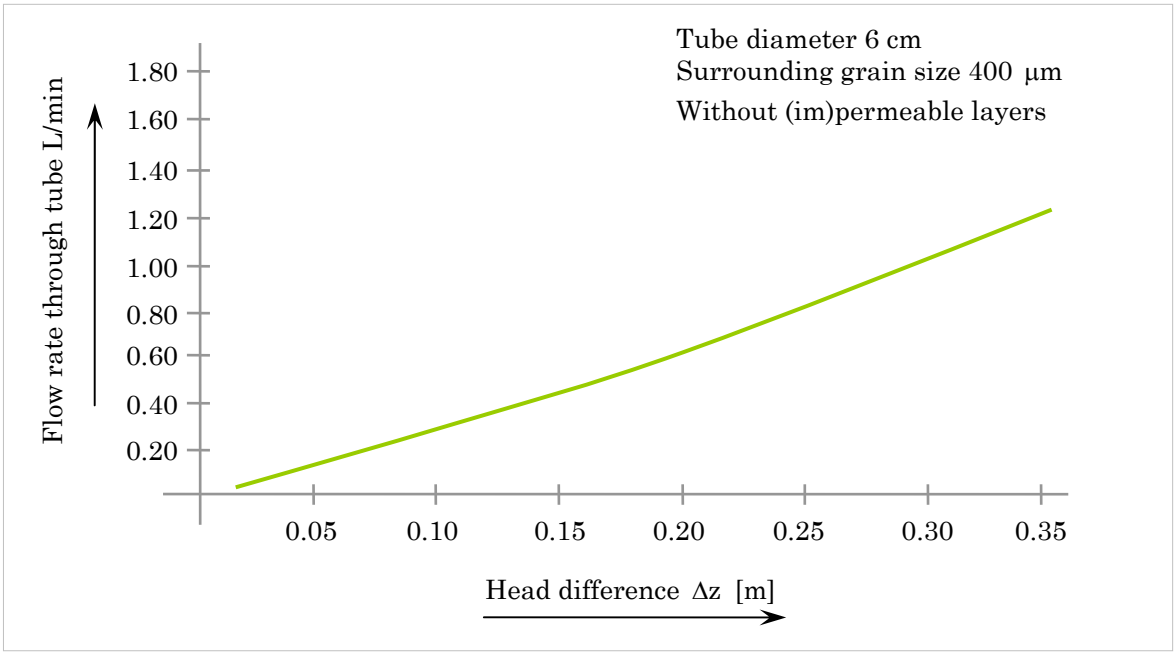

Figure 4-18 Empirical relation between the flow rate through the tube and head difference [41]

The lowering of the groundwater level can be calculated by [41];

$$z_{tube} = \frac{\left[V_{tide} \cdot (A_{tot} - A_{tube}) + V_{tube} \cdot A_{tube}\right]}{A_{tot}} \cdot t - \text{Tidal range} \qquad [m]$$

Eq.4-40

With:

z_{tube} = lowering by the tube	[m]
V_{tide} = lowering velocity of the water table in the beach	[m/s]
A_{tot} = Total affected area per tube	[m²]
A_{tube} = Area of the tube	[m²]
V_{tube} = Velocity through tube	[m/s]
t = duration of the falling water level	[s]
Tidal range = $z_{high} - z_{low}$	[m]

In case of an in-homogeneous beach, the drainage effect can be enlarged when more permeable layers are present. There are different mechanisms possible, which can be initiated by vertical drainage tubes placed in layered beaches. The most obvious is the connection of permeable layers within the beach. The requirement must be that the permeable layer is connected to the sea [41]. In that case, a low pressure can be established in the permeable layer. The pressure drop is needed to create a horizontal flow to the sea. The effect of the permeable layer is visualised in Figure 4-19.

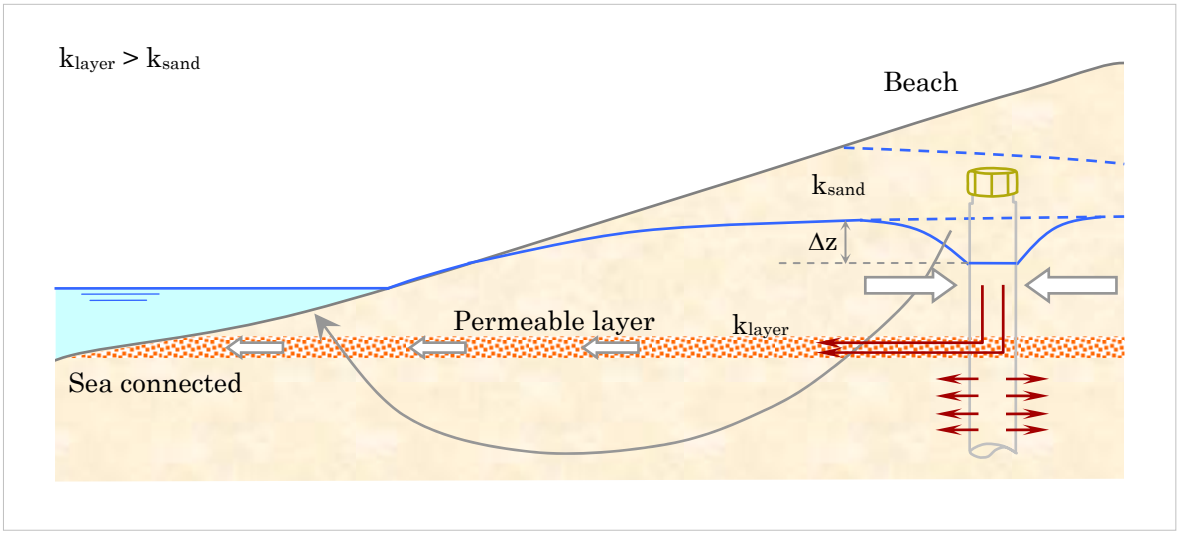

Figure 4-19 The effect of a permeable layer with vertical drainage tubes installed

The head difference Δz depends on the energy loss through the permeable layer. Thus, the drainage capacity of that layer depends strongly on the permeability of the layer (k_{layer}). The water will flow more easily through the layer. This will certainly increase the impact radius. [41]. In addition to this, the tubes can also link isolated layers (Figure 4-20). They can act as a vertical or horizontal link between different layers.

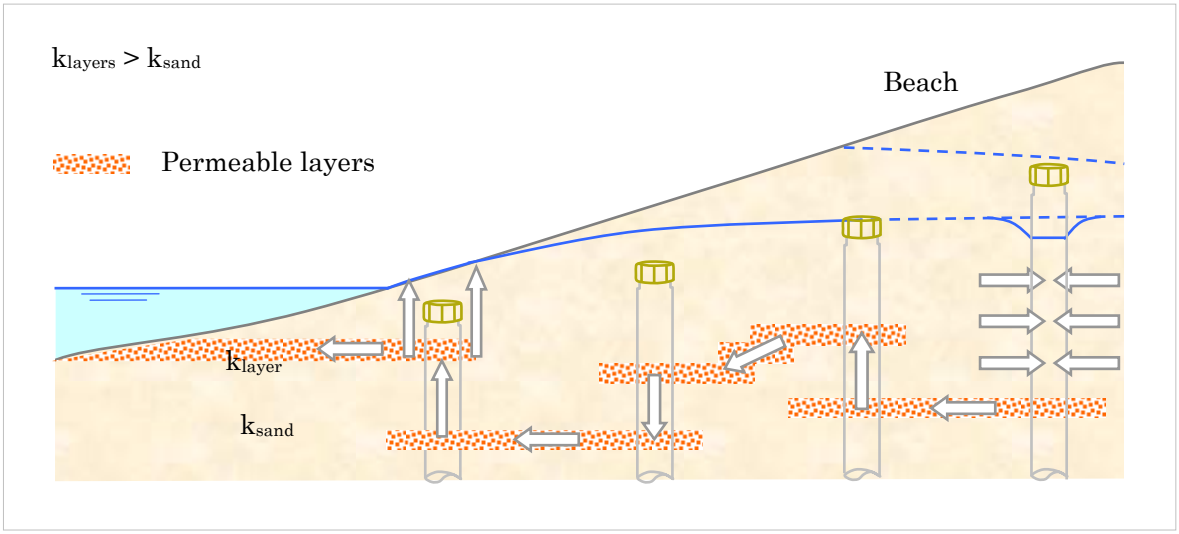

Figure 4-20 The linking effect of vertical drainage tubes penetrating different permeable layers

The local depression close to the tube, already shown in Figure 4-17, will also be established when permeable layers are present.

In case of a impermeable layer (Figure 4-21), the pressure below that layer is lower than above [41]. The vertical transport of water is jammed.

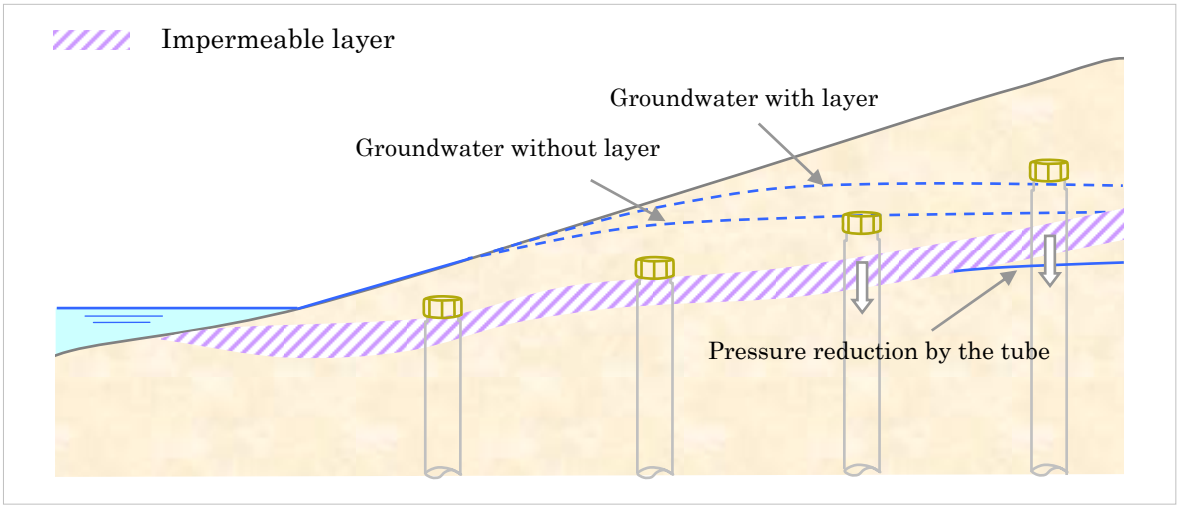

Figure 4-21 The penetration of vertical drainage tubes through an impermeable layer

The water entering the beach during high tide must be drained nearly horizontally when tide declines. This will cause a higher average groundwater level. The vertical drainage tubes may penetrate the impermeable layer, which lowers the pressure under the layer. Water can flow down through the tube when that head is lower than above the layer [41].

Results from experiments with vertical drainage tubes in Denmark [41] show that there is some impact on the pressure at the beach surface where seepage exists. During low and mean tide the flow through the tubes is often outwards. During high tide the flow is in and out. At high tide two peaks were measured: at the location of the low water level and at the high water level. This corresponds to inflow. During falling tide, an outflow at mean and low water level location could initiate, which indicates that water is drained by the tubes. The drainage tubes near the low water line actually generated higher gradients (outflow). This was suggested by the study done in 2009 [79] where fluctuations of temperature and salinity were observed. Results and descriptions of previous research were given in Chapter 2.

4.4.2 Capillary fringe

The presence of a capillary fringe influences the beach groundwater dynamics, especially in the unconfined aquifer. This fringe can have significant effect on the exchange of water between the sea and the beach aquifer. This is in particular for the storage capacity of the aquifer. Groundwater waves propagate faster and decay more slowly in aquifers with a capillary fringe [49]. The capillary fringe develops immediately above the watertable. It's a tension saturated zone where tension refers to a pressure which is negative, relative to the atmospheric pressure. The pore spaces are fully saturated. The distinction from the water table is that the pore pressures are negative. The capillary fringe depends strongly on the grain size and pores. A lowered net water table (groundwater + capillary fringe) may result in a drier beach. [51].

The capillary water level above the groundwater level does not rise to an even height. It forms an uneven fringe which is higher in fine-grained sediments because greater tensions are present. [49]

Turner and Nielsen (1997) gave an expression for the thickness of the capillary fringe within the beach;

$$h_c = \frac{10 \cdot \gamma}{\rho \cdot g \cdot D_{50}} \qquad \text{Eq.4-41}$$

With:

h_c = Thickness of the capillary fringe

γ = the surface tension

ρ = density of the fluid

D_{50} = median grain diameter of the sediment

This relation between the height of the capillary fringe and the grain diameter can be seen as a first approximation [99]. Here, the equivalent radius of pore spaces is taken D/5.

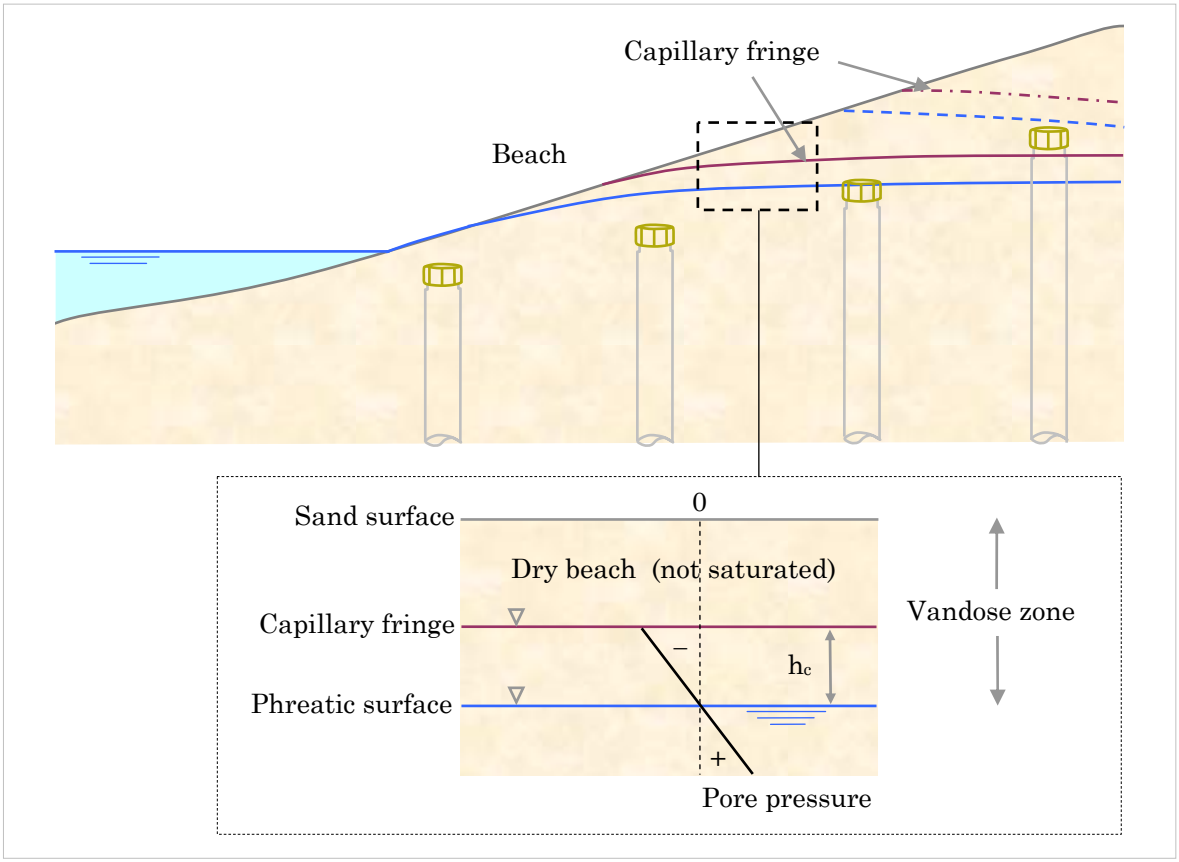

Figure 4-22 The capillary fringe above the groundwater table

The vandose zone is thicker during falling tide than at the high water level period [99]. Its thickness for grain sizes of D<0.1 mm to D>1 mm can reach values of 80 mm.

In Figure 4-23, this relation is shown. During ebb the saturated region becomes most pronounced. Rapid water table rise, which is seen on any sandy beach during a swash, results from a temporary infiltration of water. The capillary fringe coincides at that moment with the beach surface.

Rapidly after this swash, the wet region moves seaward to a lower and relatively stationary position above the groundwater table. Coarser sediment will give a lower thickness of the capillary fringe h_c. Also, the drying process will become shorter in time. [99].

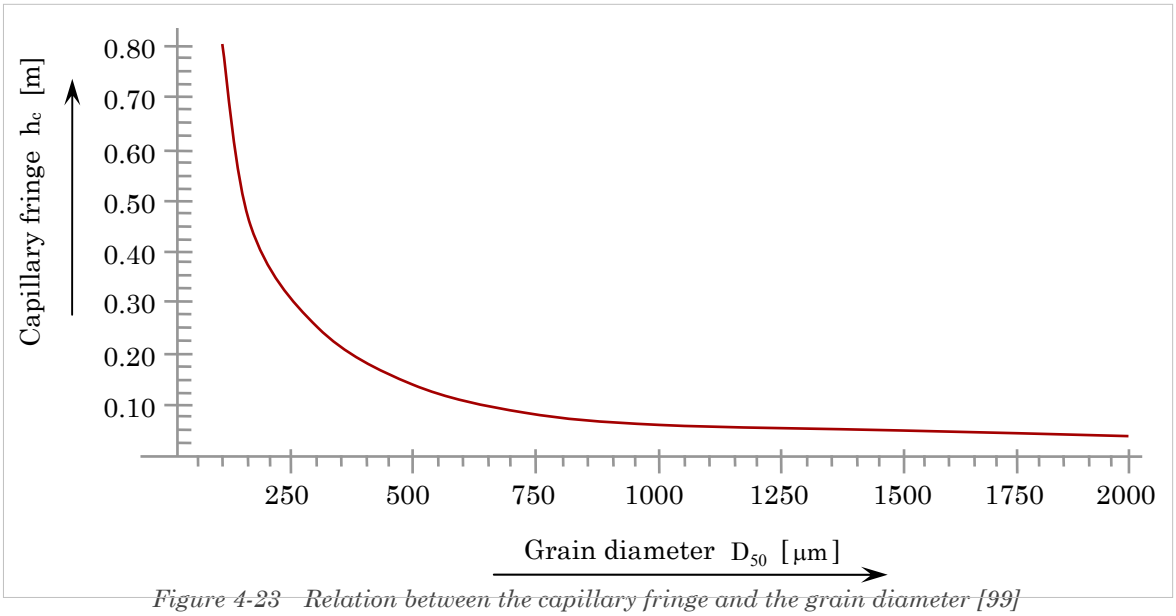

Figure 4-23 Relation between the capillary fringe and the grain diameter [99]

The rapid water table rise during swash results from downwards infiltration. The beach face hydraulic conductivity plays an important role. The sediment mobility may be decreased by swash infiltration and exfiltration effects. The next section elaborates on that thought.

4.4.3 Infiltration, exfiltration and fluidisation

The potential for infiltration and exfiltration has been linked to beach water table elevation. A low phreatic level favours infiltration and a high water table supports exfiltration. The flow velocity and shear stress at the bed are thought to increase due to boundary layer thinning during infiltration. The opposite occurs during exfiltration. Exfiltration is also expected to increase the turbulence intensity due to enhanced mixing near the bed. Infiltration increases shear stress, while exfiltration does the opposite. [49].

Nielsen (1997) gives a revised Shields parameter which includes effects of infiltration and exfiltration, which is described in Appendix M.

The effect of infiltration is bigger for a more porous bed during backwash than in uprush. [49]. The thickness of the boundary layer due to vertical flow into and out of the beach becomes thicker during backrush (exfiltration). Together with a fluctuation of the groundwater level, this will influence the sediment transport (onshore and offshore).

The infiltration and exfiltration during a swash event are explained in Figure 4-24. With an increasing grain diameter (and infiltration rate), the friction coefficient and thus bottom shear stress increases. The bottom velocity increases when the boundary layer decreases. The net onshore transport becomes higher than the net offshore transport when the grain size increases (and the parameters change). This tipping point, which depends on the grain size, is defined by Nielsen (1998) and Turner & Masselink (1998) for quartz sands.

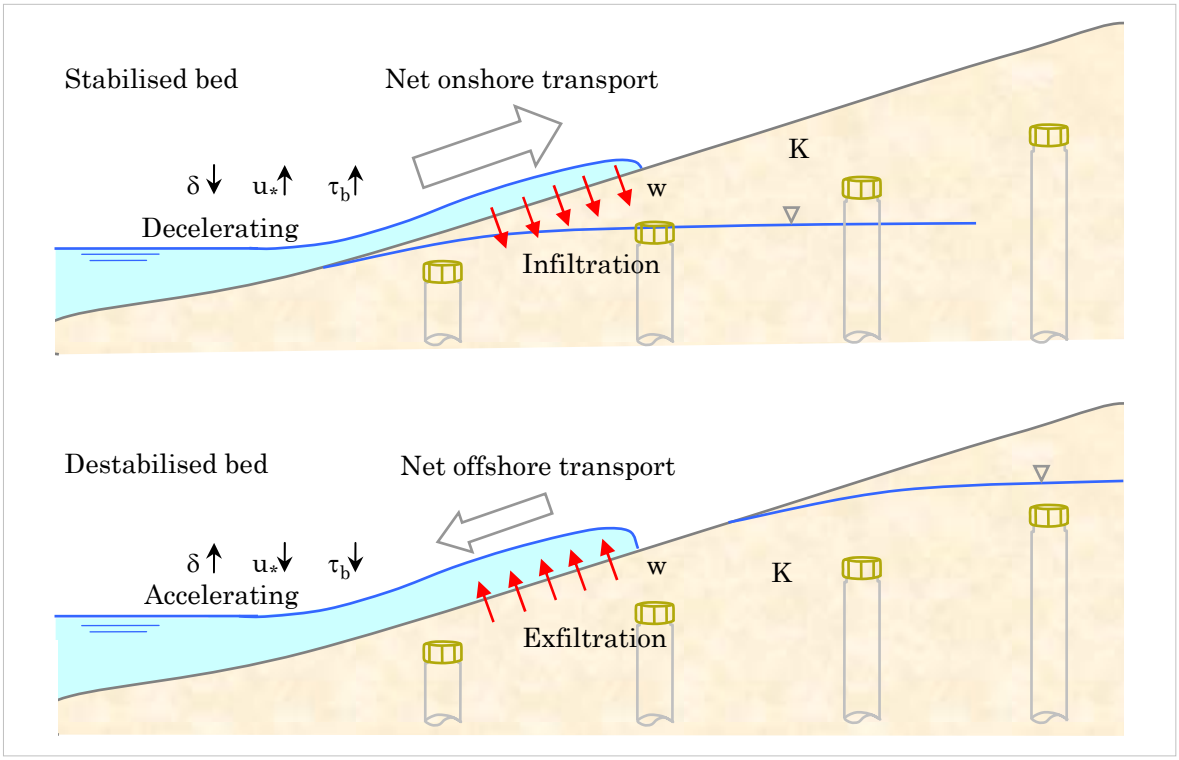

Figure 4-24 Infiltration and exfiltration during a swash event

The simulations of Butt et al. (2001) [24] suggest that onshore sediment transport due to effects of infiltration and exfiltration becomes more important as grain sizes increase. Fluidisation of the upper layer of the bed might be a significant contributing factor for sediment transport on the backwash. The condition for fluidisation of the bed is described by;

$$\frac{w}{K} \geq \frac{(S-1)}{a} \qquad \text{Eq.4-42}$$

With: w = vertical seepage velocity, K = hydraulic conductivity, S = relative density = 2.65 for sand, a ≈ 0.50 for a seepage force in the top layer which is half of that within the bed.

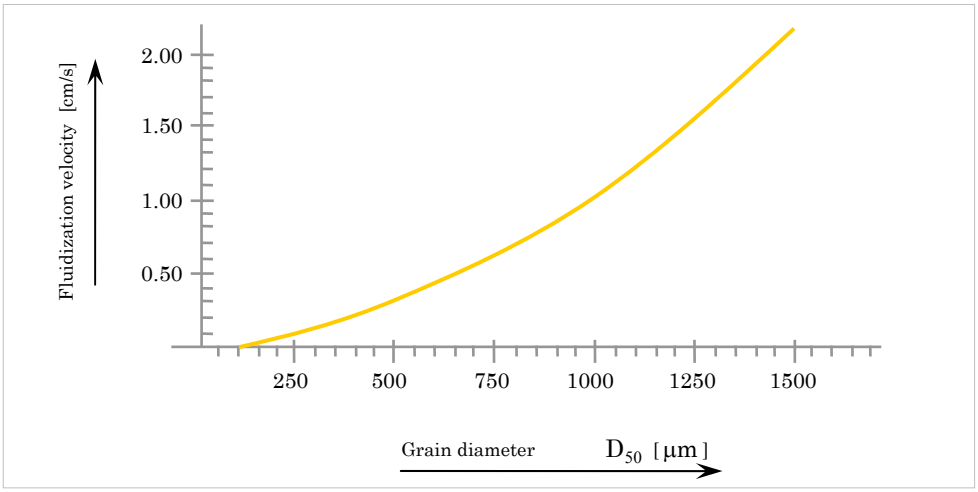

Figure 4-25 Relation between the fluidization velocity and the grain diameter [99]

Butt et al. gives an expression for the relative sediment transport due to effects of infiltration-exfiltration (which is the decrease of transport due to infiltration effects) [24];

$$Q_{\text{inf iltration}} = Q_w - Q_0 \qquad \text{Eq.4-43}$$

$$Q_{\text{inf iltration}} = \overline{u}^3 \cdot \left(\frac{f \cdot \left(1 - \frac{w}{\overline{u}} \cdot f^{-1/2}\right)}{8 \cdot g \cdot D_{50} \cdot \left(S - 1 - \frac{1}{2} \cdot \frac{w}{K}\right)} \right)^{3/2} - \overline{u}^3 \cdot \left(\frac{f}{8 \cdot g \cdot D_{50} \cdot (S-1)} \right)^{3/2} \qquad \text{Eq.4-44}$$

With:

$Q_{\text{infiltration}}$ = relative sediment transport due to effects of infiltration and exfiltration
Q_w = influenced sediment transport with through bed flow
Q_0 = sediment transport without through bed flow
$\overline{u}$ = averaged velocity [m/s]
f = the friction factor for swash flow
w = vertical seepage velocity [m/s]
g = acceleration due to gravity [m/s²]
D_{50} = mediane grain diameter of the sediment [m]
S = relative density = 2.65 for sand
K = hydraulic conductivity [m/s]

In coarse sand beds onshore sediment transport due to the effects of swash infiltration and exfiltration becomes important. This process depends on a critical grain size. Infiltration augments onshore transport and berm formation. The backwash volumes can be reduced by infiltration which occurs during uprush. At least 2% of the uprush volume has to infiltrate in order to get a net onshore sediment transport rate [67]. During the passage of a bore front, the water pressure changes. This process will only take a second. The pressure is guided directly into the surface. [67]. When infiltration occurs, the total transport rate decreases. The role of infiltration – exfiltration in the swash zone is generally to enhance uprush transport [24]. The relation between the grain diameter and the change of the total sediment transport rate is looked at (Figure 4-26). Nielsen (1998) and Turner & Masselink (1998) suggested that boundary layer effects dominate at grain diameters above $450\,\mu m \le D_{50} \le 580\,\mu m$.

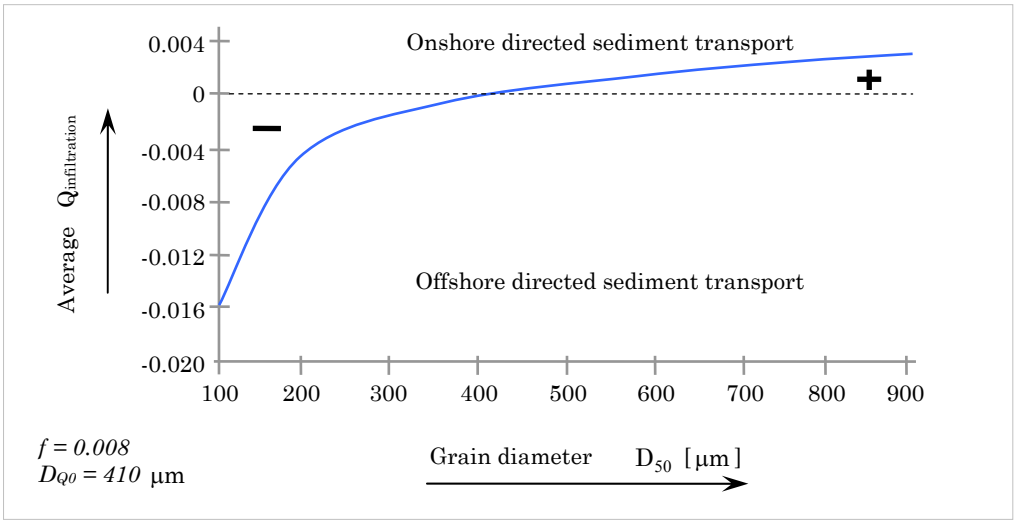

Figure 4-26 Dependency of the grain diameter to infiltration rates[24]

4.4.4 Swash asymmetry

The morphology of the swash zone is strongly influenced by the swash motion and sediment transport volumes. The swash motion can be described by an uprush and downrush flow. The sedimentology (section 4.1), beach profile (section 4.2), interaction with the beach surface (section 4.3) and the flow conditions influence this motion. If these parameters change, swash asymmetry may develop. The net sediment transport may change which means that erosion is turned into accretion. One example of this is already given in section 4.4.3.

The swash asymmetry may the result from the following effects;

- Changing beach slope when the grain size changes. The uprush motion is decelerating, while the backflow is accelerating. A larger grain size gives steeper slopes. The effect will be more.
- The duration of the uprush is significantly shorter. The peak velocities are generally the same. [81]
- The transition layer depends on the accelerating and decelerating motion of the swash. Thick transition layer during backwash gives less erosion than the relatively thin layer during uprush, where shear stress velocities are high. A larger grain size gives a higher friction factor and shear stress. The deceleration will be more.
- During uprush, just after bore collapse, the flow is turbulent. The backwash flow is more laminar. Therefore, the uprush flow can be described by larger friction terms. The sheet flow friction terms are smaller.

4.4.5 Sediment sorting principles

The cross-shore grain size distribution depends on the composition of various sediment sources and the energy level of the wind and wave forces at work in a particular environment [85]. Sorting processes along the beach occur both in settling and pick up of grains and fractions. In settling, the fall velocity is dependent on the size, shape and the density. The grains which have the same settling velocity are considered to be hydraulic equivalent. Differences in settling velocity and segregation of sediment fractions take place in the vertical, with finer fractions suspended at higher elevations. The net onshore transport of coarse material relatively close to the bed combined with finer material transported offshore in suspension, would result in cross-shore segregation leading to the offshore fining. The beach can become coarser. Over the breaker bar slight coarsening is observed. Finer material is found in the bar throughs. The adaptation time of the spatial sorting is short [69]. There exists some kind of dynamic equilibrium between the sediment size and the hydrodynamic conditions [85]. The basic rule is;

Finer grains are winnowed away from the bed in the most energetic areas by turbulent processes and carried away to less energetic areas. This leads to the simultaneous deposition of large grains with lower density and small grains with higher density.

Heavy materials can expose the hydrodynamic conditions. The percentage of total heavy minerals and the relative contribution of the high density minerals increase in shoreward direction. Selective transport will play a role. Even on different scales this effect is noticeable (offshore transport and ripples). In the past, many studies were done related to the flow dynamics of graded sediments in coastal regions comprising both theoretical and experimental investigations and statistical analysis. Many questions remain unanswered. The influence of cross-shore sediment transport on the bed grain size distribution is one still unsolved problem. [59]. Some theoretical approaches say that grain size sorting is attributed to variability of wave energy and wave related processes. Some sorting principles are described in the book of Komar (1998) and van Rijn (1998). Important mechanisms are the wave breaking and the swash run-up (see section 4.2.1). In order to get insight in changing grain properties one

should give a precise description of the velocity by waves and currents, with particular attention paid to the bedload transport and the suspended transport close to the bed.

At slopes between 1:10 and 1:30 (Egmond aan Zee and Hvide Sande) the mean grain size is greatest (coarsest) near the wave plunge point at the base of the beach face (Figure 4-27). Up to the foreshore as well as down offshore the mean grain size decreases. Rounder grains are transported towards the upper part of the swash zone. Round grains may congregate on the upper foreshore because of their larger settling velocities. Non spherical grains are transported further onshore. At the lower shore face the alongshore currents increase in strength which may result in the winnowing of relatively fine sediments [85]. According to measurements done by Pruszak (1993) fining often occurs from the water line to the dune foot. Some results of this study are shown in Appendix N. On average the fining of sediment from the swash zone to the dune foot is 15 to 30% [85] [99].

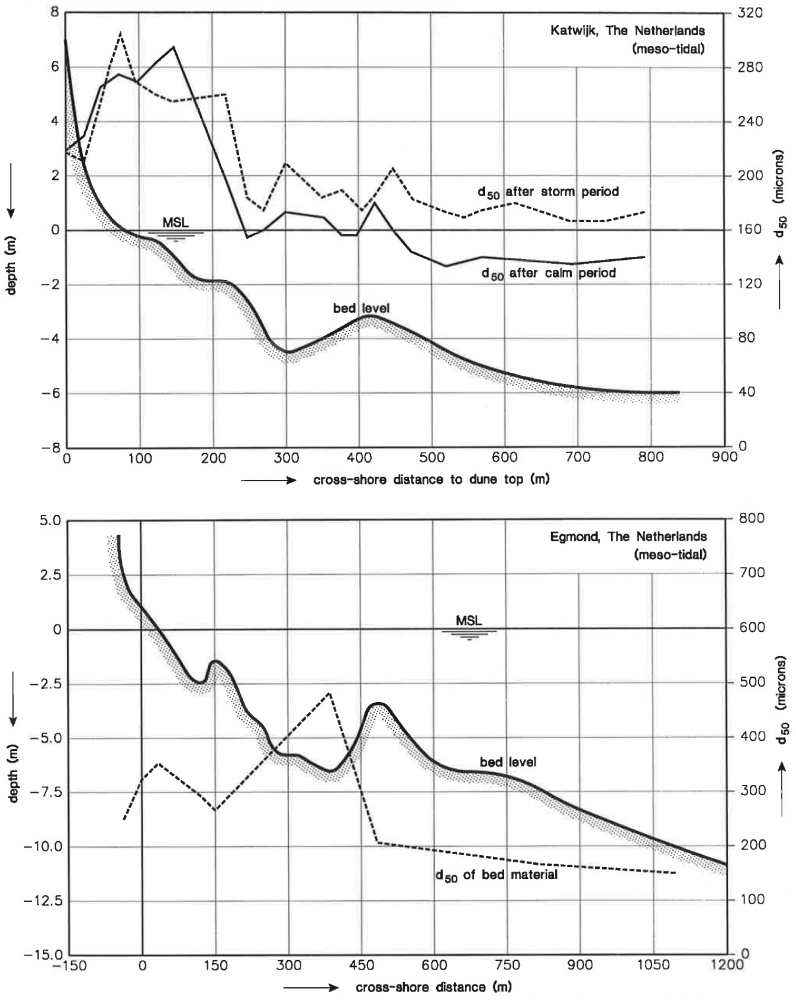

Figure 4-27 Cross-shore distribution of median grain sizes at the beach of Egmond aan Zee [48]

Studies done by Stauble and Cialone (1996) confirm that the sand at the foreshore between the waterline and breaker bar becomes relatively coarse. Especially during a storm event this effect enlarges. The median grain sizes at through zones between bars is often much coarser during stormy conditions. But during fair weather a layer of fine sediments accumulates.

Basically two different effects cause the sorting of sediment; aeolian transport at the beach and more energetic conditions by waves/currents (like wave breaking) at the nearshore beach zone.

4.5 Sediment transport

Numerical modelling has become one of the corner stones of coastal engineering. Many models are available that predict the morphological development. Here, the UNIBEST Coastal Software Package is used to describe qualitatively the influence of the sedimentology on the sediment transport rates. The Unibest-LT and CERC formulae are used for longshore transport and the Unibest-TC focuses on the cross-shore transport of sediment.

4.5.1 Longshore sediment transport

First, the dependence of the longshore sediment transport on the sedimentology is studied by the use of the well known CERC formula. The CERC (Coastal Engineering Research Center) formula for longshore sediment transport is extensively described in the Shore Protection Manual (US Army Corps of Engineers 1984). This approach is based on the energy flux and the principle that the longshore immersed weight sediment transport rate is proportional to the longshore wave power per unit length of beach. One expression of the equation is given by;

$$Q = \frac{K \cdot P_{\ell}}{(\rho_s - \rho) \cdot g \cdot (1 - p)} \qquad \text{Eq.4-45}$$

With :

K = dimensionless parameter {ranging from 0.2 (Kraus) to 2.2 (Caldwell)

P_{ℓ} = longshore component of wave power, entering the breaker zone (energy flux)

ρ and ρ_s = mass density of water and sediment

p = porosity in relation to sand weight and volume (voids)

This equation defines a constant 'K' which possibly varies with sand size, density, fall velocity and shape characteristics. Lots of research is done by many scientists to determine the right value for K. During a study done at the Leadbetter Beach, California, it was found that the total longshore suspended sediment transport could account for all of the transport predicted by this equation, with a K value of 0.77 [29]. One outcome of that research was the relation between the sediment grain size and the K-value (Figure 4-28).

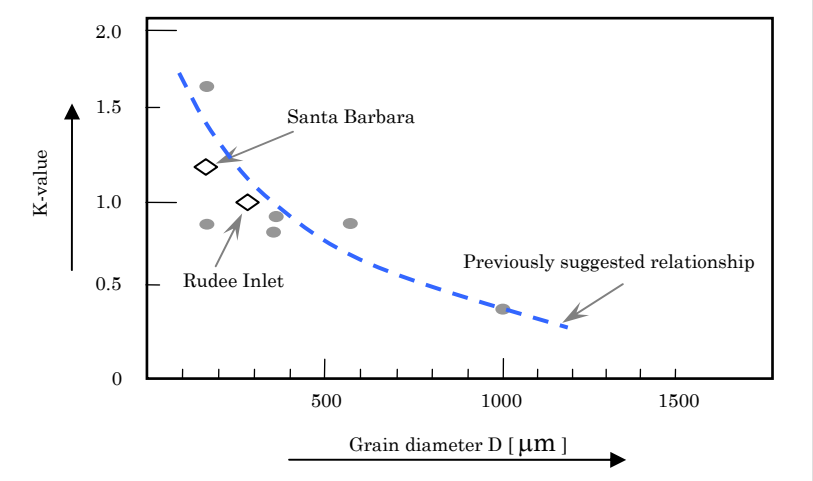

Figure 4-28 Variation of the K-value with the grain size D [29]

Van Rijn (2006) studied the relation between the longshore sediment transport and the beach slope which varies with the grain sizes (Figure 4-29). He concluded that the sand transport of fine sand is about 3 to 4 times larger than the transport of coarse sand for the same beach slope.

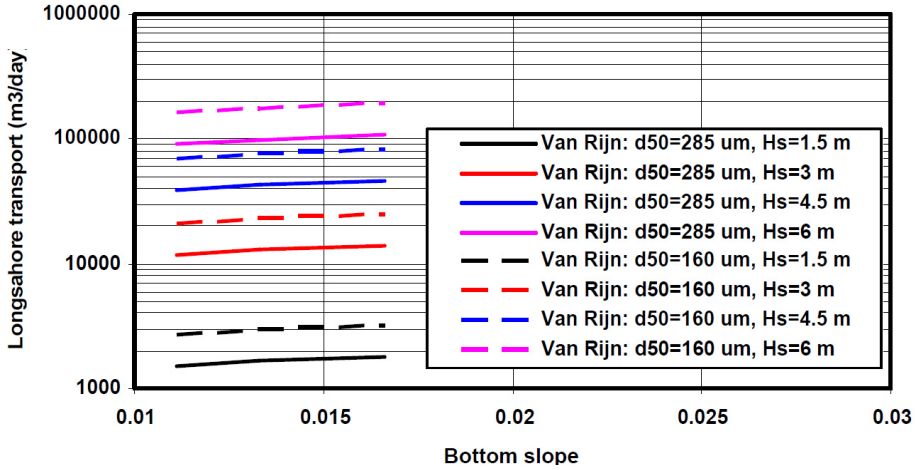

Figure 4-29 Longshore transport as function of the grain size and beach slope [85]

The computer model named Unibest-LT, which is developed by Delft Hydraulics, is designed to compute longshore sediment transports and resulting profile changes along any coastal profile of arbitrary shape under the combined action of waves, currents and wind. In order to say something about the influence and sensitivity of the roughness, wave breaking, grain size and beach slope, a model run is used. Figure 4-30 shows the output of this reference case.

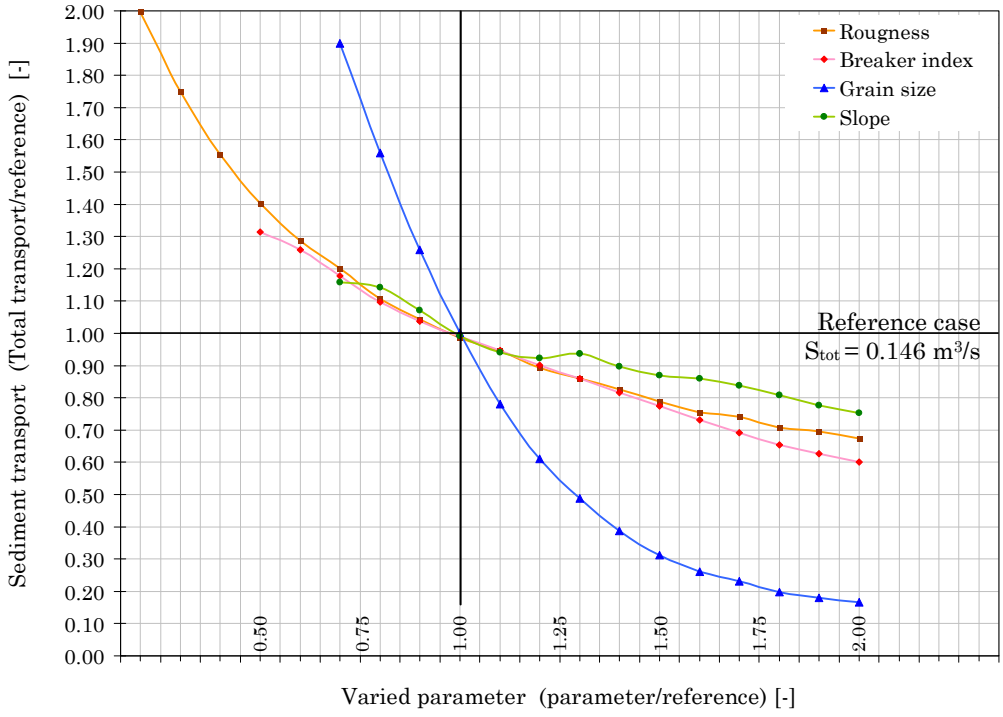

Figure 4-30 Change of sediment transport with decreasing parameters [43]

The chosen parameters used for the calculation of Figure 4-30 were; offshore wave height = 2 m, wave period = 7 s, offshore wave direction = 30^0 , bottom slope = 1:100, breaker index = 0.800, bed roughness height = 0.060 m, mean sand diameter = 200 μm , coarse sand (D_{90}) diameter = 270 μm , specific water density = 1000 km/m^3, specific sand density = 2650 km/m^3 and particle fall velocity = 0.0252 m/s. These values are fairly similar to the Egmond aan Zee case which is described in Chapter 2.

4.5.2 Cross-shore sediment transport

The profile changes along any coastal profile of arbitrary shape under the combined action of waves, longshore tidal currents and wind, can be described by the Unibest-TC model (for more detailed information see Appendix M). Figure 4-31 shows the relation between three different friction factors and the wave height. The wave height decreases with a higher friction.

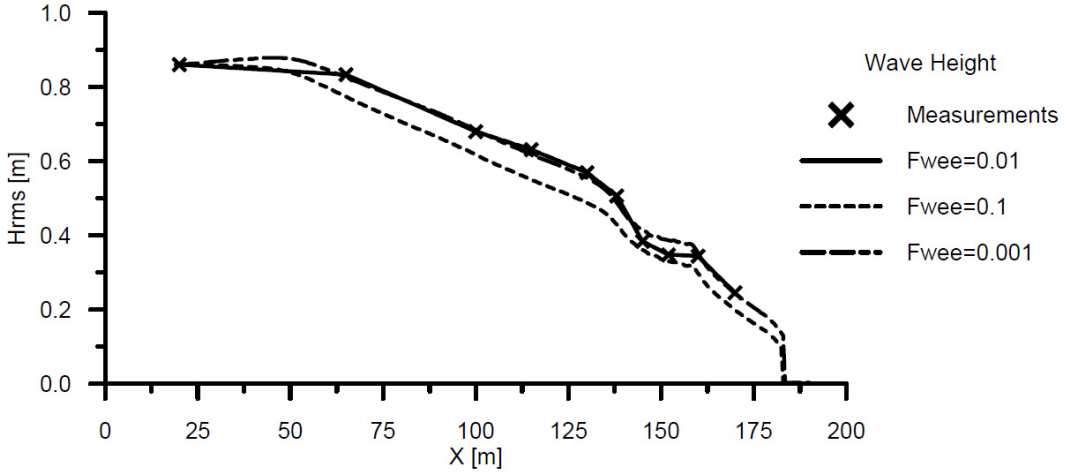

Figure 4-31 Wave height predictions for various settings of the friction factor [103]

One other important form of dissipation is wave breaking. The wave breaking parameter γ is related to the beach slope (see section 4.2.1, 4.2.2). This parameter can have a significant influence on the wave height as can be seen in Figure 4-32.

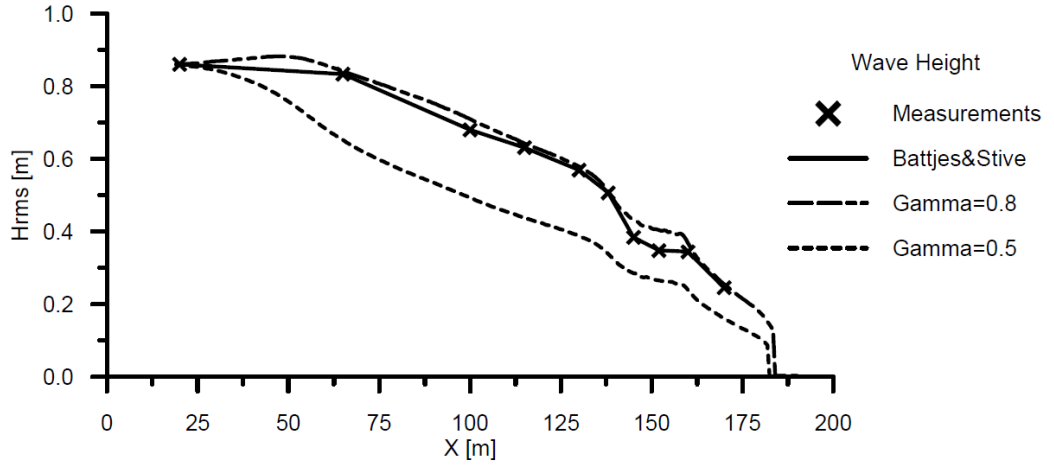

Figure 4-32 Wave height predictions for various settings of the breaking parameter [103]

The cross-shore transport depends on the median grain diameter, the shear stress (initiation of motion) and slope. For the computation of the bed shear stress the wave-current friction factor is used. In the case of a sloping bed, the transport is affected by the gravity. A steeper slope increases the transport rates in case of downslope transport and decreases the transport rates in case of upslope transport [17].

The median grain size has also an effect on the sediment transport direction (see Figure 4-33)

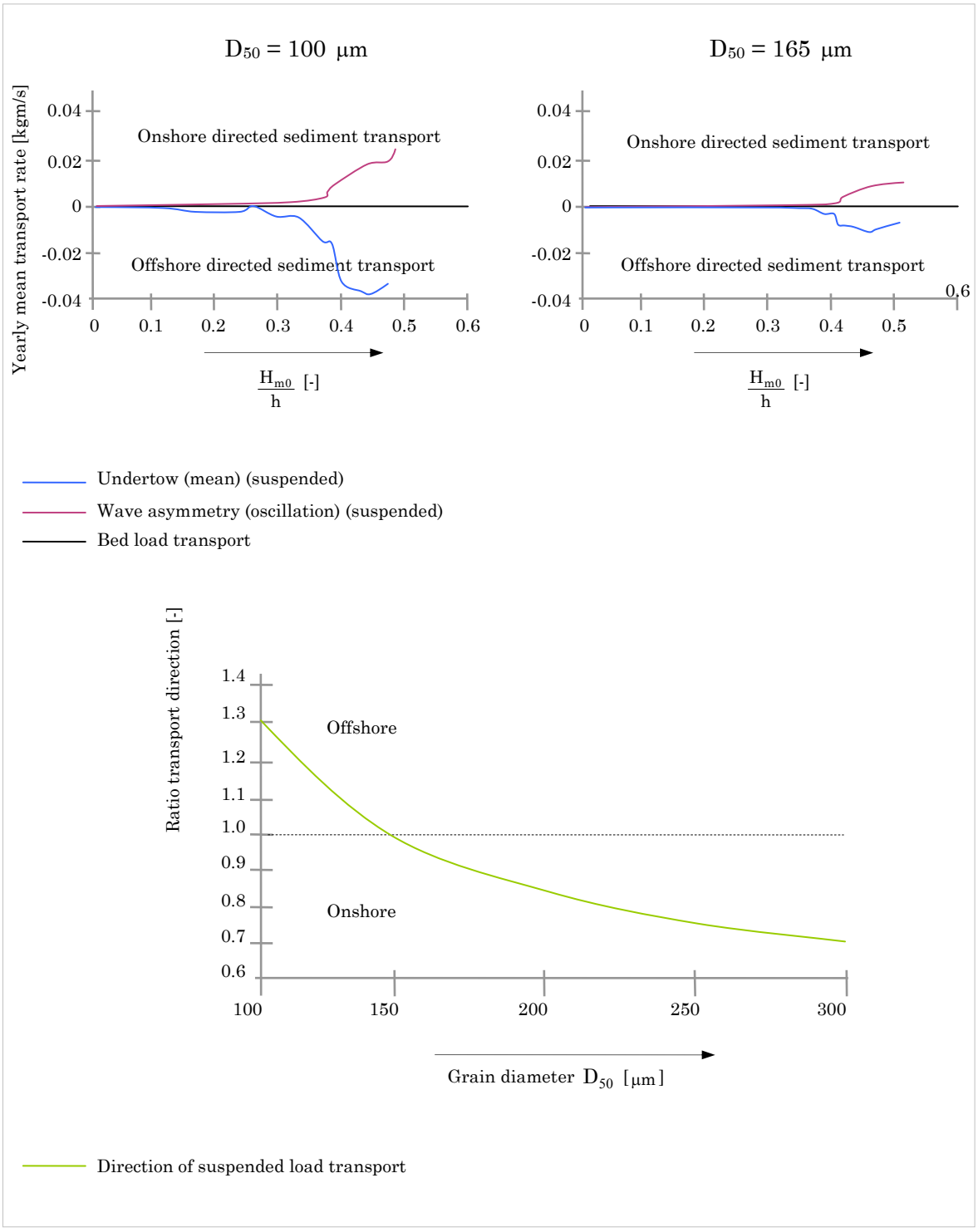

Figure 4-33 The effect of the median grain size on the sediment transport rate and direction [48]

5. Field data

The purpose of this study is to investigate the effects of vertical drainage tubes on the sedimentology of two beaches and to connect any changes of grain properties with influenced intertidal beach processes.

Theoretical models and scientific formulae require a practical input from field measurements. The theoretical part is already discussed in Chapter 4. This chapter focuses on raw data obtained from different measurements at the beaches. These findings will be used to determine the effects on beach processes and morphology and to evaluate the large scale working mechanism.

Background information of the data and an overview of the field experiments are given in Appendix B. Besides examining the sedimentology of the two different beaches, some morphological dynamics were analysed. The data of these measurements are described in paragraph 5.4. The active zone, often called the beach envelope, erodes during storm events and accretes in times of calm weather (Figure 5-1). The sediment, which forms this top layer, is mixed continuously. Therefore, it can be regarded as 'fresh sand'. The transition between this sand and older deposits is studied by the drills and deep samples. Cylinder and cone penetration tests were done to study the sand of both deposits (paragraph 5.1). The geological composition of the beaches can be studied with this data.

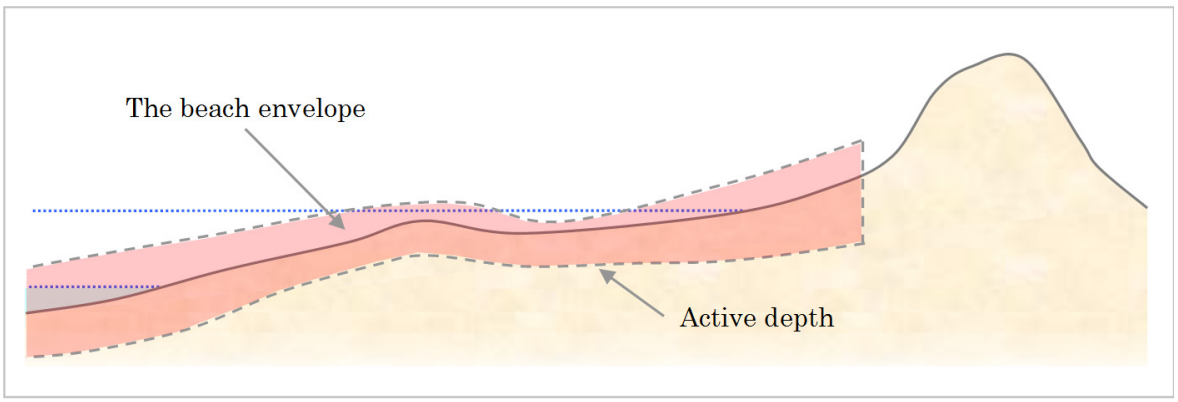

Figure 5-1 The active zone or beach envelope at the Egmond aan Zee beach

Figure 5-36 shows a map with beach profiles and isobars. From this figure the steepness of the beach can be derived. Also the height and location of bars and channels are visualised.

The vertical drainage tubes were installed at twenty centimetres below the beach surface. If these drainage tubes prevent erosion of the beach and stimulate accretion of sand, this covering layer becomes thicker. When the active depth, which refers to the beach surface level after many storms, increases, the tubes will stick out of the ground. In that case, they must be injected again with a pressure lance. Section 5.4.2 gives an analysis of this process in time for the Egmond aan Zee case. From every single tube its subsidence is recorded. Therefore, a trend can be seen when the data is combined with the prevailing hydrological conditions.

5.1 Geological composition of the beaches

The historic development of the geological composition of the beach near Egmond aan Zee is described in Chapter 2. The presence of permeable and impermeable layers would be essential to increase the probability of the validation of the large scale working mechanism, described in Chapter 3. The geological composition of the beaches is studied by analysing the presence of shells, studying the conditions of the subsurface by cone penetration tests and looking for layered structures in the subsurface of the beaches.

5.1.1 Permeable shell layers at Egmond aan Zee

The beach near Egmond aan Zee contains large amounts of shell fragments. Some of them lie on the beach surface, while others are found several metres deep. At first glance, the fragments occur along the entire coast. However, the area from the high waterline to the dune foot and beyond contains no shells at the surface and small amounts at depths of two metres or more. Here, shell layers may be covered by wind blown sand from the beach or dunes.

A large part of the intertidal beach is covered with shells. There are sorting mechanisms active which concentrate shell deposits at the beach. Shell layers in the subsurface may form permeable areas, which may form a shortcut for groundwater flow to the sea [see Chapter 3]. The presence of these layers is investigated by conducting a number of drilling tests. The locations of the measurements are shown in Figure 5-2. Depths of zero to one metre are examined at six locations along the beach. Deeper drills, up to five metres, were done at four locations.

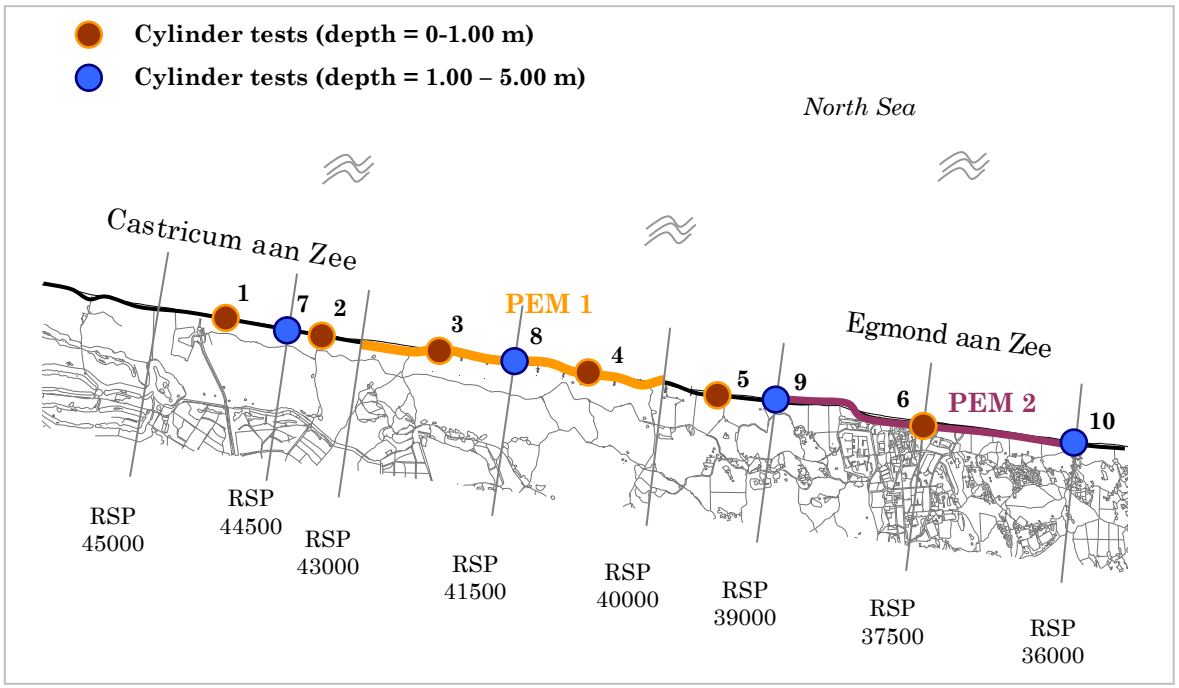

Figure 5-2 Locations of the cylinder tests

In summary, many shell layers were found at different locations. The size of the shell fragments varied considerably. Figure 5-3 and Figure 5-4 show two representative drills for both depths studied. The thickness of the layers ranges from five to forty centimetres.

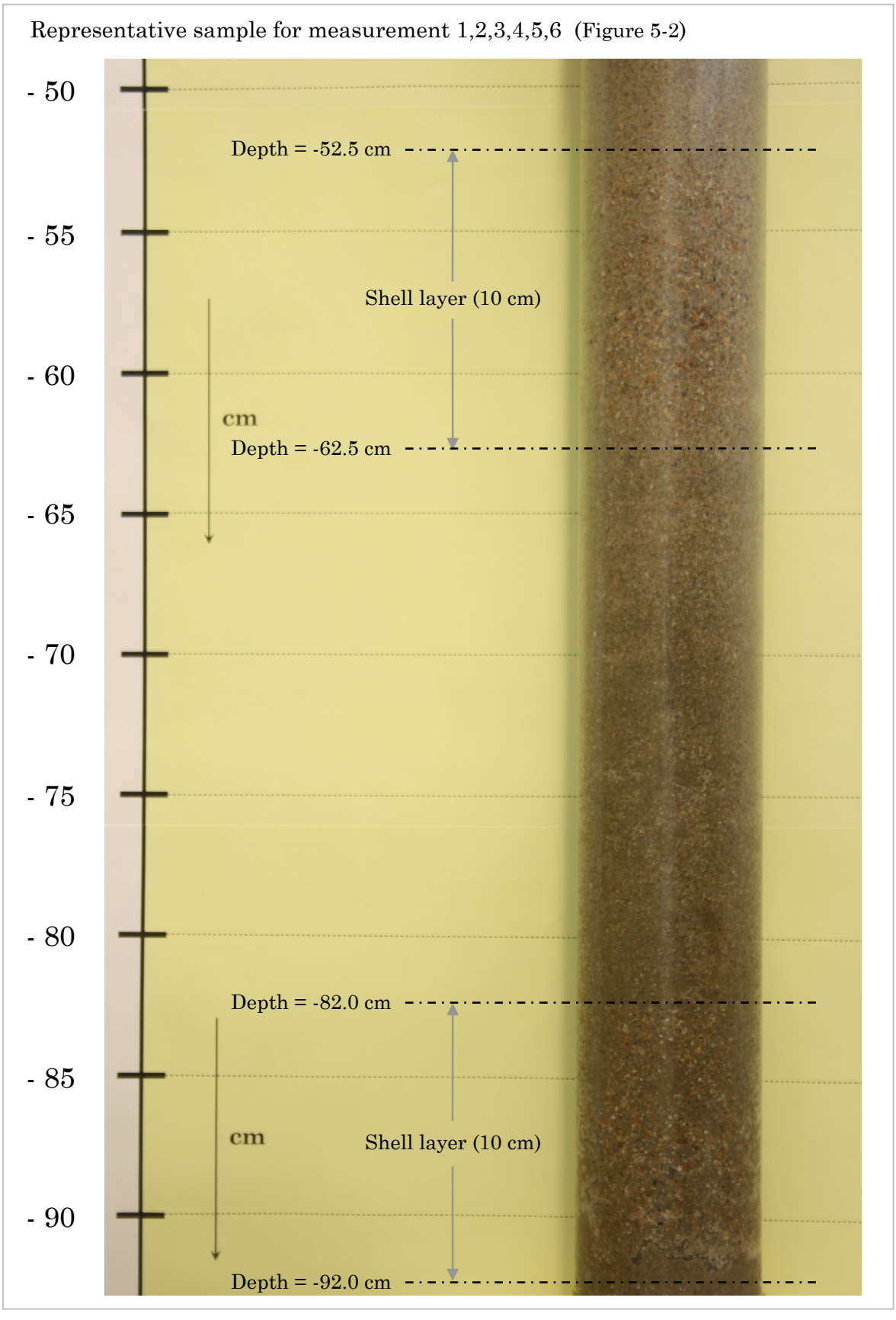

Figure 5-3 Shell layers at 0.50 to 1 metre depth [representative sample]

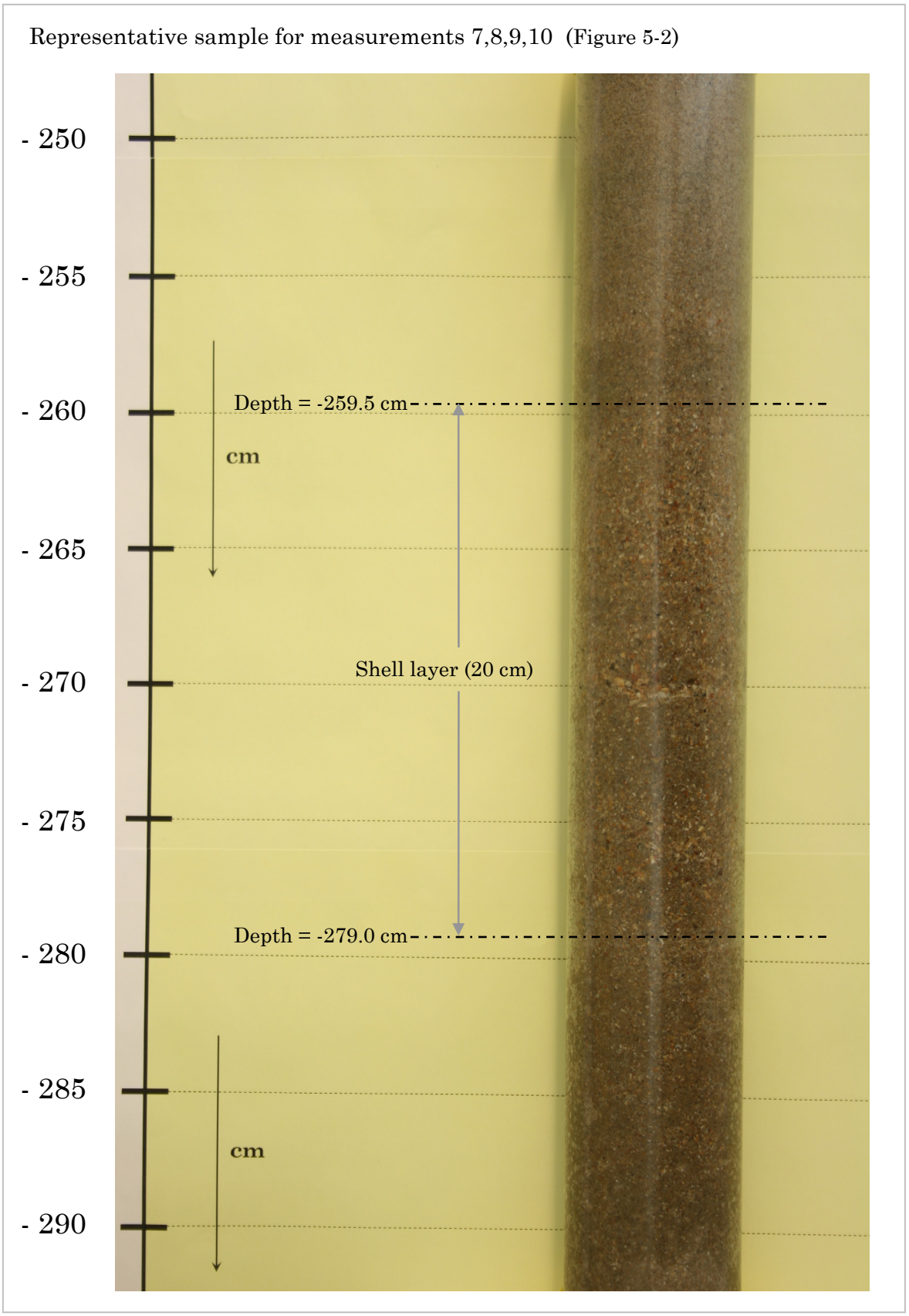

Figure 5-4 Shell layers at 2.5 to 3 metre depth [representative sample]

Figure 5-5 Shell fragments from three metres below the beach surface

The drill samples were taken between the low and high water line. The shells were arbitrarily present in the subsoil. The vertical drainage tubes at the intertidal beach zone are penetrating these shell layers. Without any accretion of sediment, the tubes are still located at a depth of -20 cm to -220 cm. Their filter, which is situated at the centre of the tube, goes through the shell layers.

The recently accreted sediment on the beach (active zone) contains shells too. This is confirmed by Figure 5-3. The presence of shells at this part of the beach is also randomly distributed. The vertical drainage tubes may connect shallow layers with deeper shell areas in order to facilitate a vertical connection.

5.1.2 Conditions of the subsurface

The cone penetration tests (CPT) were executed using a cone shaped cylindrical probe with sensors on its tip (Figure 5-6). The tests were done at two different rows at the beach of Egmond aan Zee (Figure 5-7). Their primary application is for stratigraphic profiling. The grain size distribution cannot be provided accurate enough by CPT [88]. On the other hand, the CPT classification charts provide a guide to soil behaviour.

The data consists of six graphs which show the cone resistance and friction ratio (%). These figures give an impression of the layered structure of the subsurface. Naturally, most of the measured soil is sand. Some thin layers of clay were also observed. Table 5-1 gives an overview of the soil classification, which is often used to describe the cone penetration records. The carrying capacity of the tip depends on the soil. Clay layers have a much lower cone resistance compared to sand layers. The friction ratio for clay is much higher than that of sand.

Figure 5-6 Cone penetration tests at the beach near Egmond aan Zee

Depending on the resistance of the soil, the cone was pressed twelve to eighteen metres below the beach surface. The measurements were done in the centre of the reference area and at the centre of the drainage tube area (Figure 5-7). Each row consists of three tests; one at the low, mean and high water line. The width of the intertidal beach area near the drainage tubes is fourteen metres less than that of the reference area. Figure 5-7 gives an overview of the measurement locations.

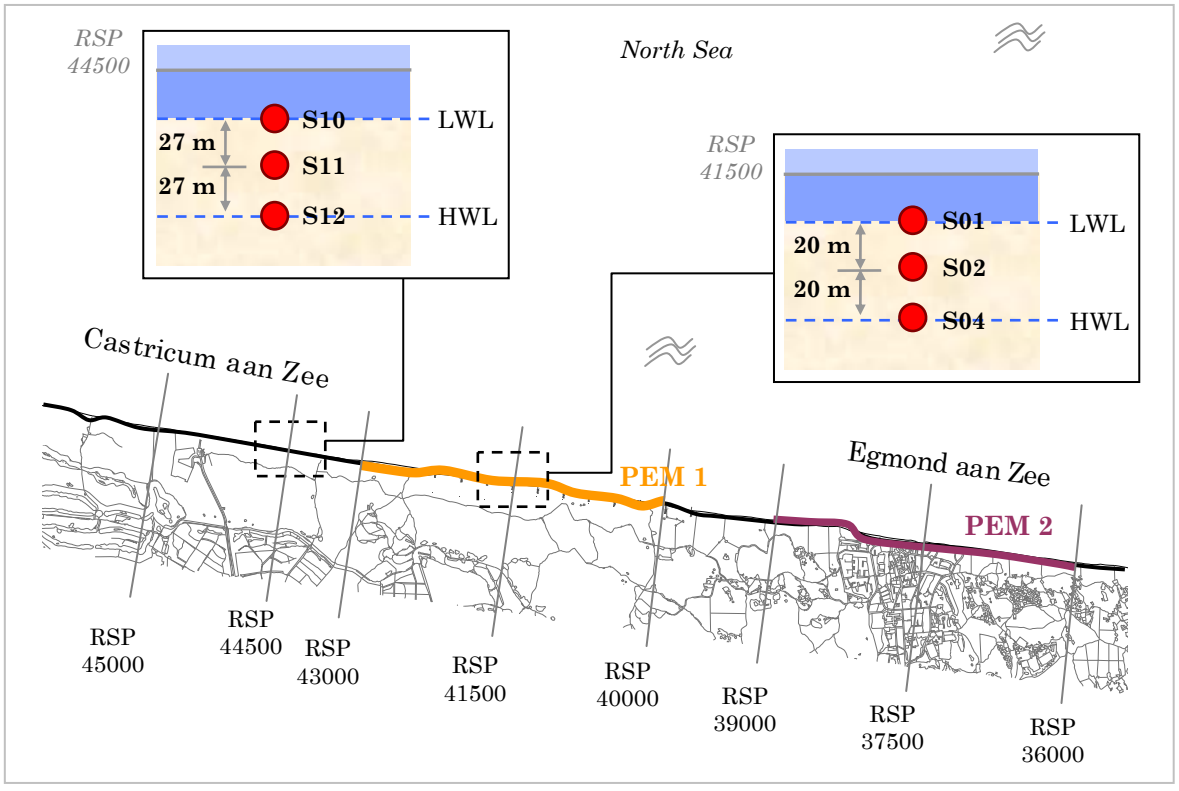

Figure 5-7 Locations of the cone penetration tests

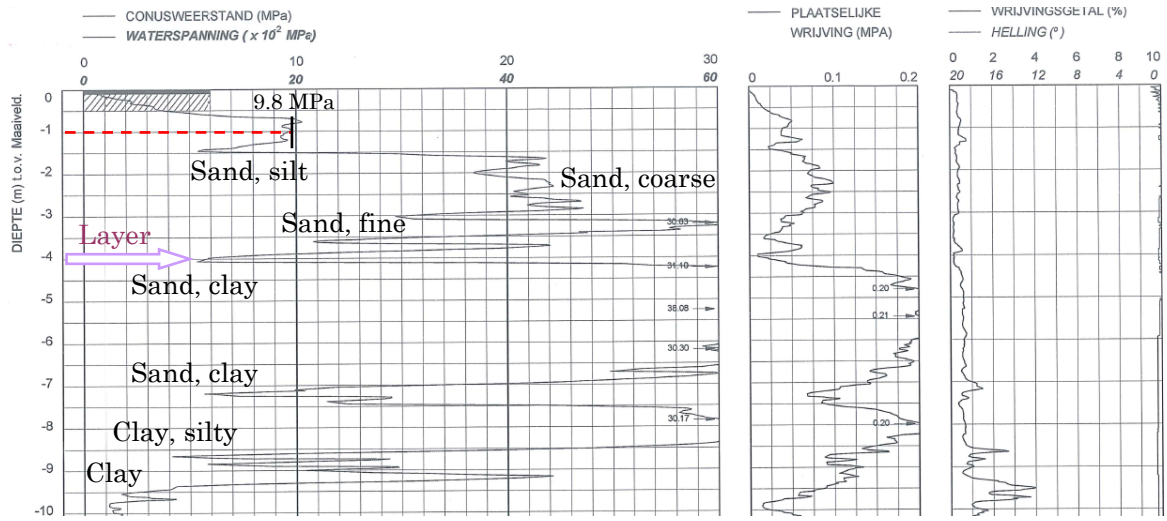

Figure 5-8 Cone penetration test S10; Reference area, low water line

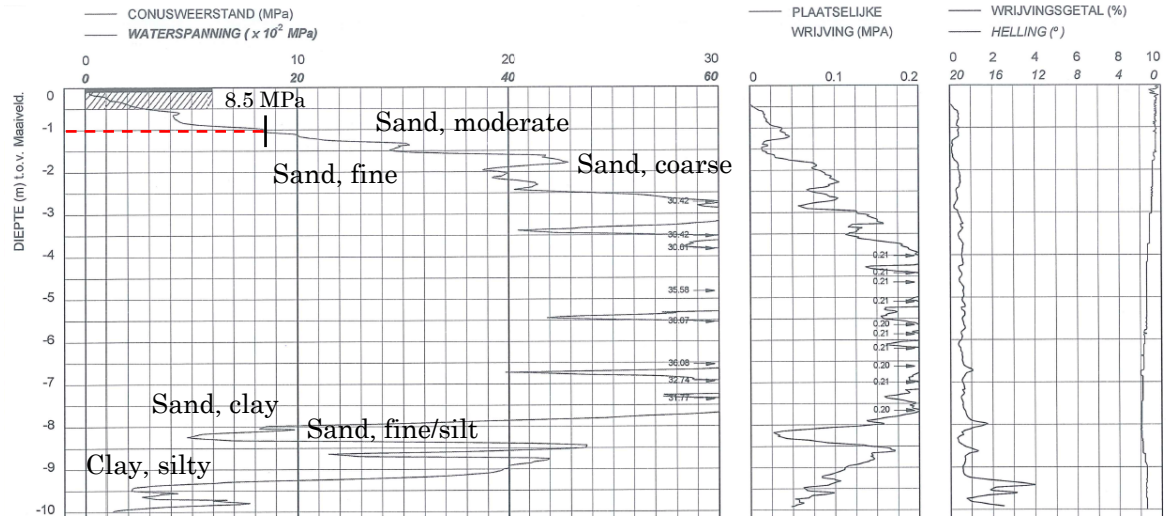

Figure 5-9 Cone penetration test S11; Reference area, mean water line

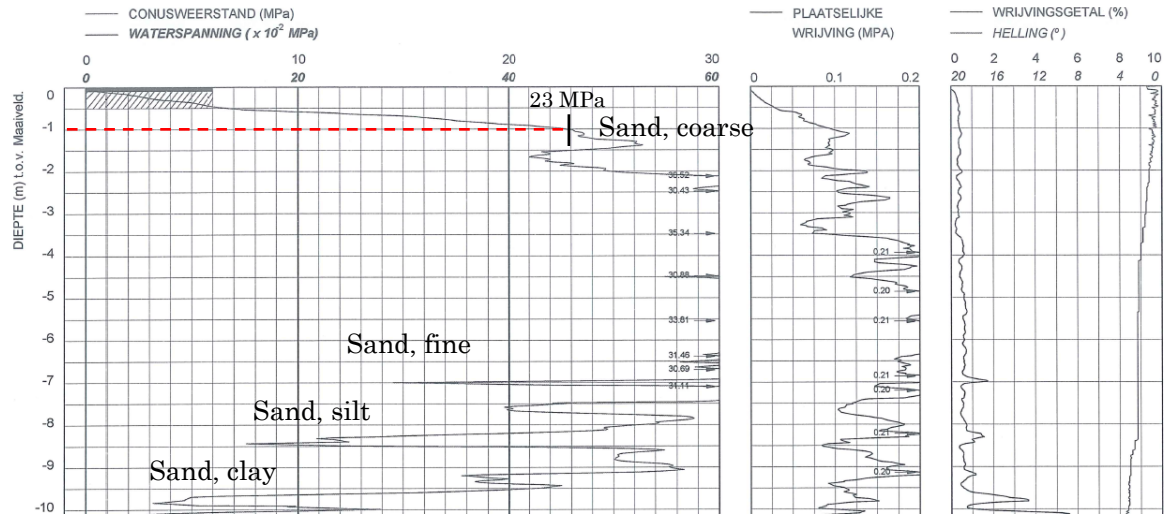

Figure 5-10 Cone penetration test S12; Reference area, high water line

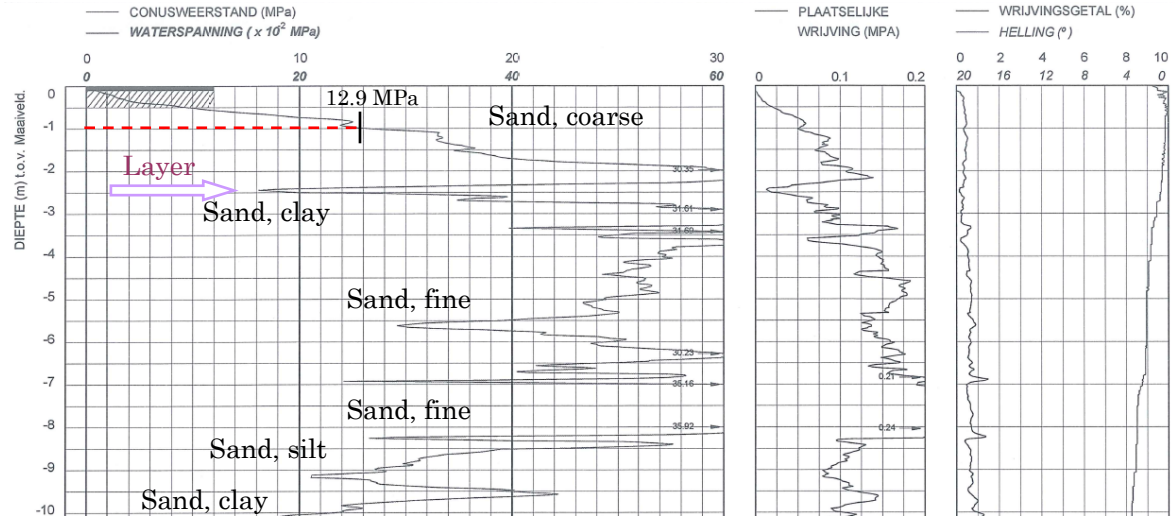

Figure 5-11 Cone penetration test S01; Drainage tube area, low water line

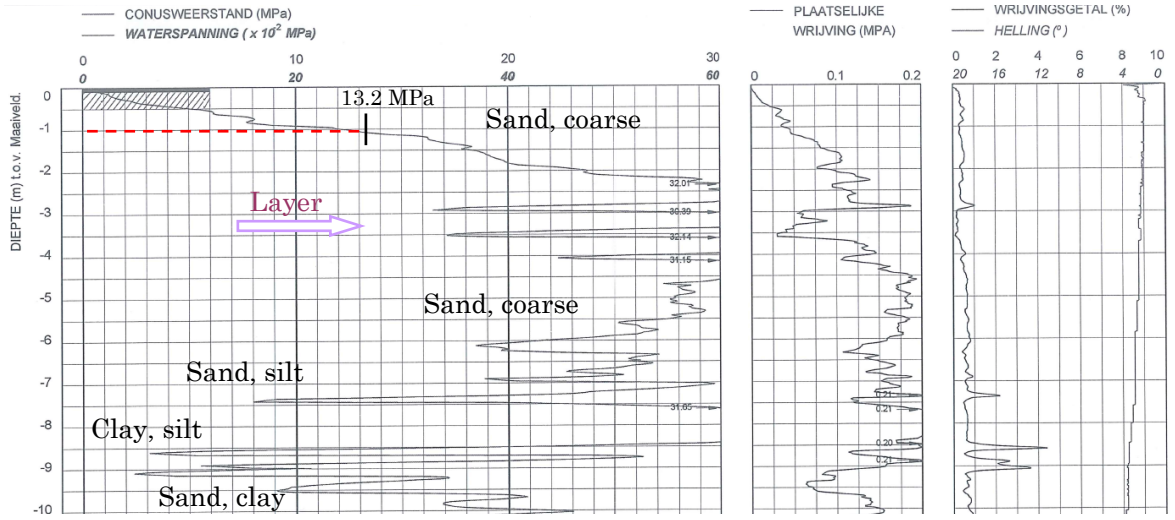

Figure 5-12 Cone penetration test S02; Drainage tube area, mean water line

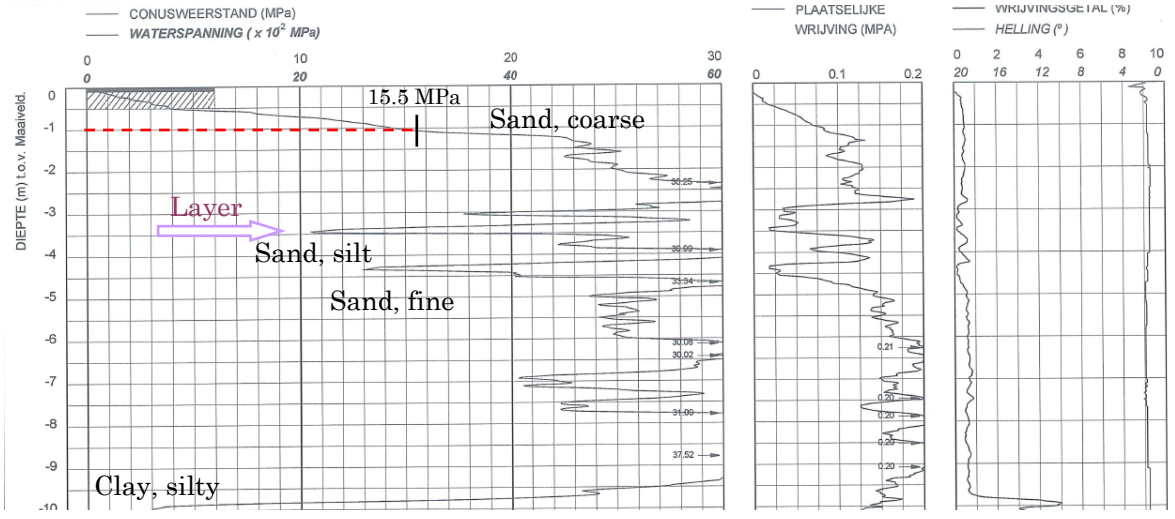

Figure 5-13 Cone penetration test S04; Drainage tube area, high water line

The results of the cone penetration tests, for depths to ten metres, are shown in Figure 5-8 to Figure 5-13. The active layer lies within this region. The cone resistance at a depth of one metre is given for each measurement.

Table 5-1 Soil type classification [2]

Soil type	Friction ratio	Cone resistance
Sand, coarse	0.4 %	
Sand, moderate	0.6 %	5 – 30 MPa
Sand, fine	0.8 %	
Sand, silt	1.1 %	
Sand, clay	1.4 %	5 – 10 MPa
Clay, loam	1.8 %	
Loam	2.2 %	
Clay, silty	2.5 %	
Clay	3.3 %	0.5 – 2 MPa
Clay, humus	5.0 %	
Peat	8.1 %	0 – 1 MPa

The cone resistance at the reference area (Figure 5-8 to Figure 5-10) is below 10 MPa for depths to one metre (active zone) at the low water line. At the high water line, this resistance becomes approximately 23 MPa. The measurements at the drainage tube area (Figure 5-11 to Figure 5-13) differ from these values. The cone resistance is approximately 17 MPa, for depths of one metre, at the low, mean and high waterline. The sand at the low and mean water line at the drainage tube area is moderate to coarse, according to the classification from Table 5-1

5.1.3 Permeable gravel layers at Hvide Sande

Unlike the Dutch shell layers the subsoil of the beach near Hvide Sande contains very permeable gravel layers. These layers are remains from the glacial period (Figure 5-14). The grain size of these granules varies between 1 - 4 mm or more. The layer thickness varies between 1- 40 cm or more. The gravel areas differ in size and depth. A shortcut between the higher and lower part of the beach is available, especially when they are connected by tubes.

Figure 5-14 Gravel layers in the active beach subsurface near Hvide Sande, Denmark

5.1.4 Impermeable layers in the beach

The cone penetration tests, shown earlier in section 5.1.2, indicate that clay and silt layers are present at the Dutch beach. The clay layers act as an impermeable layer where pore pressures are high. These layers are located at different depths. Sometimes, they can be observed at the beach surface. Field measurements, done by Pauw (2009), confirm that a thick clay layer is located at a depth of eighteen metres. A significant mixing zone is observed at the front and bottom of the developing fresh submarine groundwater tongue under this layer. The clay layer provides a seepage area which extends many metres offshore. The vertical drainage tubes, installed at the active beach surface, will only reach the thin clay layers (drills of Figure 5-15).

5.2 Sediment analysis of the beach at Egmond aan Zee

The sedimentology of the beach near Egmond aan Zee is studied by taking a large number of sediment samples. The first set of samples was taken from the surface at a depth of 30 cm near the mean waterline. These measurements were done along 21.5 km of coast (Figure 5-16). The starting point was IJmuiden, south of Castricum aan Zee. The route is divided into a number of different areas. There are two southern reference areas REF S2 and REF S1 (without tubes) and two northern reference areas REF N1 and REF N2 (without tubes). In between, two tube areas are situated; PEM 1 and PEM 2. This study focuses on PEM 1, because less than half of the number of tubes are installed at PEM 2 (see Appendix F). Near tubes measurements were done every 250 m. The space between each row of vertical drainage tubes is 100 m. In addition a number of box measurements were done (Figure 5-16). The purpose of these samples was to investigate differences in sedimentology near the drainage tubes. In this way the local variability of grain properties could be determined. One box consists of nine measurements at a depth of thirty centimetres. The distance between each sample is ten metres. At the drainage tube area PEM 1 two box measurements were done. Finally, a number samples were taken from the subsurface with a drilling rig (see Figure 5-15). The first row of measurements was sampled at RSP pole 44500 at the reference area REF S1 (Figure 5-16). Within the active zone, every forty centimetres a sample was taken. Below a depth of one metre, this was done every metre. The same measurements were done near the drainage tubes (Figure 5-16).

Figure 5-15 Drilling rig used to take deep samples from the subsurface

Field measurements of grain sizes in The Netherlands by Hugo Ekkelenkamp | Location: The coast between IJmuiden and Bergen aan Zee | Date 13th of November 2009

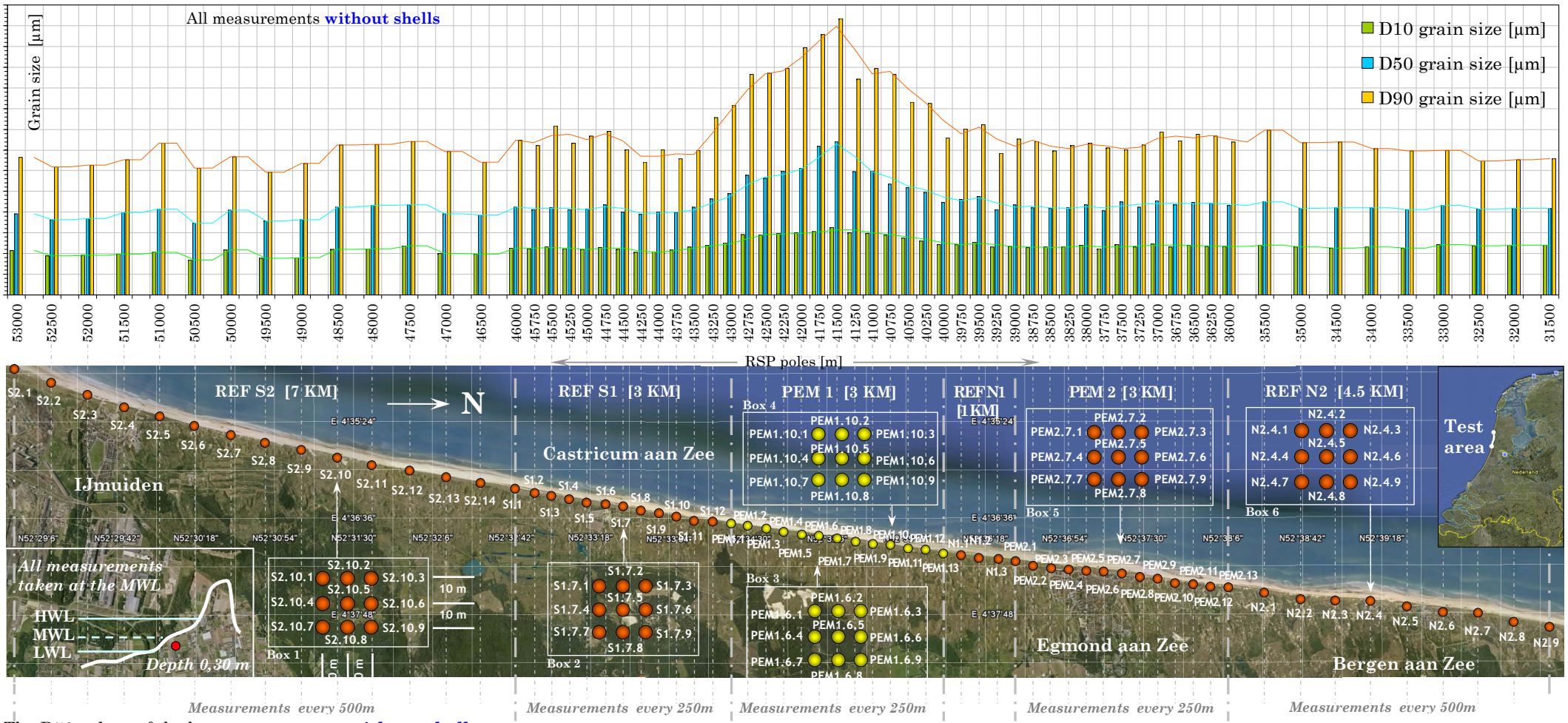

The D50 values of the box measurements without shells

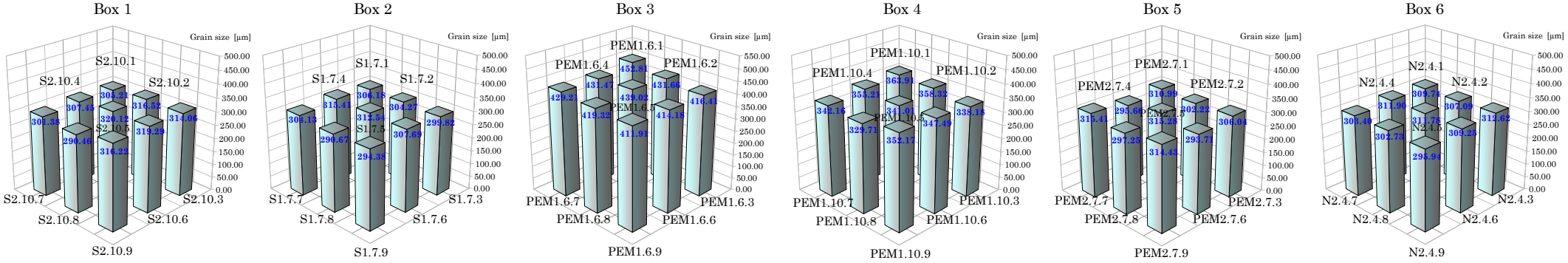

Results of the depth measurements at Egmond aan Zee

Without shells

Location: **Reference** area, at **RSP 44500**

Date of measuring 27th of April 2010
by Hugo Ekkelenkamp

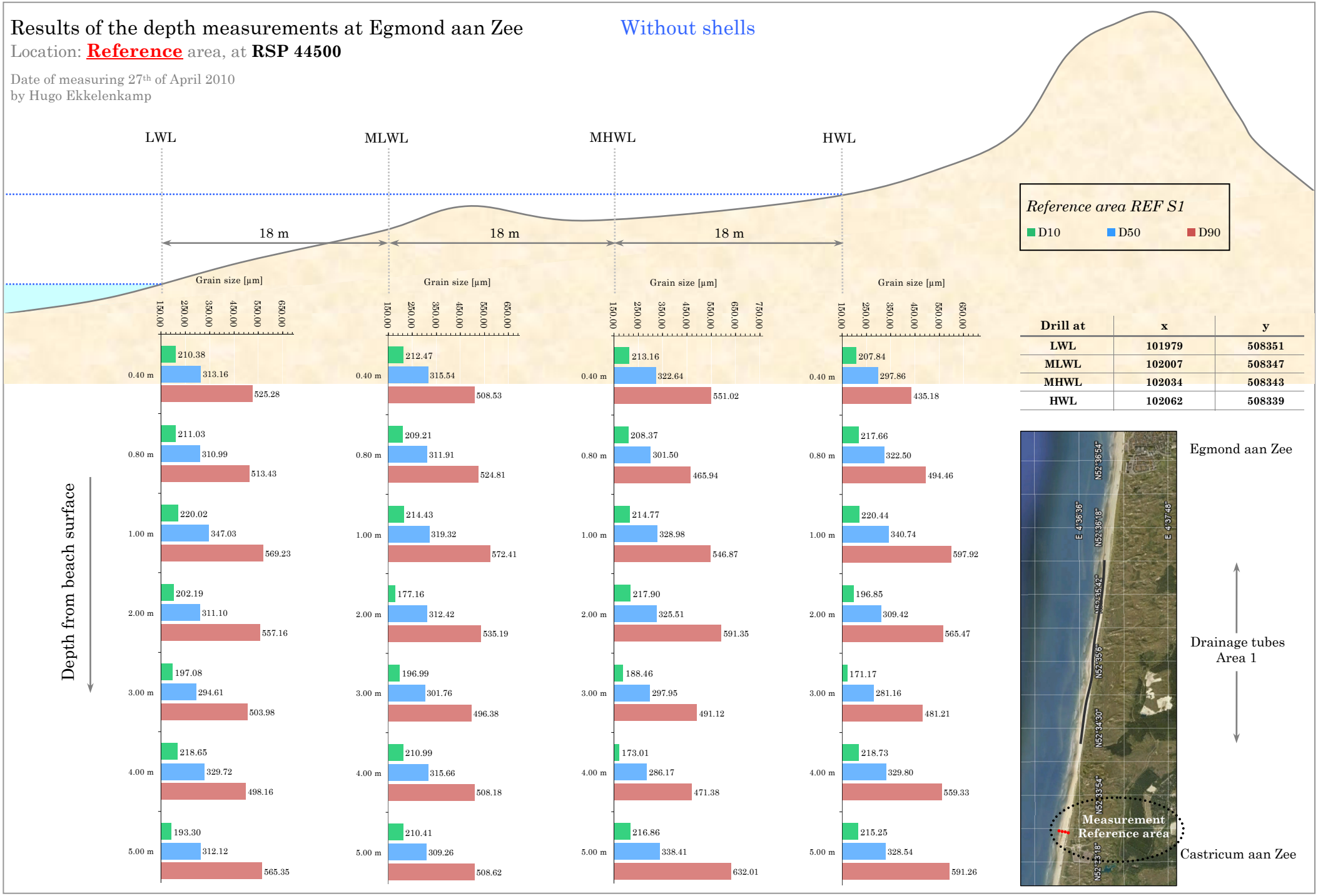

Drill at	x	y
LWL	101979	508351
MLWL	102007	508347
MHWL	102034	508343
HWL	102062	508339

Egmond aan Zee

Drainage tubes
Area 1

Castricum aan Zee

Results of the depth measurements at Egmond aan Zee

Without shells

Location: **Drainage tube** area, at **RSP 41500**

Date of measuring 27th of April 2010
by Hugo Ekkelenkamp

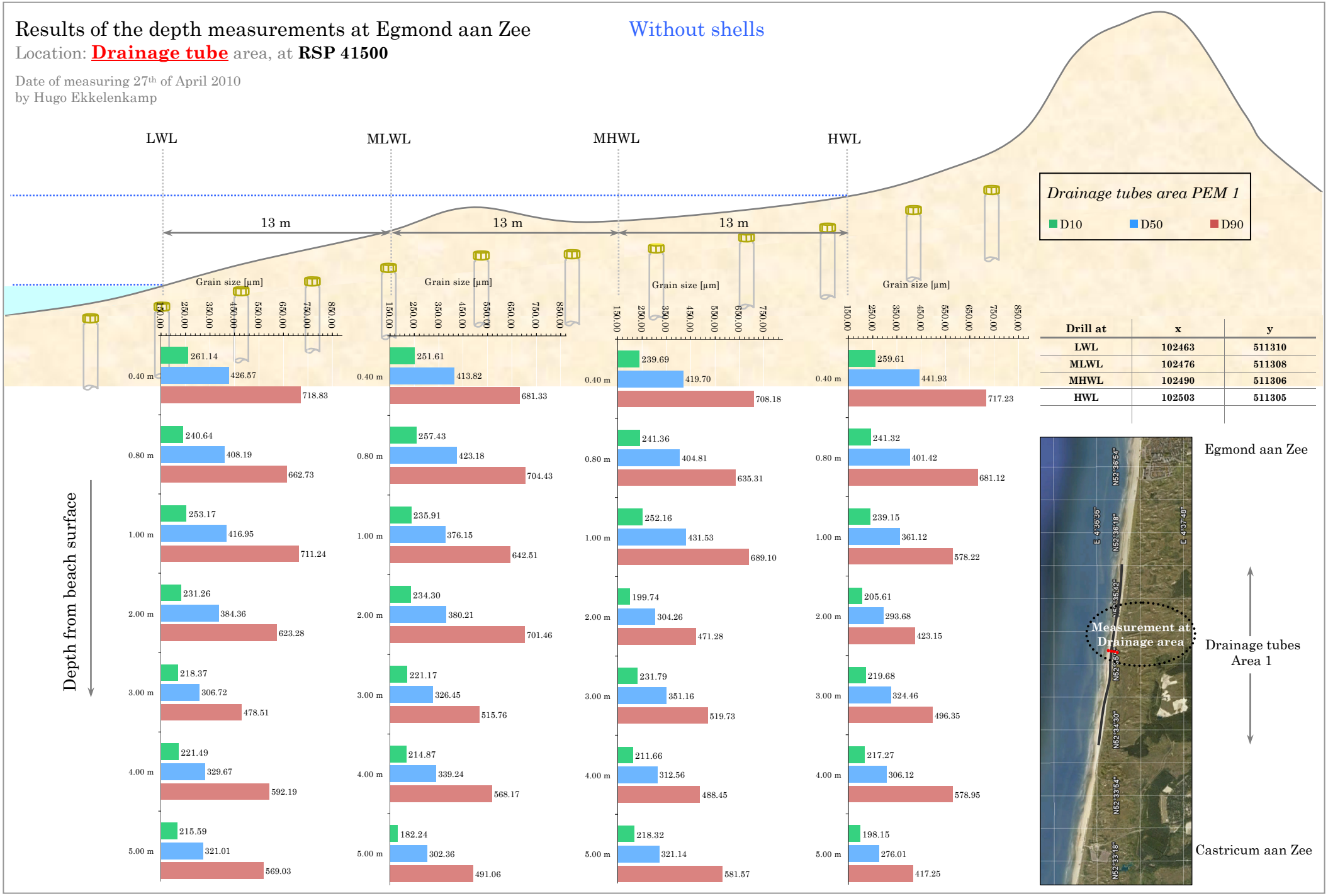

Drill at	x	y
LWL	102463	511310
MLWL	102476	511308
MHWL	102490	511306
HWL	102503	511305

Egmond aan Zee

Drainage tubes Area 1

Castricum aan Zee

5.2.1 Grain diameters

Almost all measurements, showed in de graphs of Figure 5-16, included a shell fraction. First, every sample was analysed with shells. Secondly, the shells were removed by a labour intensive method using different kinds of acids [further described in Appendix B]. Then, the samples without the shell fraction were analysed again. This resulted in the grain size of the sand fraction without any shells. The average median grain size at the southern reference areas is 302 µm (±40µm). This D_{50} value increases and decreases gradually along the drainage tube area PEM 1. It reaches a maximum value of 470 µm near RSP pole 41500. On average, the grain size at this tube area is 398 µm (±90µm). This value is, on average, 95 µm bigger than the reference area. The median diameter along the northern reference area remains more constant, where it has an average value of 312 µm (±15µm). The same pattern holds for the D_{10} and D_{90} values. The sediment at the northern reference area may consist of nourished sand. Sand from this area contains very few shell fractions and looked very homogeneous.

From the results of the box measurements (Figure 5-16), it can be concluded that the grain size varies locally with ±25µm at the reference area and ±40µm at the drainage tube area PEM 1. These values are within the natural variability according to the earlier measurements. The grain size at the drainage tube area PEM 1 is approximately 427µm (±20µm) and 347µm (±20µm) at respectively box measurement 3 and 4. Again, these values are bigger than the grain diameters at the reference areas. In addition to the measurements, made along the beach near Egmond aan Zee, ten samples from the deep subsurface were taken (Figure 5-17).

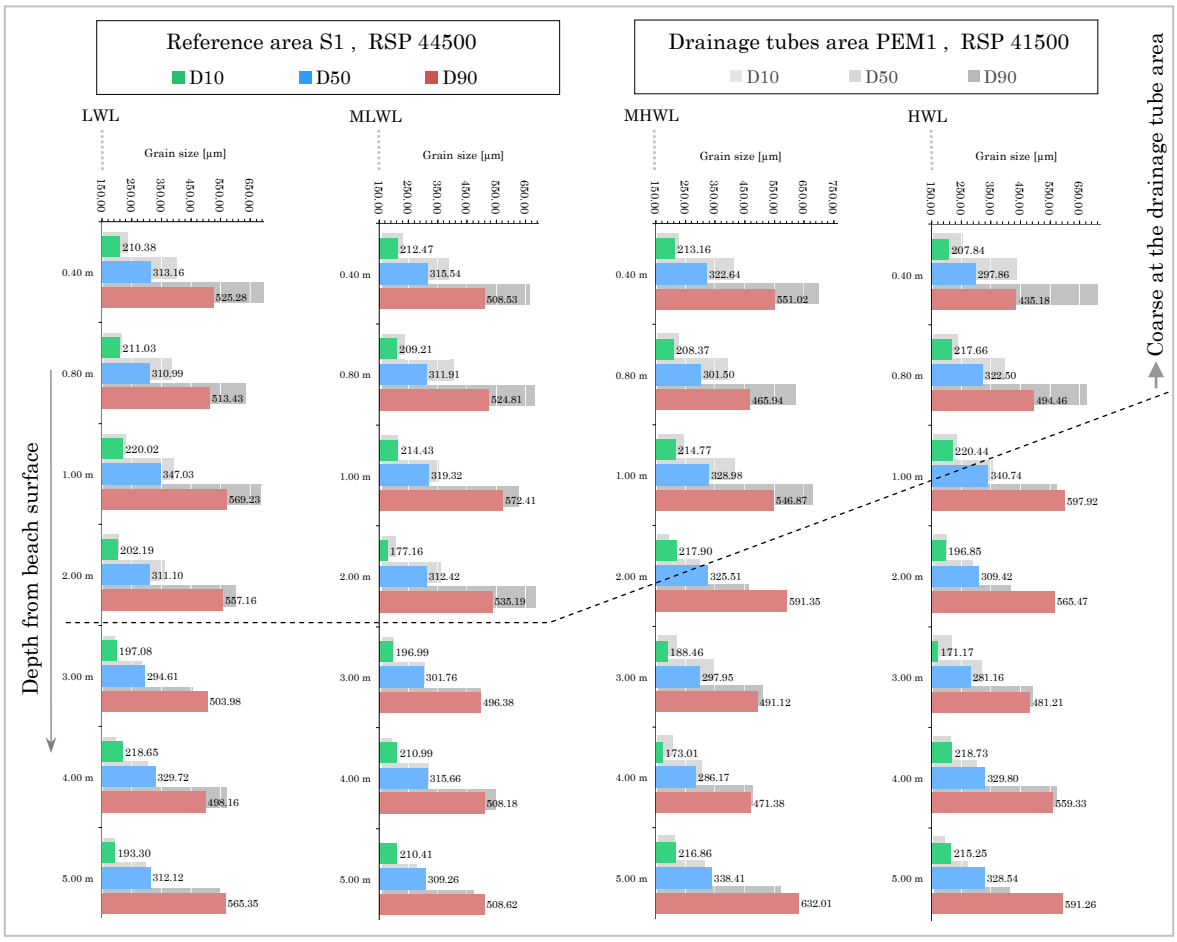

Figure 5-17 Difference between the subsurface of the reference and tube area without shells

These depth measurements, done at two different locations (Figure 5-16), confirm the findings of the field measurements along the beach. This is true, even for the decrease of the grain size with the depth, at the tubes area. Also the samples from 0.4 m depth are compared with the samples from 0.3 m depth.

The grain size at the reference area S1 is quite constant. Its average value is 315 µm (±33µm). At a depth of three to four metres the sediment is more fine. This might indicate a silty sand layer. The variation of the grain size is slightly smaller than that of the sediment from the beach surface (which is ±40µm). This could be the case due to the churned active layer which contains more homogeneous sediment. The layers present in the subsurface are from different moments in time. The grain size at drainage tube area PEM 1, also shown in Figure 5-17, differs significantly from the grain size at the reference area. In particular, the sediment at the active layer, from zero to two metre deep, is coarser. This transition depth decreases from the low to the high waterline. The grain size is on average 412 µm (±29µm). Near the high water line, only the upper eighty centimetres of beach is coarse. The reason for this could be the stronger hydrodynamic forces acting near the low water line, which cause deeper erosion of the beach during storm events. Below the coarse upper layer, the median sediment size is on average 319 µm (±40µm). This value is consistent with the grain size at the beach surface along the reference areas and box measurements at area PEM 1 (which are 302 µm ±40µm).

In summary, the sediment at the beach surface along the drainage tube area is coarser than that of the reference areas (around 95 µm bigger). Locally, the variation of the grain size does not change. At the reference area, the grain size does not vary substantially in depth. But, at the drainage tube area PEM 1, the upper one to two metres of the beach surface is coarser than the reference area. This seems to coincide with the active beach envelope.

5.2.2 Grain size fractions

The increased grain size at drainage tube area PEM 1 is reflected in the grain size fractions (Figure 5-18). The fine and medium fraction decreases, while the coarse fraction increases.

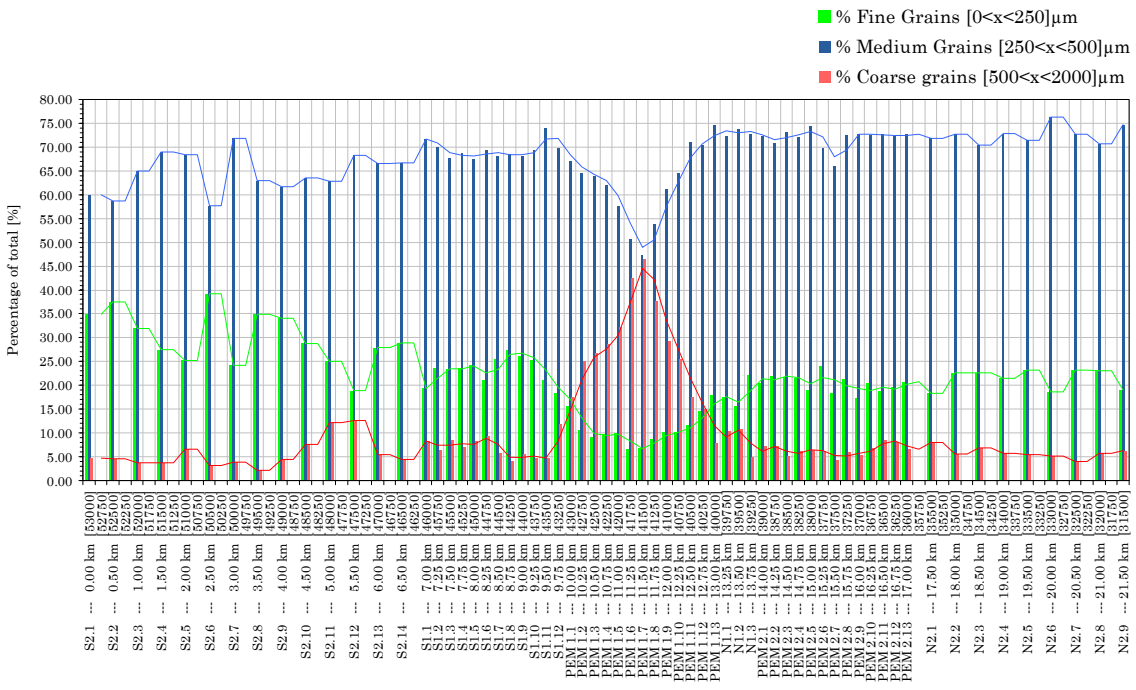

Figure 5-18 Distribution of different gradations at Egmond aan Zee, without shells

Most remarkable is the distribution of the very coarse grain fraction of 1000 to 2000 µm (Figure 5-19). Normally, only low percentages of these grain sizes are found at the beach near Egmond aan Zee [90]. One should think of peaks of 0 – 1 %. The fraction of very coarse grains along drainage tube area PEM 1 increases and decreases gradually. It reaches a maximum value of 3.85 % near RSP pole 41250.

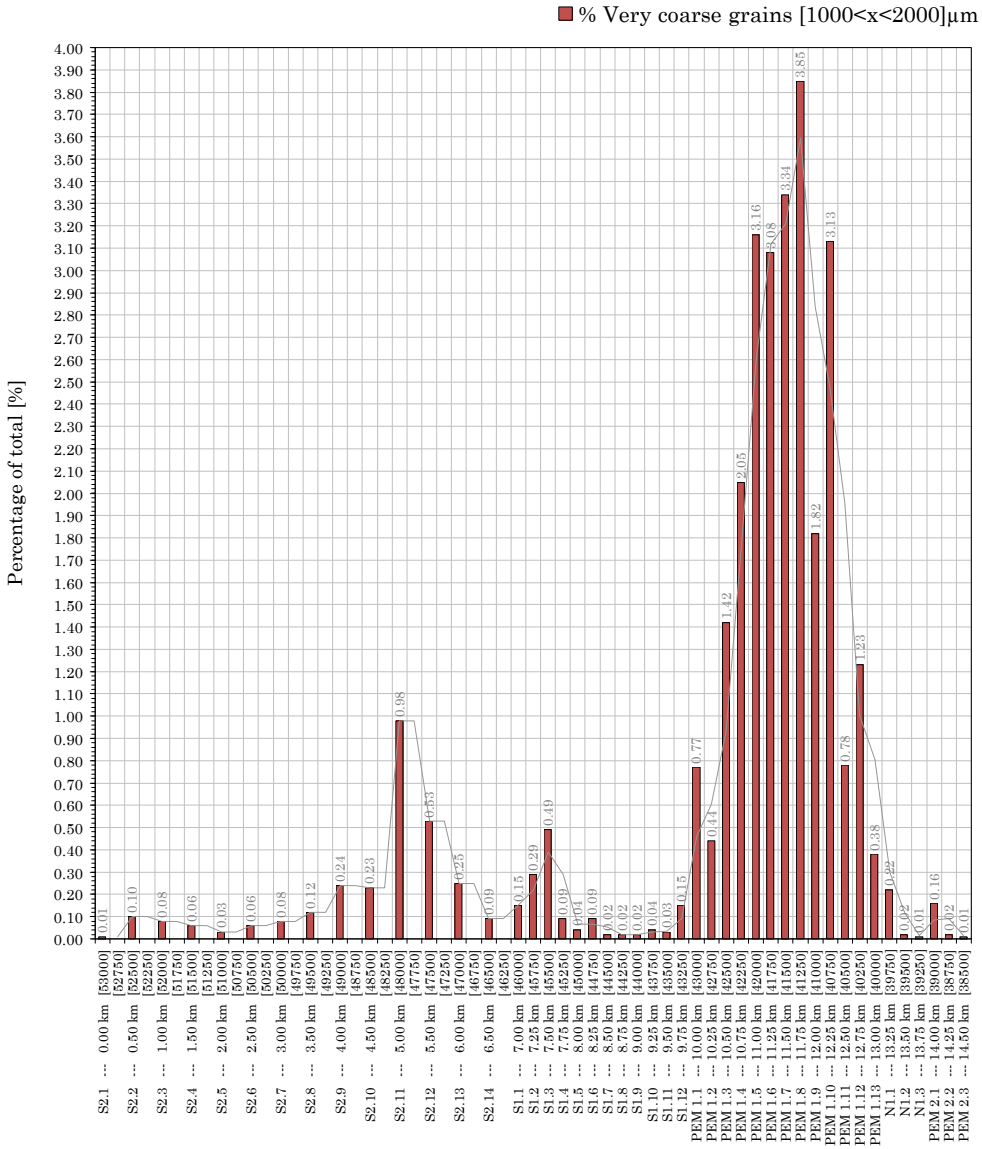

Figure 5-19 The fraction of very coarse grains at the beach near Egmond aan Zee, without shells

5.2.3 Grain size distribution

The sediment samples can also be compared by their grain size distributions. Here, a log-normal Gaussian distribution is considered with a geometric grain size scale. The grain size distribution of all sediment samples are included in Appendix D.

Most interesting is the transition between the southern reference area S1 and drainage tube area PEM 1 (Figure 5-20). Not only the grain size increases, but also the shape of the grain size distribution changes. The sorting of the sediment refers to the range of sizes present in

the sample. As the standard deviation increases, the sediment becomes poorly sorted. A wide range of grain sizes is present along the drainage tube area. This is visualised by the less sharp peak in the distributions.

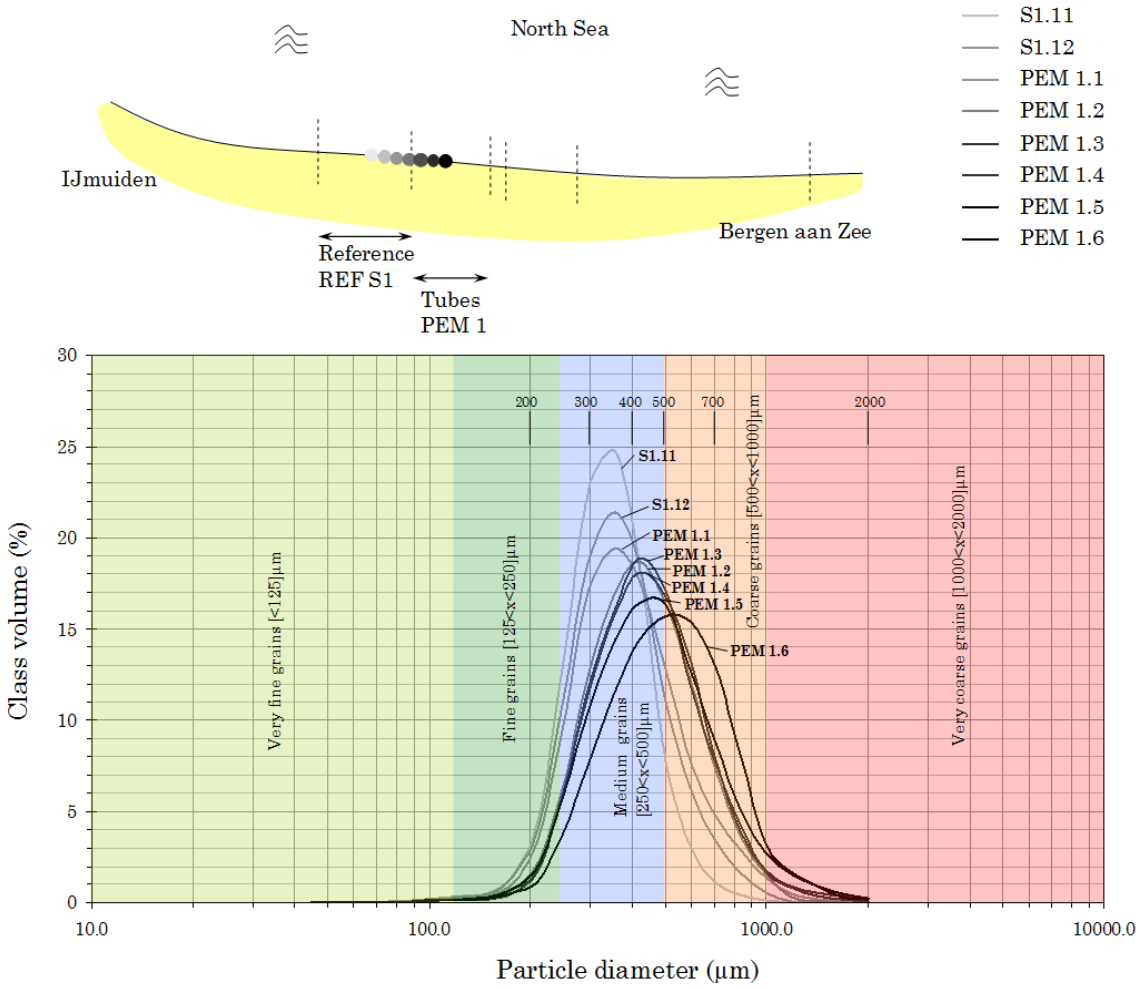

Figure 5-20 Class volume distribution of sample S1.11 to PEM 1.6 at Egmond aan Zee, without shells

Besides the sorting of the sediment, two other measures describe the distribution; the skewness and kurtosis. The transition from the reference to the drainage tube area causes the distributions to be coarse skewed (asymmetrical to the right). This indicates an erosive environment where finer material has been winnowed out by the action of currents and waves. In addition, the curves become platykurtic, which means that the peakedness of the distribution decreases. This indicates that both gravel and fine sand populations are present along the drainage tube area.

5.2.4 Shell fraction

The beach near Egmond aan Zee contains large amounts of shell. Section 5.1.1 already described the shell layer at the beach (sub)surface. At varying depths, shell layers were found. The shell fragments varied in shape and size. It is interesting to find out how the large concentrations are distributed along the beach near Egmond aan Zee.

This is examined by analysing all samples before and after a treatment with acids. Although this is a labour intensive method, it clearly shows the locations where shells are present. Figure 5-21 shows the amount of shells present along the beach near Egmond aan Zee.

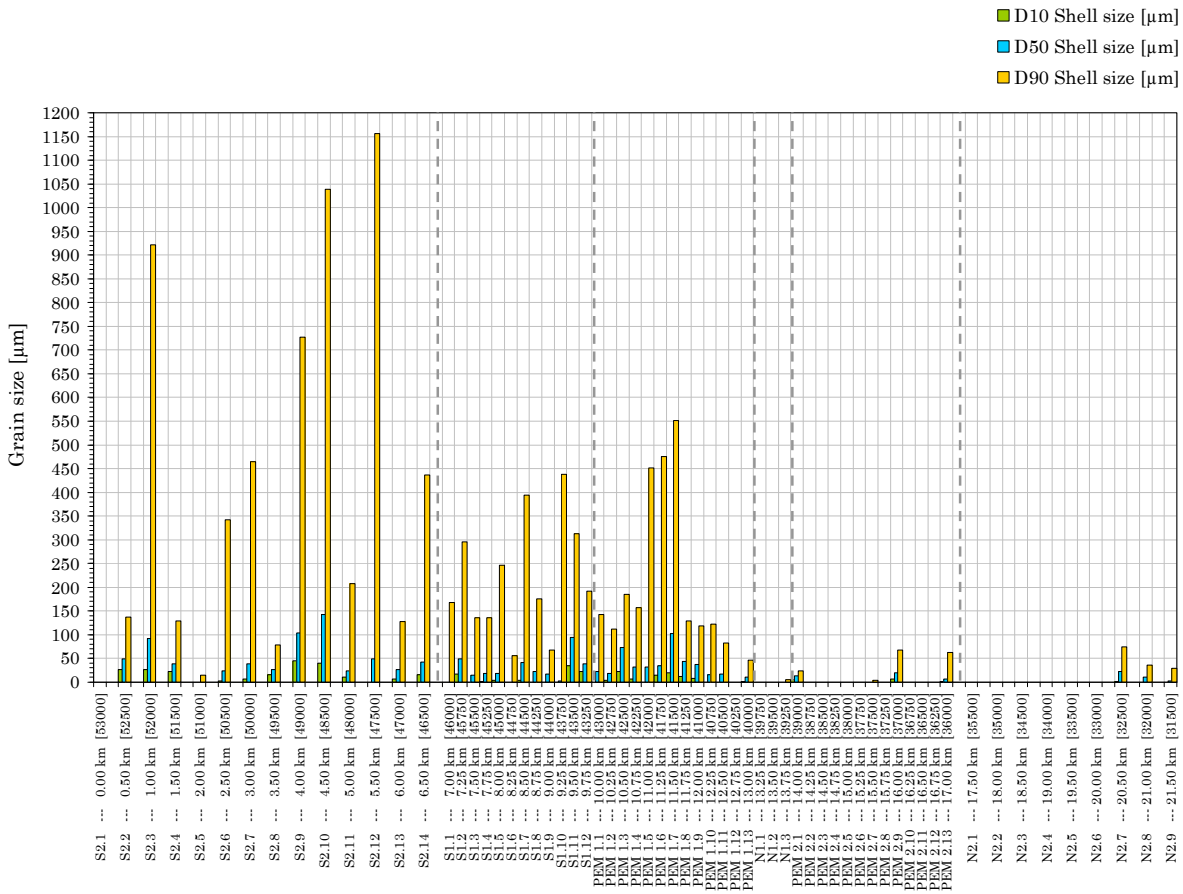

Figure 5-21 Shells present along the beach near Egmond aan Zee

Shells are present at both the southern reference areas and drainage tube area PEM 1. It is striking that along the northern reference area virtually no shells are present. This area is known for its beach nourishments, which have been made in the past. The shell fragments vary in size, with a range of 10 to 1160 µm .

5.2.5 Aspect ratio and sphericity

The shape of the sediment along the beach near Egmond aan Zee is studied using a very sophisticated device. An image was created from every single grain. The aspect ratio was calculated using the minimum and maximum Feret's diameter (Figure 5-22). The sphericity was calculated using the surface of the image and its perimeter (Figure 5-23). A large number of particles (up to 10^6) were analysed within a range of 200 to 400 µm .

The results clearly show that the sediment along the drainage tube area PEM 1 is more asymmetrical than at the reference areas (Figure 5-22). In addition, sand grains at the drainage tube area are more irregularly shaped than the sand at the reference areas (Figure 5-23).

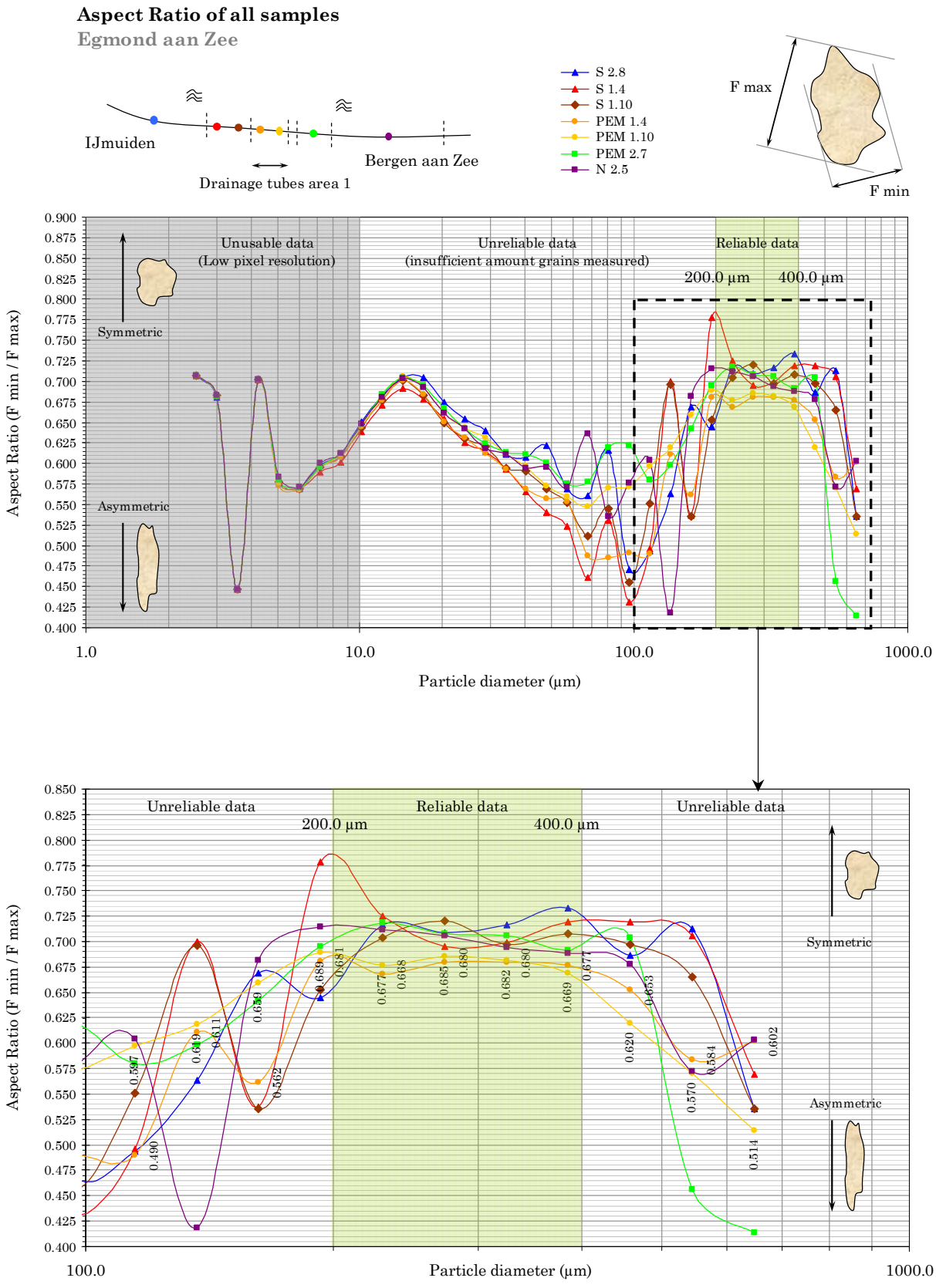

Figure 5-22 Aspect ratio of the sediment particles along the beach, without shells

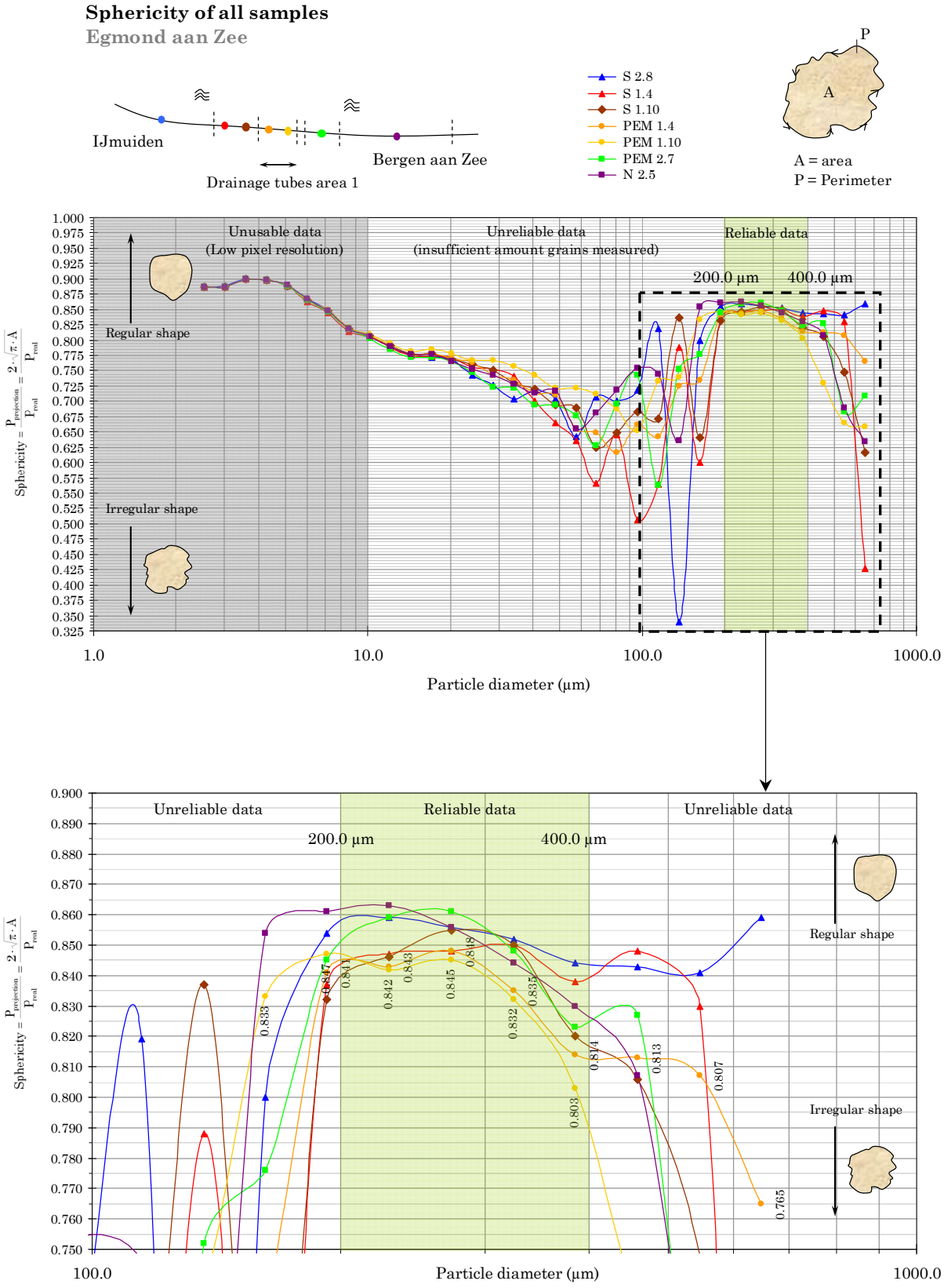

Figure 5-23 Sphericity of the sediment particles along the beach, without shells

5.3 Sediment analysis of the beach at Hvide Sande

The sedimentology of the beach near Hvide Sande is studied by taking a large number of sediment samples. The samples were taken from the beach surface at a depth of thirty centimetres near the mean waterline. These measurements were done along 27 kilometres of coastline (Figure 5-25). The starting point was Hvide Sande, north of Skodbjerge. The route was divided into a number of different areas. The layout is similar to the field measurements done at the beach near Egmond aan Zee. Again, four reference areas were chosen, with the drainage tubes areas in between. The northern reference areas are REF N1 and REF N2. Both contain measurements with a spacing of five hundred metres. The southern reference areas are REF S1 and REF S2. One additional reference area REF M1 is located between the drainage tubes areas PEM 1 and 2. This study focuses on the largest drainage tube area PEM 2, because all tubes are installed at this location. A number of extra drainage tubes at area PEM 1 were installed recently. Their upper part was exposed above the beach surface (Figure 5-24).

Near the drainage tubes all measurements were done every two hundred fifty metre along the beach. Again, the distance between each row of tubes is one hundred metres. The depth at which a sample was taken is thirty centimetres. The location of the samples was determined with modern GPS equipment and chosen at the mean water line. The coordinates are given in Appendix L.

The beach near Hvide Sande contains many granules. The gravel fraction varies along the beach. The layers of gravel near the surface can be seen at several locations. The gravel fraction is removed from the sample at the laboratory. The methodology is explained in Appendix B. The gravel fraction was analysed separately (Figure 5-25). In this case, the definition of sand is 1 to 2 mm. Fragments larger than 2 mm are categorized as gravel. Shape parameters like the aspect ratio and sphericity could not be analysed, because the sediment along this beach is too coarse.

Figure 5-24 Exposed vertical drainage tube after a storm near Hvide Sande, Denmark

Field measurements of grain sizes in Denmark by Hugo Ekkelenkamp | Location: The coast between Henne and Hvide Sande | Date 15th of December 2009

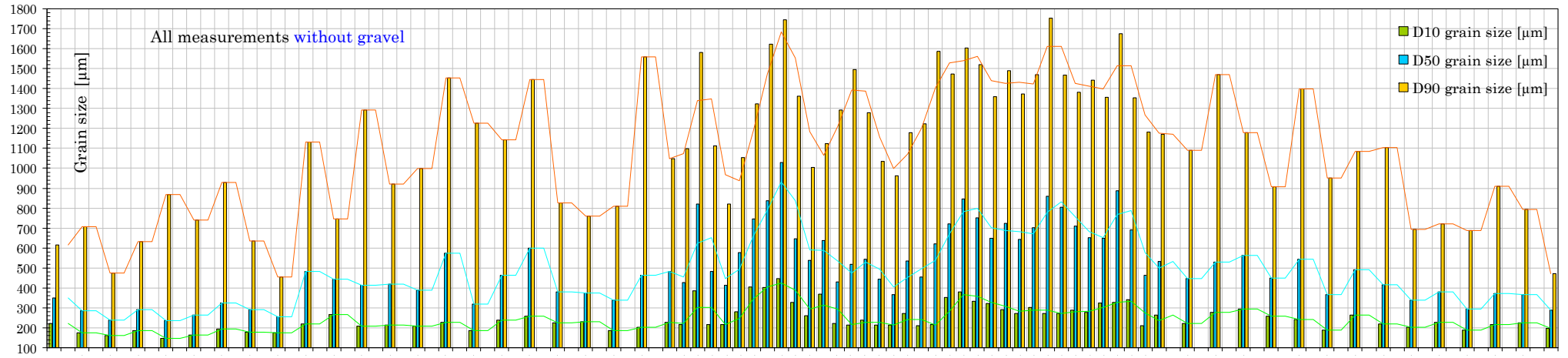

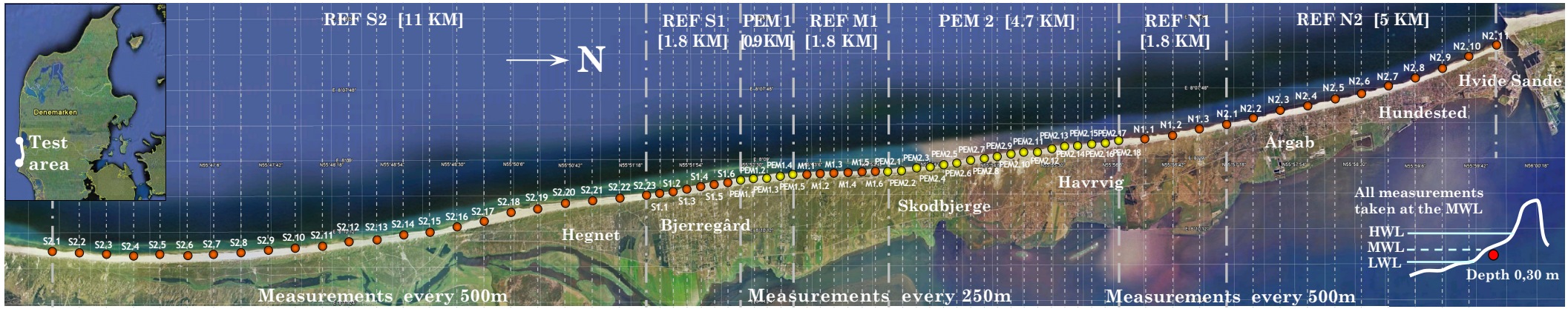

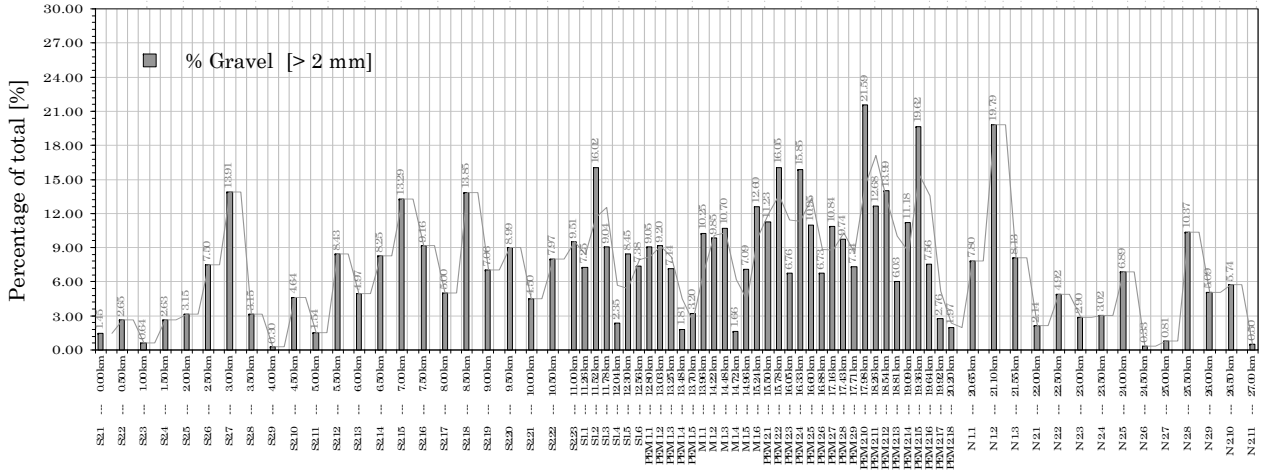

Layers of gravel in the beach

Gravel along the intertidal beach area

5.3.1 Grain diameters

Almost all measurements, showed in Figure 5-25, included a gravel fraction. Every sample was analysed after this fraction was removed from it. The values of D_{10}, D_{50} and D_{90} vary along the beach. Again, near the area where vertical drainage tubes are installed, the sediment is coarser. The average median grain size at tube area PEM 2 increases and decreases rapidly at the borders of this area near PEM 2.2 and PEM 2.17. It reaches a maximum value of 887 µm at sample PEM 2.14. On average, the grain size at this tube area is 687 µm (±208µm). Nearly the same pattern is observable at tube area PEM 1. Although this area has a length of nine hundred metres, an increase of the grain size is recognizable. Along this area the average grain size equals 716 µm (±310 µm).

At the southern reference areas REF S1 and REF S2, the grain diameters are smaller. Here, the average size is 401 µm (±199µm). The median diameters along the northern reference areas are very similar with an average value of 417 µm (±145µm). The pattern of the grain sizes is quite random. The northern part of REF N2 is continuously nourished by a sediment by-pass at the Hvide Sande harbour. In the past, many beach nourishments were carried out from Hvide Sande to Skodbjerge. The largest amount of sediment, almost ten million cubic metres, was applied near the beach of Skodbjerge.

In summary, the grain sizes along both drainage tube areas are larger than at the reference areas. On average, this difference equals circa 320µm. Although this value corresponds to the variation of the grain sizes at drainage tube area PEM 1, the distribution of the extreme values is much more concentrated along the drainage tube area. A clear trend is visible along area PEM 1 and 2. The impact of beach nourishments is less clear than at the beach near Egmond aan Zee.

5.3.2 Grain size fractions

The increased grain sizes at both drainage tube areas PEM 1 and 2 are reflected in the grain size fractions of these areas (Figure 5-26). The fine and medium fraction decreases, while the coarse fraction increases.

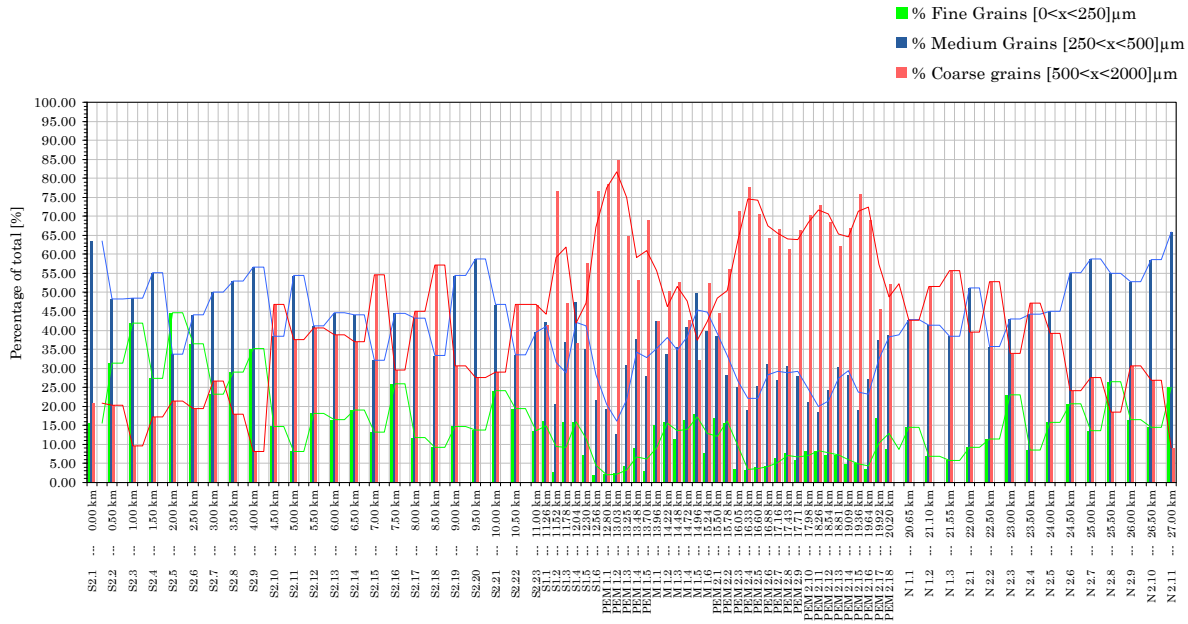

Figure 5-26 Distribution of different gradations at Hvide Sande, without gravel

5.3.3 Grain size distribution

The sediment samples can be compared by their grain size distributions. The transition between the reference area and drainage tube area is one of the most interesting locations to look at. Here, two different locations are amplified. The grain sizes larger than two millimetres are too inaccurate to include. The transition between reference area REF S1 and drainage tube area PEM 1 is shown by Figure 5-27. The sorting of the sediment refers to the range of sizes present in the sample. As the standard deviation increases from REF S1 to PEM 1, the sediment becomes poorly sorted.

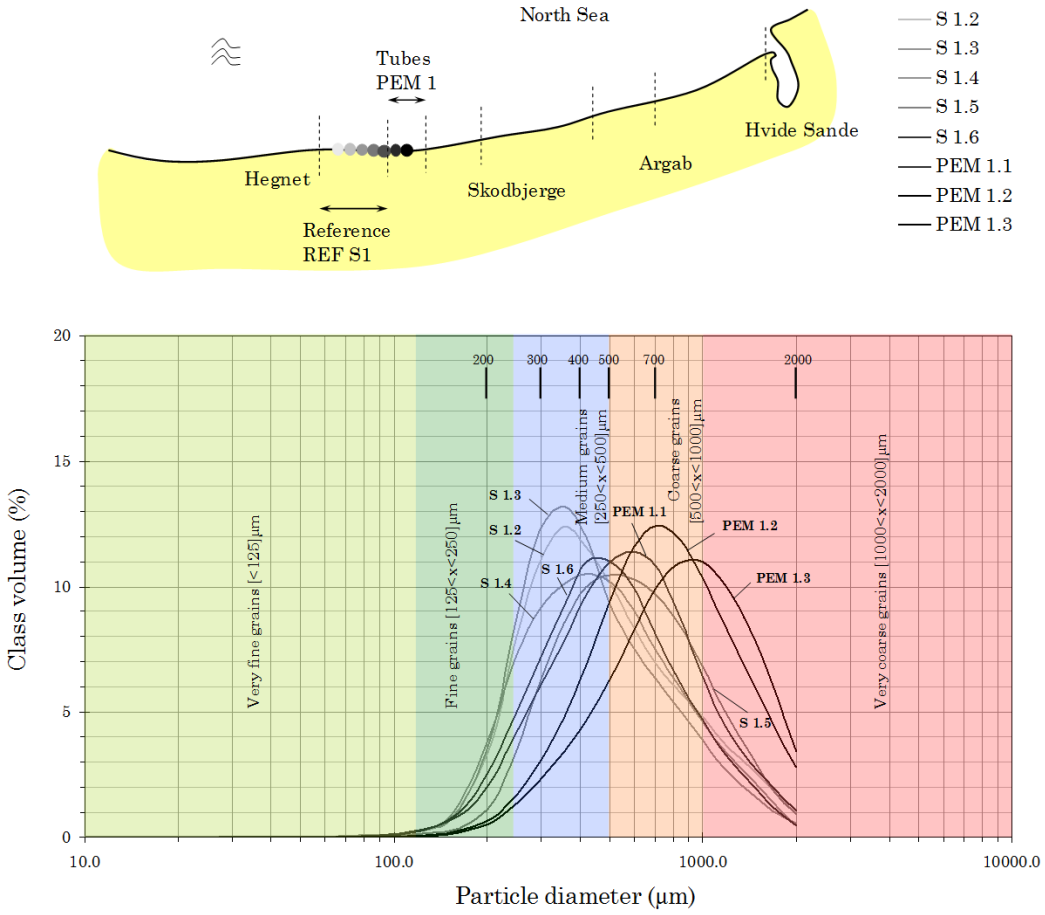

Figure 5-27 Class volume distribution of sample S 1.2 to PEM 1.3 at Hvide Sande, without gravel

Also the skewness changes. The distributions, plotted in the figure, transform from a negative skewness (REF S1) to a more positive skewness (PEM 1). This indicates that the finer materials haven been winnowed out by the action of currents and waves (Duane 1964). The system transforms from a depositional to a more erosive environment.

The platykurtic shape of the distributions at the drainage tube area corresponds to the situation at Egmond aan Zee. The peakedness of the REF S1 distributions is less than that of PEM 1. The extreme populations (coarse and fine) are more present in the samples.

Nearly the same picture can be drawn near drainage tube area PEM 2 (Figure 5-28). Again, the samples become coarser.

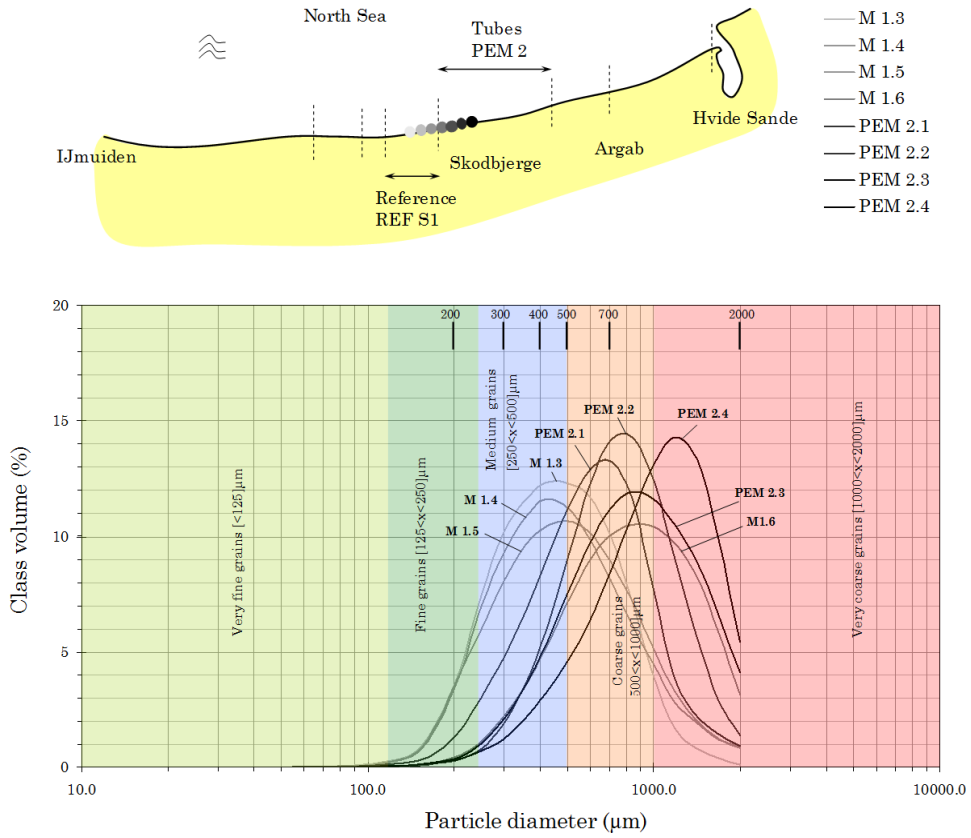

Figure 5-28 Class volume distribution of sample M 1.3 to PEM 2.4 at Hvide Sande, without gravel

It is noteworthy that this time the distributions develop into more leptokurtic curves. This means that the degree of polymodality of the sediments changes the other way. The samples turn out to be better sorted.

5.3.4 Gravel fraction

The gravel fraction is evenly distributed along both the reference and drainage tube areas.

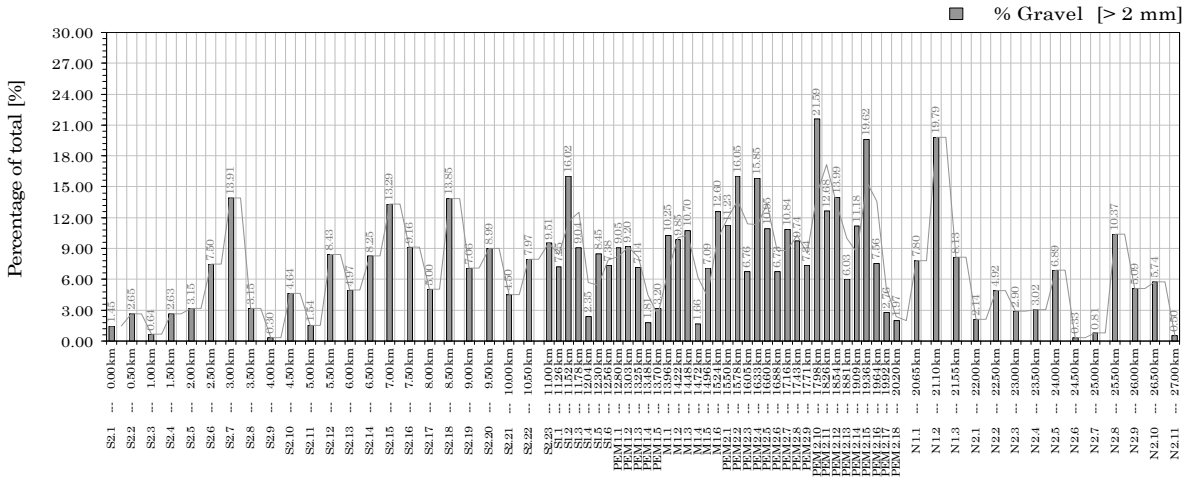

Figure 5-29 Gravel fraction along the beach near Hvide Sande

5.4 Morphological dynamics

Some aspects of the morphological dynamics are studied by measurements of the beach profile, shoreline position and an analysis of the maintenance of the drainage tubes at Egmond aan Zee.

5.4.1 Beach envelope and profiles

The beach profiles along the beach near Egmond aan Zee have been measured many times in the past. Here, the beach envelope is studied by a number of measurements before and after a storm (Figure 5-30 to Figure 5-33). The wind speed and wave height were approx. 16.5 m/s and 4.5 m.

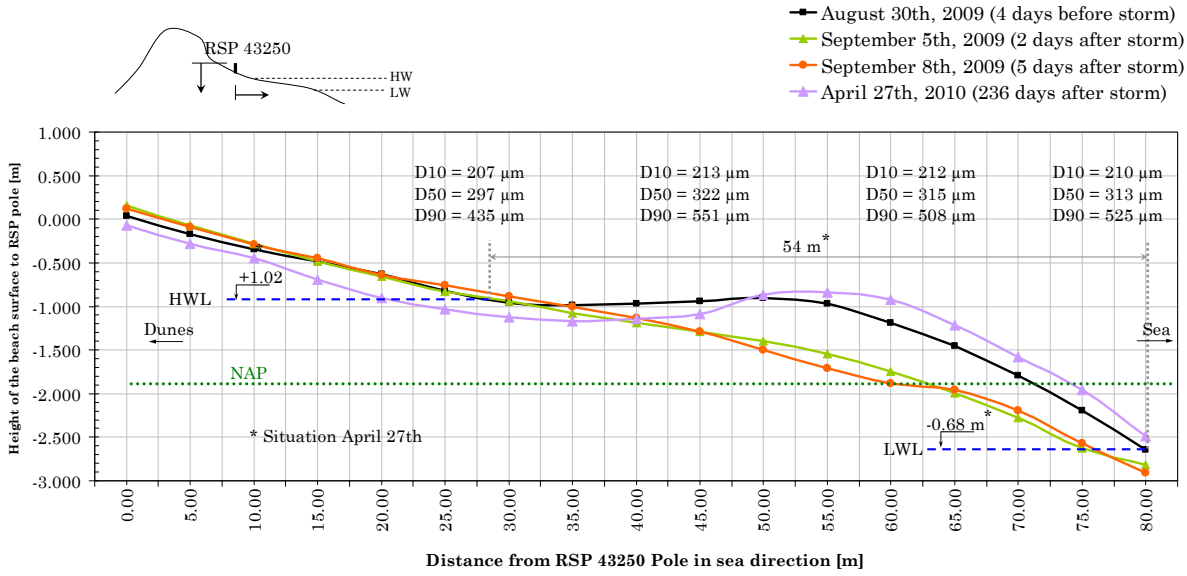

Figure 5-30 Change and adjustment of the beach profile after a storm at the reference area

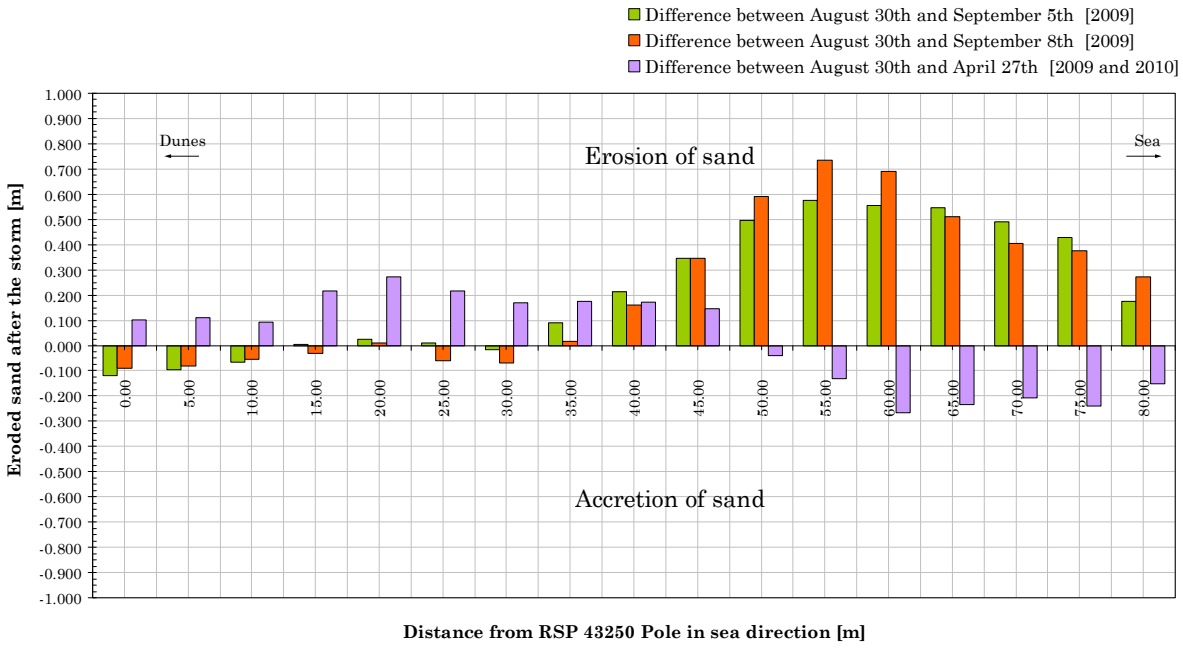

Figure 5-31 Erosion of the beach profile after a storm at the reference area

The beach profile is measured against the RSP poles, which were used as the reference level. Four days before the storm, the first measurement of the beach was made. The erosion and accretion are determined by comparing two consecutive profiles. Two days after the storm, a significant erosion of approx. half a metre near the foreshore of the reference area was recorded (Figure 5-31). The beach continued to erode during the following days. The last measurement, done during the 27th of April, shows a recovery of the beach with an accretion of twenty centimetres on average.

Figure 5-32 shows the measurement done at drainage tube area PEM 1. Again, four measurements of the beach profile were executed. The RSP 42000 pole is used as reference level. As well as the reference area, the foreshore was eroded again. This time, the erosion was limited to thirty centimetres (Figure 5-33).

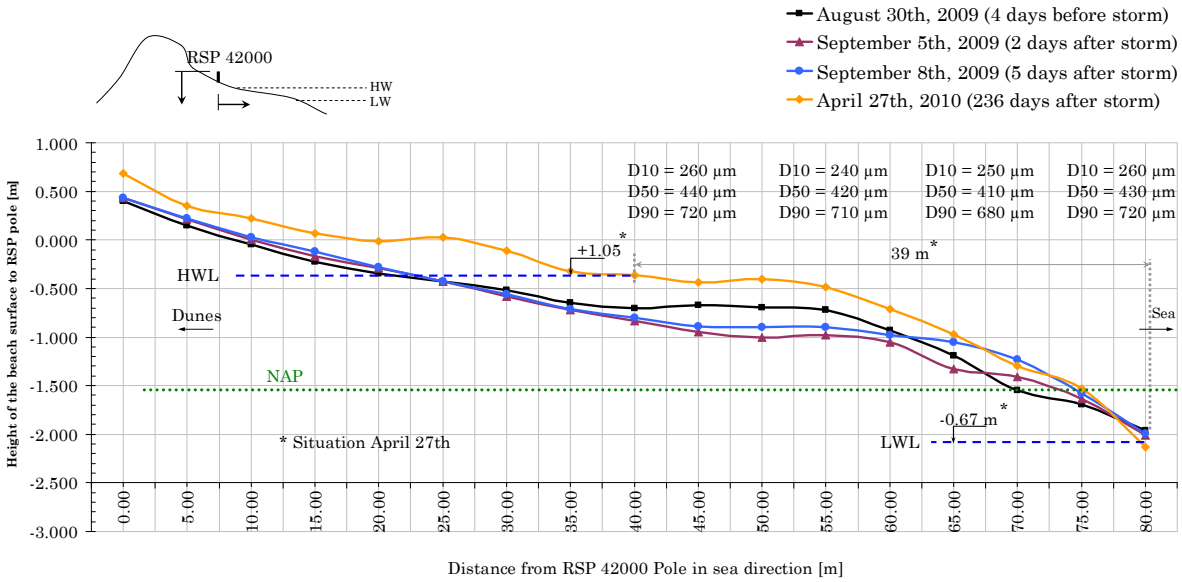

Figure 5-32 Change and adjustment of the beach profile after a storm at the drainage tube area

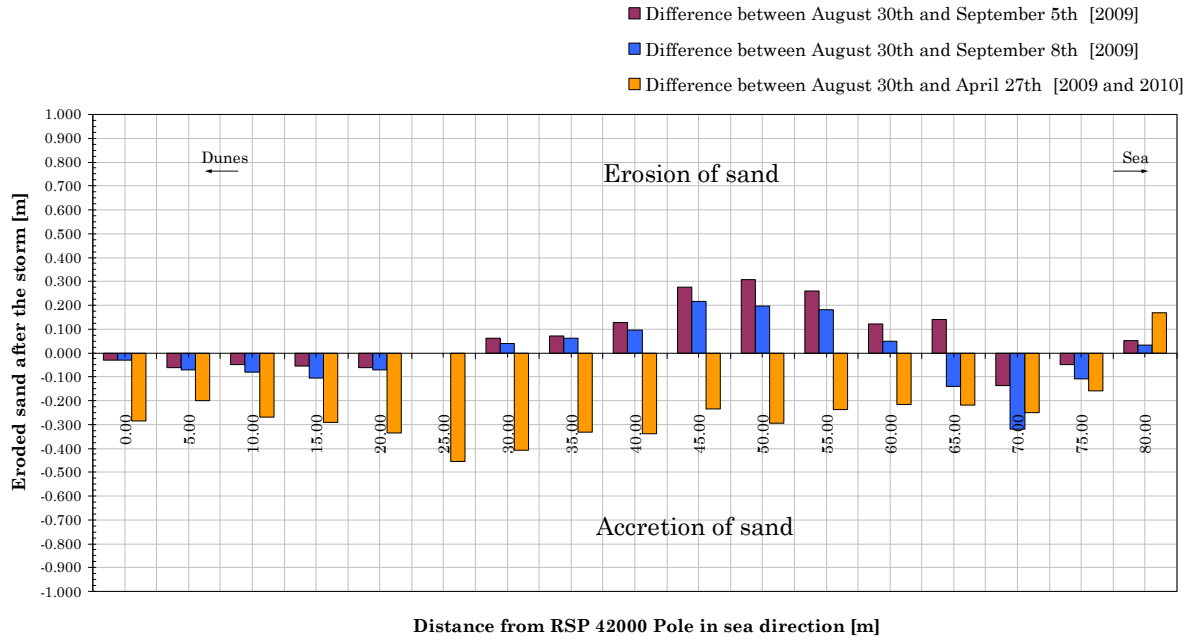

Figure 5-33 Erosion of the beach profile after a storm at the drainage tube area

The data of (Figure 5-30 to Figure 5-33), combined with the Jarkus coastal data, can be used to define the beach envelope (Figure 5-34 and Figure 5-35). This depth can be regarded as the active zone in which the beach erodes or accretes.

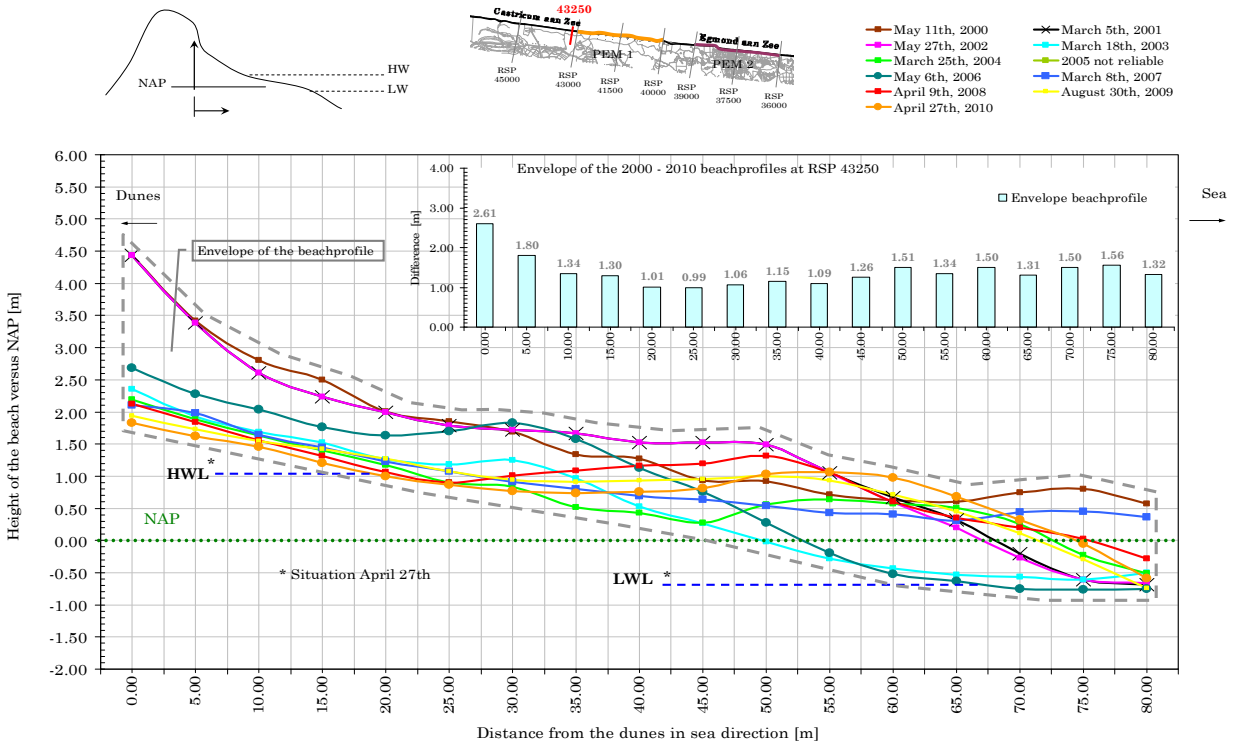

Figure 5-34 Beach envelope at the reference area of Egmond aan Zee [2000 to 2008 Jarkus]

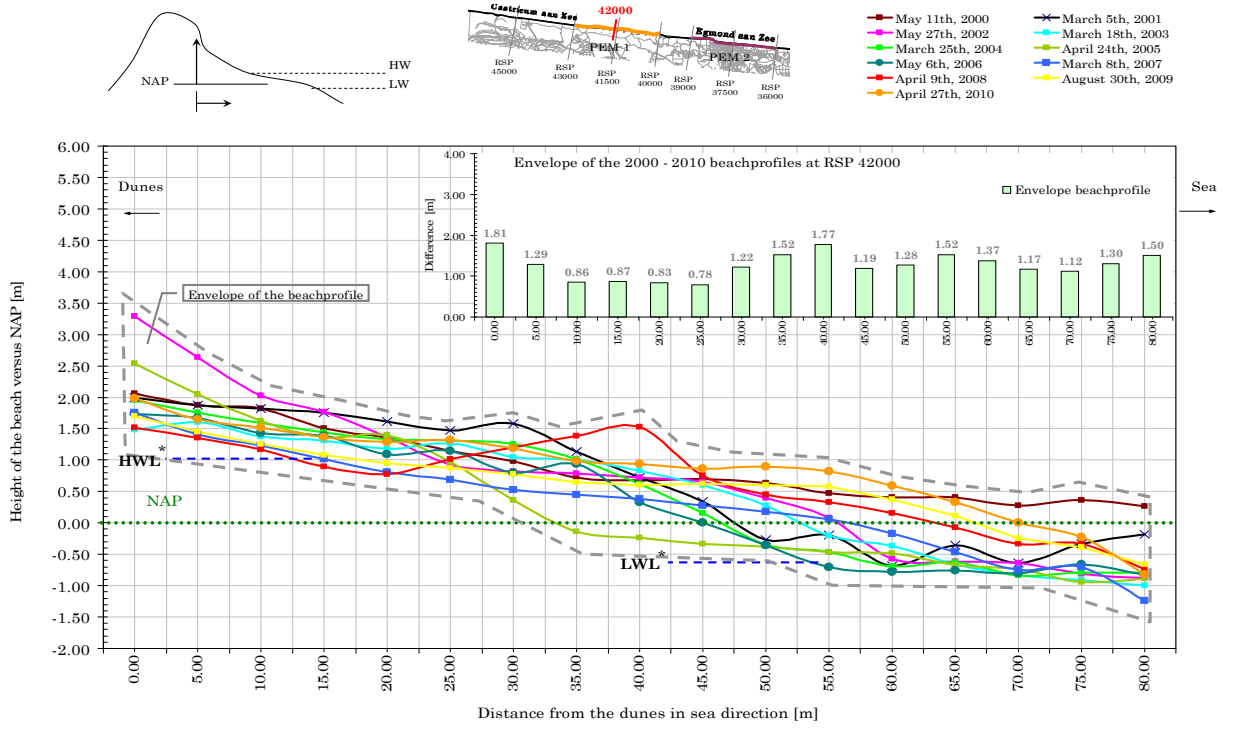

Figure 5-35 Beach envelope at the drainage tube area of Egmond aan Zee [2000 to 2008 Jarkus]

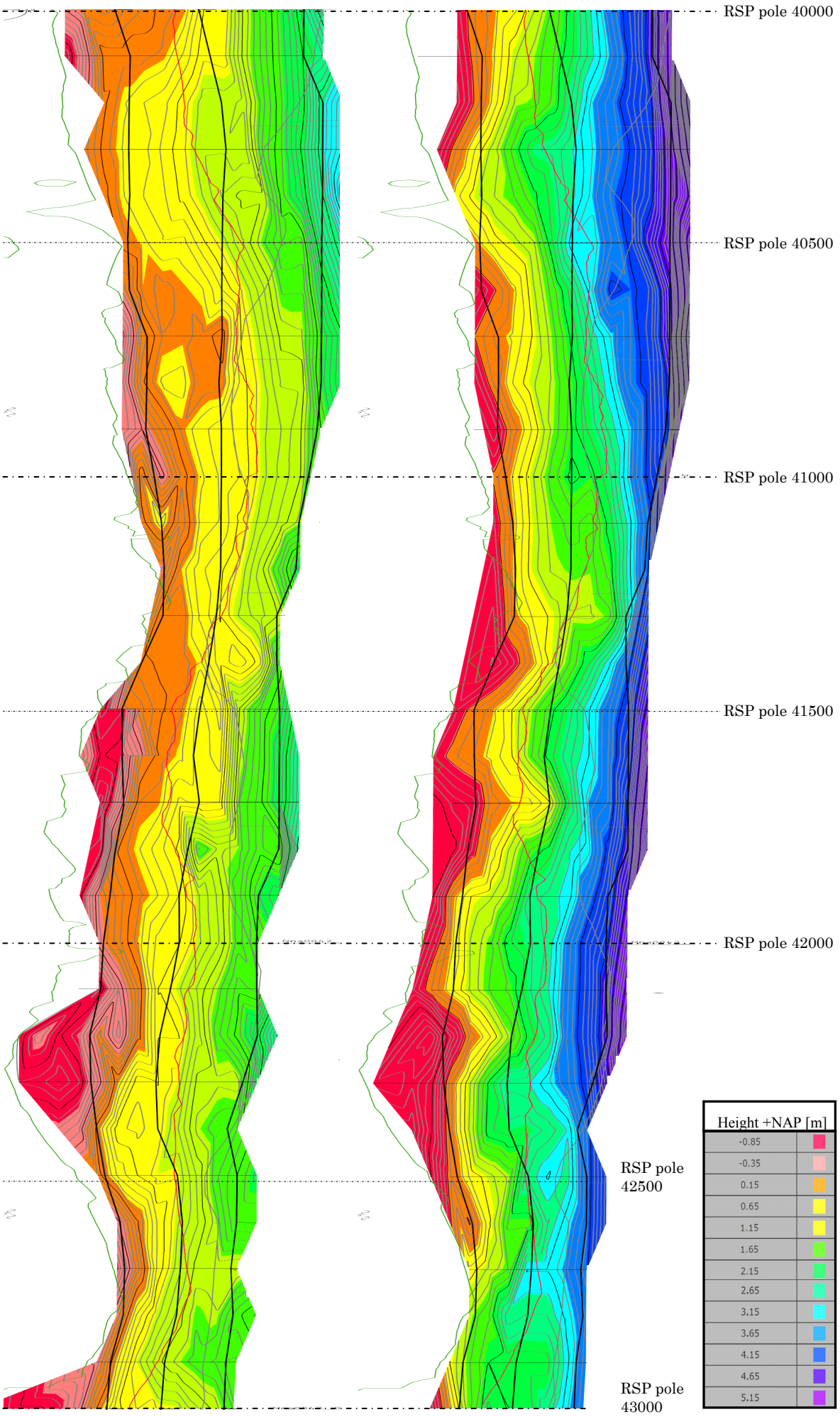
RSP pole 40000
RSP pole 40500
RSP pole 41000
RSP pole 41500
RSP pole 42000
RSP pole 42500
RSP pole 43000
Height +NAP [m]
-0.85
-0.35
0.15
0.65
1.15
1.65
2.15
2.65
3.15
3.65
4.15
4.65
5.15

5.4.2 Analysis of injected drainage tubes

The contractor, who installs the drainage tubes, must maintain the system by injecting a tube when it sticks out of the ground. This can be the case when sediment is eroded after a storm. The depth of each tube was recorded. This data is analysed and visualised by Figure 5-37. A clear decreasing trend is observable, which means that fewer tubes are injected.

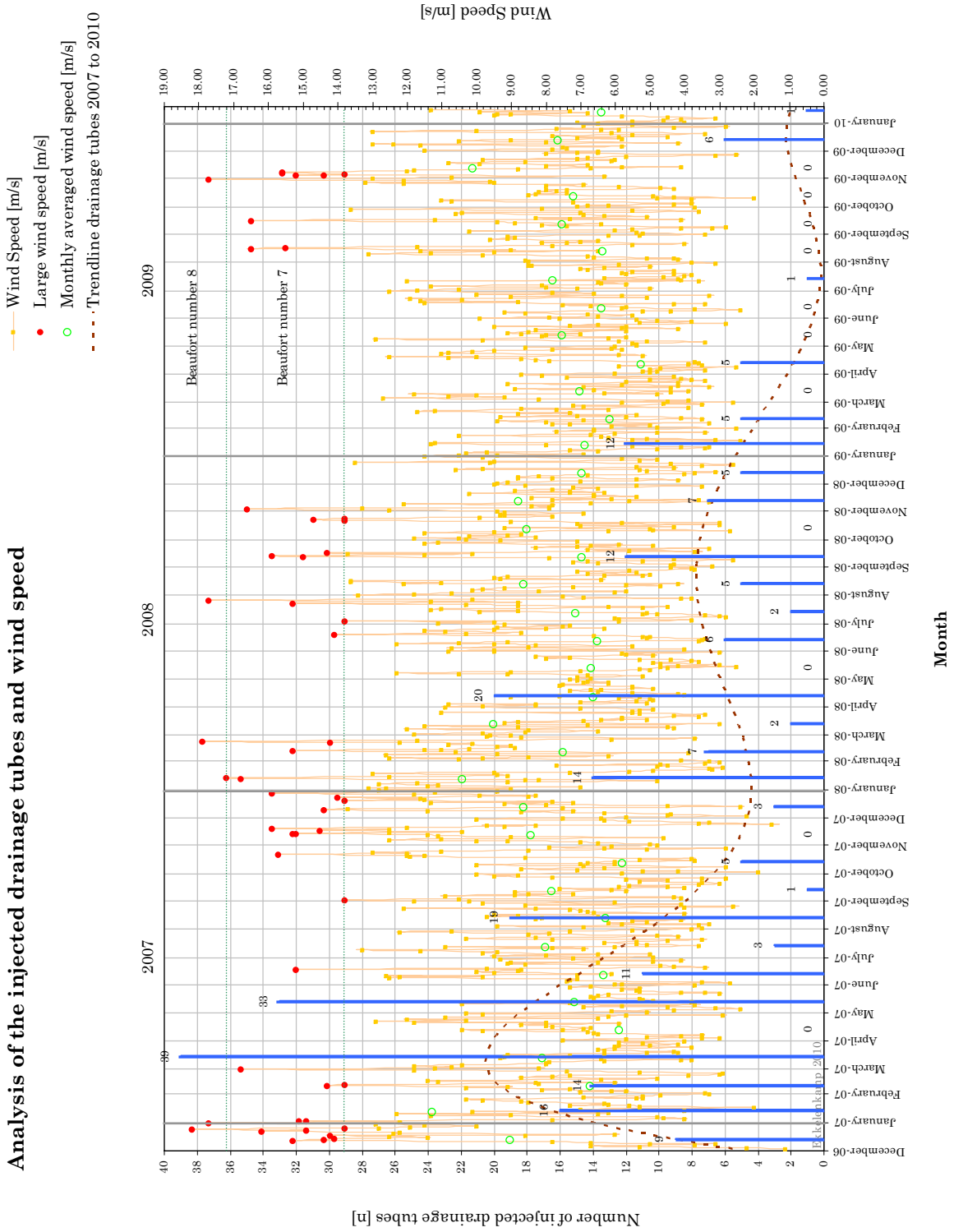

Figure 5-37 Analysis of injected drainage tubes

6. Synthesis of mechanisms and measurements

The development of the intertidal beach zone and beach processes is partly influenced by the sedimentology of the beach surface. The changed sediment properties will affect the beach morphology. This chapter reflects the collected data with the theoretical principles and mechanism described in Chapter 4.

6.1 Sediment parameters

The sediment at the drainage tube area near Egmond aan Zee is almost entirely composed of quartz sand. The same holds for the beach near Hvide Sande where drainage tubes are installed. Only low percentages of minerals like feldspar, hornblende and garnet were detected in the Dutch sand. The sand from Egmond aan Zee contains about 1 to 2 % heavy minerals. The sediment samples from Hvide Sande show around 5 to 7 percent [61]. These figures are usual for Dutch coasts. Therefore, no specific sediment sorting principles of heavy minerals at the studied areas are found.

The governing sediment parameters described in this study are the grain size, sorting, skewness and kurtosis. These values determine the permeability and settling velocity which occur in sediment transport formulae and influence beach processes. The aspect ratio and sphericity may indicate some changes in aeolian sediment transport at the dry part of the intertidal beach area and settling behaviour in the marine environment.

6.1.1 The size and sorting of the sand grains

According to the grain size measured at Egmond aan Zee and Hvide Sande the beach sediment can be categorized as medium to coarse sand. At both drainage tube areas, the measured grain size at thirty centimetres depth exceeds the average grain size along the entire stretch of coast. The PEM areas contain coarser sediment then the reference areas. At the beach near Egmond aan Zee an increase of 95 µm was measured (compared with the historic data of Chapter 2). The sediment at the PEM areas near Hvide Sande are on average 320 µm coarser than surrounding beach areas. The same trend is even visible at one to five metres deep below the beach surface of Egmond aan Zee. Here, the upper layer consists of sand diameters which are 90 µm larger than the sand below this active layer. This depth seems to be the same as the active depth of the beach envelope.

Compared to the historic data described in Chapter 2, both beaches are coarser along the drainage tube areas. There is no evidence of these coarse historic layers at the active beach envelope (see 2.2.3). Before the installation of the drainage tubes near Egmond aan Zee the average grain size varied between 180 and 360 µm (Figure 5-23). Near Hvide Sande the average median size at Skodbjerge [54] was between 430 and 560 µm.

The beach envelope at Egmond aan Zee has varied between one to two metres over the last eight years (Figure 5-35 and Figure 5-36). This means that only the upper part of the beach (< 2 m depth) is built from 'fresh sand'. The coarse sand at depths of 2 to 5 m (412 µm) was not found during former research [54]. Therefore, it is likely that this sediment was accumulated

during the presence of the vertical drainage tubes. The depth indicates that new coarse sand could accumulate at the intertidal beach area. It is not certain whether the same applies to the beach near Hvide Sande. This study does not supply sufficient data to substantiate this.

The grain size fractions follow the same pattern. Near the Dutch and Danish drainage tube areas the fine fraction is replaced by the coarse fraction. Most remarkable is the very coarse grain fraction of one to two millimetres present at the beach near Egmond aan Zee. Very high concentrations are found at the drainage tube area (up to 3.85%). This indicates that even very large quartz grains settle at the beach or very fine grains are washed away. The sedimentation process is illustrated by the balances showed in Figure 6-1.

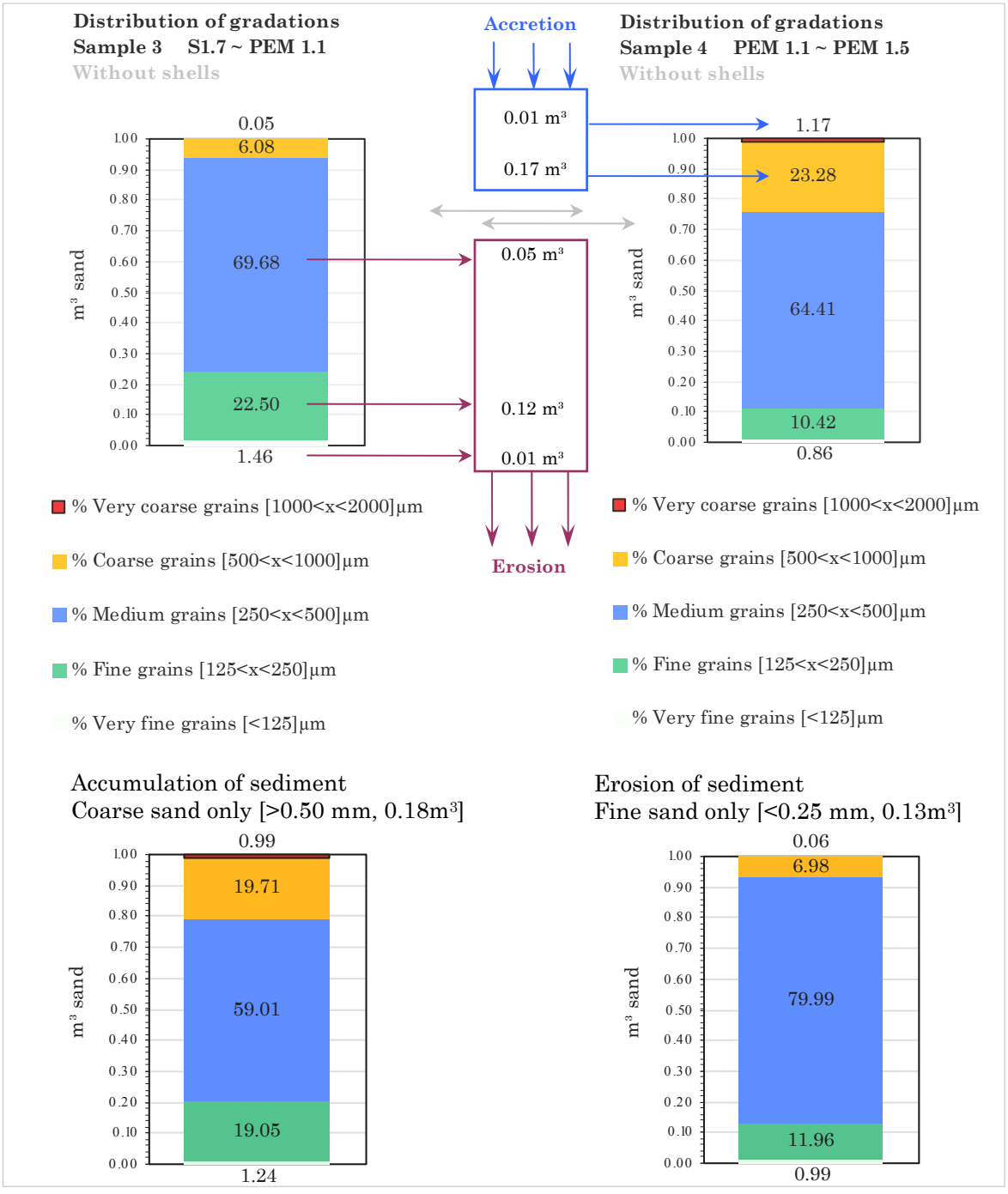

Figure 6-1 Sediment balances at the transition from Ref S1 to PEM 1

Three different situations are possible: the beach accretes (coarse sand >0.50 mm accumulates), erodes (fine sand <0.25mm erodes) or remains at its reference level. Some assumptions are made:

- The sediment at the beach area becomes coarser
- One of the three situations given above happens
- Both figures given in Figure 6-1 consist of averaged values
- Medium sized fractions do not change significantly
- The grain size distribution of trespassing sediment is similar to that of reference areas
- The pore volume remains about the same (volume analysis)
- The grain shape does not influence the analysis made in Figure 6-1
- Sediment transport along the beach remains the same (fraction ratios)
- Nourishments do not influence the balance given by Figure 6-1
- A qualitative analysis is made of the fraction ratios, not of real volumes
- Coarse sand is defined by a grain size of >0.50 mm
- Fine sand is defined by a grain size of <0.25 mm
- Fine sand erodes from the beach by aeolian sediment transport
- Coarse sand accumulates by morphodynamic beach processes
- A qualitative comparison is made between cubic metres of sand (volumetric)

If the total volume of sand at the beach remains the same, the amount of accumulated coarse sand is compensated by the erosion of fine sediment. This seems plausible because the amount of medium sized sediment increases only by 0.05 m^3. An almost equal amount of coarse and fine sediment goes through the system. If the beach accretes, coarse sediment is accumulated (Figure 6-1). The ratio of size fractions changes. Compared to the reference situation at Ref S1, the amount of fine sand decreases with 3.67 m^3. The assumption that the beach accretes with only coarse sand does not seem plausible. If the beach erodes, fine sand is removed (Figure 6-1). Again, the ratio of size fractions changes. This time the amount of coarse grains increases with only 0.91 m^3, compared to the reference situation at Ref S1. The assumption that the beach erodes with only fine sand also does not seem plausible.

In summary, the assumption that coarse sand accumulates and fine sand erodes seems to be most probable. It is difficult to quantify the amount of sediment passing through the system. As trespassing sediment has probably a similar grain size distribution as that of the reference areas, some sorting mechanisms may act at the intertidal beach area. Coarse sediment could accumulate by less energetic conditions while fine sediments could blow away by aeolian sediment transport mechanisms.

The data from the beach near Hvide Sande is not suitable to be analyzed in the same way. Not much information is available about the gravel fractions and pore volumes. The grain size distribution of the sediment samples is analysed by three other descriptive parameters. The average values are presented in Table 6-1. The reference areas of the beach near Egmond aan Zee contain well sorted sediment. The sediment along the drainage tube area is moderately well sorted. This means that this sand contains a wider range of sizes compared to the reference sands. In the case of the beach near Hvide Sande, only drainage tube area 2 shows the same type of distributions.

The grain size distributions of the sediment found at the Dutch reference areas are symmetrical. The distributions from the samples at the drainage tube area are a bit more coarse skewed which indicates an erosive environment. The finer materials have been winnowed out. The opposite holds for the sediment at Hvide Sande. The grain size distribution of the sand near the drainage tubes is fine skewed while it is coarse skewed at the reference areas. This indicates a more depositional environment at the beach near the drainage tubes.

Finally, the presence of both coarse and fine grain populations are analysed. The sand at Egmond aan Zee is meso to lepto kurtic along the reference areas and meso to platy kurtic at the drainage tube areas. This means for the last case that the polymodality of the sample decreases. Both populations are more equally present here. The results of the calculations at Hvide Sande show no specific change in polymodality. The large values of gravel may influence this figure.

Table 6-1 Calculated sediment parameters of the sediment samples of both beaches

Beach	Section	Sorting	Skewness	Kurtosis
Egmond aan Zee	REF S2	1.38	0.00	1.10
	REF S1	1.37	0.02	1.11
	PEM 1	1.47	0.04	1.03
	REF N1	1.36	0.03	1.08
	PEM 2	1.35	0.01	1.09
	REF N2	1.35	0.00	1.09
Hvide Sande	REF S2	1.73	0.13	0.98
	REF S1	1.70	-0.02	0.94
	PEM 1	1.65	-0.08	1.02
	REF M1	1.84	0.10	0.90
	PEM 2	1.81	-0.09	0.93
	REF N1	1.77	0.10	0.95
	REF N2	1.66	0.11	1.04

6.1.2 The hydraulic conductivity of the soil

The permeability of the sediment samples is determined by the use of formulae given in Chapter 4. It is recommended to calculate the permeability routinely when characterizing sediment properties of marine sand deposits [106]. Empirical relationships like Hazen (1892), Beyer (1964) and Krumbein and Monk (1943) should be treated with caution. Baird et al. (1998) found an order of magnitude difference between measured and calculated hydraulic conductivity. Therefore, three different empirical relations are used to calculate averaged values over several beach sections. The detailed output of the calculations is given in Appendix K. From literature it is known that the relation of Krumbein and Monk gives results which are a factor ten less [51]. The variation by orders of magnitude is a major conceptual difficulty. The hydraulic conductivity values given in Table 6-2 are used qualitatively (relative) to compare the permeability of the drainage tube area with that of the reference areas.

The permeability at the drainage tube area near Egmond aan Zee increases by the changed sedimentology. On average the permeability increased with 31% to approximately $6 \cdot 10^{-4}$ m/s. The drainage tube areas near Hvide Sande show both large increases. PEM area 1 consists of to few measurements to draw conclusions. PEM 2 shows an increase of 42% to $8.5 \cdot 10^{-4}$ m/s. The immersed sediment weight during the swash motion may be adjusted for infiltration (uprush) and exfiltration (backflow). For a more permeable beach, infiltration will have little effect on the uprush compared to the significantly reduced backwash depth. The resulting

velocity asymmetry is increased by the hydraulic conductivity. The amount of water infiltrating into the beach is almost linearly related to the hydraulic conductivity [51]. The higher hydraulic conductivity values will influence the infiltration and exfiltration and reduce the backwash depth. The beach accretes because of the onshore transport of sediment. Bar and step formations may develop. The subaerial beach volume is positively related to the increased permeability.

*Table 6-2 Calculated permeability coefficients *10-4 [m/s] of the sediment samples of both beaches*

Beach	Section	Hazen (1892)	Beyer (1964)	Krumbein & Monk (1943)
Egmond aan Zee	REF S2	4.04	4.38	0.109
	REF S1	4.48	4.86	0.120
	PEM 1	5.94	6.30	0.168
	REF N1	4.91	5.31	0.134
	PEM 2	4.73	5.13	0.129
	REF N2	4.73	5.14	0.126
Hvide Sande	REF S2	4.22	4.47	0.113
	REF S1	8.87	9.28	0.304
	PEM 1	13.50	14.0	0.504
	REF M1	5.27	5.48	0.156
	PEM 2	8.77	8.93	0.351
	REF N1	7.06	7.43	0.200
	REF N2	4.93	5.26	0.132

Kozenzy-Carman [84] developed a formula which can be used to calculate the permeability of the beach by using the porosity, average grain size and the sphericity of the sediment particle. The average sphericity at the reference area near Egmond aan Zee equals 0.849 and at the drainage tube area 0.825. This results in a permeability coefficient of respectively $k = 4.39 \cdot 10^{-4}$ m/s and $k = 5.65 \cdot 10^{-4}$ m/s. In this case the permeability increases with 29% . This is a smaller change which could arise from the fact that grain particles become rounder. Irregularly shaped particles interlock easily. This decreases the permeability slightly.

6.1.3 The settling velocity of the sand

The depositability of the sediment depends on the settling velocity. Three different formulae were presented in Chapter 4; Cheng (1997), Gibbs (1971) and van Rijn (1993). The calculated settling velocities are presented in Appendix K. The velocity of the sediment at the reference areas near Egmond aan Zee is approximately 0.0355 m/s. At the drainage tube area this value increases to 0.048 m/s. This is an increase of 35%. The same applies to the beach near Hvide Sande. Here, the average fall velocity at the reference areas equals 0.0714 m/s. This value increases with 48% to 0.106 m/s.

For the quantitative analysis of the sediment transport, knowledge of the settling velocity is a pre-requisite. Sorting processes along the beach occur both in settling and pick up of grains and fractions. The grains which have the same settling velocity are considered to be hydraulic equivalent. Differences in settling velocity and segregation of sediment fractions take place in the vertical, with finer fractions suspended at higher elevations. The net onshore transport of coarse material relatively close to the bed combined with finer material transported offshore in suspension, would result in cross-shore segregation. The beach can become more coarse in time.

Kriebel (1991) and Dean (1987) formulated the relation between the settling velocity and the nearshore bed slope. Section 6.2 describes the change of the beach parameter and bed slope. With an increased settling velocity by 35% the beach shape parameter becomes 27% higher. By the theory of Dean (1977) this results in a steeper bed slope. A steeper nearshore bed profile may reduce the swash length. The beach becomes drier in time.

6.1.4 The shape of the grain particles

The shear strength of granular materials like sand depends on the shape of the grains. It is defined by the structural arrangement of the particles. The average aspect ratio of the sediment particles from the reference areas at the beach near Egmond aan Zee equals 0.714. The samples from the sand taken from the drainage tube area have an average aspect ratio of 0.668. This is an decrease of more than six percent. These values relate to the median sediment sizes of 0.200 to 0.400 mm. The sediment at the drainage tube area is more asymmetrical than the sand along the reference areas. The same holds for the sphericity of the sediment grains. Again, samples from the reference area were analysed which resulted in a average sphericity of 0.849. The data reveals that the sphericity value of the drainage tube area equals 0.825. The sediment at the drainage tube area has a more irregular shape compared to the sediment found at the reference areas.

Both shape parameters can be used in formulas related to sediment stirring mechanisms and the development of critical shear stresses. The values can also be used to study aeolian transportation of sand. Folk (1978) suggests a relation between the mean roundness or sphericity and the grain size of the accumulated or transported sediment. Accumulated sand grains are often rounder when they are smaller (Folk (1978)). These grains are saltated and have endured abrasion. In addition, it is assumed that round and more spherical grains are more readily transported by the wind.

A hypothesis could be that the asymmetrical and irregular shaped grains found along the drainage tube could have suffered less abrasion during their transport by waves and currents. This could indicate less aeolian transport into the area. This is in accordance with the findings at the drainage tube area near Egmond aan Zee which could indicate that less aeolian sand is accumulated here (decrease of fine fraction). This would suggest that the increase of sediment volume along the drainage tube area is created by suspended sediment transport. However it is still not proven that the abrasion during hydraulic transport is lower compared to aeolian transport. The premise is therefore inconclusive.

One other hypothesis would be that if the sphericity factor lowers, the beach erodes by aeolian transport. This should be a kind of natural selection. Irregular shaped particles stay on the surface when the beach encounters large aeolian sediment transport rates. As less irregular shaped grains should be transported by wind the sediment becomes more irregular shaped (sediment sorting). Folk (1978) suggests that when it comes to the sphericity of the particle in particular large grains of 0,400 mm are easier transported than small grains of 0.100 mm. The measured increase of the sediment volume along the drainage tube area contradicts with the assumption that the aeolian transport increases. This falsifies the hypothesis.

6.2 Beach profiles and surface

The profile of the beach and nearshore zone will be influenced by the hydrodynamic conditions and sedimentology. The waterline will shift under changing steepness of the beach profile. The berm which is situated between the foreshore and backshore moves seaward if the beach front gets steeper. This influences the moment when waves start to break. The shape of the beach profile determines the vulnerability of the coast to storms. The dynamic equilibrium profile can be described roughly by the Bruun relation. Within this rule the profile is related to the

shape parameter and the water depth. Table 6-3 shows the shape parameters according to changing sedimentology. Three different prediction methods are compared and averaged.

Table 6-3 Calculated beach shape parameters of the sediment samples of both beaches

Beach	Area	Kriebel (1991)	Moore (1982)	Vellinga (1986)
Egmond aan Zee	REF south	0.1059	0.1117 ; 0.1330	0.0858 ; 0.0849
	PEM	0.1330	0.1298 ; 0.1725	0.0997 ; 0.0987
	REF north	0.1103	0.1147 ; 0.1372	0.0881 ; 0.0872
Hvide Sande	REF south	0.1427	0.1360 ; 0.1864	0.1044 ; 0.1084
	PEM	0.2264	0.1844 ; 0.2119	0.1416 ; 0.1492
	REF north	0.1427	0.1360 ; 0.1881	0.1044 ; 0.1081

The nearshore beach profile becomes steeper at the drainage tube areas (see Figure 6-2).

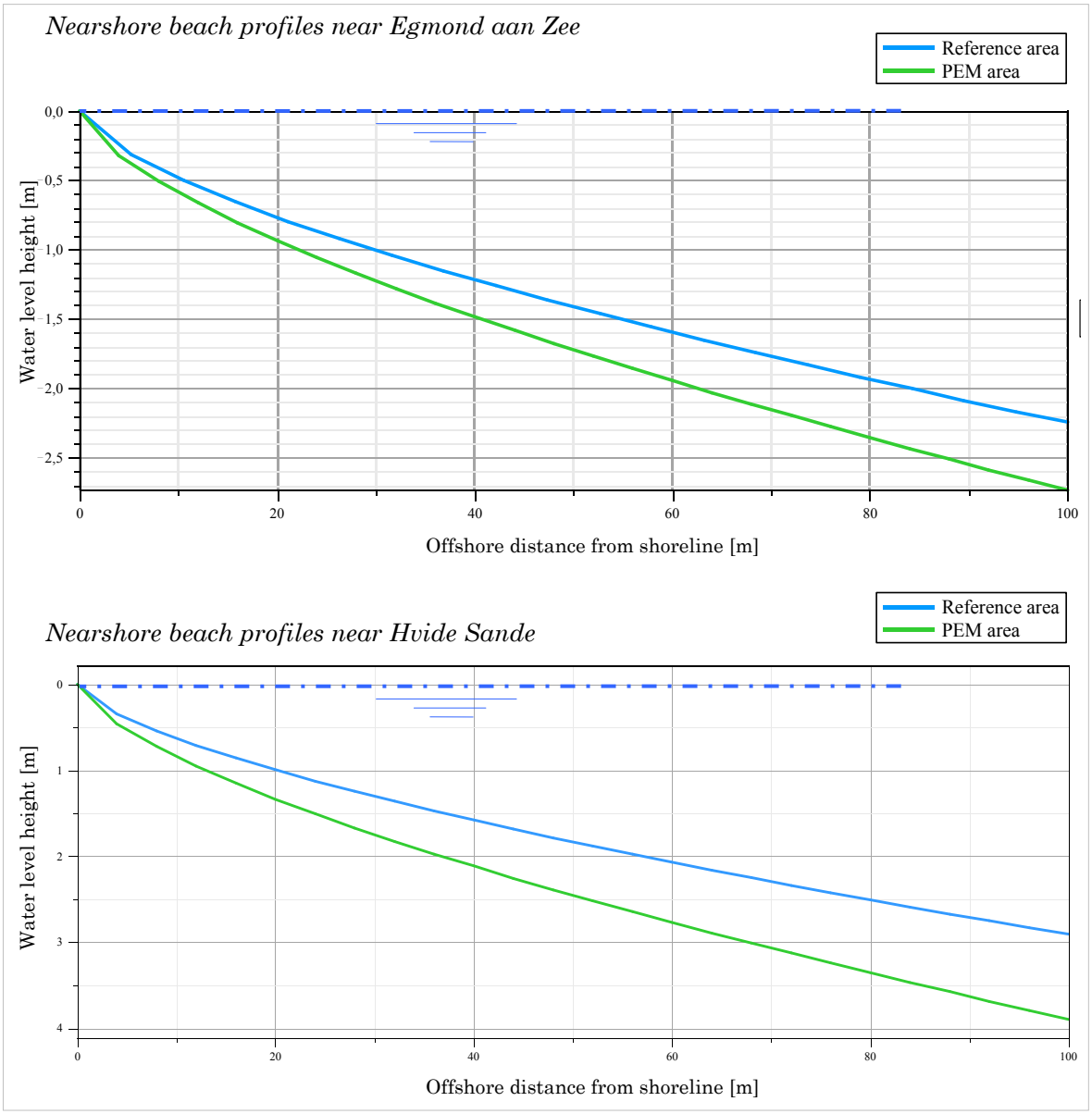

Figure 6-2 Nearshore beach profiles of Egmond aan Zee and Hvide Sande (averaged values)

The steep nearshore beach profile is observed at the drainage tube area PEM 1 near Egmond aan Zee (Figure 6-3). Many local people stated that they observe a steeper beach (based on four different interviews with local people). Passing bikers said that the swash area decreased so they were forced to ride closer to the water line (based on three stories). This photograph is taken in the summer. The summer beach profile is often wider than the profile during the winter. Compared to the reference area at the same day this part of the beach is clearly steeper.

Figure 6-3 Steep nearshore zone at the beach near Egmond aan Zee along PEM 1

The changed beach sedimentology influences the dynamic equilibrium. The steeper nearshore beach profile influences the swash dynamics. Waves start to break earlier and the swash length decreases. The turbulence generated during the breaking of a wave will suspend sediment. The fall time of a particle may become less than one-half wave period (see section 6.1.3). This may result in a net onshore sediment transport rate. The Dean number [N] indicates whether the beach will erode or accrete. For an accreting coast the turning point is N<3.2. The data of Egmond aan Zee gives N_{REF} = 7.6 and N_{PEM} = 4.8. This indicates that the drainage tube endures less erosion than the reference area. The values for the Danish coast are N_{REF} = 4.7 and N_{PEM} = 3.1. This indicates that at the drainage tube areas near Hvide Sande accretion occurs while at the reference areas erosion is probable. Although this is a rather crude estimator for the beach morphodynamics state, it gives some insight in the consequences of the changed sedimentology.

6.2.1 The beach slope

The larger sediment grain size along the drainage tube areas influences the beach slope. It becomes steeper when the grain size increases. With the graph of Wiegel (1965) (see Appendix N) the beach slope can be theoretically determined. The average slope at the reference areas near Egmond aan Zee equals 1:33. The drainage tube area PEM 1 should have a slope of 1:19. The same holds for the beach near Hvide Sande. Here the average beach slope along the reference areas equals 1:18. At the drainage tube areas this slope gets steeper to 1:7. Steep

beach profiles were observed at the drainage tube areas near Hvide Sande (Figure 6-4). The swash area was clearly short.

Figure 6-4 Steep nearshore zone at the beach near Hvide Sande along PEM 1

The beach slope can be calculated in relation to the proportionality between the beach face and the sediment size or to swash infiltration and hydraulic conductivity. The backwash will reduce when more water is infiltrated in the beach. The beach slope will increase with a higher permeability. The beach slope is calculated by the method of Reis (2010).

At the reference areas near Egmond aan Zee the expected beach slope is $\beta = 0.03264 = 1:31$. The average slope at the drainage tube area is expected to be $\beta = 0.04756 = 1:21$. These values correspond to the earlier findings. This would theoretically mean an steepening of 32%.

The calculated beach slope near Hvide Sande equals $\beta = 0.04275 = 1:23$ for the reference areas. The slope at the drainage tube areas are is on average $\beta = 0.09065 = 1:11$. Again, the beach slope is steeper, with in this case a difference of 52%.

These values should be used qualitatively as many factors determine the morphology. Dean (1977) suggests that other features, like wave dissipation per volume unit of water across the beach profile, influence the beach slope. This directly affects the beach slope calculations if the parameters would change.

From the beach height measured before and after the placement of the drainage tubes (see Figure 5-39 and Figure 6-5) it is clearly visible that the beach becomes steeper. The isobars representing different heights are more densely distributed at the drainage tube area. In addition to this the height of the beach increases in offshore direction. This indicates accumulation of the beach combined with a steeper slope which makes the beach more robust. The swash distance decreases and the beach becomes drier in time. This enhances the effect of aeolian transport (see section 4.3.3).

After the drainage tubes were installed the dunes with heights up to 3 to 5m grew extensively [30]. The dune foot moves in offshore direction (Figure 6-5). The dunes are fed with wind blown sediment from the beach. The increased sediment volume is caused by the larger aeolian transport rates. Future research must be done at the dunes to study the sediment on their volume, size, shape and origin.

The safety against flooding and erosion becomes higher when the beach height increases and front slope becomes steeper. Also the recreational area increases. Beach nourishments at the drainage tube area are less needed.

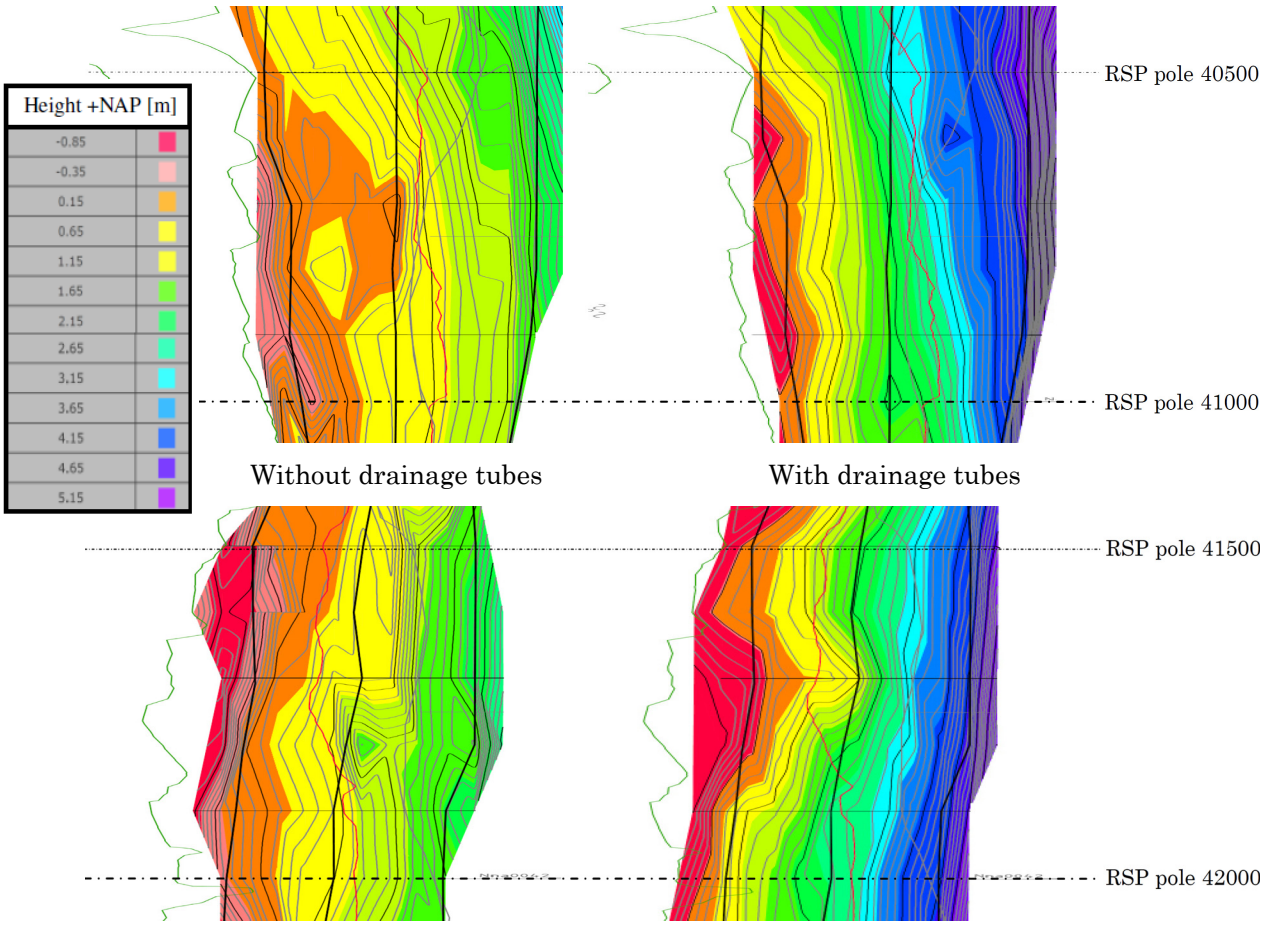

Figure 6-5 More densely distributed isobars indicate a steeper slope (before (l), with (r) tubes)

6.2.2 Swash dynamics

The breaking factor depends strongly on the wave steepness and the bed slope. The breaking wave height is mainly controlled by the depth (h) at the crest. The γ - values range from 0.4 (flat bed) to 1.2 (steep slope). Figure 6-6 shows data from USA beaches and The Netherlands. The breaking factor ranges from roughly 0.4 to 0,9 with a wave steepness of 0,02 to 0,06, depending on the significant wave height and length.

For very steep slopes the influence of the wave steepness becomes significant and constant, which means that waves will break almost instantly when the breaker depth reaches the breaker wave height. The beaches along the Dutch coast have a width varying from 100 to 200 metre [94] (Egmond aan Zee aprox. 104 to 160 metre [33]), measured from the dune foot to the low water line. The average slope varies between 1:20 and 1:60 [94]. The bed slopes at Egmond aan Zee (Figure 6-6) are in roughly 1:30 to 1:40. At Egmond aan Zee the waves approach the coast most often from north-westerly directions during fair-weather conditions. During more stormy conditions the wave direction changes to south-westerly directions. For the period of a large storm the waves are coming from west to northwest direction. The wave steepness is on average 0.03 with $\gamma = 0.42$.

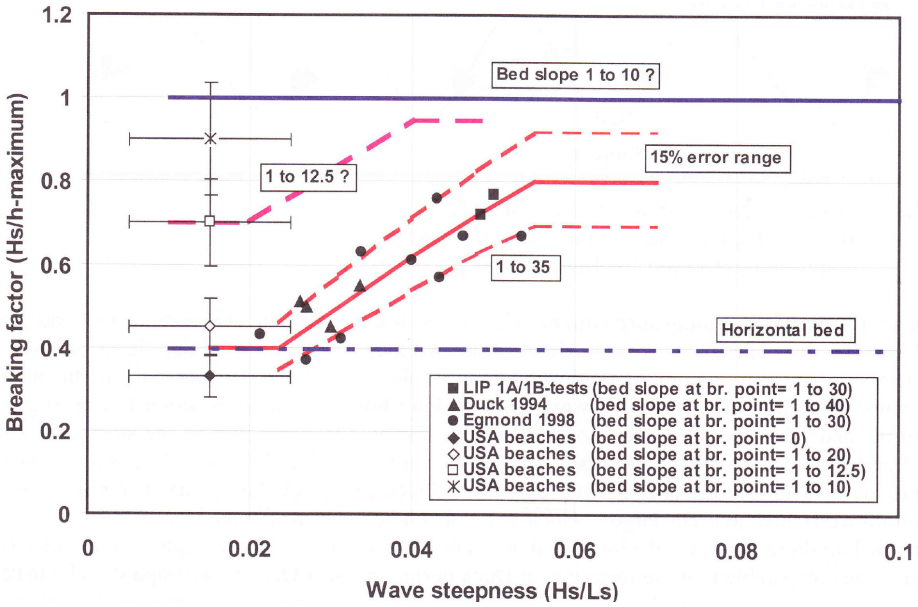

Figure 6-6 The maximum values of the breaking factor as function of wave steepness and bed slope

If the beach slope at the drainage tube area near Egmond aan Zee changes from 1:31 to 1:21, the breaking factor becomes $\gamma = 0.61$. At the tube areas near Hvide Sande this parameter changes from $\gamma = 0.69$ to $\gamma = 0.92$. At both beaches the breaking depth increases. This causes waves to break more offshore. The turbulence which is created by the breaking waves will wash out small ripples. High sand concentrations will move in a sheet along the bed.

The wave set-up is a consequence of mass flux piling up. This set-up follows from the breaking factor and wave breaking height (Figure 6-7). The wave set-up at the reference areas near Egmond aan Zee are 0.4 m and along the drainage tube area 0.5 m. Together with the steeper slopes this results in a set-up length of respectively 12.5 and 10.5 metre. The beach gets drier and wider.

The reference areas near Hvide Sande encounter a wave set-up of 0.7 m. For the Danish drainage tube areas the set-up equals 0.98 m. The theoretically swash length decreases from 16.1 m to 10.8 m, while the beach width increases.

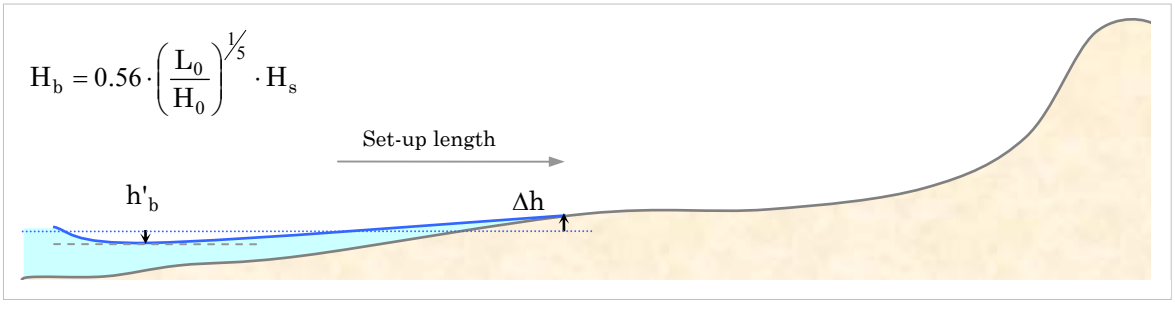

Figure 6-7 Wave set-down and set-up which influence the water level

The steeper beach slope will cause more turbulence when the waves are breaking. Sediment sorting may occur when the fine fraction is winnowed out by the more energetic environment. This could, among other effects, explain the coarser sediment at both drainage tube areas.

6.2.3 Geology of the subsurface

The geologic composition of the beach near Egmond aan Zee and Hvide Sande is considerably different. Besides the grain sizes and shapes, some other aspects are studied on a bigger scale. The presence of permeable and impermeable layers and the conditions of the subsurface are mapped.

Measurements done at both beaches give information about layers in the subsurface and local deposits. The beach near Egmond aan Zee contains large amounts of shell fragments. In longshore direction the deposits of these fragments are randomly distributed. But in cross-shore direction the fragments were only found between the low and high water line. The cylinder tests were done at depths up to 5 metre. Below this level more shell layers could be present. The thickness of the permeable shell layers varied considerably. On average the shell layers were ten to thirty centimetres thick. Even the density varied, which may be an indicator for changed hydrodynamic conditions in the past. The depths at which the layers were found, fluctuated between 0.5 to 4.0 metres in cross-shore and longshore direction. This makes it very plausible that the tubes are penetrating these permeable layers with their filters. Without any accretion of sediment, the tubes are still located at a depth of 0.2 to 3 metre deep. If sand is accumulated at the drainage tube area over time, the tubes could reach depths up to 5 metre. Still the permeable layers are penetrated by the tubes. The same story holds for the beach near Hvide Sande. Many gravel layers from glacial periods are found at the (sub)surface. These layers are also very permeable. The grain size of these granules varies between 1 to 4 mm which is classified as very coarse. Again the observed layers occur at different places and levels on the beach. Their thickness varies on average between one and thirty centimetres.

A rough estimate of the soil type can be made using the data from the cone penetration tests (CPT). The CPT tests near Egmond aan Zee indicate that clay and silt layers are present at the subsurface of the beach. At the reference area at the beach near Egmond aan Zee the upper part of the beach (depth of one metre) consists of sand which deforms easily (pressures up to 10 MPa at the low water line (LWL) and 23 MPa at the high water line (HWL)). This indicates that this sand is fine (silty) at the LWL and coarse at the HWL. So the packing of the sand differs significantly from the LWL to the HWL. At the drainage tube area near Egmond aan Zee the results of the cone penetration measurements show a different situation. This data is consistent with the results from the research done by Pieterse (2008) [79] (see Figure 6-8).

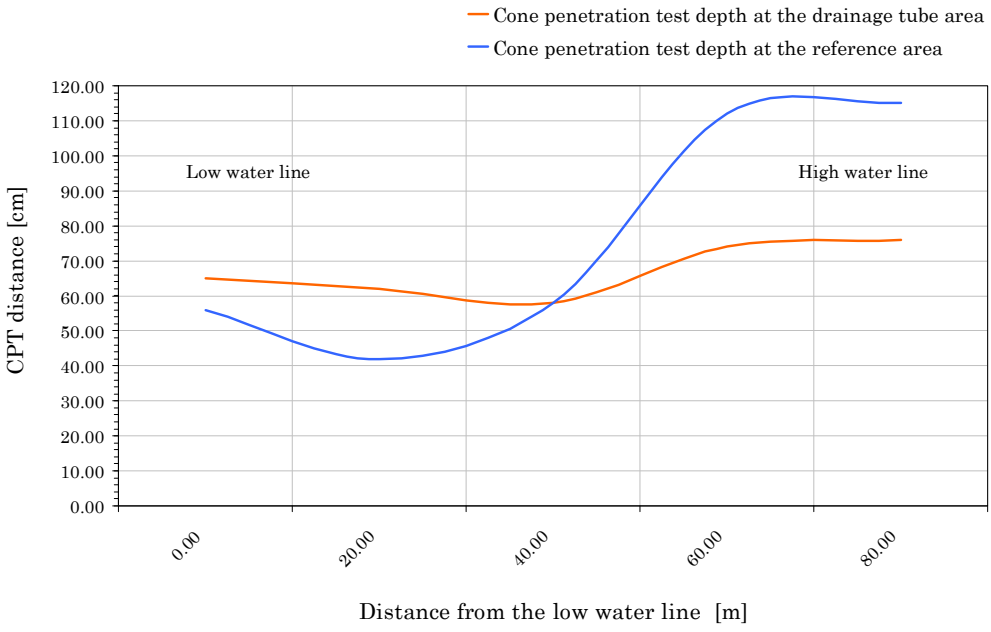

Figure 6-8 Cone penetration test done at Egmond aan Zee in year 2008 at the same locations [79]

The upper part of the whole intertidal beach area consists of sand with a cone resistance of 16 MPa which remains almost constant over the entire cross-shore intertidal beach profile. This sand can roughly be classified as (moderately) coarse. At a depth of 2,5 metre a clay/sand layer exists. It is unclear whether this could be a shell layer which is relatively loosely packed.

The higher pressure resistance at the drainage tube area results from a lower moisture level. If the groundwater level and capillary fringe are lowered the sand becomes more packed. More research must be done at the pore pressures to validate this reasoning.

6.2.4 Changes of the beach surface

The development of the swash zone is to a large extent dominated by the uprush and downrush flows. The bottom friction is a dominant factor in swash dynamics. The bottom friction is calculated with the roughness values employed to characterize the bottom resistance. Difference is made between steady flows and oscillatory flows.

The roughness for oscillatory flows is used to calculate the friction in the swash area. The commonly employed value for the friction f in the nearshore zone is generally taken as current related friction. At the swash zone f values tend to be much larger [81]. The average roughness at the reference area of the beach near Egmond aan Zee equals 0.0476 m. At the Dutch drainage tube area this value increases to 0.0578 m. These values give a friction term of 0.046 and 0.052 respectively (H=1.7m, T=6s, $\lambda = 57\,\mathrm{m}$, $u_0 = 1\,\mathrm{m/s}$). The roughness values of the reference and drainage tube areas along the coast near Hvide Sande are respectively 0.07 and 0.12. These values result in a friction of 0.053 and 0.074 (H=2.2m, T=6s, $\lambda = 56\,\mathrm{m}$, $u_0 = 1.5\,\mathrm{m/s}$). These values are estimates and must be used qualitatively.

The friction is closely related to the rate of momentum transfer at the bed. The slightly higher friction values cause more energy to dissipate. In addition to this resistance, different bedforms with ripples may develop by changing grain sizes. Ripples have an effect on the friction. Camenen (2003) describes the complex effect of ripples to the friction of the sand surface. Under flows of intermediate strength and wave motions the bed will become more active. Vortex ripples will develop. According to the formula of Nielsen (2002) the Shields' (Appendix M9) parameter changes when the grain size increases. If the flow conditions remain the same and the grain size increases, the bed becomes more stable and less ripples may develop. The increased grain size at the drainage tube area near Egmond aan Zee results in a Shields' parameter of $\theta_{2.5;\mathrm{REF}} = 0.956$ to $\theta_{2.5;\mathrm{PEM}} = 0.776$. Vortex ripples are still likely to occur for the same velocities. At the beach near Hvide Sande these values are $\theta_{2.5;\mathrm{REF}} = 1.525$ to $\theta_{2.5;\mathrm{PEM}} = 1.04$. Instead of mega ripples, the surface along the drainage tube area will have vortex ripples when the same velocities occur. This means that the total friction decreases due to current velocities, while it increases for velocities due to waves. The motion within the boundary layer is too complex to quantify the increase of the friction term due to ripples. Therefore this friction must be used qualitatively in sediment transport formula.

6.2.5 Swash motion

The swash zone is dominated by the uprush and backwash motion. As described in section 6.2.2 and Appendix M4 and M6, the vertical flow into the bed influences the swash motion. The swash length depends partly on the resistance from the beach surface. After the maximum rise of the bore on the beach face, the uprush edge reverses direction and becomes backwash (under gravity). Energy is dissipated by bed friction and vertical flow.

During the swash motion, the friction influences the excursion. When the friction coefficient is raised the swash trajectory becomes asymmetric. This effect is an important factor for beach change (Baldock and Holmes, 1997).

If the beach near the drainage tube areas has a constant beach slope, the excursion may be reduced by the increasing friction factor. This decreases the duration of the swash cycle. This can be up to several metres. The swash motion becomes increasingly asymmetric as the friction is increased. For the drainage tube areas of both beaches this means that the foreshore becomes drier in time. The cross-shore sediment transport rate also changes. As energy dissipates, the flow velocity and transport rate are reduced.

The beach slope is also of importance. As the beach gets steeper, the excursion distance reduces. However, the friction factor at the drainage tube areas near Hvide Sande increases more than at Egmond aan Zee which results in the same effect on the excursion distance.

Based on the literature described in Chapter 4, the combined effect of the increased friction factors and steeper slopes may result in a decreased excursion distance of 1 to 2 metres.

In addition to the friction as a function of the grain roughness, some other mechanisms may influence the swash motion. It would be unwise to ignore these effects. The dissipation of energy may be increased by bed irregularities like ripples. Also, the movement of individual grains influences the skin friction. The flow itself will also exert a resistance due to any appreciable sediment load carried by the flow. Finally the influence of infiltration and exfiltration cannot be neglected. The total resistance should be given as a combination of these four mechanisms.

6.3 Beach processes

Several beach processes are influenced by the grain size and shape of the sediment. These processes are mostly related to groundwater flow, as the vertical drainage tubes are highly permeable elements which transport water and drain the beach. The beach groundwater dynamics control the foreshore sediment transport. If the water table drops, the beach tends to accrete. The conceptual groundwater system includes the variation of the water table caused by the tidal movement. At the low waterline near the surface, short wave fluctuations are inundating the beach. The unsaturated zone increases when the foreshore gets steeper, the permeability increases and the swash motion decreases.

The beach fills more easily than it can drain under gravity. The difference between high water and low water creates a gradient. After the water level starts to lower during the ebb movement, a curved groundwater pattern is introduced which causes flow in the beach. With the use of the tidal information, the hydraulic conductivity of the beach and the specifications of the drainage tubes the influenced mechanisms of the system can be studied.

6.3.1 Vertical drainage of groundwater

The drainage capacity of the tubes is largely determined by the outflow capacity. The resistance of the surrounding soil decelerates the water flow through the tube (in and out). If the filter constipates the tube stops to operate (see Appendix A). The increased grain size of the soil surrounding the tubes at the drainage tube areas gives a higher permeability which reduces the piezometric head difference of the level in and out at the tube. On the other hand, when the hydraulic conductivity increases, water may leave the tube more easy. This effect increases the drainage capacity of the tube. Other factors which may have the same result are the lengthening of the tubes and the centre to centre distance of the rows of tubes. These optimizations of the drainage tube technology could enlarge possible effects. Some empirical relations were studied in the past by Fredsoe (2008). He found that the drainage capacity increases with the piezometric head difference. The same tests must be repeated when parameters like permeability, length, distance or radius change. Yet it is too difficult to formulate one expression to calculate the flow rate through the tube.

As part of the large scale working mechanism, here the moisture level of the beach is studied. Lowering of the groundwater table will reduce the moisture level at the beach surface [51]. This mechanism could be initiated by the drainage effect of the tubes. The significance of this effect will become apparent from the real flow rates through the tube. The calculated lowering of the beach near Egmond aan Zee and Hvide Sande is given by (Figure 6-9). The perceived dissimilarity between the two beaches follows from the different hydrodynamic and tidal conditions. The theoretical backgrounds of these calculations are described in section 4.4.

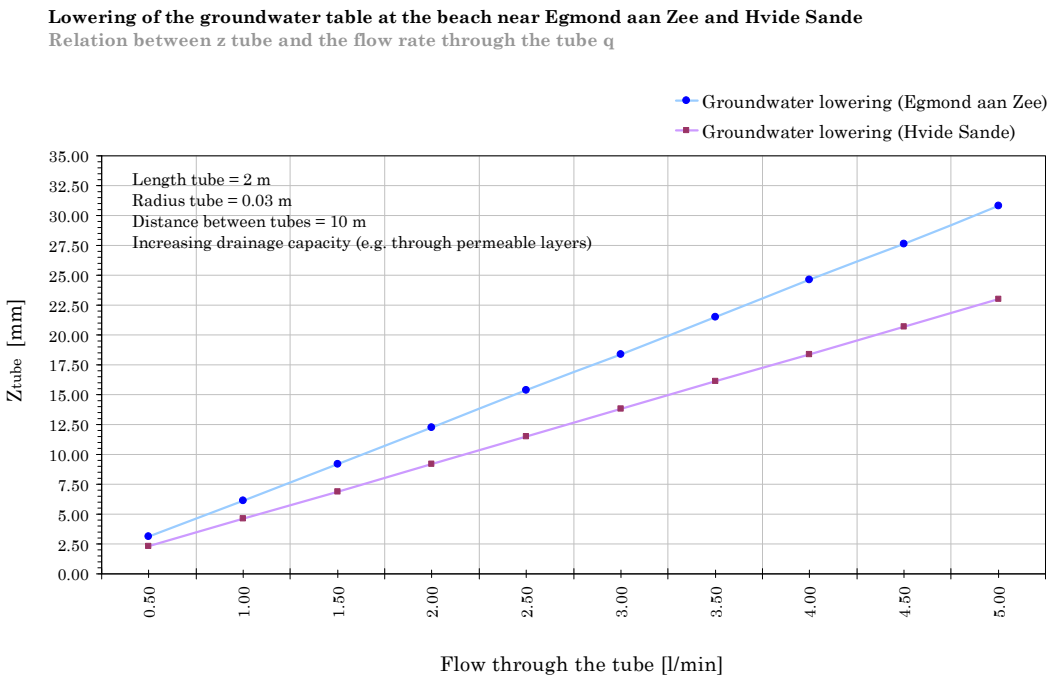

Figure 6-9 Influence of the tube drainage capacity

Very permeable layers may facilitate higher flow rates through the tubes when they are connected to the sea. Water chooses the path of least resistance. In the case that no permeable gravel or shell layers are present in the subsoil, the flow capacity at the beach near Egmond aan Zee equals 1.21 litre per minute. This could lower the local groundwater level by 7 mm. If the same principles hold for the beach near Hvide Sande, the calculated flow rate equals 0.79 l/min. In this case the groundwater level is lowered locally by only 4 mm. These values for the two beach areas are very small when they are modelled with a homogeneous subsurface. The drills at Egmond aan Zee and Hvide Sande show that the vertical drainage tubes were penetrating the permeable layers. If these layers are connected to the sea either by themselves or through the drainage tubes, the flow rate capacity would increase. This results in a lower groundwater level near the drainage tubes. It is quite possible that the measured layers initiate this effect. More research of the stratification and permeability of the beaches must be done. The real flow rate must be measured to compare the theory with reality. The theoretical implication of the calculated change of groundwater level on the moisture level of the beach surface must also be studied. The local groundwater levels must be measured in more detail. Starting point would be the study of Pieterse (2009).

In case of an impermeable layer, the pressure below that layer can decrease when the tubes are penetrating that layer. The cone penetration tests showed that clay/silt layers are present in the subsurface at depths around three metre. Additional tests and research should prove whether or not these layers are impermeable and influencing the pore pressures. Research done by Fredsoe et al (2008) and Pieterse (2009) shows that some impact on pressure at the beach surface could be measured. This effect increases where seepage exists. During falling

tide, an outflow at mean and low water has been recorded. The drainage tubes near the low water line generated higher gradients. In addition to the flow capacity of the tubes, the influence of the length of the tube is calculated (Figure 6-10). Some important assumptions here are the constant drainage capacity per unit length and the homogenous subsoil. Longer tubes will increase the effect on the groundwater level. In addition more underground layers will be penetrated.

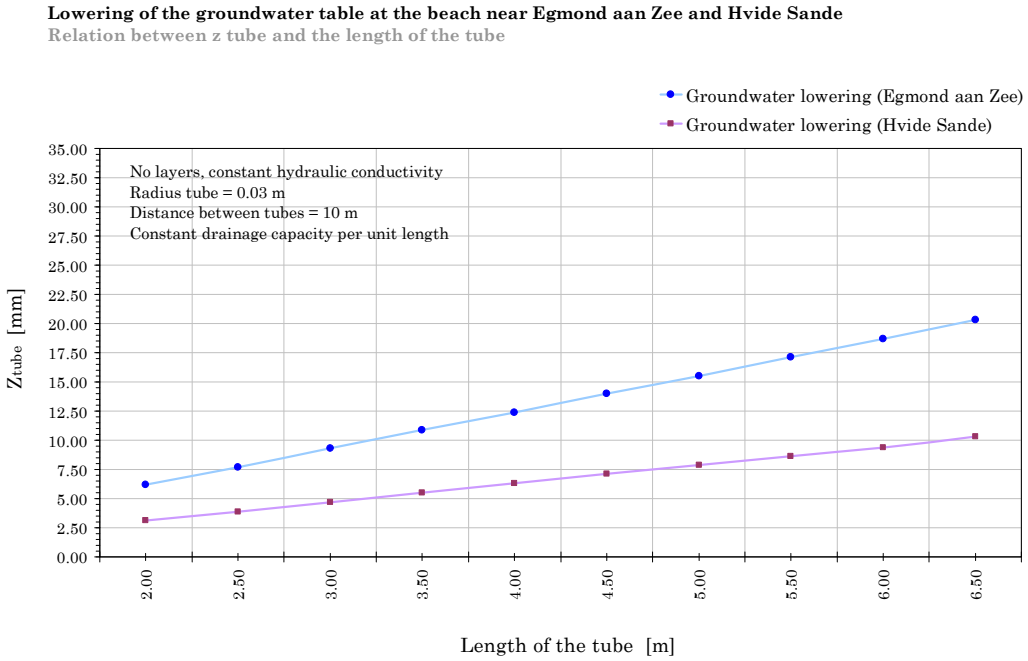

Figure 6-10 Influence of the length of the tube

The distance between each vertical drainage tube has a larger impact on the lowering of the groundwater table (Figure 6-11). The exponential relation gives an increase of 225 to 262% when the distance between the tubes is halved.

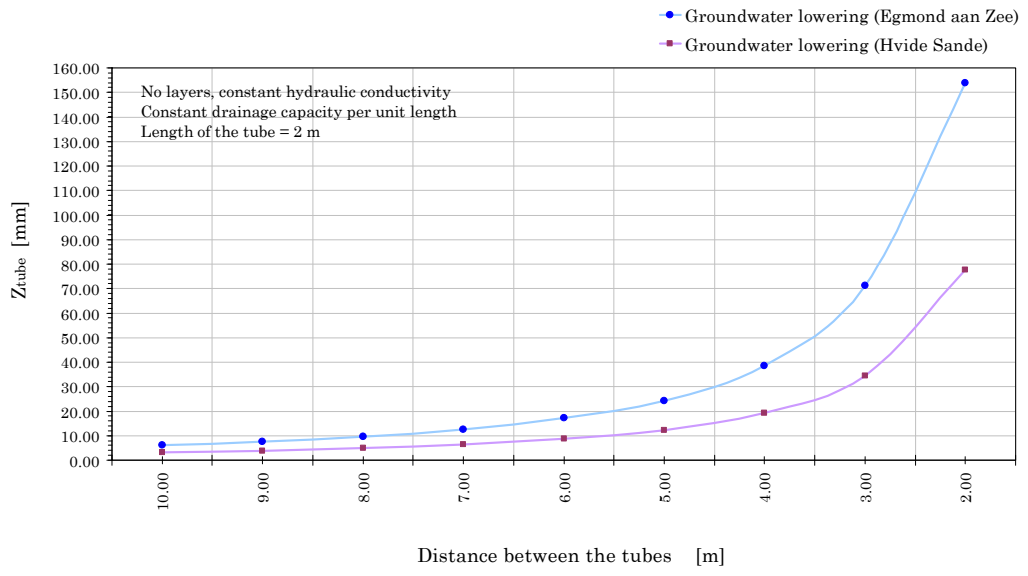

Figure 6-11 Influence of the distance between the tubes

6.3.2 Capillary fringe and moisture content

The storage capacity and moisture level of the beach is influenced by the capillary fringe. This fringe develops immediately above the ground water table. The changed sediment characteristics at the beaches near Egmond aan Zee and Hvide Sande influence the capillary fringe. A lowered net groundwater table may result in a drier beach.

The thickness of the capillary fringe becomes less with larger grains in the beach soil (section 4.4.2). This is the case at the drainage tube areas. This effect is exponential. The surface tension for fine-grained sediment is bigger than for coarse grains. In addition to this the higher hydraulic conductivity of the subsoil increases the infiltration rate. At the swash area the capillary fringe coincides with the beach surface. A wet surface can be seen here. Along the beach the vandose zone consists of a dry part of the beach which is not saturated.

Due to an increase of the average grain size at the drainage tube area near Egmond aan Zee the capillary fringe decreases from 0.27 to 0.16 m. The same holds for the Danish drainage tube area with a reduction from 0.15 to 0.08 m. An average decrease of ten centimetres of the net water table is considerably larger than the reduction of the water level by the drainage capacity of the tubes. Therefore bigger effects on the beach processes are more likely when the sediment at the beach becomes coarser. These values are only illustrative, not quantitative. The effects on the capillary fringe and moisture content must be studied by field measurements.

6.3.3 Infiltration and exfiltration

Beach groundwater dynamics determine the beach morphology. An elevated beach groundwater table gives an intensified erosion while a lower groundwater level promotes accumulation. Draw down of the water table increases infiltration at the beach face and reduces the duration, the volume and the mean flow velocities of the backwash. The beach foreshore gets steeper and deposition is stimulated. Percolation into the unsaturated beach face increases the stabilizing drag on the sediment. The effects on flow into or out of the bed are subject to the loss or addition of the swash volume.

The vertical seepage velocities at the reference and drainage tube areas near Egmond aan Zee are respectively 0.001 and 0.002 m/s. This small change gives a condition for fluidization (w/K – value = 3.33). Fluidization may occur on a very small scale. In the case of Hvide Sande the critical velocities are too large to result in fluidization of sand grains [41].

The effects of infiltration and exfiltration bias the potential sediment transport. These two opposing effects quantify the balance between the uprush and backwash. The effect of infiltration is bigger for a more porous bed during backwash than uprush. If the infiltration rate increases by the larger grain sizes along the drainage tube areas, the bed becomes more stable. Although the boundary layer gets thinner (which increases the shear stress velocity) this stabilizing effect becomes dominant.

Coarser sediment along the drainage tube area near Egmond aan Zee increases the influence of filtration processes. The grain sizes, which where measured, fluctuate around the crossover point D_{q0}. This means that in some cases the sediment transport (uprush vs. backflow) could become onshore directed. According to Nielsen (1998), the boundary layer effects dominate at grain diameters above $450\mu m \leq D_{50} \leq 580\mu m$. The grain sizes at the drainage tube areas near Hvide Sande fluctuate around $700\mu m$. The swash friction factor increases a bit by a changing water depth and hydraulic conductivity. Nevertheless D_{q0} remains within the range defined by Nielsen. Onshore directed sediment transport due to infiltration effects is likely to occur at the Danish drainage tube areas near Hvide Sande.

6.3.4 Sediment sorting along the beach profile

The sorting of sediment along the cross-shore profile depends on the local energy level of the wind and wave forces. The fine and coarse grain size fractions behave differently under the same hydrodynamic conditions. The mechanism of onshore bedload and offshore suspended transport is an important mechanism responsible for sediment sorting. Near the bed, coarse sediment is transported while fine sediment moves in suspension. The sediment flux is related to the ratio of local wave height and local water depth (wave breaking conditions). Often the suspended load (undertow, fine fractions) is offshore directed while the onshore directed bed load (coarse fraction) is initiated by wave asymmetry (oscillation). If the beach becomes coarser, the onshore directed transport processes prevail. The main reason for this effect is the changing relative contribution of both suspended transport components related to their height above the bed.

According to field measurements described in literature (see Appendix G) the measured grain sizes at the drainage tube areas are an exception. It's not customary that the grain sizes vary locally with 33% and remain constant over the cross-shore beach profile, measured from the plunging point to the high waterline. Therefore it is not obvious that sedimentological changes at the drainage tube areas are completely caused by natural sorting mechanisms at the beach. It is even stranger that at the drainage tube areas large differences appear compared to the adjacent reference area where almost identical hydrodynamic conditions prevail.

Changed swash dynamics (like infiltration), wave breaking and surface properties may cause more bed load transport. This must be further investigated in future research. In any case the ratio of offshore versus onshore directed suspended load fluxes will differ by an changing grain size. The onshore directed transport will prevail at the drainage tube areas near Egmond aan Zee and Hvide Sande by the segregation of grain size fractions and selective transport. Consequently, both the oscillating and mean suspended transport will decrease.

In addition to the selective sediment transport mechanisms operating in the nearshore zone. Wind blow transport could sort the sediment along the beach profile. Aeolian transport influences the fine fraction at the upper part of the beach from the waterline to the dunes (the dry part). The coarser sediment lowers the moisture level which makes the beach drier. Aeolian sediment transport increases. This will again lead to selective transport. The fine fraction is removed from the surface and blown in longshore and cross-shore direction. More data about the ratio of suspended and bed load transport, the hydrodynamic conditions, the moisture level and the amount of aeolian transport must be collected in order to prove the assumptions just described.

6.4 Sediment transport

The morphology at the Dutch and Danish beach is strongly influenced by the amount of sediment transported by waves and currents. In longshore direction the transport rate is proportional to the longshore wave power. According to the CERC formula, the suspended sediment transport decreases with 23% (Egmond aan Zee) and 29% (Hvide Sande) with an increase of the measured sediment grain size at the drainage tube areas. The Unibest-LT model also suggests a decrease in sediment transport when the sediment gets coarser. The most influential parameter is the grain size, which could lead to a reduction of 80%. As a result of coarser sediment, the beach becomes steeper and waves start to break more offshore. These two effects also decrease the sediment transport by approximately 20-25%, according to the calculated values of the drainage tube areas near Egmond aan Zee and Hvide Sande. For more background information see section 4.5.

From the Unibest-LT analysis it becomes clear that the total transport of sediment decreases when bottom roughness increases. If the sedimentology of the beach surface changes, the bed roughness will change too. An increasing sediment size together with a more asymmetrical

shape gives a higher roughness value. This means that the sediment transport decreases. Any change of the roughness value is quite complex. The roughness at the drainage tube area near Egmond aan Zee increases with 18%. At the tube area near Hvide Sande this increase equals 71%. According to the rough prediction based on the model run for a reference case, these values give an average longshore sediment transport decrease of 10 to 30%.

The cross-shore sediment transport depends on the grain properties and hydrodynamic conditions of the beach. The sedimentology influences the dissipation of wave energy which consists of bottom friction and wave breaking. The Unibest-TC model is used to give insight into the sensitivity of the sediment transport to various parameters. The driving force from waves and flows is balanced by the bottom friction and wave breaking dissipation. At the swash area, friction may cause an asymmetric swash motion and a smaller excursion length. The calculated bottom friction at the foreshore has little influence on the wave height.

Coarse sand gives a steeper foreshore (section 6.2.1). The wave breaking parameter is related to the beach slope. This parameter increases for both tube areas at the Dutch and Danish beach. The increased wave height causes waves to break. As waves are breaking more energy dissipates. Research done by Hoekstra et al (1997) suggests that the effect of increased median grain sizes on the computed cross-shore suspended load components could be large. The transport rate decreases extensively.

The larger roughness heights (wave and current) at the drainage tube areas of both beaches may also significantly reduce the total offshore sediment transport at the nearshore zone. In addition to this, the transport rate by the undertow reduces more rapidly than the waves asymmetry part. This effect becomes larger for higher waves and a steeper beach (H_s/h – rate). Ergo the sediment transport rate is reduced. Even its direction changes from offshore to onshore. This could stimulate accumulation at the beach which enforces and widens the beach.

6.5 Exploration of the drainage tubes

Some field information can be extracted from the data concerning the maintenance of the systems like the number of drainage tubes injected over the three years when the system was tested at the beach near Egmond aan Zee. In addition to this, the average depth at which the tubes were found confirms the morphological development of the beach.

6.5.1 Injection of the tubes

The drainage tube system must be maintained by the contractor. If tubes are sticking out of the sand they must be injected for safety reasons. The active layer at the beach is measured by considering the beach envelope. At the beach near Egmond aan Zee, its thickness equals 1 to 2 m. This means that for future projects the tubes should be installed below this depth to prevent unnecessary maintenance.

The analysis of injected drainage tubes shows that especially during the start up period, many tubes were re-injected. Almost 90% of these tubes were different every time repair was made. The injections were randomly distributed over the drainage tube area. The data shows a decreasing trend (see Figure 5-37). This means that fewer tubes had to be injected over time. There is no clear connection with the wind speed data for the same period. All three years had severe storms with wind speeds above 17 m/s. It is very likely that the active top layer of the beach eroded during severe weather conditions. The beach profile measurements shown in Figure 5-33 to Figure 5-38 confirm this. In some cases, nearly one metre of sediment was eroded from the beach. The top part of the vertical drainage tubes, which were initially installed at twenty centimetres below the surface, was above the surface after stormy weather conditions. Afterwards the beach accumulated to its dynamic equilibrium and several tubes were injected again.

There are three possible explanations; the beach height remains stable (with accretion after storm), the beach erodes or the sediment accumulates. In the first case, no decreasing trend should be observed because the repaired drainage tubes are injected only a few decimetres within the active layer. Therefore an average number of tubes must be injected after severe weather conditions (if the erosion rate varies within a certain range over the years). Structural erosion of the beach would enlarge this effect with even more tubes to be injected after erosion. Accumulation of sediment at the beach is most likely to be the case. Although almost every single tube (239 different tubes) was injected over the three years period, the active layer of one metre was not reached. This accumulation of sediment and the higher beach levels, correspond with the decreasing trend of the number of injected drainage tubes.

6.5.2 Removal of the tubes

After four years of testing, the vertical drainage tube field at Egmond aan Zee was removed by the contractor. Although no signs of any disturbances were recorded, the project was ended by contract. The GPS location of each drainage tube was recorded in a data base. This made it possible to localize and remove the tubes with an excavator (Figure 6-12).

Figure 6-12 Removal of the vertical drainage tubes near Egmond aan Zee

The depth at which the drainage tubes were found varied between 1 and 3,5 metres. On average a depth of one metre was measured. This means that since their installation the tubes have become covered by a layer of more than one metre of sand. These facts are in compliance with the conclusions drawn in section 6.5.1. Sediment accumulated at the Dutch drainage tube area and the beach has become wider.

Discussion

The data collected from the Dutch and Danish beaches forms the basis for this study. The starting point was the search for any effect at both beaches where vertical drainage tubes were applied. Most remarkable facts are the sedimentological state of the beach near Egmond aan Zee (2009 and 2010) and that of the beach near Hvide Sande (2009). When this data is compared to the historical data of the sediment from these two beaches, the differences become clear. The active zone of both beaches seems to be coarser than before. This will influence the beach state significantly. Many beach processes like groundwater flow, capillary fringe, infiltration and exfiltration and the sediment transport will be affected in one way or another. It would be very difficult to predict the new conditions in a quantitative way because the morphodynamic system is to complex. At this moment only a qualitative analysis could be made based on raw data of the sedimentology, calculated soil properties and beach characteristics like the profiles, bathymetry and swash dynamics.

Former studies

As a start five basic hypothesis were mentioned in paragraph 3.1 and critically reviewed in Appendix A. Several researchers have studied effects underlying these working mechanisms. Pieterse (2009) and Pauw (2009) found that things happened near the tubes. Pressure drops were measured at the high water line and at the low water line. Channelling exfiltration flows through the vertical tubes were located. This seems to indicate that the tubes could influence the beach system on a small scale. They may form a conductor to guide pressures into the sand. Their filtration capacity influenced the swash motion and reduced swash volumes. During the tests by Pieterse some digital divers were used. As Pieterse noticed some differences in output he thought that the divers were sometimes inaccurate. Therefore his data could include measurement errors. But his data clearly shows that minor changes of pressure, salinity and temperature could happen near the tubes. More (practical) research with better equipment must be done onto this subject.

Theoretical framework

Between the small scale mechanisms at the tubes and the large scale change of sedimentology (also measured by Pieterse (2009)) a knowledge gap exists. It is very difficult to understand the physics behind any working mechanism of the drainage tubes. In science, evidence should be based on theoretical understanding combined with raw data to get an explanation of the changed situation. In order to find all missing pieces, a lot of data must be collected. Data obtained during the present study can only give insight into changes of sediment properties over a short period of time (three years). This data does say something about the effects on the beach processes at the intertidal beach zone. Much work on the link between small and large scale changes is still to be done. Computer models like Unibest use large quantities of data. In order to study the natural variability of the sedimentology more data over the past and present must be collected. The beach must be continuously monitored.

The large scale mechanism gives a plausible explanation of how the system with vertical drainage tubes might work. It all starts with infiltration and exfiltration of water through the tubes. A starting point or 'trigger' could be the outflow of groundwater already measured by Pieterse (2009). According to the hypotheses from the large scale mechanisms, water stored inside the beach flows from the high water line to the low water line by a groundwater gradient. The drainage capacity of the tubes is largely determined by the outflow capacity. As the water chooses the path of least resistance the very permeable shell layers at Egmond aan

Zee or gravel layers near Hvide Sande increase the flow through the tube significantly. For both drainage tube areas the water level over a tidal cycle might be lowered by centimetres. This is just a trigger. If the tubes are removed again or not working after a while (because they are too deep or not influencing groundwater flows anymore), the system should stop working as it is only a trigger. From the present data it is still unclear whether the changes (like sediment distributions) stop.

Influence on groundwater

By just theoretically reasoning one could think of the following concept. Levelling of the groundwater gradient increases the storage capacity of the upper part of the beach. The moisture level of that area lowers. The beach becomes drier in time. Aeolian transport increases and sorts the sediment at the beach. Fine grains are blown away along the coast and into the dunes. The fine grain fraction at the drainage tube area is more angular (less abrasion) which suggests that the sand is transported by aeolian transport. The grains are also more irregularly shaped, which might indicate that sediment erosion by wind becomes less. Because of their shape the grains interlock with each other. Therefore only the fine fraction could be transported by wind. This might change the sediment distribution locally. Data presented in this study does not prove this. The relation between the measured shape and size of the grains could not yet be associated with aeolian transport.

If future research proves that vertical drainage tubes cause (little) changes in groundwater flow, it becomes plausible that the beach protection system could work. These studies must include sedimentological data from the past and present. The problem will be that the active part of beach systems will change constantly. For example, ancient estuaries only leave their mark in the very deep soil layers. The active beach envelope consists of the upper few metres of sand which are not that old. This layer is mixed and rebuilt every couple of years. Very little data is available of the sediment from this layer. In this way it is not possible to compare present data of the sediment with historical data of deeper sediment layers.

The measured sediment

Still the question remains whether or not it is coincidence that at two completely different beaches the sediment at the drainage tube areas seem to be coarser compared to historic records. The answer might be found in statistics. The confidence interval could be found by comparing the data from the reference areas and tube areas. Such an analysis should be done in order to find out the chance that the beach became coarser by natural mechanisms. This would be a comparison without the time dimension.

Present research suggests that the sediment at both drainage tubes areas has become coarser after the tubes were installed. The used technique for measuring the sediment is state of the art. This allows us to use the data for detailed calculations. The changed sedimentology influences a number of soil parameters like the fall velocity, bottom shear stress and permeability. Even the bathymetric shape of the beach changes. The steeper beach affects the swash dynamics. The swash length could be reduced and the breaking factor increased.

Some changes of the beach were observed by local people at Egmond aan Zee. They confirm that the beach feels more packed when they are cycling on it. Large sediment changes could be noticed at the beach by looking at the shape of the beach, state of the sediment and development of the dunes (see Figures).

The measured sediment sizes can be qualified as rare. Processes like infiltration of water, the draw down of the water table and the stabilizing drag on the sediment could be influenced. The effects of the more porous bed during backwash are bigger than during uprush. The crossover point (moment offshore transport transforms to onshore transport) could be reached more often. This means that the beach volume would increase. It is interesting to know at what point any influence of the tubes stops when they are covered with a thick sand layer.

New dunes were formed over the last four years at the drainage tube area near Egmond aan Zee

The beach volume at Egmond aan Zee

The increased volume of sand at the beach and dunes was measured by yearly recordings done by the Dutch coastal authority (JARKUS data). At the drainage tube area both the dune and beach volume increased over the last three years. A large quantity of sand is transported to the dunes. At the reference areas only the beach volume increased. This phenomenon is clearly visible at the beach with the tubes installed. New dunes are formed and fresh vegetation can be observed. This is not the case with the reference beach area (lower photo). Here less dune development can be observed.

At reference area REF S1 less dune development is observed at the Dutch beach

In order to get scientific evidence of these processes, computer models could be made which calculate sediment volumes and transport rates into the system. Also more practical measurements like using sand traps can be done. Compared to this study the same problems arise concerning the need for fresh data. Also the detail level (scale) of this data must fit the small scale processes near the drainage tubes. It is not easy to find a method for comparing large volumetric changes of sand.

Drainage tubes instead of nourishments

The question rises whether beach nourishments will still be needed in the future. Unfortunately there is no straightforward answer. This depends on the orientation of the coast, the hydrological conditions, the groundwater system and the structure of the soil. Until now two different beaches were studied which both had sand nourished at the nearshore zone. At the drainage tube areas no nourishments were done. Therefore the added value of the tubes to beach nourishments is unclear. The influence of the tubes on the nourishments done at the northern drainage tube area near Egmond aan Zee could not be studied. The reason was that only 52% of the necessary tubes were installed. The fact that no shells (and layers) were found at this part of the coast indicates that at this location the active beach layer consisted of nourished sediment. Also the stratification of the beach subsurface seems to be a requirement.

The key question, whether or not the passive vertical drainage system could work still remains. This study clarifies some ambiguities concerning the changed sedimentology at the intertidal beach area and explains any transformations using historical data and large reference areas. In addition, the consequences of changes concerning the morphology, bathymetry, groundwater circulations and aeolian transport are described. The field data and calculated effects support the concept of the large working mechanism. The missing piece continues to be the link between a local small effect near the tubes (the trigger) and the large scale mechanism. Given the extraordinary findings and observations, the scientific study must continue. New tube areas should be installed and monitored. This study gives some leads which can be used to start new study programmes. A good start would be to decrease the distance between the tubes.

Also the development of the tubes themselves becomes important. By changing their length, size and filter some changes to the beach morphodynamics could be studied.

Conclusions and recommendations

One main goal of this research was to study the sedimentology of two beaches where vertical drainage tubes were installed and to describe effects on beach processes. By analysing a large number of sediment samples, measuring beach profiles and drilling into the subsoil, some very interesting data was collected. This data is used to evaluate the effects of working mechanisms which could be triggered by the drainage tube system.

Sedimentology

The sediment at the beaches near Egmond aan Zee and Hvide Sande consists mainly of quartz sand. The median sediment grain size at the drainage tube areas near Egmond aan Zee is 0.1 mm larger than the sediment of the reference areas. The sediment at the tube areas near Hvide Sande is 0.3 mm larger than the sediment of the reference areas. Box measurements show no variation of the grain size near the tubes. The coarse sediment was not locally found but was well distributed over the entire intertidal beach zone. The active surface layer (or beach envelope) near Egmond aan Zee has a long term (5 years) variation between 0 and 2.3 metre. Drill samples taken from the subsurface indicate that only the active layer (depth of 2.0 m at LWL and 0.8m at HWL) consists of coarse sand. The values of the very coarse fractions are remarkable. Near the Dutch drainage tube areas these fractions were 3.85% while at the reference areas values of 0 to 1 % were measured. Also the shape of the grain size distributions from both beaches was analysed. As the standard deviation increases, the sediment at the tube areas was poorly sorted. A wide range of grain sizes is present along the these areas. Also the shape of the grains seems to be different. Compared to the reference areas it was found that the sediment at the drainage tube area is more asymmetrical than the sand along the reference areas. The sediment at the drainage tube area had also a more irregular shape compared to the reference areas.

At the beach near Egmond aan Zee a number of processes might initiate large scale sediment sorting along the beach. Basically, one can distinguish four different periods in time, the OerIJ, the following erosive period, period of beach nourishments (after 2005 to present) and the vertical drainage tubes (2006 to 2011). At this moment the Kreftenheye formation consists mainly of very coarse sediment (sands) which are carried by the river Rhine during the last glacial period 'the Weichselien'. In this sediment very coarse particles are present with sometimes even gravel or marine shells which are remains of older 'Eem' deposits. These coarse layers lie at depths deeper than twenty metre. Above this layer Holocene deposits are present which consist of fine to medium sized spisula sands.

The coarse sediments found at the drainage tube area near Egmond aan Zee can not be explained by any historic development other than the presence of a drainage tube system. The coarse beach envelope shows us that the coarse sand is relatively new (formed over the last couple of years). This can be substantiated by the findings of several researchers from the period 1980 to 1988. The median size from all data sources varies between 180 and 320 μm with some extremes up to 360 μm (Figure 5.23.). Therefore it is likely that the beach became coarse after the drainage tubes were installed.

Geological composition

Both beaches have a stratified subsoil which contains mostly permeable layers. The beach near Egmond aan Zee has shell layers while at the Danish beach gravel layers are present. The depths where these layers were found fluctuates between 0.5 to 4.0 metres in cross-shore and longshore direction. The cone penetration tests indicate that the entire intertidal beach

zone at the drainage tube areas consists of well packed (16 MPA) sand. The sand at the reference areas has well packed sand at the HWL (23 MPA) while the area at the LWL has weaker sand layer (10 MPA).

The depths where permeable layers where found make it very plausible that the tubes penetrate these layers with their filters. The drainage capacity of the tubes is largely determined by the outflow capacity. This capacity is influenced by the presence of permeable layers like the Dutch shells and Danish gravel. For both beach systems the water level over a tidal cycle could be lowered by centimetres if a bypass is formed by tubes via the permeable layers. The real flow rate of the installed tubes must be measured to compare the theory with reality.

Beach profiles

The beach profiles along the beach near Egmond aan Zee have been measured many times in the past. The steep nearshore beach profile was observed at the drainage tube area PEM 1 near Egmond aan Zee (Figure 6.3). Coarse sediment found at the drainage tube areas might cause steeper beach slopes. At the Dutch tube area, the slope near the tube area would be 32% steeper. At the Danish tube areas this effect is even larger with a steeper slope of 52%. From the beach height measured before and after the placement of the drainage tubes (see Figure 5-39 and Figure 6-5), it is clearly visible that the beach has become steeper. In addition to this, the height of the beach has increased in offshore direction (see Figure 5-36). After the drainage tubes were installed, the dunes with heights up to 3 to 5m seem to grow extensively. The dune foot moved in offshore direction (Figure 6-5). The dunes were probably fed with wind blown sediment from the beach area.

Accumulation of sediment at the beach combined with a steeper slope makes the beach more robust. The swash distance decreases with a steeper foreshore and the beach becomes drier in time. This enhances the effect of aeolian transport. Wind transports the fine fraction which makes the sediment distribution coarser and more robust.

Beach processes

Several beach processes are present at the intertidal beach area. Many of them are strongly influenced by the sedimentology of the beach surface. As the beach gets steeper the excursion distance reduces. The combined effect of the increased friction factors and steeper slopes will result in a decreased excursion distance of 1 to 2 metre. The wave set-up length decreases with 2 metre at Egmond aan Zee and 5 metre at Hvide Sande. The 'lost' beach width by the effect of wave set-up makes the surface drier.

If the phreatic level drops, the beach surface tends to accrete with sediment. If the foreshore gets steeper, the unsaturated zone increases, the permeability increases and the swash motion decreases. The capillary fringe can have a significant effect on the exchange of water particularly in terms of the storage capacity of the aquifer. If the tubes form a bypass via the permeable layers, larger flow capacities towards the sea can be reached. This very small lowering of the groundwater table could be the trigger to start the large scale mechanism (Figure 3-8). This is still not proven by this study as more research on this effect must be done. As the sorting process starts, the beach gets coarser and more permeable. Because of the larger grains found at the drainage tube area, the thickness of the capillary fringe decreases. An average decrease of 10 cm of the net phreatic level is considerably larger than the reduction of the water level by the drainage capacity of the tubes. The moisture level of the beach surface lowers and the storage capacity of the beach increases. This would explain the stronger, steeper and higher beach. More detailed research on the moisture level and groundwater levels must be done.

The effects of infiltration and exfiltration influence the potential sediment transport. These two opposing effects quantify the balance between the uprush and backwash. The coarse sand

found at the drainage tube areas influences the filtration processes. The grain sizes fluctuate around the crossover point D_{q0}. Especially for the Danish case it is very likely that the crossover point is reached. The cross shore sediment transport might become onshore directed. Also in the Dutch case the transport directions might change. This could explain the steeper beach and increased sand volumes.

Morphology

Both longshore and cross-shore sediment transport are affected by coarse sediment (compared to normal sediment 100 μm smaller). Also the direction of the transport changes from offshore to onshore, which could stimulate accumulation at the beach. The increased volume of sand on the beach and dunes is measured by yearly recordings done by the Dutch coastal authority (JARKUS data).

At the end of the drainage tube testing period, the depth at which the tubes were found varied between 1 and 3,5 metres. On average a depth of one and a half metre was measured. This means that the tubes became covered with a layer of more than one metre of sand over the past four years. These facts support the conclusions drawn in section 6.5.1. Sediment is accumulated and the beach has become wider.

Working mechanism

After the exciting story of the Danish contractor who thought he had discovered the magical tubes, still one question remains: can the system work? After studying the sedimentology of two different beaches, looking at the possible influences on beach processes and comparing the outcomes with beach profile measurements, it became clear that some observations are significant (very coarse sediment found at the drainage tube areas) while others not (lowering of the groundwater table). The measured grain sizes and particle shapes could not be explained by natural phenomena. Based on this observation, it is likely that the vertical drainage tubes could have an effect on the sedimentology and thus on the beach processes. This could explain the changed beach morphology registered by the Dutch coastal authority. It is recommended that future researches start looking at the link between a small scale physical effects near the tubes. Also by studying the beaches evidence must be found which proves any relation between the coarse sediment found at the drainage tube areas and any effect of the drainage tube system.

References

1. Aagaard, T., Kroon, A., Hughes, M.G., Greenwood, B. 2007 *Field observations of nearshore bar formation.* Earth surface processes and landforms, Vol 33, iss 7
2. Adel, H. den 1986 *Correlaties tussen uniformiteitsgradatie en spreidingscoefficient.* Delft, Grondmechanica
3. Alpen, J. van 1987 *De morfologie en lithologie van de brandingszone tussen Terheijde en Egmond aan Zee.* Rijkswaterstaat, Den Haag
4. Alphen, J. van, Damoisseaux, M.A. 1998 *Geomorfologische kaart van de Nederlandse kustwateren.* Geografisch tijdschrift 22
5. Arens, S.M. 1996 *Rates of aeolian transport on a beach in a temperate humid climate.* Geomorphology 17 3-18, The Netherlands
6. Baird, A.J., Mason, T., Horn, D.P. 1998 *Validation of a Boussinesq model of beach ground water behaviour.* Marine Geology 148, UK
7. Baker, V.R. 1988 *Geological fluvial geomorphology.* Bulletin of the Geological Society of America
8. Baker, V.R. 1994 *Geological understanding and the changing environment.* Transactions of the Gulf Coast
9. Baker, V.R. 1994 *Geomorphological understanding of floods.* Geomorphology
10. Bauer, B.O., et al. 2009 *Aeolian sediment transport on a beach: Surface moisture, wind fetch and mean transport.* Geomorphology 105, USA
11. Beets, D.J., Van der Valk, L., Stive, M.J.F 1992 *Holocene evolution of the coast of Holland.* Marine Geology 103, Amsterdam
12. Bemmelen, C.E. van 1988 *De korrelgrootte-samenstelling van het strandzand langs de Nederlandse Noordzee-kust.* Geopro, Utrecht University, The Netherlands
13. Bijker, E.W., Dillingh, D., et al. 1984 *Leidraad voor de beoordeling van de veiligheid van duinen als waterkering,* TAW rapport, 's- Gravenhage, The Netherlands
14. Black, K. P. , Oldman, J. W. 1999 *Wave mechanisms responsible for grain sorting and nonuniform ripple distribution across two moderate-energy, sandy continental shelves.* Marine Geology
15. Blott, S.J., Pye, K. 2001 *Grain size distribution and statistics of unconsolidated sediments.* Earth Surf.Process. Landforms 26, UK
16. Blott, S.J., Pye, K. 2008 *A grain size distribution and statistics package for the analysis of unconsolidated sediments.* Earth Surf. Process. Landfor 26, 1237–1248
17. Bosboom, J. et.al. 2000 *Unibest-TC 2.0 Overview of model formulations*. Delft Hydraulics
18. Boussinesq, J. 1872 *Theorie des ondes et des remous qui se prpagant le long d'un canal rectangulaire horizontal, en communiquant au liquide contenu dans ce canal des vitesses sensiblement paralleles de la surface au fond.* Journal de Math, vol 17
19. Bowman, D., Ferri, S., Pranzini, E. 2007 *Efficiency of beach dewatering*. Coastal Engineering 54, Alassio, Italy
20. Bruun, P. 1962 *Sea-level rise as a cause of storm erosion.* Journal of the Waterways and Harbors Division
21. Burcharth, H. F. 2008 *Coastal Protection Performance of the SIC Pressure Equalizing Modules,* Dep. Of Civil Engineering, Aalborg University, Denmark
22. Butt, T., Russell, P. 2000 *Hydrodynamics and cross-shore sediment transport in the swash-zone of natural beaches.* Journal of coastal research 16, pp. 125–268

23. Butt, T., Russell, P., Miles, J., Turner, I. 2007 *Sediment transport processes in the swash zone of sandy beaches.* Journal of Coastal Research SI 50 636 – 640

24. Butt, T., Russell, P.,Turner, I. 2001 *The influence of swash infiltration-exfiltration on beachface sediment transport: onshore or offshore.* Coastal Engineering 42, pp. 35–52.

25. Camenen, B., Larroude, P. 2003 *Comparison of sediment transport formulae for the coastal environment.* Coastal Engineering 48 111-132, France

26. Camenen, B., Larson, M., Bayram, A. 2009 *Equivalent roughness height for plane bed under oscillatory flow.* Estuarine, Coastal and Shelf Science 81 409–422

27. Cheng, N. S. 1997 *Simplified settling velocity formula for sediment particles.* Journal of Hydraulic Engineering

28. Cox, M.R., Budhu, M. 2008 *A practical approach to grain shape quantification.* Engineering Geology, 96, 1-16, USA Tucson

29. Dean, R.G., Dalrymple, R.A. 2002 *Coastal Processes with engineering applications.* Chpt. 2,3,6. Cambridge University Press, UK, 475p.

30. Dinoloket TNO NITG 2009 *Data and information of the Dutch subsurface.* TNO Utrecht, The Netherlands

31. Eisma, D. 1968 *Composition, origin and distribution of Dutch coastal sands between Hoek van Holland and the island of Vlieland.* Ph.d. thesis, University of Groningen, The Netherlands

32. Eisma, D. 1992 *Suspended matter in the aquatic environment.* Springer Verlag, Berlin Heidelberg New York

33. Ekkelenkamp, H.H.M. 2009 *Ecobeach workshop, The scientific research program,* Gouda, The Netherlands

34. Enckevort, I.M.J., Ruessink, B.G. 2003 *Video observations of nearshore bar behaviour, part 1.* Continental Shelf Research 23, Pergamon, The Netherlands

35. Enckevort, I.M.J., Ruessink, B.G. 2003 *Video observations of nearshore bar behaviour, part 2.* Continental Shelf Research 23, Pergamon, The Netherlands

36. Engesgaard, P. 2006 *Effect of vertical drains on tidal dynamics in beaches.* Geological institute, Copenhagen

37. Engesgaard, P. 2008 *Simulation of tidal effects on groundwater flow and salt transport in a coastal aquifer with artificial drains (PEM).* Dep. of Geography, University of Copenhagen

38. Fentie, B., Yu, B., Rose, C.W. 2004 *Comparison of seven particle settling velocity formulae for erosion modelling.* ISCO 2004, Australia

39. Fredsøe, J. 1984 *Turbulent boundary layer in combined wave–current motion.* Journal of Hydraulic Engineering, ASCE 110, Denmark

40. Fredsøe, J., Deigaard, R., 1992 *Mechanics of coastal sediment transport.* Advanced Series on Ocean Engineering, World Scientific, Singapore

41. Fredsøe, J., et.al. 2008 *Report on field tests with the PEM-system at the West Coast of Jutland 2005-2008.* Dep. Of Mech. Eng., DTU, Denmark

42. Glennie, K.W. 1970 *Developments in Sedimentology, Desert Sedimentary Environments.* Elsevier, Amsterdam

43. Graaff, J. de 2009 *Coastal Morphology & Coastal Protection.* Delft Un. Techn. Publication course. Ct5309

44. Groot, A.V. de 2000 *Tidal Groundwater fluctuations in a beach with swash bars.* Msc. Thesis, Groningen

45. Guillén, J. and Hoekstra, P. 1996 *The "equilibrium" distribution of grain size fractions and its implications for cross-shore sediment transport: a conceptual model.* Marine Geology

46. Guillén, J. and Hoekstra, P. 1997 *Sediment distribution in the nearshore zone, grain size evolution in response to shoreface nourishments.* Estuarine, Coastal and Shelf Science, Utrecht University, The Netherlands

47. Haff, P.K. 1996 *Limitations on Predictive Modeling in Geomorphology*

48.	Hoekstra, P., Houwman, K.T.	1997	*Selective sediment transport in the nearshore zone, field observations and potential mechanisms.* Coastal Dynamics, Utrecht University
49.	Horn, D. P.	2006	*Measurements and modelling of beach groundwater flow in the swash-zone: a review.* Continental Shelf Research 26, University of London
50.	Horn, D. P., Walton, S.M.	2007	*Spatial and temporal variations of sediment size on a mixed sand and gravel beach.* Sedimentary Geology, University of London, UK
51.	Horn, D.P.	2002	*Beach groundwater dynamics.* Elsevier Geomorphology, London
52.	Houwman, K., Hoekstra, P.	1994	*Shoreface hydrodynamics, Part 1, Field measurements Egmond aan Zee.* IMAU, Utrecht
53.	Iribarren, C.R., Nogales, C.	1949	*Protection des port.* Lisbon
54.	Jakobsen, P., Brøgger, C.	2006	*Evaluation of the function of the PEM system.* Skagen Innovation Centre, Denmark
55.	Jakobsen, P., Brøgger, C.	2007	*Evaluation of the function of vertical drains.* International Coastal Symposium, Australia
56.	Janssen, G.M., Mulder, S.	2004	*De ecologie van de zandige kust van Nederland.* RWS RIKZ OSW, NL
57.	Jimenez, J.A., Madsen, O.S.	2003	*A Simple Formula to Estimate Settling Velocity of Natural Sediments.* Journal of waterway, port, coastal and ocean engineering
58.	Jonkers, L., et al.	2009	*Experimental insights into laser diffraction particle sizing of fine-grained sediments for use in palaeoceanography.* Sedimentology, NL
59.	Kaczmarek, L.M., Biegowski, J., Ostrowski, R.	2004	*Modelling cross-shore intensive sand transport and changes of bed grain size distribution versus field data.* Coastal Engineering 51, Poland
60.	Kaczmarek, L.M., Ostrowski, R.,	2002	*Modelling intensive near-bed sand transport under wave-current flow versus laboratory and field data.* Coastal Engineering 45, pp. 1–18.
61.	Kasse, K., Spek, A. van de	2009	*Personal contact brainstorm session and analysis of the results.* NL
62.	Kriebel, D.L., Dally, W.R., Dean, R.G.	1986	*Beach profile response following severe erosion events.* University of Florida, USA
63.	Lancker, V. van, Lanckneus, J., Martens, C., Moerkerke, G.	1998	*Small-scale morphology and sedimentological response of the nearshore area of Egmond aan Zee.* Marine and Sedimentary Geology, Ghent University, Belgium
64.	Liiv, T.	1999	*The effect of bottom roughness on the flow quantities under plunging breaking wave motion.* Tallinn Technical University,19086
65.	Lorentz, E.	1993	*The Essence of Chaos.* University of Washington, Seattle
66.	Martins, L.R., Barboza, E.G.	2005	*Sand gravel marine deposits and grain size properties.* Gravel, nr 3, 59 - 70, comar
67.	Masselink, G., Li, L.	2001	*The role of swash infiltration in determining the beachface gradient.* Marine Geology 176, 139 - 156
68.	Masselink, G., Puleo, J.	2006	*Swash-zone morphodynamics.* Continental Shelf Research, 26, 661-680
69.	Meijer, R. J., Bosboom, J., Cloin, B., Katopodi, I., Kitou, N., Koomans, R. L., Manso, F.	2002	*Gradation effects in sediment transport.* Coastal Engineering 47
70.	Meyer-Peter, E., Muller, R.	1948	*Formulas for bed-load transport.* Hydraulic Structures Research. pp. 39-64
71.	Moore, B	1982	*Beach profile evolution in response to changes in water level and wave height.* University of Delaware, Newark
72.	Nielsen, P.	1990	*Tidal dynamics of the water table in beaches.* Water Resources Research 26, Syney, Australia
73.	Nielsen, P.	1992	*Coastal bottom boundary layers and sediment transport.* Ocean Engineering. World Scientific, nr 4

74.	Nielsen, P.	2002	*Shear stress and sediment transport calculations for swash zone modelling.* Coastal Engineering 45, University of Queensland, Australia
75.	Nielsen, P.	2006	*Sheet flow sediment transport under waves with acceleration skewness and boundary layer streaming.* Coastal Engineering 53, 749-758.
76.	Nielsen, P., Callaghan, D.P.	2003	*Shear stress and sediment transport calculations for sheet flow under waves.* Coastal Engineering 47, 347-354
77.	Ostrowski, R., Szmytkiewicz, M.	2006	*Modelling longshore sediment transport under asymmetric waves.* Oceanologia 48, Inst. Of Oceanology, Poland
78.	Pauw, P.	2009	*The onshore and offshore groundwater salinity distribution between Egmond aan Zee and Castricum aan Zee.* MSc. Thesis, University of Amsterdam
79.	Pieterse, J.J.	2009	*The influence of an Ecobeach PEM on beach development.* MSc. Thesis, Delft University, The Netherlands
80.	Pilkey, H.	1994	*Mathematical modeling of beach behavior doesn't work.* Journal of Geological Education, Duke University, Durham
81.	Puleo, J.A., Holland, K.T.	2001	*Estimating swash zone friction coefficients on a sandy beach.* Coastal Engineering 43 25-40, USA
82.	Ramiah, B.K.	1970	*Experimental study of permeability characteristics in sands.* Proc. Sec. Southeast Asian Conf. SMFE, Singapore
83.	Reeve, D., Chadwick, A., Fleming, C.	2004	*Coastal Eningeering, processes, theory and design practice.* Chpt. 2,5,6. Spon Press, 416p.
84.	Reis, A.H., Gama, C.	2010	*Sand size versus beachface slope.* Geomorphology 114, 276 - 283, Evora, Portugal
85.	Rijn, L.C.	1998	*Principles of coastal morphology.* ISBN 90-800356-3-7
86.	Rijn, L.C., Ruessink, B.G., J.P.M. Mulder	2002	*The behaviour of a straight sandy coast on the time scale of storms and seasons.* Coast 3D, Egmond aan Zee, EC Mast Project, NL
87.	Rijn, L.C., Boer, S.	2006	*The effects of grain size and bottom slope on sand transport in the coastal zone.* Coastal Engineering 3066-3078, NL
88.	Robertson, P.K.	1989	*Soil classification using the cone penetration test.* Dept of civil eng. University of Alberta, Canada
89.	Schiereck, G.J.	2001	*Introduction to bed, bank and shore protection.* DUP Blue print, Delft University Press
90.	Short, A.D.	1992	*Beach systems of the central Netherlands coast: Processes, morphology and structural impacts in a storm driven multi-bar system.*Marine Geology 107, Sydney, Australia
91.	Sleath, J.F.A.	1987	*Turbulent oscillatory flow over rough beds.* Fluid mechanics, vol 182
92.	Sleath, J.F.A.	1990	*Bed friction and velocity distributions in combined steady and oscillatory flow.* International conf Coastal Engineering, Delft
93.	Soulsby, R.L., Whitehouse, R.J.S.W.	1997	*Threshold of sediment motion in coastal environments.* Pacific Coasts and Ports '97, volume 1
94.	Stolk, A.	1989	*Zandsysteem kust - Een morfologische karakterisering Kustverdediging na 1990.* Geopro 02, Utrecht University, The Netherlands
95.	Svendsen, I.A., Lorentz, R.S.	1989	*Velocities in combined undertow and longshore currents.* Coastal Engineering 13
96.	Thieler, R.E. et al.	2000	*The use of mathematical models to predict beach behavior for U.S. Coastal Engineering: A Critical Review.* Journal of coastal research, Royal Palm Beach, Florida
97.	Thomas, D.S.G.	1987	*The roundness of aeolian quartz sand grains.* Sedimentary Geology 52, 149-153, Dep of Geography Sheffield UK

98.	Turker, U., Kabdashi, M.S.	2006	*The effects of sediment characteristics and wave height on shape-parameter for representing equilibrium beach profiles.* Ocean Engineering 33, 281-291, Turkey
99.	Turner, I.L., Nielsen, P.	1997	*Rapid water table fluctuations within the beachface.* Coastal Engineering 32 45-59, USA, Australia
100.	Vos, P.C., Eerden, R.A. van, Koning, J. de	2010	*Paleolandschap en archeologie van het PWN duingebied bij Castricum.* Deltares, The Netherlands
101.	Vries, R. de	2009	*Korrelgrootte karakteristiek van het strand.* Kust&Zeemanagement v Hall Larenstein, NL
102.	Wal, D. van der	1998	*Effects of fetch and surface texture on aeolian sand transport on two nourished beache.* Journal of Arid Environments 39
103.	Walstra, D.J.R.	2000	*Unibest-TC Userguide.* WL Delft Hydraulics Z2897
104.	Wellen, E. van, Chadwick, A.J., Mason, T.	2000	*A review and assessment of longshore sediment transport equations for coarse-grained beaches.* Coastal Engineering 40, School of Civil and Structural Engineering, UK
105.	Wiegel, R.L.	2005	*Oceanographical Engineering.* Dover Publications
106.	Wilson, A.M., Huettel, M., Klein, S.	2008	*Grain size and depositional environment as predictors of permeability in coastal marine sands.* Estuarine, Coastal and Shelf Science 80 193–199, USA
107.	Yanagishima, S., Sato K., (burcharth)	2003	*Development of beach stabilization by gravity drainage system.*P&A Research institute, Japan vol.42;no.1
108.	Zhiyao, S., Tingting, W., Fumin, X., Ruijie, L.	2008	*A simple formula for predicting settling velocity of sediment particle.* Water science and engineering vol 1, China

Notations

Symbol	Description
A	Orbital amplitude of fluid just above the boundary layer
A	Shape parameter (Bruun and Dean rule beach profile)
$\hat{a}_0$	Maximum horizontal water particle displacement outside the boundary layer
c	Volumetric concentration of sediment
c	Wave celerity. phase speed
c_0	Solid concentration, bed fluidization
c_b	Bed concentration
c_a	Concentration at reference level
C_D	Drag coefficient
C_M	Mass coefficient
D	Grain diameter
D_{10}	10% of the total volume is smaller than this grain diameter
D_{50}	Median grain diameter, 50% of the total volume is smaller than this grain diameter
D_{90}	90% of the total volume is smaller than this grain diameter
D_f	Grain fall diameter
E	Wave energy
E_{kin}	Kinetic wave energy
E_{pot}	Potential wave energy
f	Friction factor
f	Angularity factor
fc	Current friction factor
f_w	Wave friction factor
f_e	Energy loss factor for the wave boundary layer
$f_{2.5}$	Grain roughness friction factor
F_D	Drag force
g	Acceleration due to gravity
h	Water depth
h_b	Water depth at the wave breaking point
h'_b	Wave set-down
Δh	Wave set-up
δh	Depth of the leading edge at swash
H	Wave height

H_r	Ripple height
H_s	Significant wave height, average wave height of highest one third of measured waves
H_b	Wave height at breaking
H_{rms}	Root mean square wave height
H_0	Deep water wave height
i	Hydraulic gradient
k	Permeability of the soil
k_n	Equivalent sand roughness of the bed
k_e	Effective roughness of moveable bed
k_s	Effective skin roughness of moveable bed
k_v	Empirical coefficient sediment transport
K	Intrinsic permeability
K	Hydraulic conductivity
L_0	Wave length at deep water
L_B	Equivalent bed-load thickness
L	Wave length
l	Mixing length
l_{tube}	Length of the tube filter
n	Number of particles per unit area
n	Porosity of the bed sediment
N	Dean number for accretion or erosion
p	Pressure
q	Net sediment transport rate per unit width [m^2/s]
q_y	Net longshore sediment transport rate per unit width [m^2/s]
q_x	Net cross-shore sediment transport rate per unit width [m^2/s]
Q	Net sediment transport rate at beach profile [m^3/s]
r	Bottom roughness
RE	Reynold's number
s	Relative density of grains
t	Time
t_{tide}	Duration drop high to low tide
T	Wave period
T_s	Significant wave period
u	Velocity
u_t	Velocity at height ez_0
$\bar{u}$	Averaged velocity
U_0	Free stream wave orbital velocity near the bed
u_*	Shear stress velocity
u_f	Friction velocity, time varying

u_c	Current velocity
u_b	Bed load velocity
u_δ	Velocity at the top of the boundary layer
U	Wave period averaged velocity
U_f	Friction velocity
U_*	Wave period averaged shear stress velocity
V_{tide}	Lowering velocity of the water table in the beach
V_{tube}	Flow velocity in the tube
w	Velocity in z-direction
w_s	Settling / fall velocity of a sediment grain
w_*	Dimensionless settling velocity
x	Horizontal coordinate
y	Horizontal coordinate
z	Vertical coordinate
z_0	Zero intercept velocity level
z_b	Bed level
z_*	Rouse number
z_{high}	Water level at high tide
z_{low}	Water level at low tide
z_{tube}	Lowering of the groundwater table by the tubes

α	Wave direction
α_0	Deep water wave direction
β	Bed slope angle
γ	Angle between the current and wave propagation
γ_s	Specific gravity of the sediment grains
δ	Boundary layer thickness
δ_b	Thickness of the bedload layer
δ_c	Thickness of the contact load layer
δ_s	Sheet layer thickness
ε	Dissipation of turbulent energy
ε_s	Turbulent diffusion coefficient for sediment
θ	Shields parameter, dimensionless bed shear stress
θ_{cr}	Critical Shields' parameter
$\theta_{2.5}$	Grain roughness Shields' parameter
ξ	Surf similarity parameter
ρ	Water density
ρ_s	Grain solid mass density

η	Water surface elevation
κ	Von Kármán's constant
ν	Kinematic viscosity
ν_t	Eddy viscosity
λ	Wave length
λ_0	Deep water wave length
λ	Ripple length
μ	Dynamic viscosity
μ_0 μ_1 μ_2	Coefficients in bedload layer model
τ	Shear stress
$\hat{\tau}$	Maximum shear stress
τ_b	Bed shear stress
τ_c	Current bed shear stress
τ_w	Wave bed shear stress
τ_{cw}	Combined bed shear stress
ω	Angular frequency in wave motion
ϕ	Porosity
σ	Sediment sorting
ψ	Angle between major stress and horizontal direction
ψ	Mobility number

Appendix A. Reflection on the hypothesis

A.1 Reflection on the small scale hypotheses

It is trivial that the adoption of an mysterious beach protection system will lead to wrong assumptions. Therefore, one should only look at facts when the technology is judged. Basic concepts must be checked, like the coarsening of the beach. Every new theory or hypothesis raises new questions. It would be an almost impossible task to verify every hypothesis or effect. This study restricts itself to the changes of the sedimentology and some influenced beach processes. For additional research it is wise to give an critical reflection on the hypotheses beforehand. The exploration of an innovative technology must be considered from a theoretical and practical perspective. One example is the filter at the top of the tube. Trapped air in the top of the drainage tube, which dampens pressure changes, may only occur when the cap filter of the tube is constipated. This can not be rationalized theoretically.

The five different hypothesis are reviewed in the paragraph. This is done by means of tables, where arguments are given. These can be in favour or against the working mechanism. Also, suggestions are given which can be used to formulate new research questions.

Table A-1 Arguments for the better conductor of pressures

	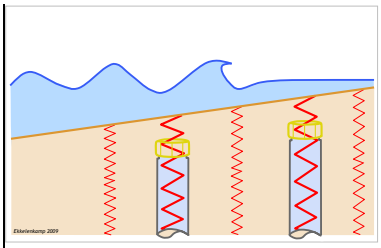 Variations by pressure a guided through the tubes into the soil	The tubes form a better conductor of pressure during rise of water	Less erosion during stormy events because the beach surface is firmer and more stable
Arguments in favour	▪ Since the beach has become coarser, the permeability increased. A more open bed structure allows a better guidance of pressure variations. This will lead to a stronger beach (sub)surface. Eventually the slope will be steeper. ▪ It is possible that a very short time difference occurs. However, it is necessary to use very accurate measurement equipment to determine this change. The influence of these small differences may trigger structural effects on beach processes. ▪ The grain structure is more elastic than water. There might be a discrepancy between the grains and the behaviour of water in the drainage tube. ▪ The coarser grains can provide a better guidance of the various pressures in the sand, because voids will react.		
Arguments against	▪ The detected pressure variations near a drainage tube and at a distance from the tube are not significant. This suggests that the		

	cause-effect relation is not proven. ▪ The high frequency measurements are done to register pressures. Again, these results do not show significant differences. ▪ One must think of bigger space scales when the transfer of pressures through a fluid or sand subsurface are considered. Transfer speed differences between water and sand may be extremely small. In addition, possible effects are very local. ▪ The grain tensions may hardly vary. Normally, these tensions are absorbed by the water surface. A rising water level will not provide an increase in grain tension directly. There is a hydrostatic situation.
Suggestions	▪ There is still not a clear picture of the impact of vertical drainage tubes on a larger time and space scale. Therefore, low frequency measurements are needed to assess the impact on a larger scale. These measurements must be repeated at many different places. ▪ It must be checked whether the pressure is guided exactly parallel into the ground. ▪ The propagation speed of the pressures must be checked in order to compare the tubes with the reference area. ▪ The propagation speed of pressure through dry sand or wet sand must be calculated or tested in practice. Also, the presence of air must be examined. ▪ The amount of air, stored in the subsurface, must be measured. It is important to know the exact location of air chambers and stratification of the subsurface. ▪ Measuring the cohesion of the subsurface may indicate pressure changes. A penetration test could reveal the differences. ▪ It is important to make a distinction between short waves and long waves. Present studies focus on short waves. Tidal waves, which are much longer, may penetrate at a much longer distance into the beach, affecting the groundwater table. ▪ Examine whether the vertical drainage tubes work with average pressure heights or extreme pressure fluctuations. ▪ Past and future research must be (re)done with more accurate measuring equipment.

Table A-2 Arguments for the better damping of pressures

	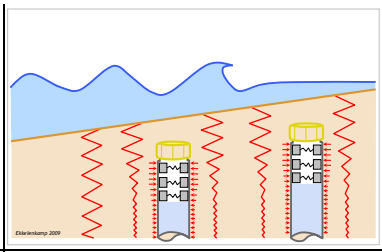 Trapped air in the top of the tubes dampens pressure changes	Pressure from waves weakens by the dampening squeezed air effect	Erosion becomes less along the waterline when the cap filter of the tube is constipated
Arguments in favour	▪ At the high water line this working mechanism may occur more likely, because the water level differences are bigger. The drainage tube will have the opportunity to fill its upper side with air. ▪ The presence of air may initiate the flow of water through the tube. This can lead to a bigger infiltration capacity of the tube. The physical transport of water increases.		
Arguments against	▪ The compressed enclosed air at the upper side of the tube is not yet observed. The top filter must be constipated quite a bit. ▪ The vertical drainage tubes, installed at the lower side of the beach (low water line), are probably under the waterline. Therefore, no air can be hold in the tube which can initiate this working mechanism. ▪ The effect of compressed air, acting like a damper, would be very local. It only occurs every ten to hundreds of metres, depending on the installation grid of the tubes. If it has any effect, it would be an initiating mechanism. For example, it could wash out the fine grains locally. ▪ The high frequency measurements [79] do not show that the measured under pressure in the top of the tube, is due to a quantity of air captured in the tube. ▪ The filters are not tested for constipation.		
Suggestions	▪ The effect of the filter should be properly studied. The drainage capacity must be mapped to different pressures. ▪ It should be examined whether the filters are blocked. If they are blocked, how often will this be the case. ▪ The sedimentology must be examined in order to find fine grain fractions which could obstruct the filter at the top of the tube. ▪ During ebb and flood, the captured air in the tube must be measured with more accurate equipment.		

Table A-3 Arguments for the ventilation of air in the beach

	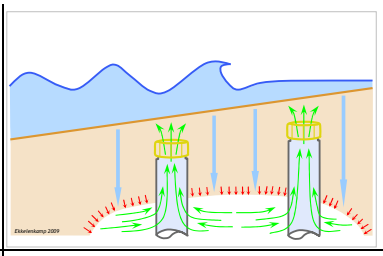 The beach is ventilated by the tubes during water pressure	Air from the beach surface escapes through the tubes	Softening of the beach surface becomes less because air escapes and water infiltrates
Arguments in favour	▪ There are almost always air bubbles trapped in the beach. During flood, they are below the ground waterline near the beach surface. ▪ If the filter of the vertical drainage tube makes contact with the confined air, then it will always affect the ventilation of air during rising tide. ▪ This working mechanism will work properly at the upper beach near the high water line, where bigger volumes of air are stored in the beach. ▪ Probably, the influence of the tide (long waves) is the most significant. Most air is ventilated during rising tide.		
Arguments against	▪ The air, trapped in the beach, is often located near the beach surface. The drainage tubes may be installed out of reach. ▪ If the top filter is blocked and the centre filter is located below the air volume, the tube will not affect the ventilation of the beach. I.e. there must be interaction of the filter with the air in the subsurface. ▪ Drops of pressure are still not observed in practice. ▪ The capillary force, of the water in the drainage tube, may block the filter top. In that case, the ventilation of air through the top of the tube is prevented. ▪ Beaches with fine sediments will block the top filter instantly. The transport of air through the filter is very limited if this filter is blocked by fine grains.		
Suggestions	▪ Measurements must be done with a sealed top filter. These results must be compared with present findings to see if there is a difference that indicates the top filter is blocked. ▪ The presence of air volumes should be mapped. One must know the depth, volume and location of the air, in order judge whether or not these air volumes are penetrated by the drainage tubes. ▪ The infiltration and exfiltration of water during a swash cycle will influence the air ventilation for short waves. In addition to visual observations, the formation of air bubbles must be examined with accurate divers.		

Table A-4 Arguments for the downwards transport of water

	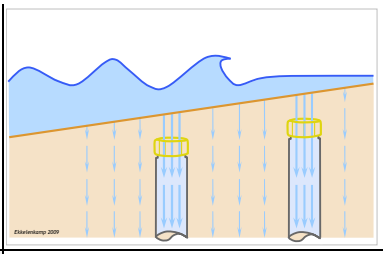
Arguments in favour	▪ During uprush, the water infiltrates at the beach surface. The rise of the water level increases the water pressure. At the bore front, exfiltration occurs. The theory behind the swash dynamics and vertical transport of water confirm the occurrence of vertical transport through the drainage tubes. ▪ Short waves cause infiltration of water at the swash line. Tidal waves, which cause the groundwater circulation, will cause infiltration at the high waterline. Tubes, installed at the upper side of the beach, will influence the physical transport of water. ▪ Field observations confirm that the filters in the middle of the tube continues to operate. If the water can penetrate into the subsurface, the tubes will transport a certain amount of water.
Arguments against	▪ The drainage capacity is strongly reduced if the permeability of the subsurface is to low. The water, which is transported downwards through the tube, encounters resistance when it tries to flow out of the tube. ▪ It is still not proven that vertical transport of water through the tube occurs. The small pressure variations, which are measured in the past, do not confirm this mechanism. ▪ Still no relation between the drainage effect and sediment transport is proven. ▪ Physical transport through the tubes is not yet determined. Indications are only based on pressure variations.
Suggestions	▪ It is important to investigate whether there are differences between short waves and long waves. The relation between short waves and sediment transport differs from the case with long waves. Short waves are characterized by a more dynamic behaviour. ▪ Investigate the permeability of the beaches where vertical drainage tubes are installed. This can be done by taking several sediment samples from different depths. ▪ The relation between long tidal waves and groundwater oscillations in the beach is important to understand. Within this model the tubes should be involved. ▪ The effect of under pressure, caused by infiltration, should be investigated. If the filter at the top of the tube is blocked, downwards movement of water will create an unsaturated zone. Suddenly, the filter will break through when this zone reaches a height of thirty centimetre [33]. This may influence mechanisms

	whereby the top filter should remain blocked. ▪ The actual discharge through the tubes should be investigated. This could be done by using a propeller in the tubes to register the transport velocities accurately. ▪ This working mechanism is vertically oriented. Groundwater circulations, which could be effected by the vertical drainage tubes, also have an important horizontal component. It is essential to study the depth below the beach surface where groundwater circulation takes place. ▪ The groundwater flow in the beach is often described using a conceptual model (Figure A-1). If shells or gravel layers are present, this flow adjusts itself. Even an impermeable layer, like the thin clay layer under the beach of Egmond aan Zee [78] changes the return flow of groundwater. In that case, it extends much further offshore.

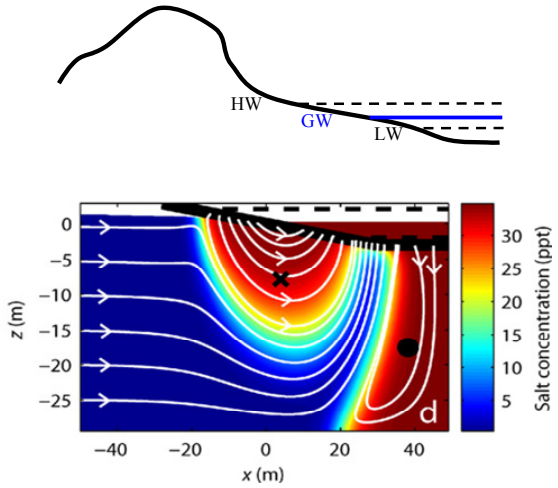

Figure A-1 Conceptual model of groundwater flow in a beach

Table A-5 Arguments for the upwards transport of water

	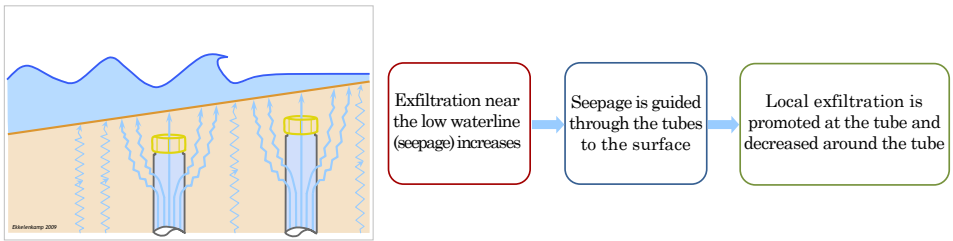
Arguments in favour	▪ This mechanism has a strong influence on exfiltration. The vertical oriented flow influences the grain stability. The fine fraction may be washed away, while the surrounding area of the tube is more stable. There, the exfiltration might be reduced. ▪ The specific outflow situation near the low water line is stimulated

	by the presence of vertical drainage tubes. If the flow is upward directed, the flow through the tube is increased. ▪ Seepage of fresh water at the low water line which destabilizes the beach surface, is canalized. ▪ Measurement show that the transition region between the groundwater and beach surface is affected [79]. ▪ Sediment transport is affected near the tubes on a small scale, because grains are lifted more easily. ▪ The boundary layer thickens which causes the bed velocity to decrease. Less grains will suspend, while the capacity of the flow increases. ▪ Impermeable layers, like clay deposits, may form a blockade for vertical transport of groundwater. The drainage tubes may form a shortcut between water levels and various soil layers. ▪ The groundwater gradient, especially in the case of a layered soil structure (with shells of gravel), will be affected. ▪ Flattening of the groundwater gradient provides an increase in storage capacity.
Arguments against	▪ The transport of water through the drainage tubes is not guaranteed, if the permeability of the surrounding subsurface is unknown. ▪ This mechanism is expected to be only applicable at the low water drainage tubes. ▪ Still no relation between the exfiltration of the drainage tubes and the transport of sediment is confirmed. ▪ If the tubes are to deep below the bed, this effect will decrease. This would only happen if sediment accretes at the beach, i.e. the system works.
Suggestions	▪ The effect of exfiltration near the bed surface is local. It would be wise to study the difference between the tube area and reference area (taken some metres away). ▪ Exfiltration leads to the transport of water, if the required conditions are met. One important issue is water pressure. It is suggested that one should investigate the beach permeability. ▪ Permeable layers may be connected by the vertical drainage tubes which may lead water pressures to the sea bed. It must be investigated whether or not the tubes are penetration these layer. ▪ The transport of sediment is influenced by the amount of exfiltration. This balance and sensitivity must be studied. ▪ The relation between the permeability and grain size distributions must be investigated, because exfiltration is strongly influenced by the sedimentology of the beach. ▪ The divers, used in previous research, were not accurate enough to confirm that the groundwater level around the drainage tubes is affected. More detailed field research must be done to register changes of the phreatic level and vandose zone around the tubes.

A.2 Reflection on the large scale working mechanism

Table A-6 Arguments for the global hypothesis; groundwater levelling and desiccation

	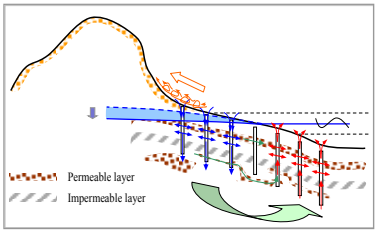 Groundwater levels because the circulation is enforced by filtration. Infiltration and exfiltration via a layered structure provides a lower gradient. Adjusting the groundwater level during falling tide goes quicker. The beach will become more dry in time
Arguments in favour	▪ The vertical drainage tubes act like a drain. The groundwater circulation is enforced. ▪ Layers of coarser grains or shells are connected with each other. If this route is connected to the sea, this path of least resistance will be chosen. ▪ Impermeable layers may be penetrated which induces pressure adaptations. The groundwater level lowers when water pressures are decreased. ▪ A lower beach groundwater level provides a more dry beach in time. Aeolian transport will remove the fine fraction from the beach surface. ▪ The beach will become coarser. The more robust beach will be wider. The recreational area increases. ▪ The dunes are fed by fine sand, supplied from the beach. ▪ The increased storage capacity delays the saturation of the beach. The beach will remain dry for an extended period of time. The duration of aeolian transport will be increased. ▪ Air, trapped in the beach, is ventilated. Additional storage capacity is obtained. ▪ The active layer of sand at the beach, the beach envelope, will become coarser in time. The permeability increases. The effect of the vertical drainage tubes will be enhanced. The tubes act like a trigger. ▪ If the sediment becomes very coarse, the vandose zone (level of capillary fringe) decreases. Again, the beach becomes more dry in time.
Arguments against	▪ The flow capacity of the drainage tubes may be to low in order to achieve any changes. ▪ The dimensions of the tubes may be insufficient. The same can be said about the chosen amount of tubes per square metre. ▪ It is not proven that the drainage tubes are penetrating permeable or impermeable layers. ▪ There is no evidence that the tubes provide a highly permeable route from the dune foot to the sea.

	▪ The storage capacity may be to small to initiate any change.
Suggestions	▪ The subsurface of the beach must be studied. One should know the existence of (im)permeable layers and shells. ▪ By doing falling head tests, the permeability of the beach can be determined. ▪ The drainage capacity of the tubes should be checked, by testing the flow rate through the tubes when they are placed in sand with different types of sediment. ▪ Calculation of the flow rates for different beach permeability. ▪ Check if layers are penetrated by the drainage tubes. ▪ Sediment samples must be taken at the drainage tube area and a reference area. ▪ The increases steepness of beach profiles should be analysed ▪ Sand traps can be used to measure the amount of aeolian transport to the dunes. ▪ The dune foot position can be compared with data from the past. ▪ Vegetation at the dunes should increase in volume and become more green. ▪ Groundwater measurements may indicate an increase of the storage capacity below the beach surface. ▪ The beach envelope should be registered and analysed. If the beach sediment becomes coarser, only this part of the beach could change. ▪ The width of the drained beach compared with a reference area forms an important figure.

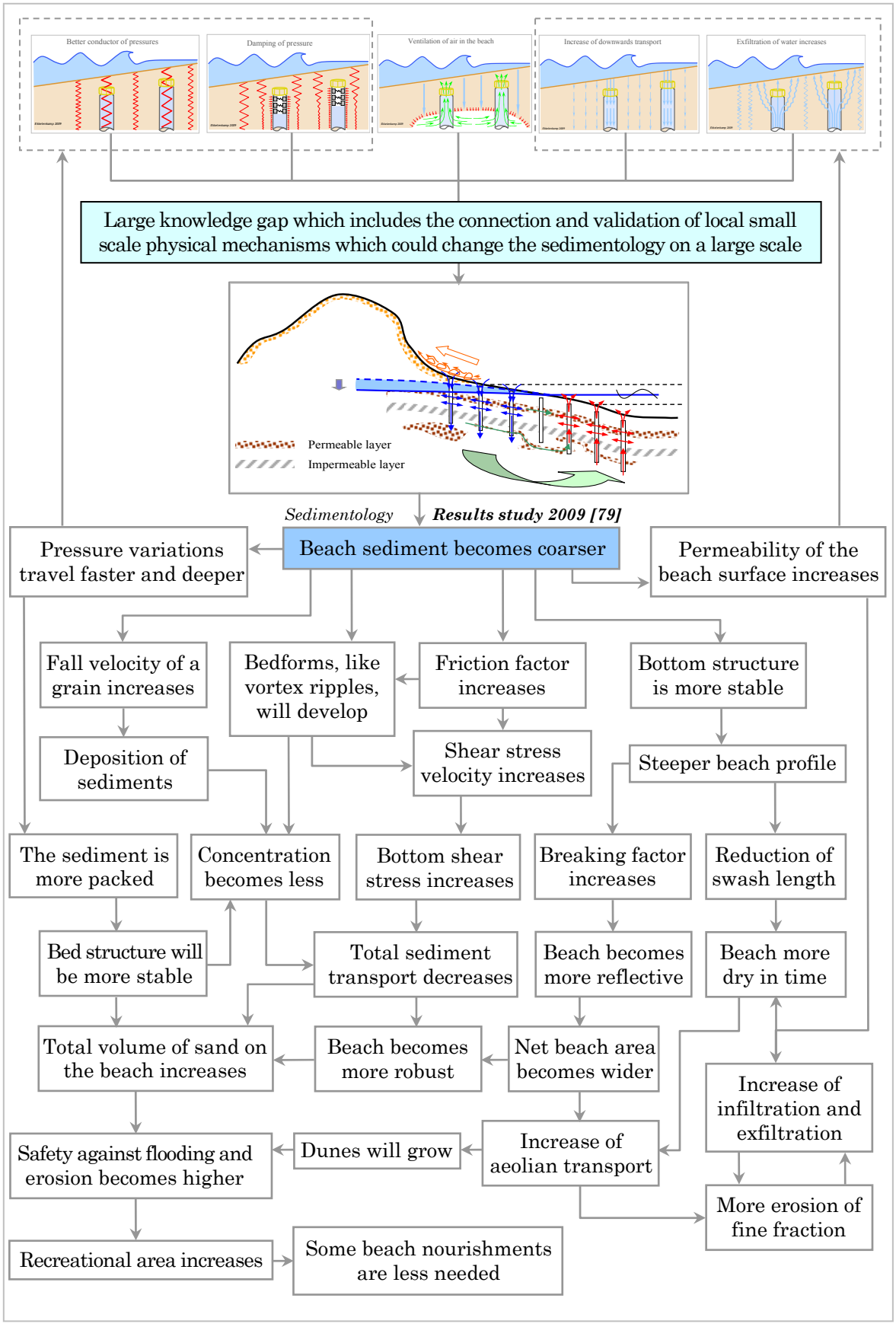

Figure A-2 Event tree of the process from small to large effects on the beach zone

Appendix B. Details of the research and analyses

B.1 Field research

The field data consists of a number of experiments, done during the years 2009 and 2010. Appendix B gives an overview of these field tests. The weather conditions during the tests varied. The water levels during calm conditions were approximately -0.60 NAP at low tide and +0.70 NAP at high tide. The tidal range increased during stormy conditions with nearly thirty centimetres. The measured wind speeds were approx. 7 m/s during calm weather and 17 m/s (almost eight Beaufort) in stormy conditions. The corresponding wave heights were respectively 1,2 m to 4,5 m. The more detailed hydrological data is showed in Appendix J.

Table B-1 Overview of the field experiments

Date	Weather conditions	Experiments done
August 30th, 2009	Calm	Beach profile survey Egmond aan Zee
September 2nd, 2009	Little windy, sunny	Sediment samples Egmond aan Zee
September 5th, 2009	Stormy	Beach profile survey Egmond aan Zee
September 8th, 2009	Windy	Beach profile survey Egmond aan Zee
September 11th, 2009	Calm, wet	Impermeable layers at Egmond aan Zee
November 13th, 2009	Windy, wet	Sediment samples near Egmond aan Zee
December 15th, 2009	Very calm	Sediment samples near Hvide Sande
December 18th, 2009	Little windy, sunny	Permeable gravel layers Hvide Sande
February 18th, 2010	Stormy, wet	Depth measurements shells Egmond aan Zee
April 16th, 2010	Cloudy, dry, calm	Dune vegetation Egmond aan Zee
April 26th, 2010	Calm, little windy	Cone penetration tests Egmond aan Zee
April 27th, 2010	Calm, sunny	Depth samples at Egmond aan Zee
April 27th, 2010	Calm, sunny	Beach profile survey Egmond aan Zee
May 4th, 2010	Little windy	Permeable shell layers Egmond aan Zee
May 17th, 2010	Clear, dry, calm	Locations/intensities shell fractions
June 8th, 2010	Rainy, windy	Dune foot measurements Egmond aan Zee

A large part of the field data concerns the analysis of the sediment samples (par. 5.2 and 5.3). Two field measurements were done in the year 2009. Samples were taken during the 13th of November at the Dutch coast near Egmond aan Zee. During the 15th of December a number of sediment samples were collected from the Danish beach near Hvide Sande.

The geological composition of the beaches is studied by analysing different soil layers in the subsurface (paragraph 5.1). Shell layers were found at the beach near Egmond aan Zee while gravel layers dominated the beach near Hvide Sande. Both permeable and impermeable layers were found. The shell and gravel layers can be considered as very permeable. The clay layer, found at Egmond aan Zee, is very impermeable.

The sediment at the beach near Egmond aan Zee contains a large amount of shell fractions. These fragments are, compared to the sand particles, very large. They form very permeable areas in the beach subsurface. The percentage of shells in the sediment samples is determined, by measuring the fraction before and after their removal from the sample. This was done by adding different kinds of acids [see Appendix B for a more detailed description of the analysing process in the laboratory]. The depth in which the shell fractions occur is also investigated. The intensities and spatial scales varied considerably. Sections 5.1.1 and 5.2.4 show the results from these studies in more detail.

The gravel layers, present at the beach near Hvide Sande, are likewise very permeable. Many glacial deposits exist at the beach. These layers are exposed after severe storm events. They are found along the entire coast. Their presence has been demonstrated by looking at the sides of pits, which were dug in the beach. As with the shells, the gravel fraction of the sediment sample was determined. This was done by heating and drying the sediment sample in an oven. [see Appendix B for a more detailed description of the analysing process in the laboratory].

All samples were analysed with state of the art devices which use laser diffraction sensors to measure the grain size. Another device took photographs of the grain particles and determined the aspect ratio and sphericity of every single grain. The sediment samples were taken from the intertidal beach zone of both beaches. This location was determined using modern Global Positioning equipment (GPS). The exact locations of the measurement are listed in Appendix L. The sediment samples were taken from thirty centimetres depth. This measure was chosen because the composition of the upper part of the beach surface may change during the field measurements. The active zone of the beach is at least half a metre deep. The drills were done using a hand drill. Before the measurements were done, the swash bars and rip channels were analysed. The feeder channels, running along the beach, were mapped. The measurements were done at the mean water level, between the bars and the high water line.

The spacing density of the sediment sample measurements varies. At the areas where vertical drainage tubes are installed, every 250 metre measurements were done. The rest of the soil samples have a distance of 500 metre from each other. In addition to the measurements at Egmond aan Zee, a number of box measurements were done near the drainage tubes. A 'box' of nine samples, with a mutual distance of ten metres, give the grain size variations near the vertical drainage tubes. These measurements are also taken at a depth of thirty centimetres. The results of both beaches are explained in detail by section 5.2 and 5.3.

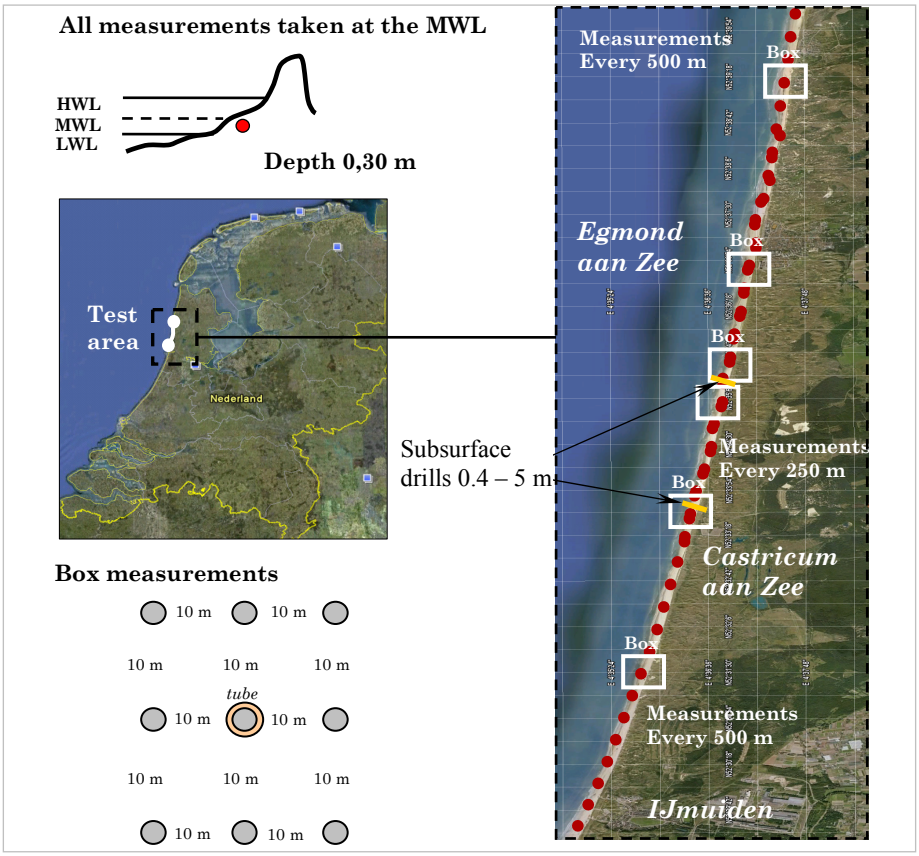

Figure B-1 Field measurements at Hvide Sande (Denmark)

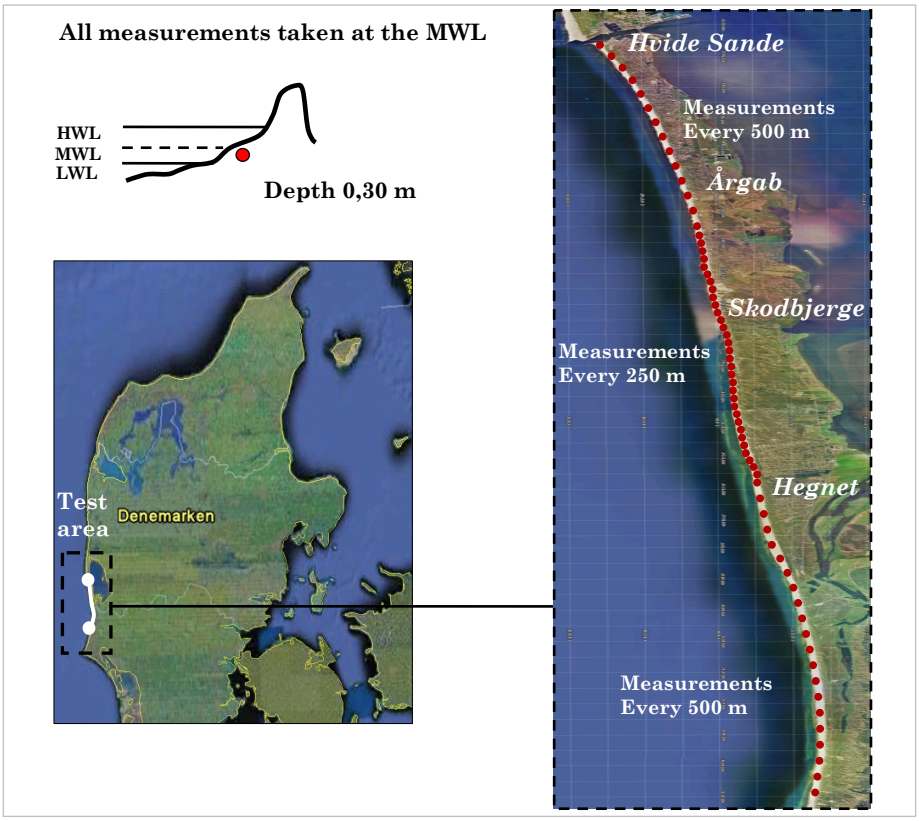

Figure B-2 Field measurements at Egmond aan Zee (The Netherlands)

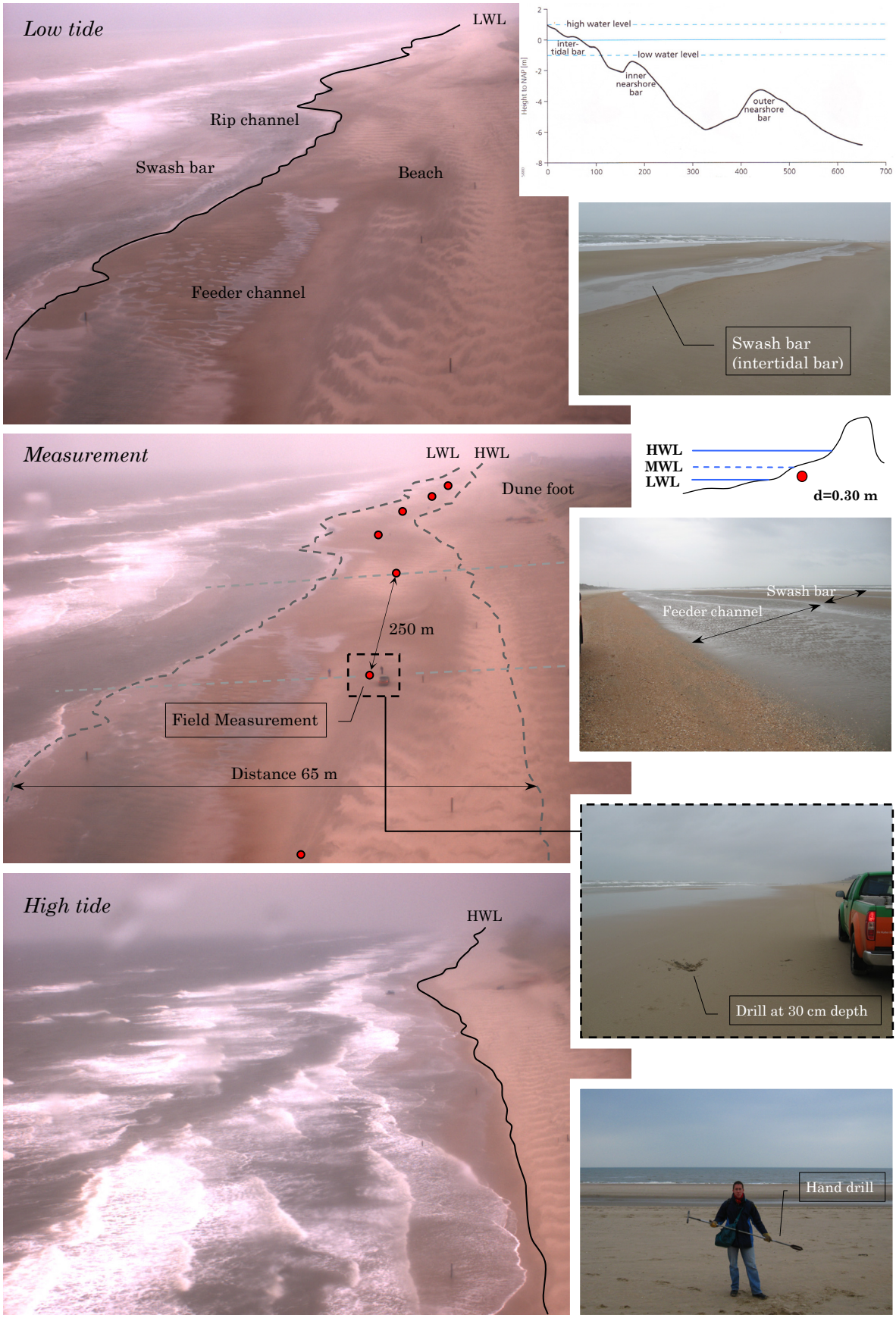

Figure B-3 Locations of the sediment samples between the high and low water level

B.2 Laboratory research

The sedimentology of the beaches was studied by taking a large number of sediment samples. The set of samples was taken from the subsurface at a depth of 30 to 50 cm near the mean waterline. In this way the sediment of the active beach zone is analysed. Every sample is carefully analysed in a certified geotechnical laboratory. The newest Laser diffraction sensor HELOS/BR with measuring zone for the insertion of dry / wet dispersers or sample couplers for particle size analysis. HELOS, the well proven laser diffraction sensor is the first system using one measuring principle laser diffraction in the parallel laser beam. The combination of measuring ranges allows the analysis of extremely wide size distributions at highest precision.

Figure B-4 The Laser Diffraction Sensor HELOS/BR, used during the analysis of the samples

It is the classical instrument for particle size analysis of dry and wet samples, i.e. of powders, suspensions, emulsions or sprays. It is entirely built to the specifications of ISO 13320 "Particle size analysis - laser diffraction methods" - and designed for absolute precision measurements to typically ±1% deviation with respect to the standard metre. High resolution and guaranteed reproducibility results in superior solutions. After the sediment samples are taken they prepared for analysis. First any organic/carbonated material is removed from the sample by adding a number of acids. The sediment is threatened by H_2O_2 15% and HCl 0.5%.

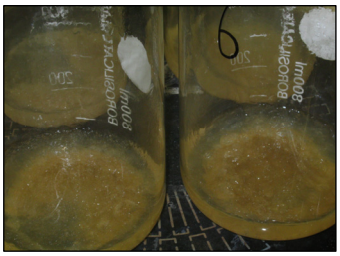

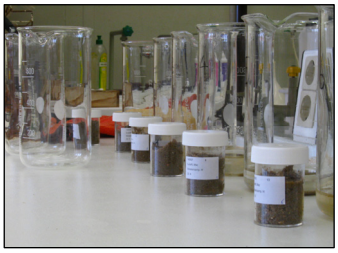

After washing out ions of the sand the samples are suspended in $Na_4P_2O_7$ and $10H_2O$ 1%. Next the suspended sediment is inserted into the Helos KR and analysed. The output consists of the grain sizes and distributions. This data will be used to study the effects of the PEM system on the sedimentology of the intertidal beach area, dunes and surrounding coast.

Appendix C. Field measurements Egmond aan Zee

C.1 D_{10} grain sizes

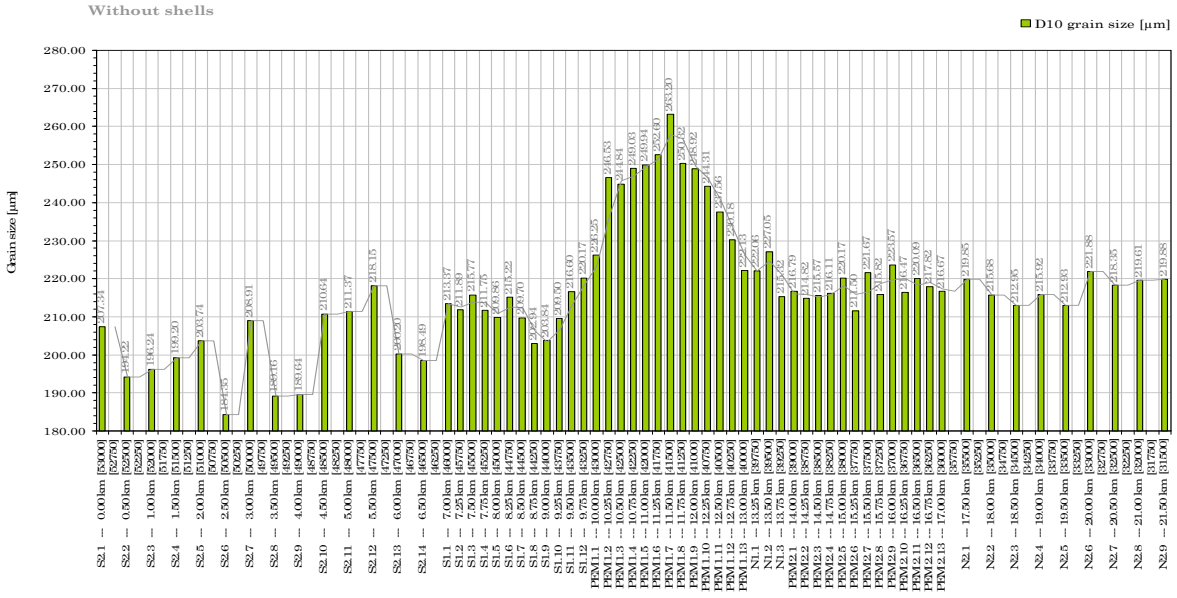

Figure C-1 D_{10} grain sizes at Egmond aan Zee without shells

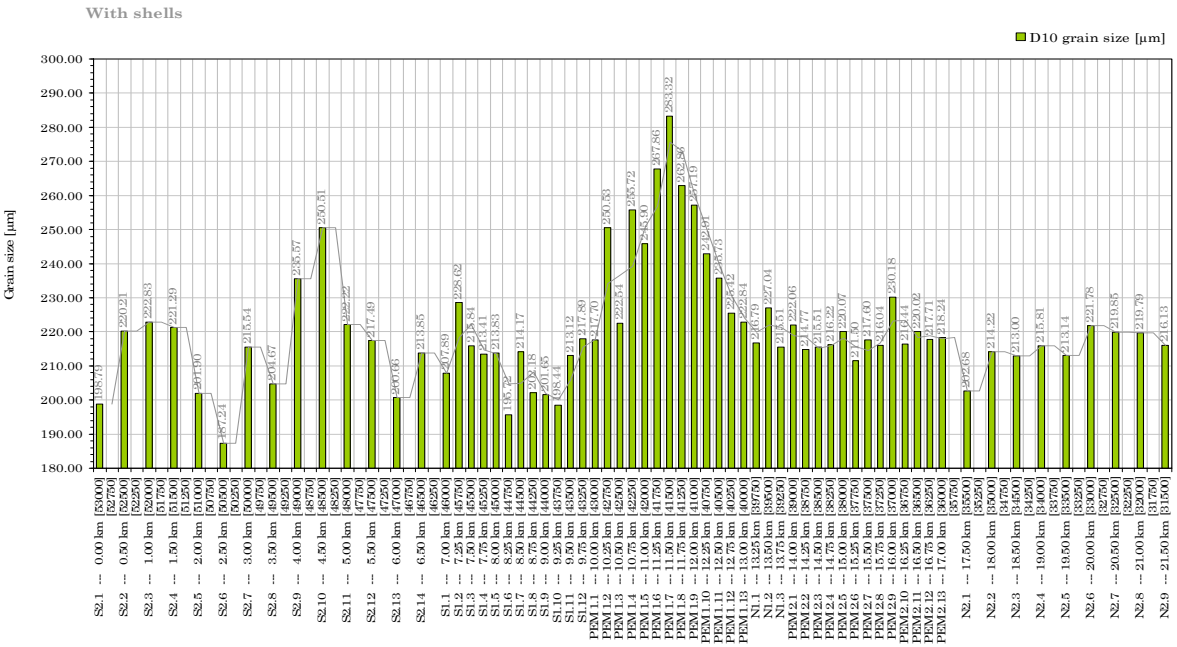

Figure C-2 D_{10} grain sizes at Egmond aan Zee with shells

C.2 D_{50} grain sizes

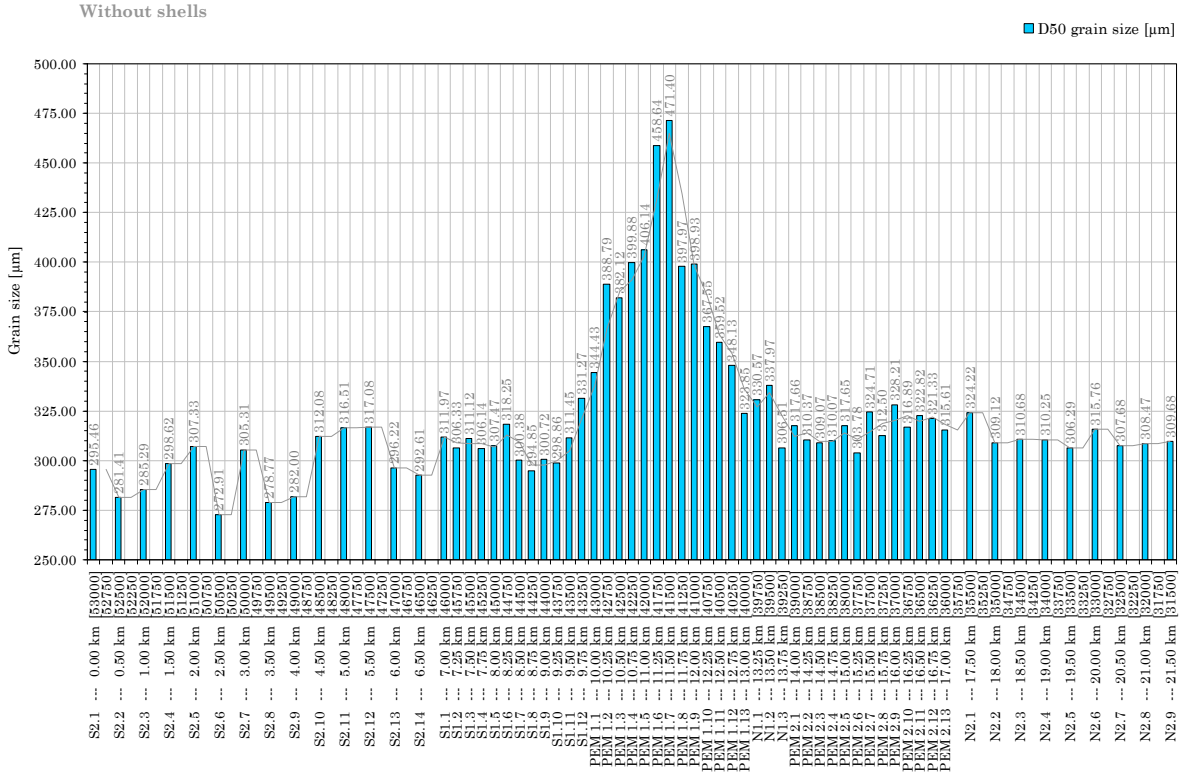

Figure C-3 D_{50} grain sizes at Egmond aan Zee without shells

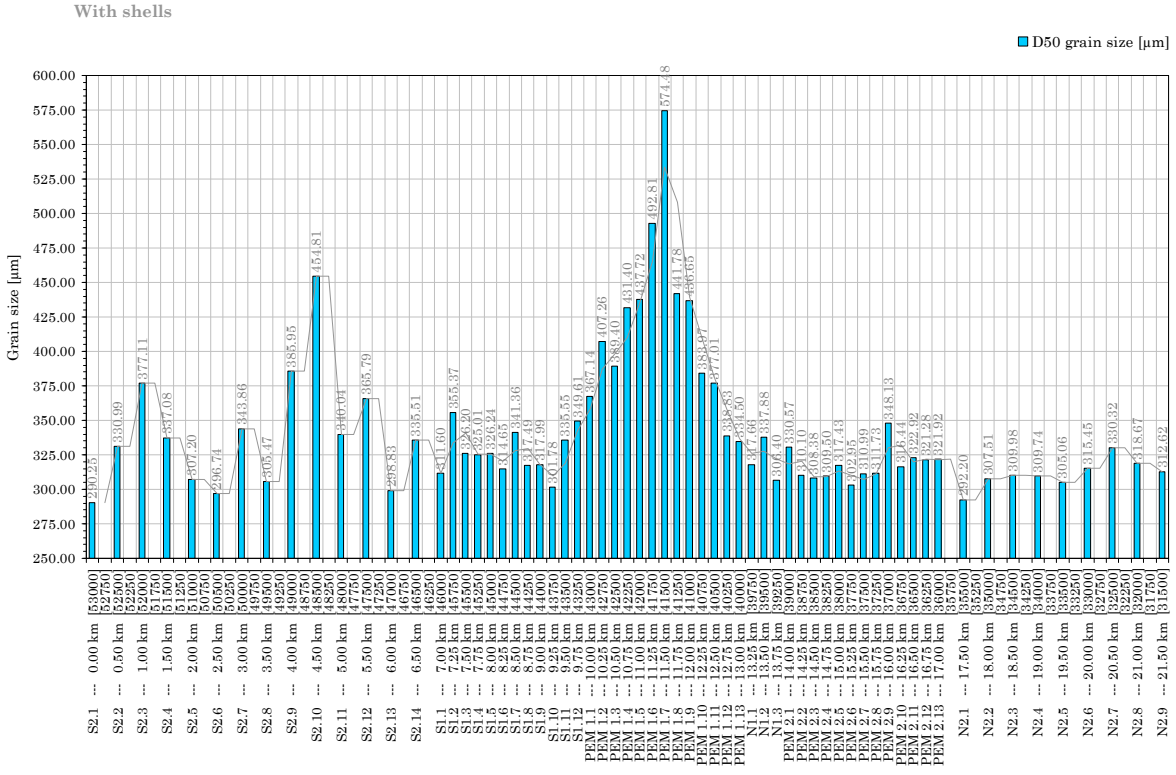

Figure C-4 D_{50} grain sizes at Egmond aan Zee with shells

C.3 D_{90} grain sizes

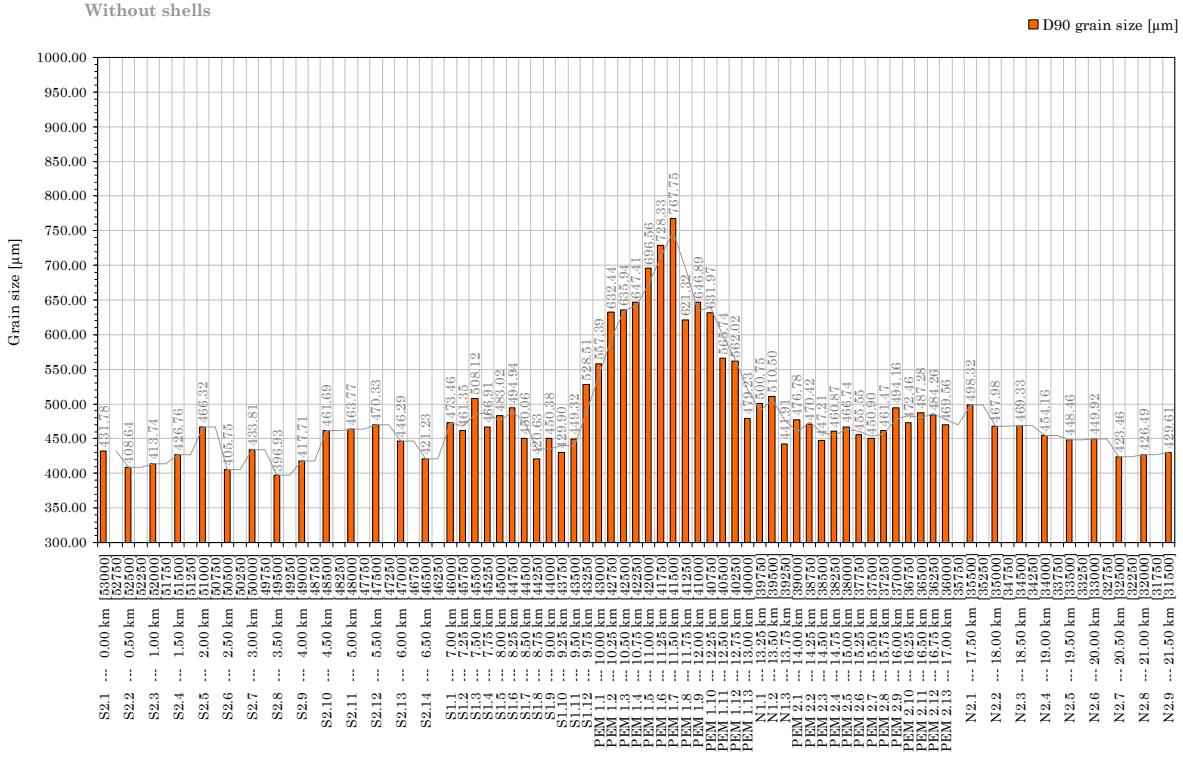

Figure C-5 D_{90} grain sizes at Egmond aan Zee without shells

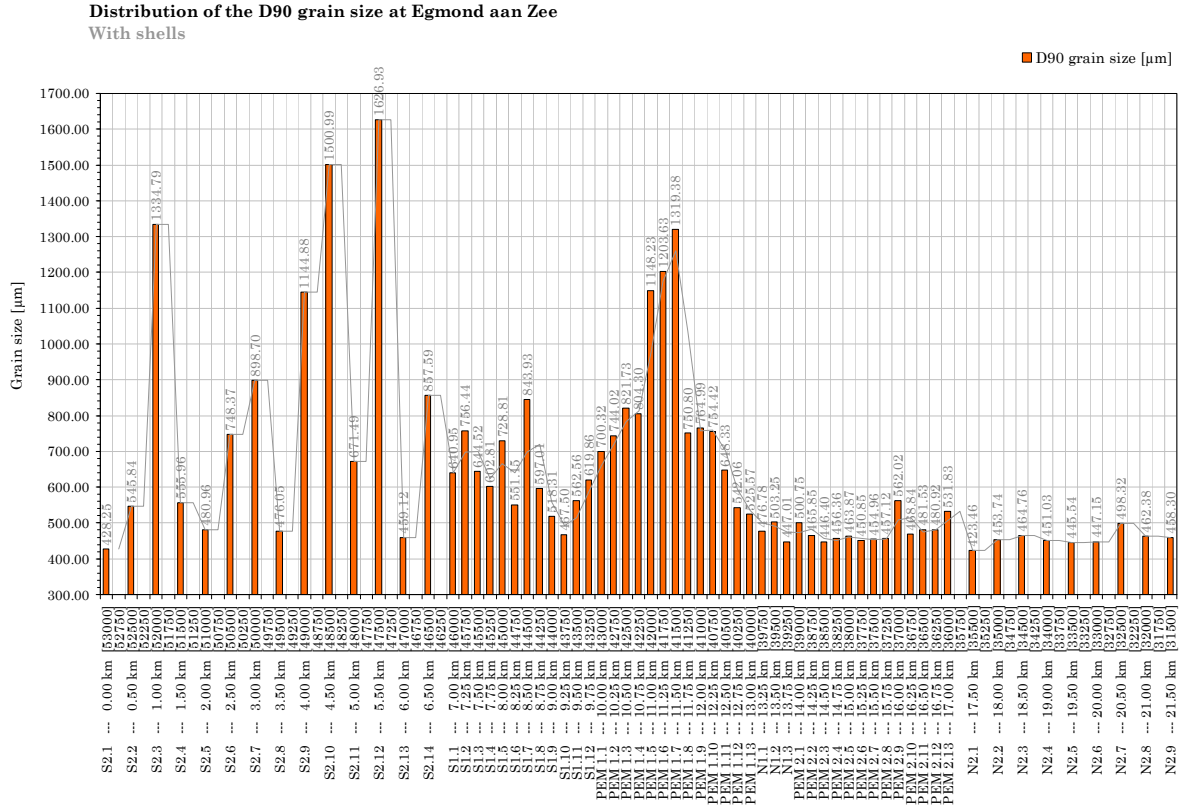

Figure C-6 D_{90} grain sizes at Egmond aan Zee with shells

C.4 D_{63} grain sizes

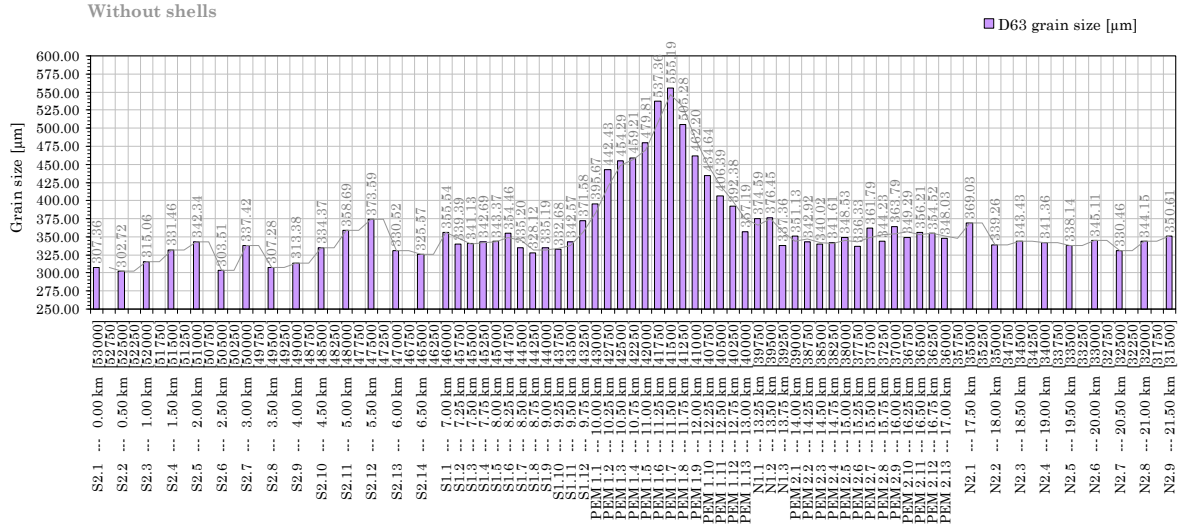

Figure C-7 D_{63} grain sizes at Egmond aan Zee without shells

C.5 Very fine fraction

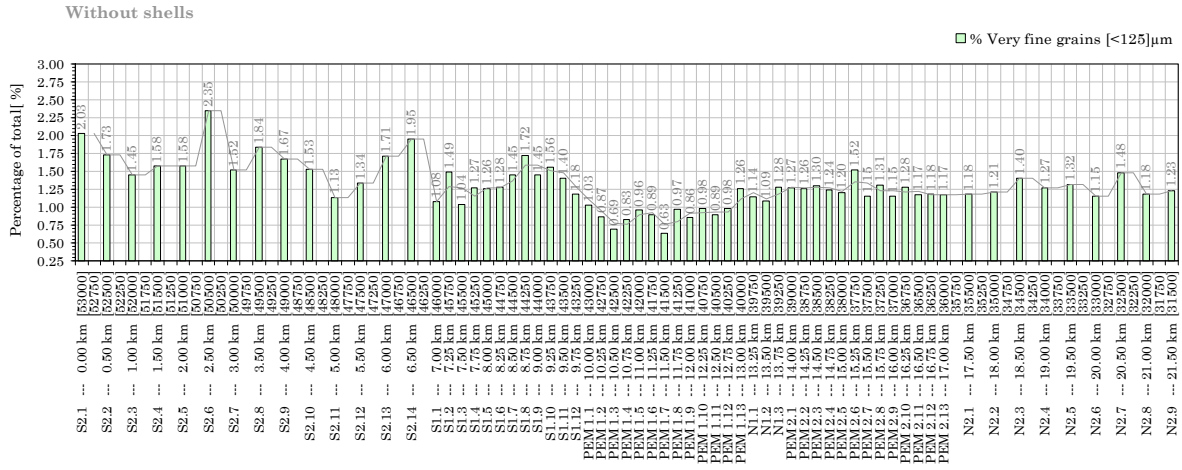

Figure C-8 Very fine fraction at Egmond aan Zee without shells

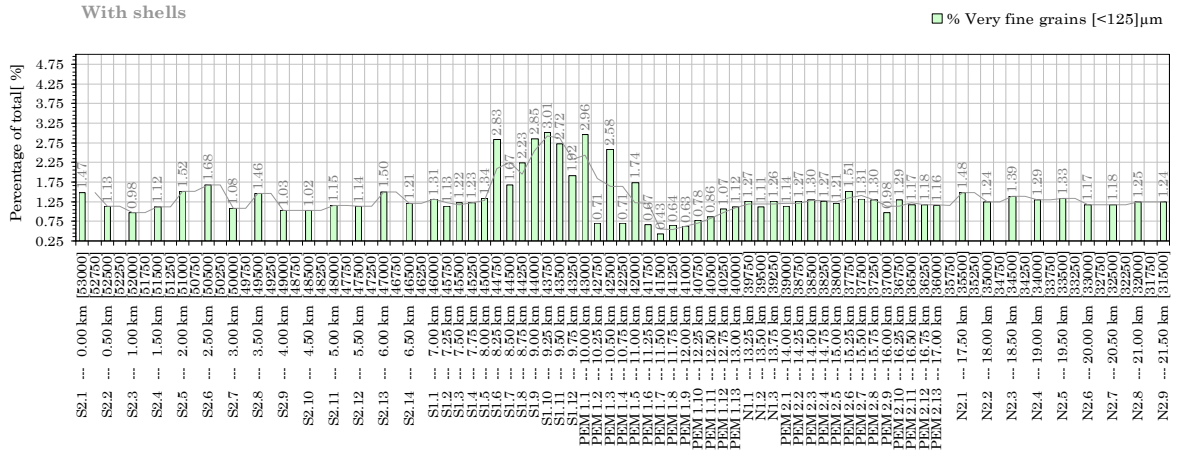

Figure C-9 Very fine fraction at Egmond aan Zee with shells

C.6 Fine fraction

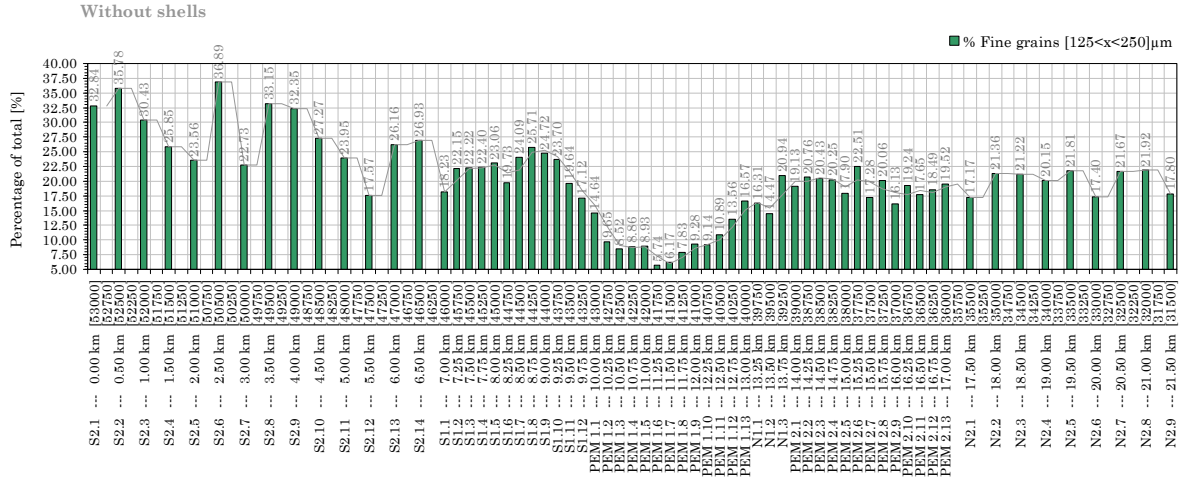

Figure C-10Fine fraction at Egmond aan Zee without shells

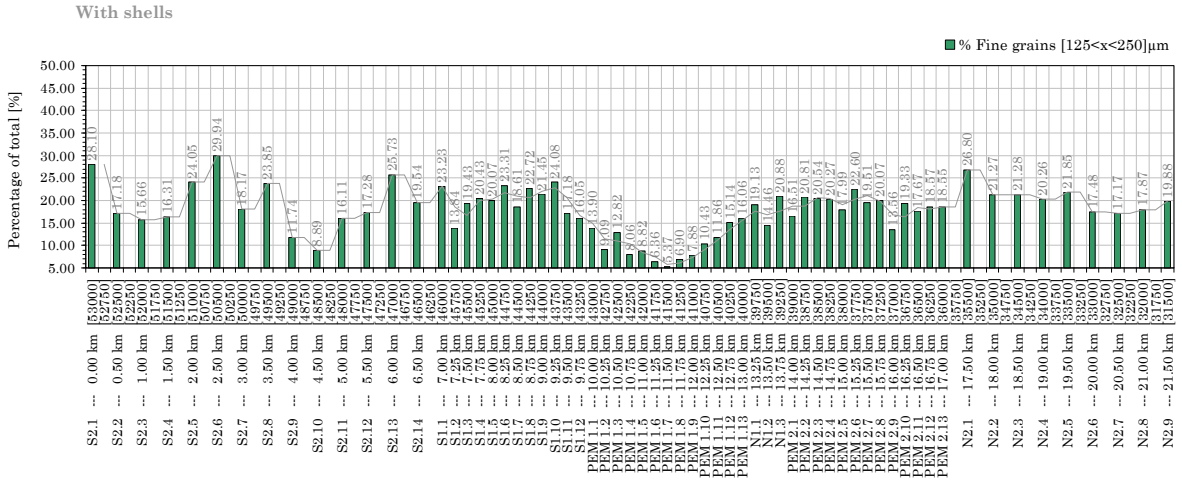

Figure C-11Fine fraction at Egmond aan Zee with shells

C.7 Medium fraction

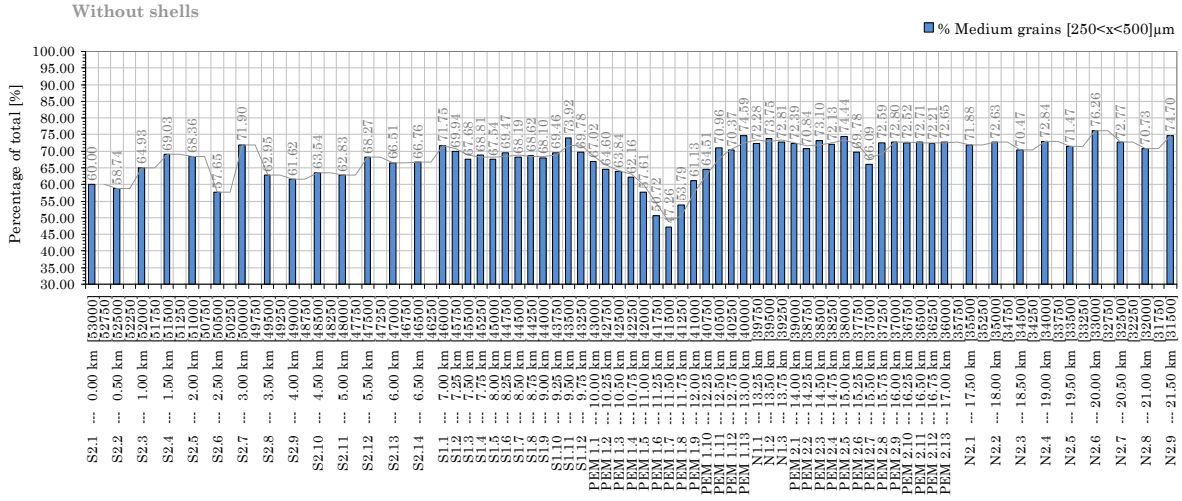

Figure C-12Medium fraction at Egmond aan Zee without shells

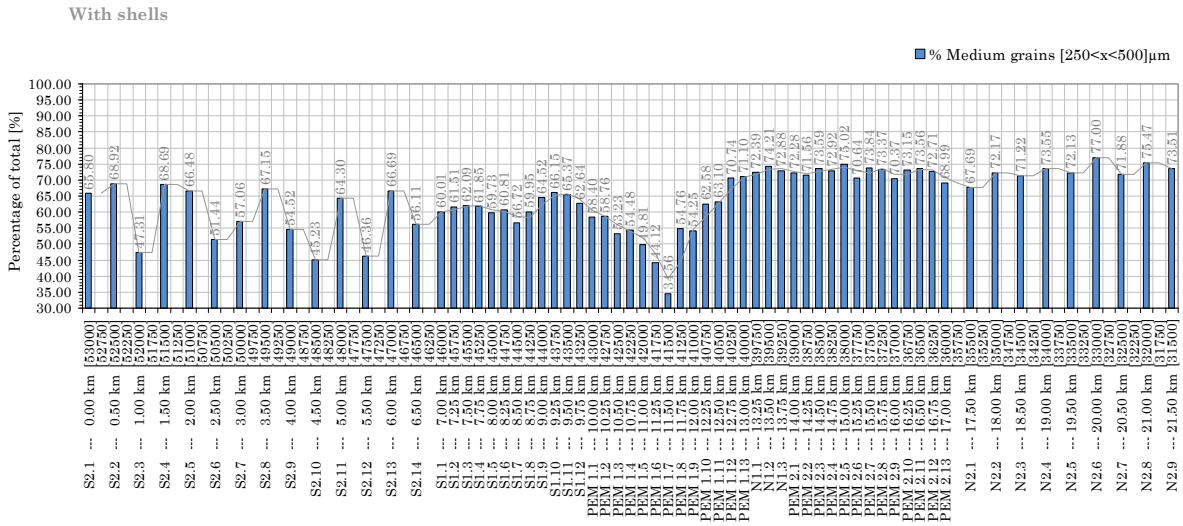

Figure C-13Medium fraction at Egmond aan Zee with shells

C.8 Coarse fraction

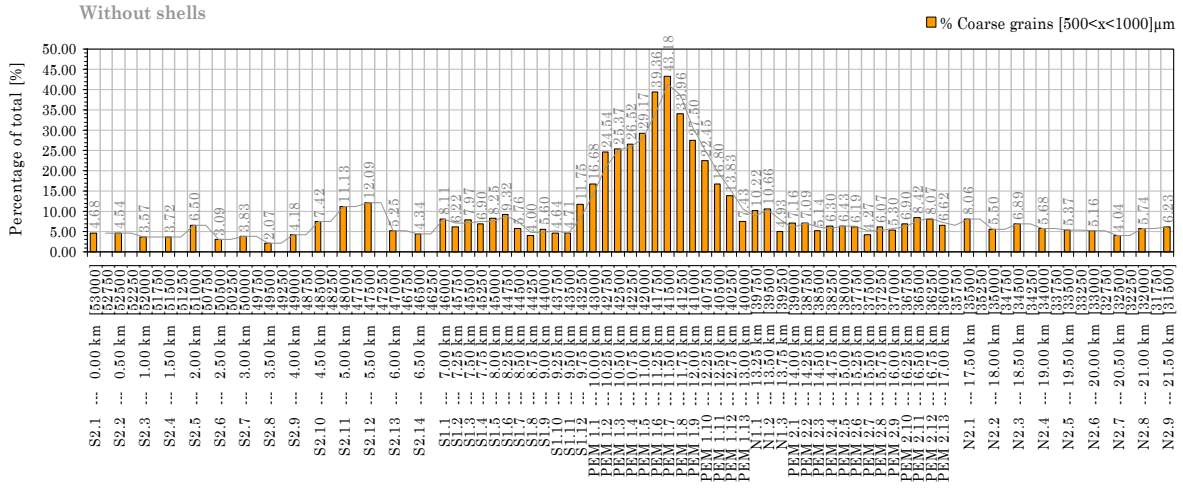

Figure C-14Coarse fraction at Egmond aan Zee without shells

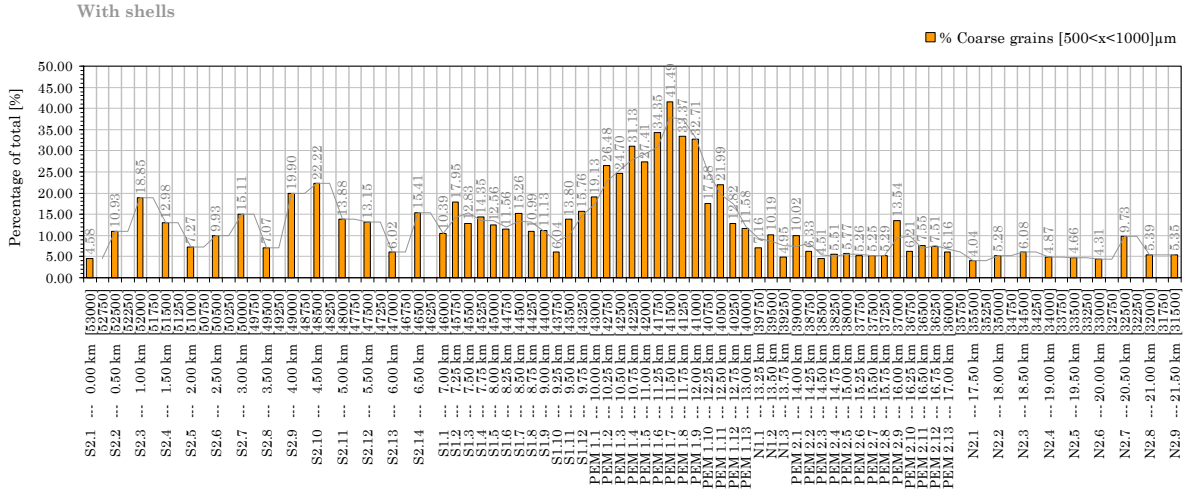

Figure C-15Coarse fraction at Egmond aan Zee with shells

C.9 Very coarse fraction

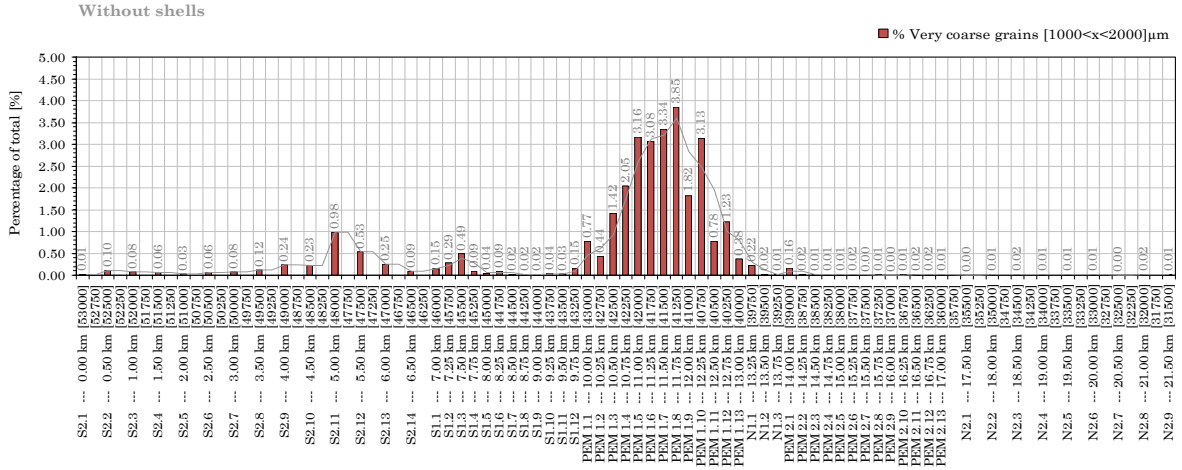

Figure C-16Very coarse fraction at Egmond aan Zee without shells

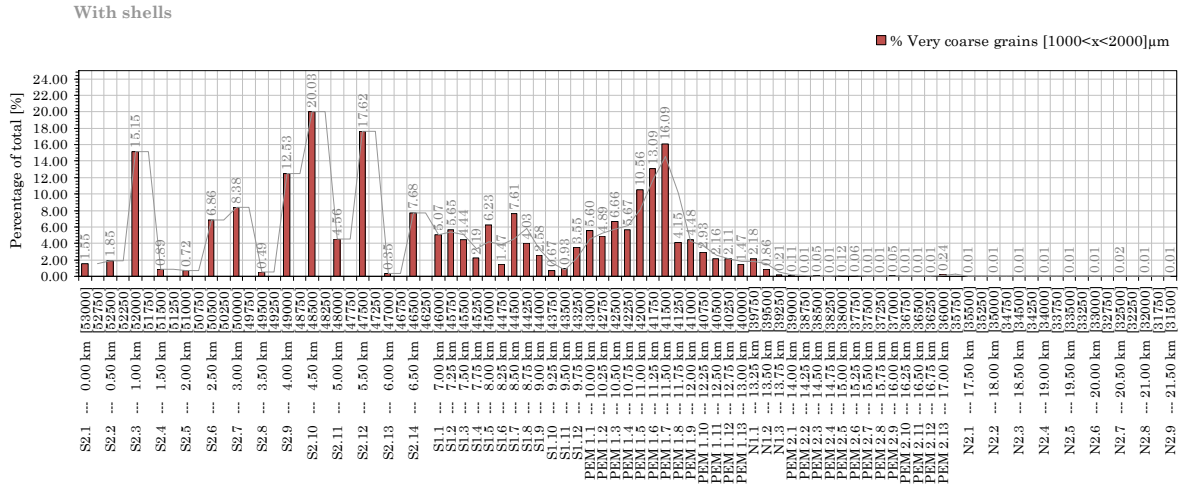

Figure C-17Very coarse fraction at Egmond aan Zee with shells

C.10 Cumulative distribution of gradations

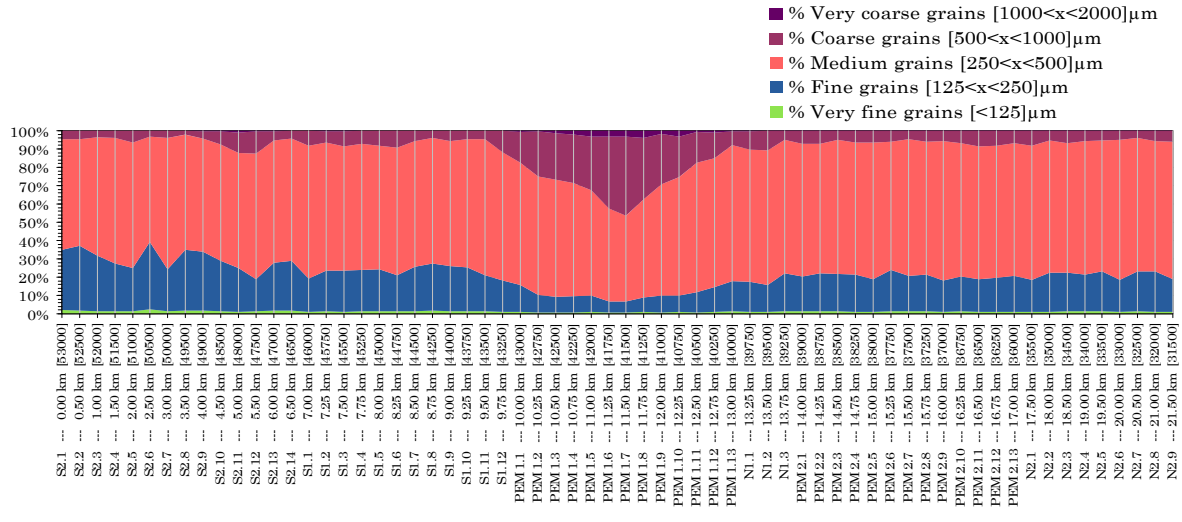

Figure C-18Cumulative distribution at Egmond aan Zee without shells

Class volume distribution of sample S2.1 to S2.4
Egmond aan Zee without shells

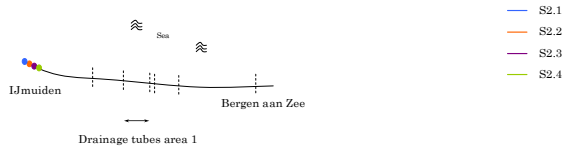

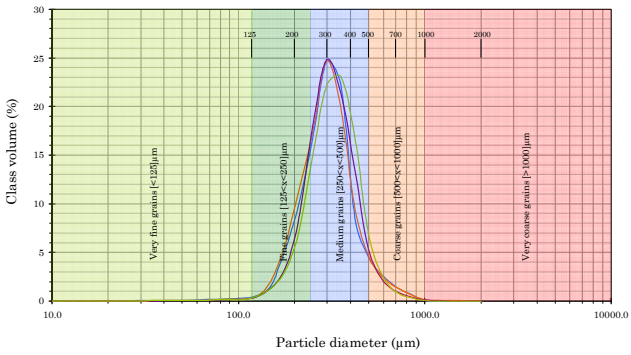

Class volume distribution of sample S2.5 to S2.8
Egmond aan Zee without shells

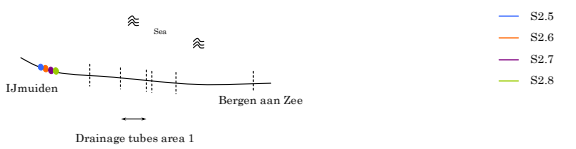

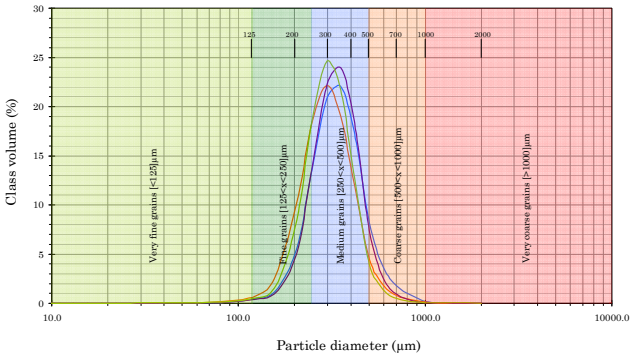

Class volume distribution of sample S2.9 to S2.12
Egmond aan Zee without shells

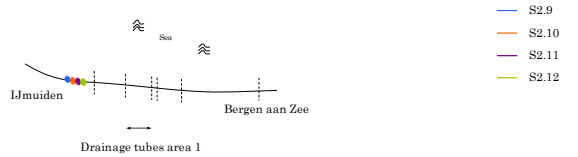

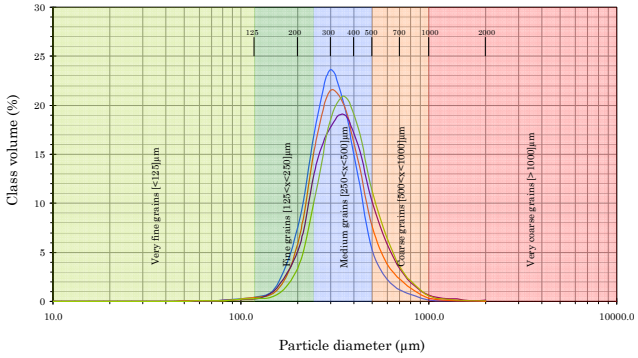

Class volume distribution of sample S2.13 to S1.2
Egmond aan Zee without shells

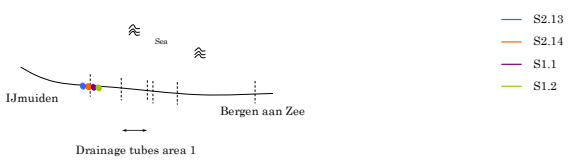

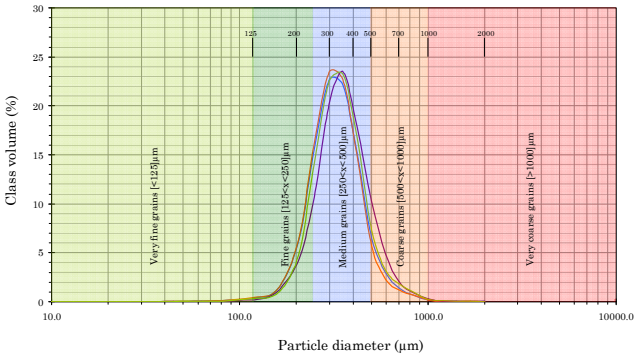

Class volume distribution of sample S1.3 to S1.6
Egmond aan Zee without shells

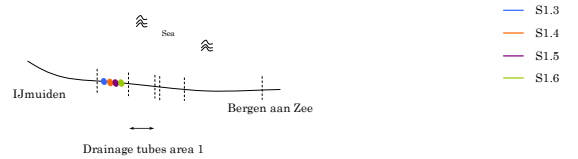

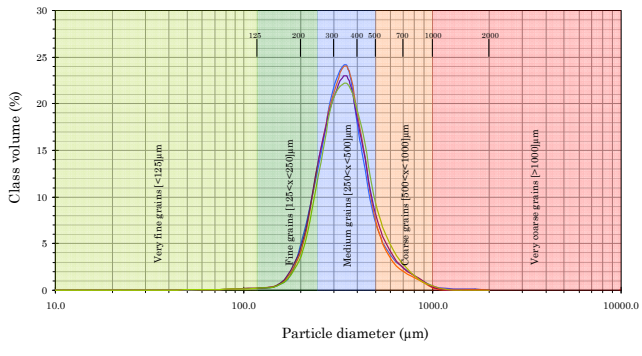

Class volume distribution of sample S1.7 to S1.10
Egmond aan Zee without shells

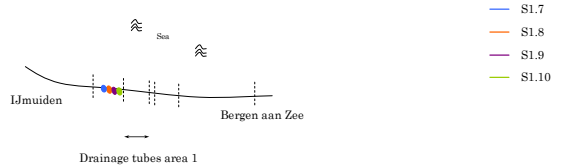

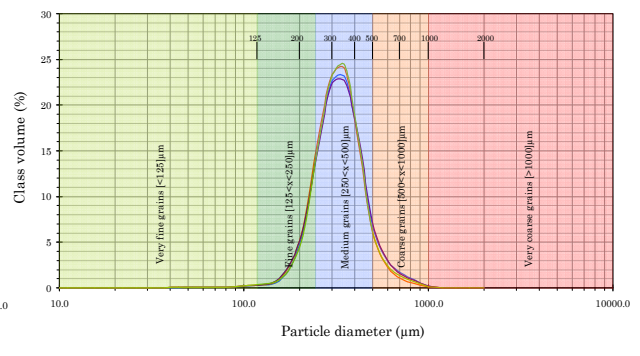

Class volume distribution of sample S1.11 to PEM 1.2
Egmond aan Zee without shells

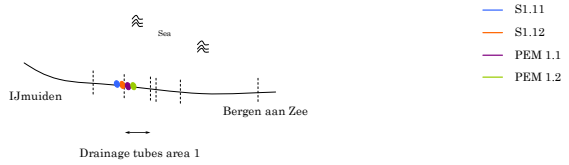

S1.11
S1.12
PEM 1.1
PEM 1.2

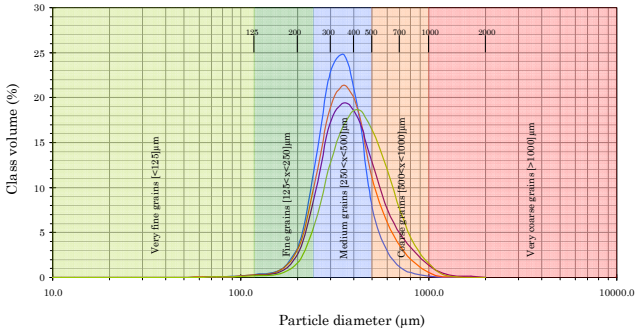

Class volume distribution of sample PEM 1.3 to PEM 1.6
Egmond aan Zee without shells

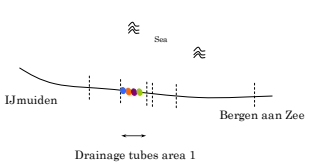

PEM 1.3
PEM 1.4
PEM 1.5
PEM 1.6

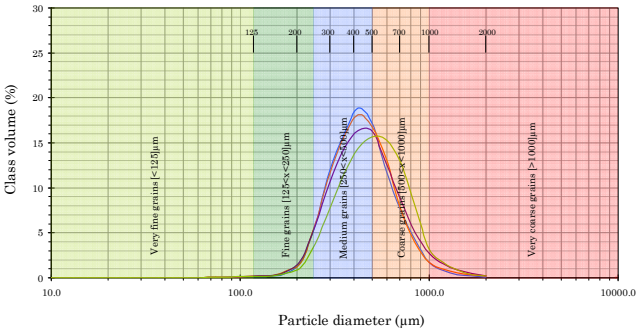

Class volume distribution of sample PEM 1.7 to PEM 1.10
Egmond aan Zee without shells

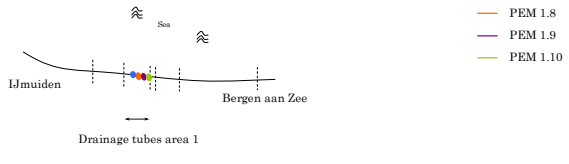

PEM 1.7
PEM 1.8
PEM 1.9
PEM 1.10

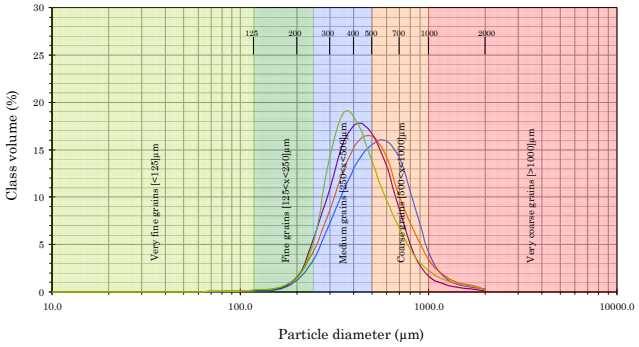

Class volume distribution of sample PEM 1.11 to N1.1
Egmond aan Zee without shells

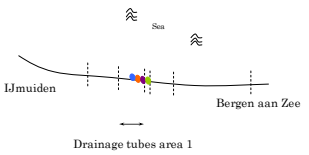

PEM 1.11
PEM 1.12
PEM 1.13
N1.1

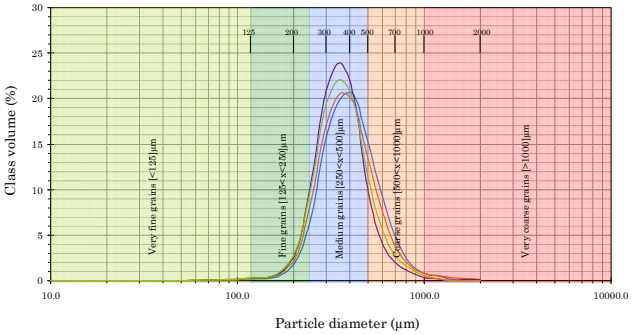

Class volume distribution of sample N1.2 to PEM 2.2
Egmond aan Zee without shells

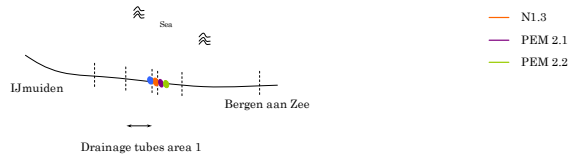

N1.2
N1.3
PEM 2.1
PEM 2.2

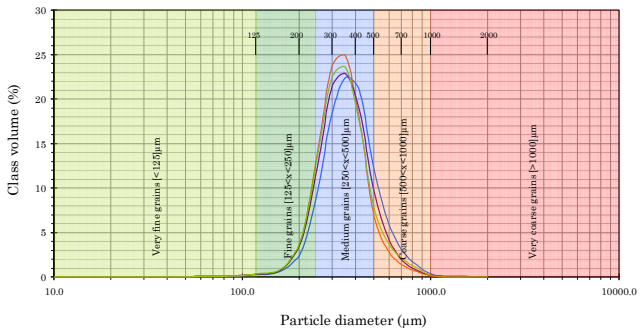

Class volume distribution of sample PEM 2.3 to PEM 2.6
Egmond aan Zee without shells

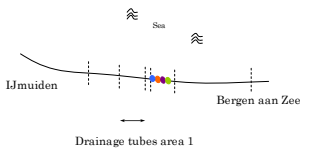

PEM 2.3
PEM 2.4
PEM 2.5
PEM 2.6

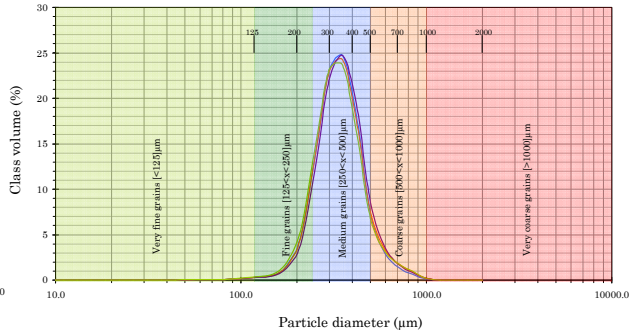

Class volume distribution of sample PEM 2.7 to PEM 2.10
Egmond aan Zee without shells

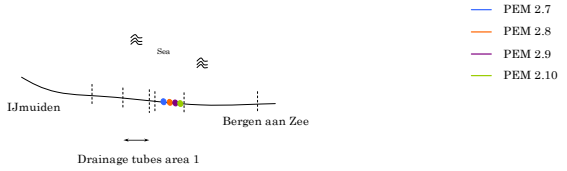

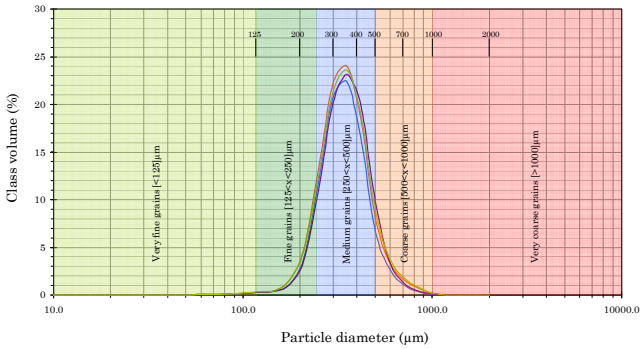

Class volume distribution of sample PEM 2.11 to N2.1
Egmond aan Zee without shells

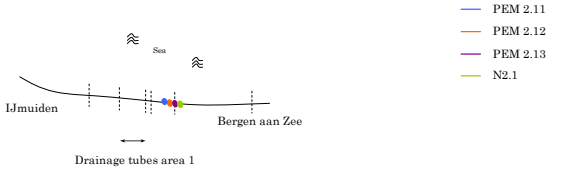

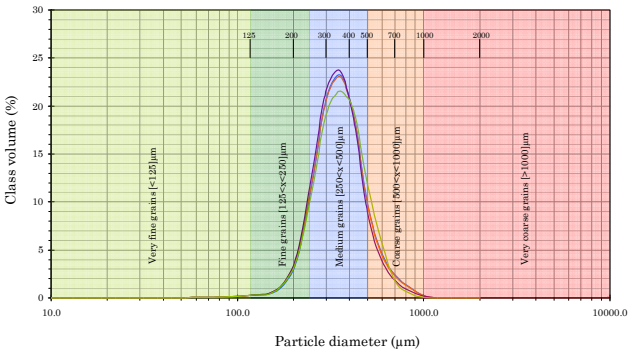

Class volume distribution of sample N2.2 to N2.5
Egmond aan Zee without shells

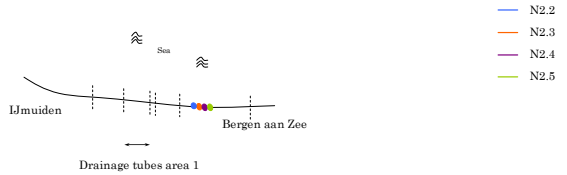

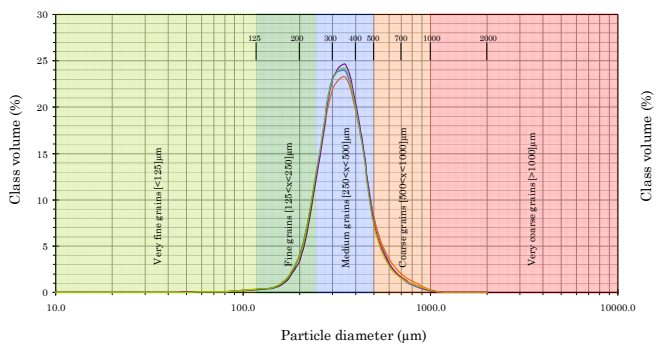

Class volume distribution of sample N2.6 to N2.9
Egmond aan Zee without shells

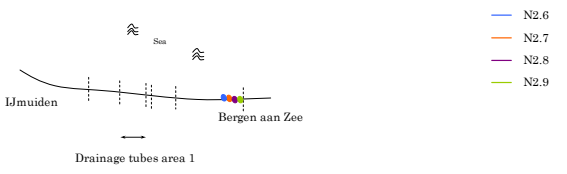

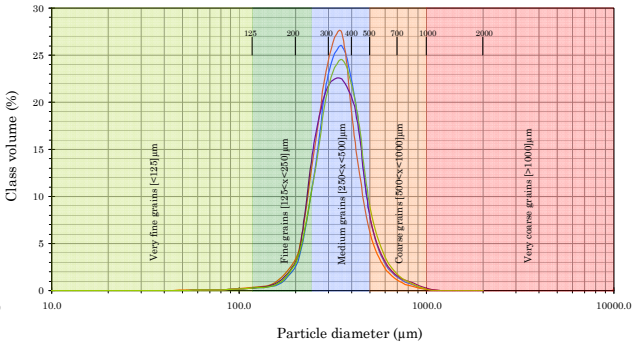

Class volume distribution of sample S1.11 to PEM 1.6
Egmond aan Zee without shells

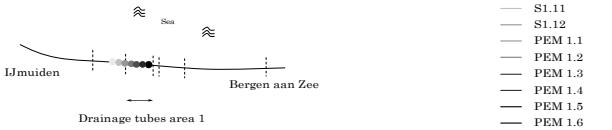

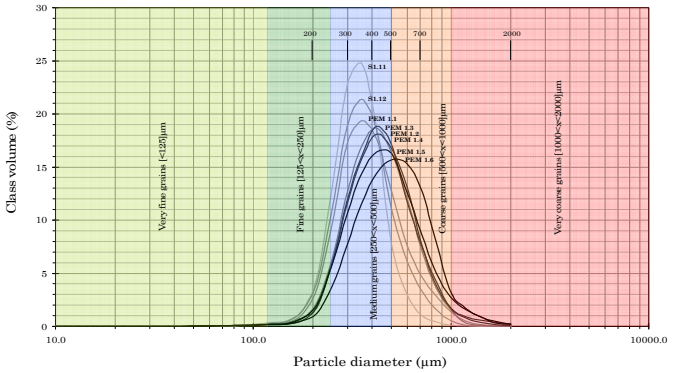

Appendix D. Field measurements Hvide Sande

D.1 D_{10} grain sizes

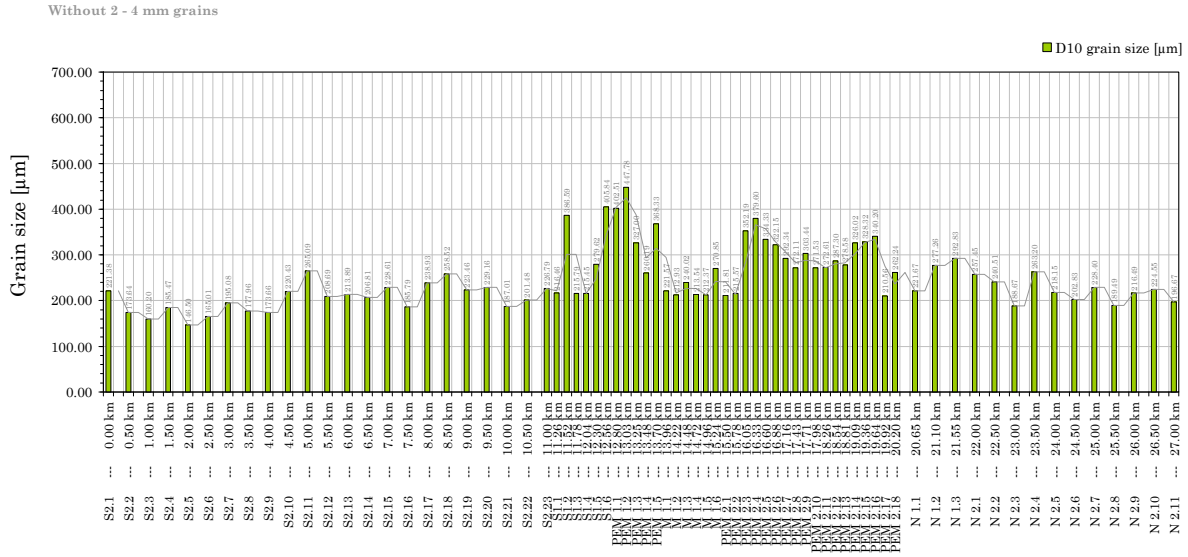

Figure D-1 D_{10} grain sizes at Hvide Sande without coarse grains

D.2 D_{50} grain sizes

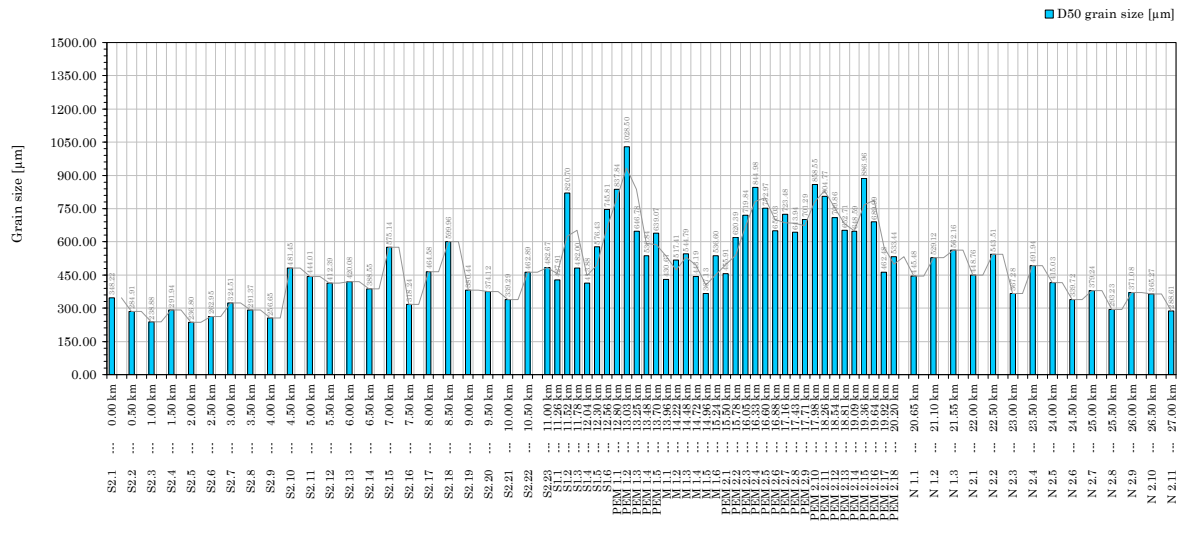

Figure D-2 D_{50} grain sizes at Hvide Sande without coarse grains

D.3 D_{90} grain sizes

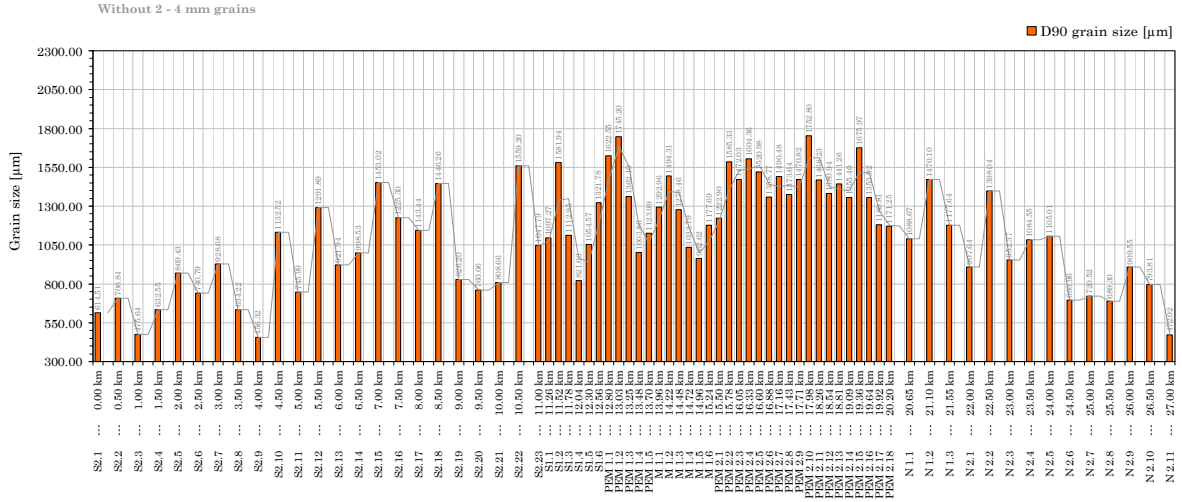

Figure D-3 D_{90} grain sizes at Hvide Sande without coarse grains

D.4 Very fine fraction

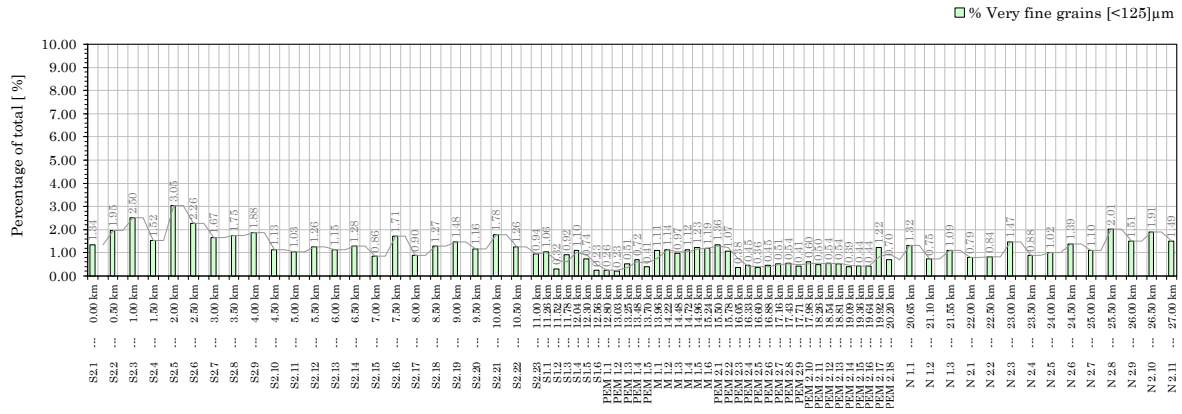

Figure D-4 Very fine fraction at Hvide Sande without coarse grains

D.5 Fine fraction

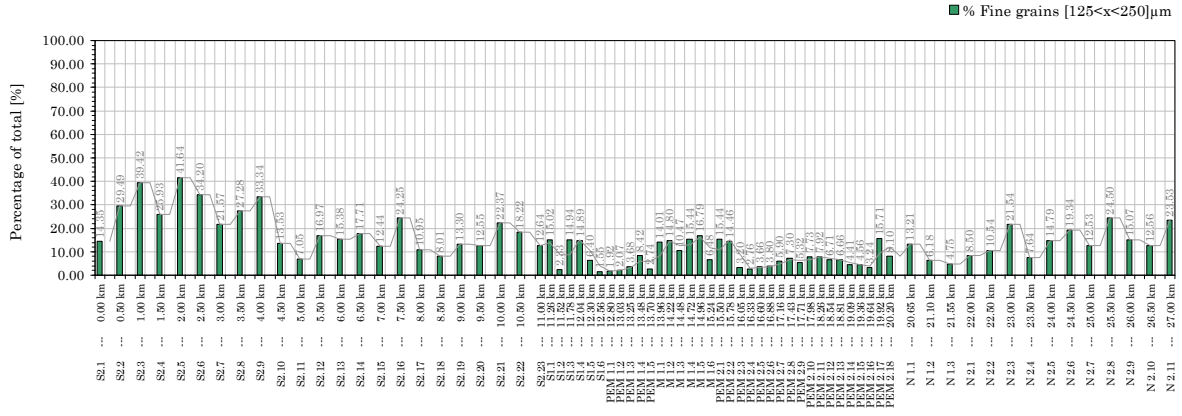

Figure D-5 Fine fraction at Hvide Sande without coarse grains

D.6 Medium fraction

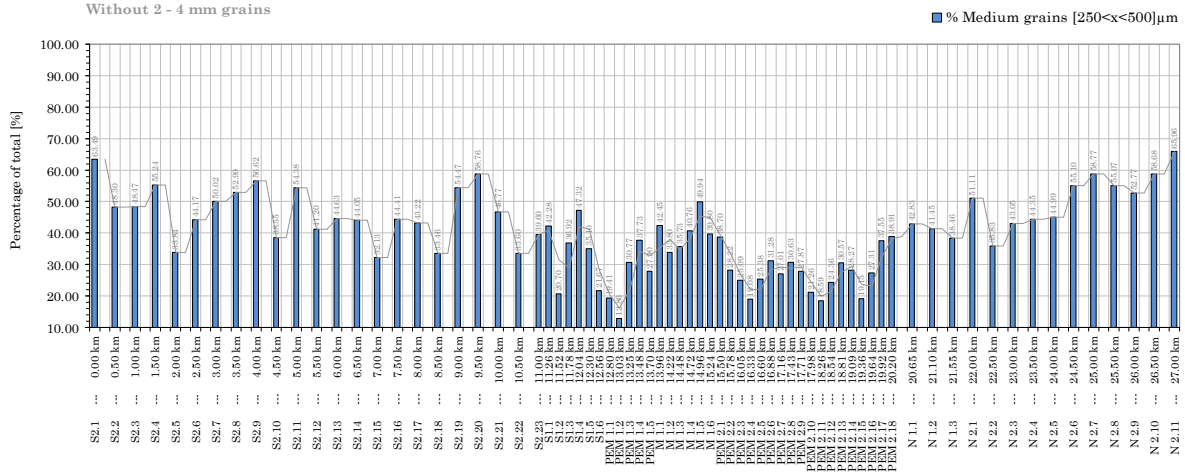

Figure D-6 Medium fraction at Hvide Sande without coarse grains

D.7 Coarse fraction

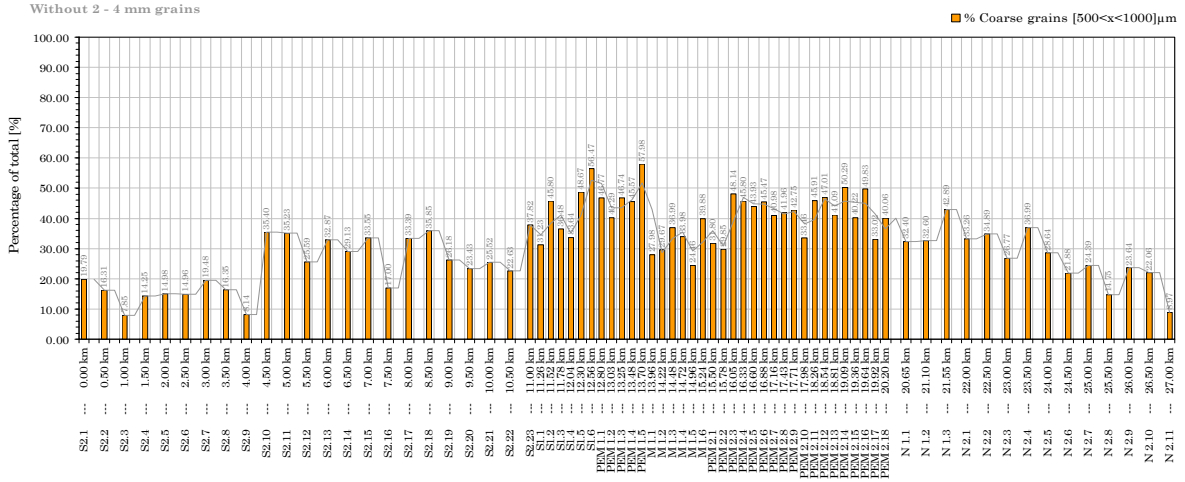

Figure D-7 Coarse fraction at Hvide Sande without coarse grains

D.8 Very coarse fraction

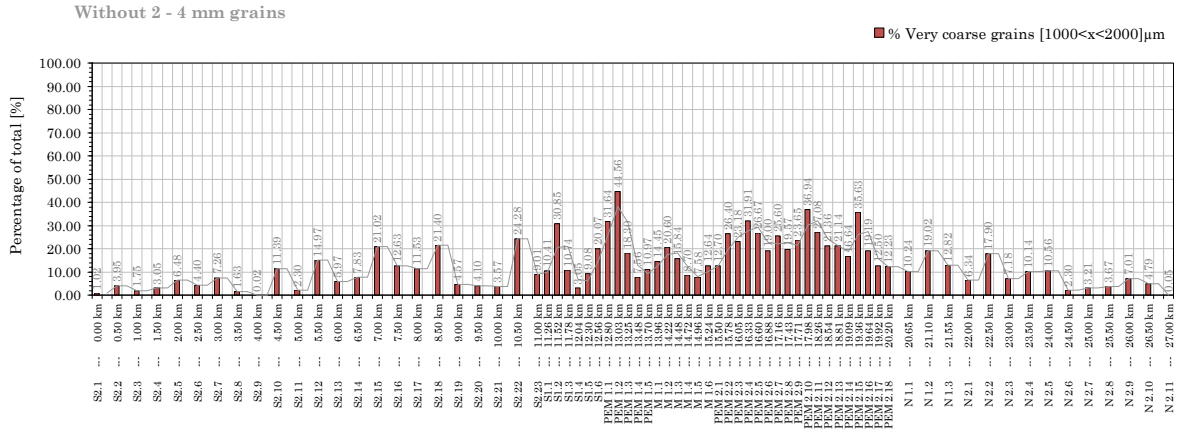

Figure D-8 Very coarse fraction at Hvide Sande without coarse grains

D.9 Cumulative distribution of gradations

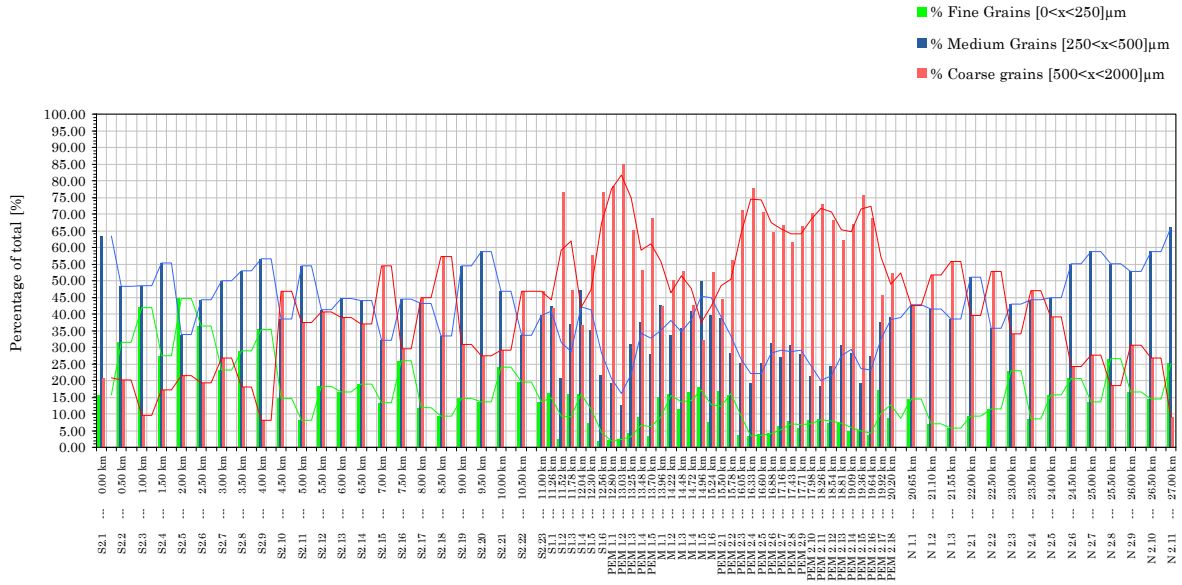

Figure D-9 Distribution of different gradations at Hvide Sande without coarse grains

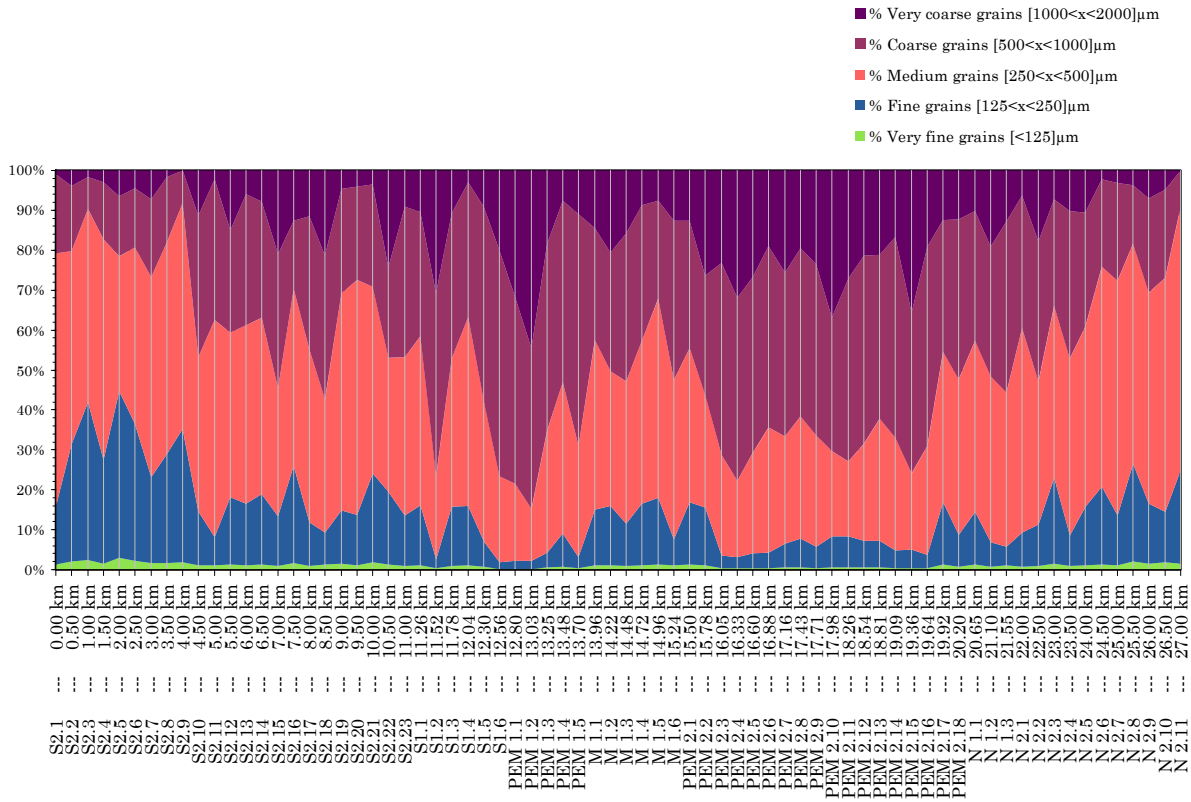

Figure D-10 Cumulative distribution of samples at Hvide Sande without coarse grains

Appendix E. Descriptive parameters of the samples

Here the calculated descriptive parameters (sorting, skewness and kurtosis) of the sediment samples at the beach of Egmond aan Zee and Hvide Sande are presented.

E.1 Egmond aan Zee

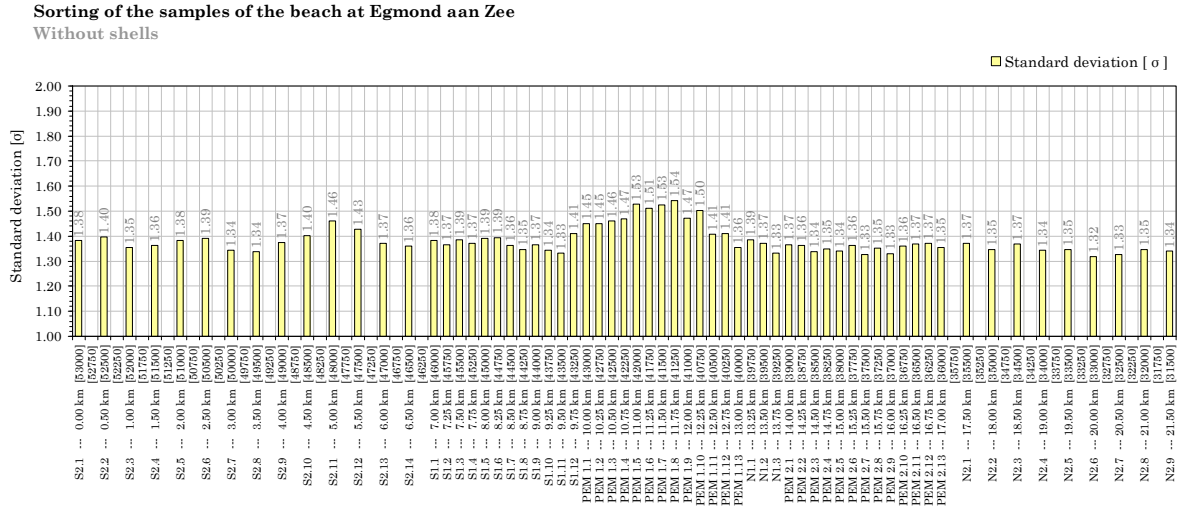

Figure E-1 Sorting of the samples at Egmond aan Zee

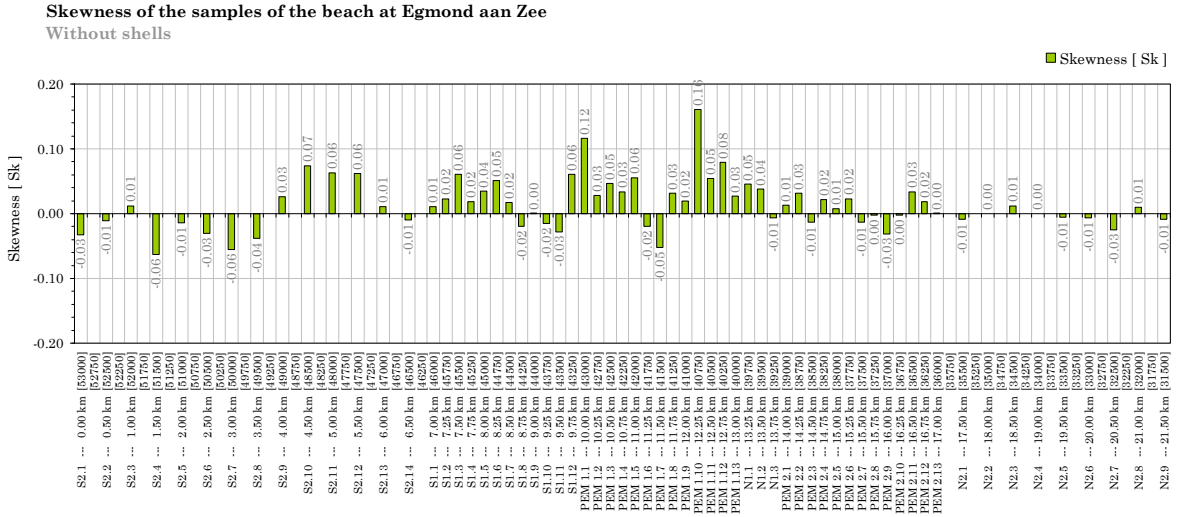

Figure E-2 Skewness of the samples at Egmond aan Zee

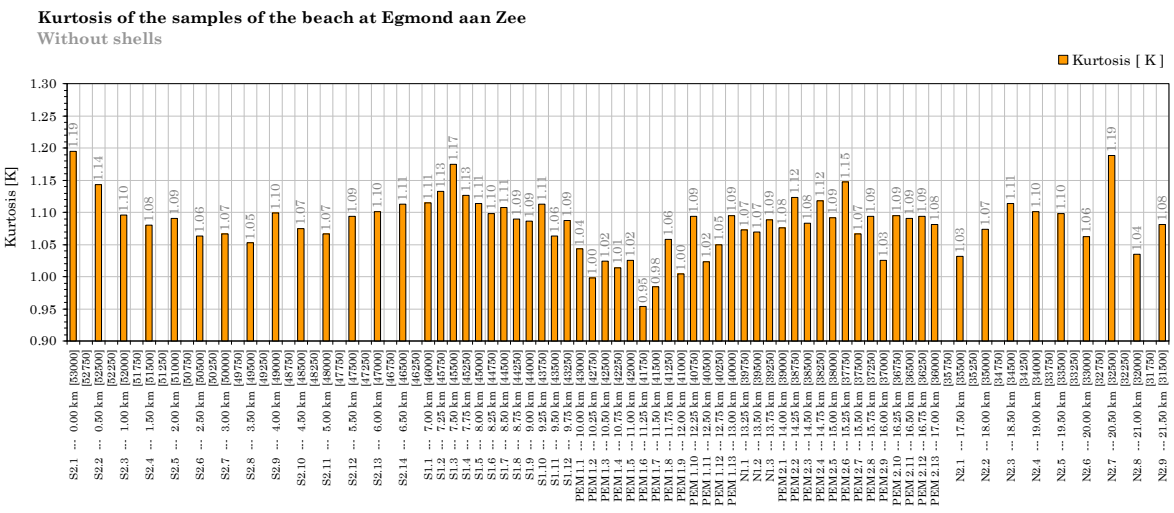

Figure E-3 Kurtosis of the samples at Egmond aan Zee

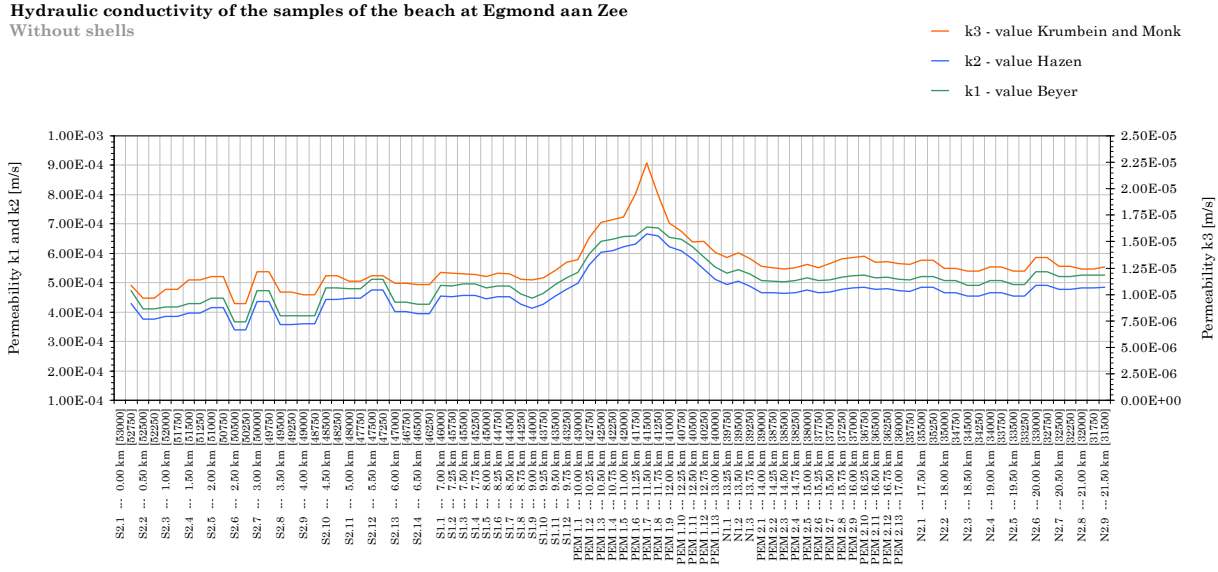

Figure E-4 Hydraulic conductivity of the samples at Egmond aan Zee

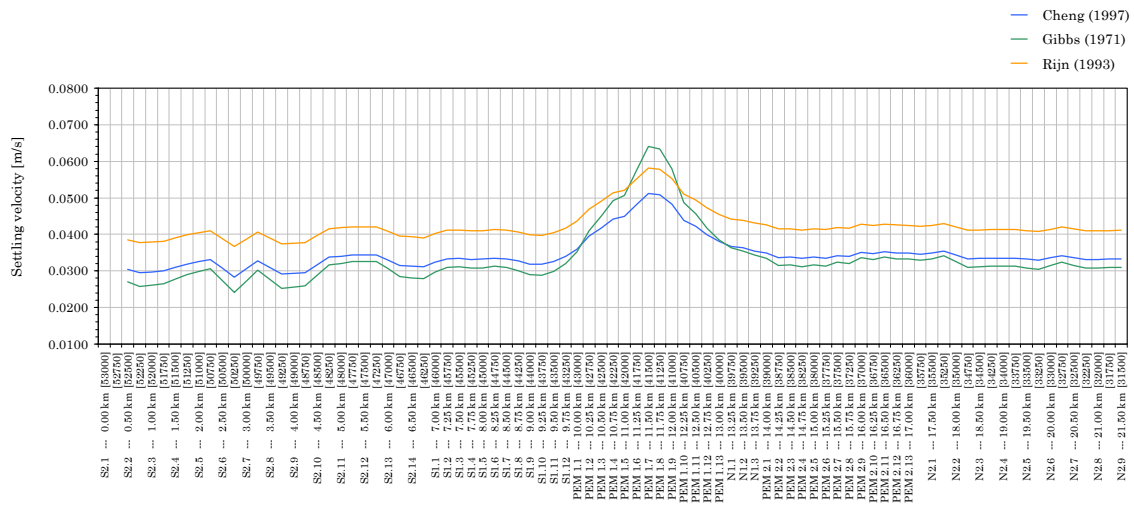

Figure E-5 Settling velocity of the samples at Egmond aan Zee

E.2 Hvide Sande

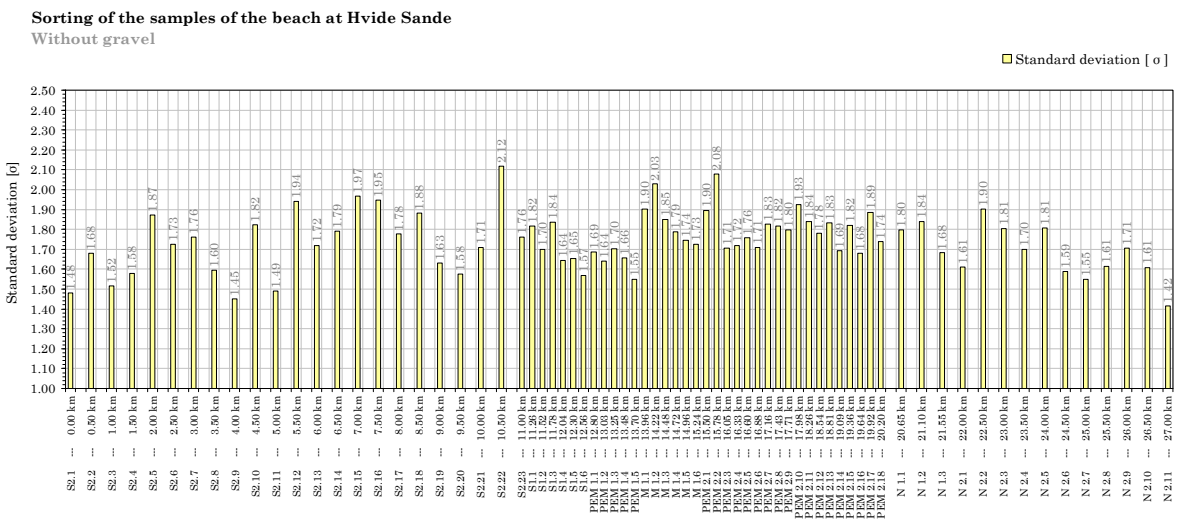

Figure E-6 Sorting of the samples at Hvide Sande

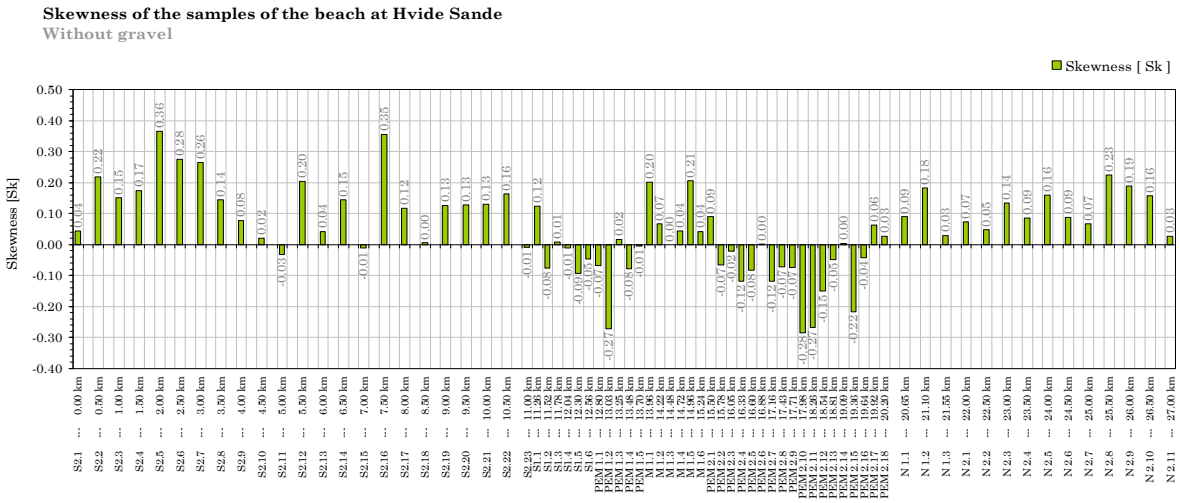

Figure E-7 Skewness of the samples at Hvide Sande

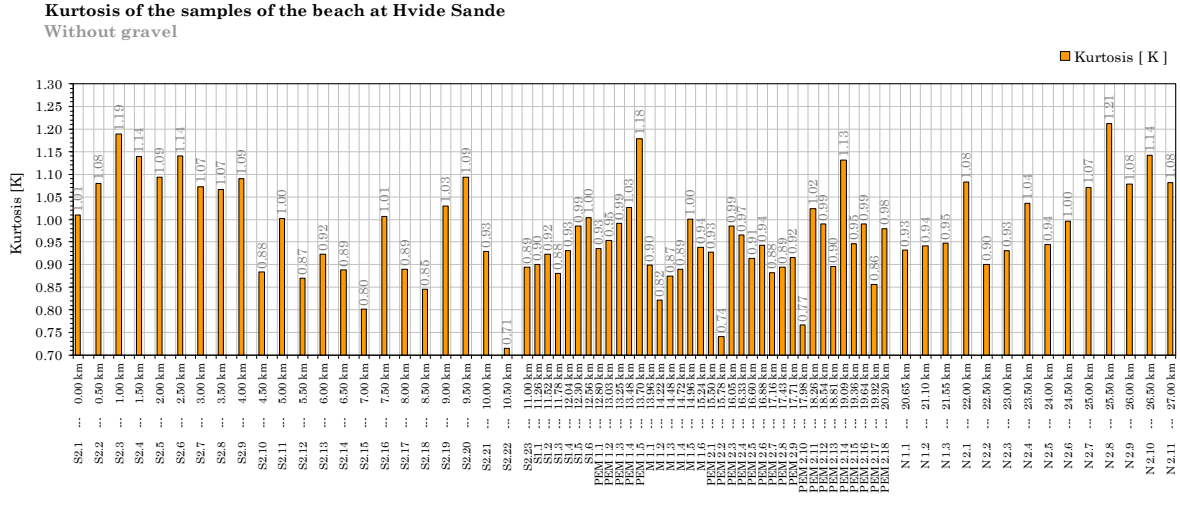

Figure E-8 Kurtosis of the samples at Hvide Sande

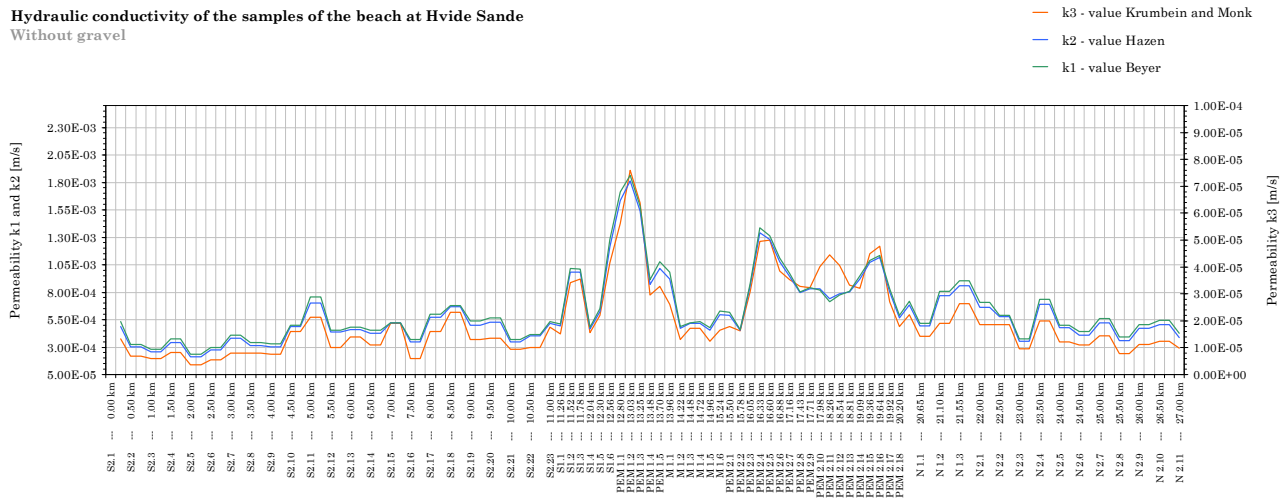

Figure E-9 Hydraulic conductivity of the samples at Hvide Sande

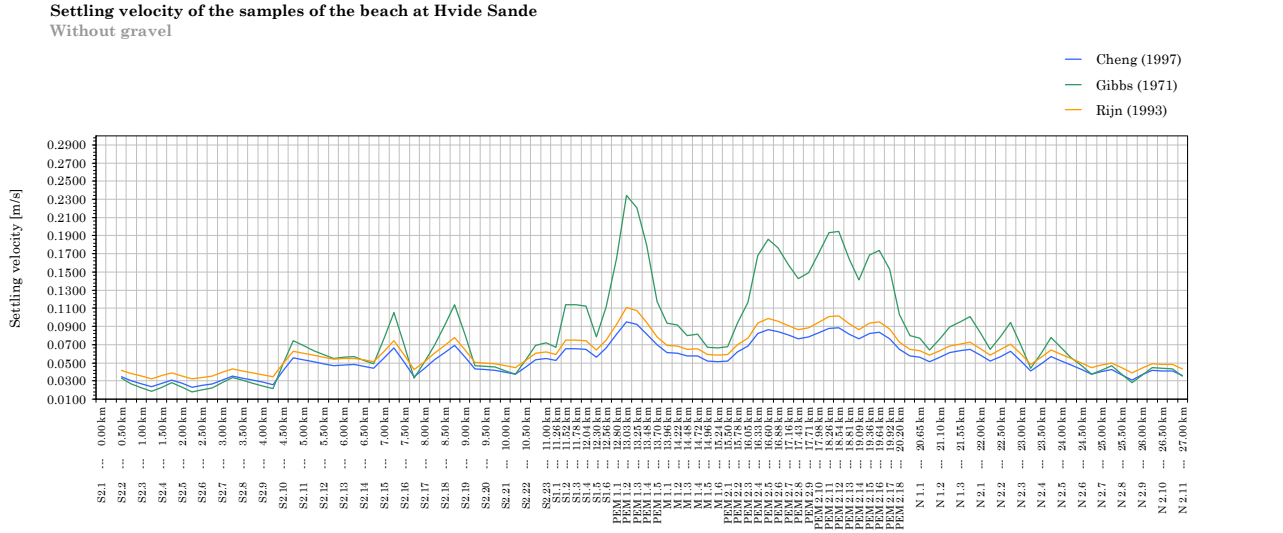

Figure E-10Settling velocity of the samples at Hvide Sande

*Table E-1 Calculated settling velocities * [m/s] of the sediment samples of both beaches ress*

Beach	Section	Cheng (1997)	Gibbs (1971)	Van Rijn (1993)
Egmond aan Zee	REF S2	0.0315	0.0285	0.0395
	REF S1	0.0332	0.0309	0.0410
	PEM 1	0.0438	0.0492	0.0510
	REF N1	0.0355	0.0343	0.0431
	PEM 2	0.0343	0.0325	0.0420
	REF N2	0.0336	0.0315	0.0414
Hvide Sande	REF S2	0.0420	0.0491	0.0497
	REF S1	0.0642	0.1072	0.0730
	PEM 1	0.0823	0.1766	0.0947
	REF M1	0.0543	0.0732	0.0617
	PEM 2	0.0776	0.1515	0.0883
	REF N1	0.0591	0.0847	0.0665
	REF N2	0.0440	0.0511	0.0514

Appendix F. Installation layout of the systems

F.1 Ecobeach near Egmond aan Zee

PEM Area 2 [3km]

52% of the drainage tubes installed

Most of them at the high waterline

PEM Area 1 [3km]

120% of the drainage tubes installed

Some extra drainage tubes at the low water line

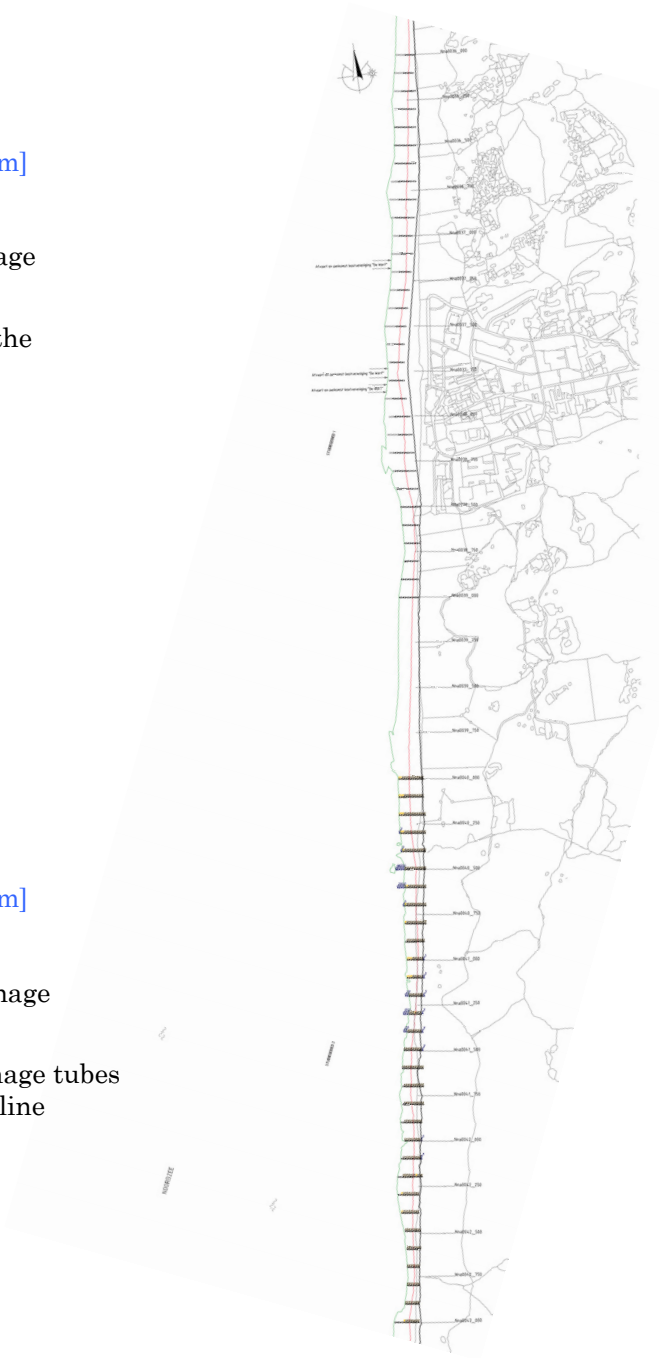

Figure F-1 Installation layout of the drainage tube system at Egmond aan Zee

A scientific study of Ecobeach in The Netherlands was done by Pieterse (2009). This research focused on the groundwater behaviour in the vicinity of a drainage tube and the influence of it on the pressure guidance. Measurements on the groundwater table [79] were done with divers measuring pressure variances (Figure 2-15). The divers used to measure the differences could be too inaccurate [79]. Also the natural variability could be too large.

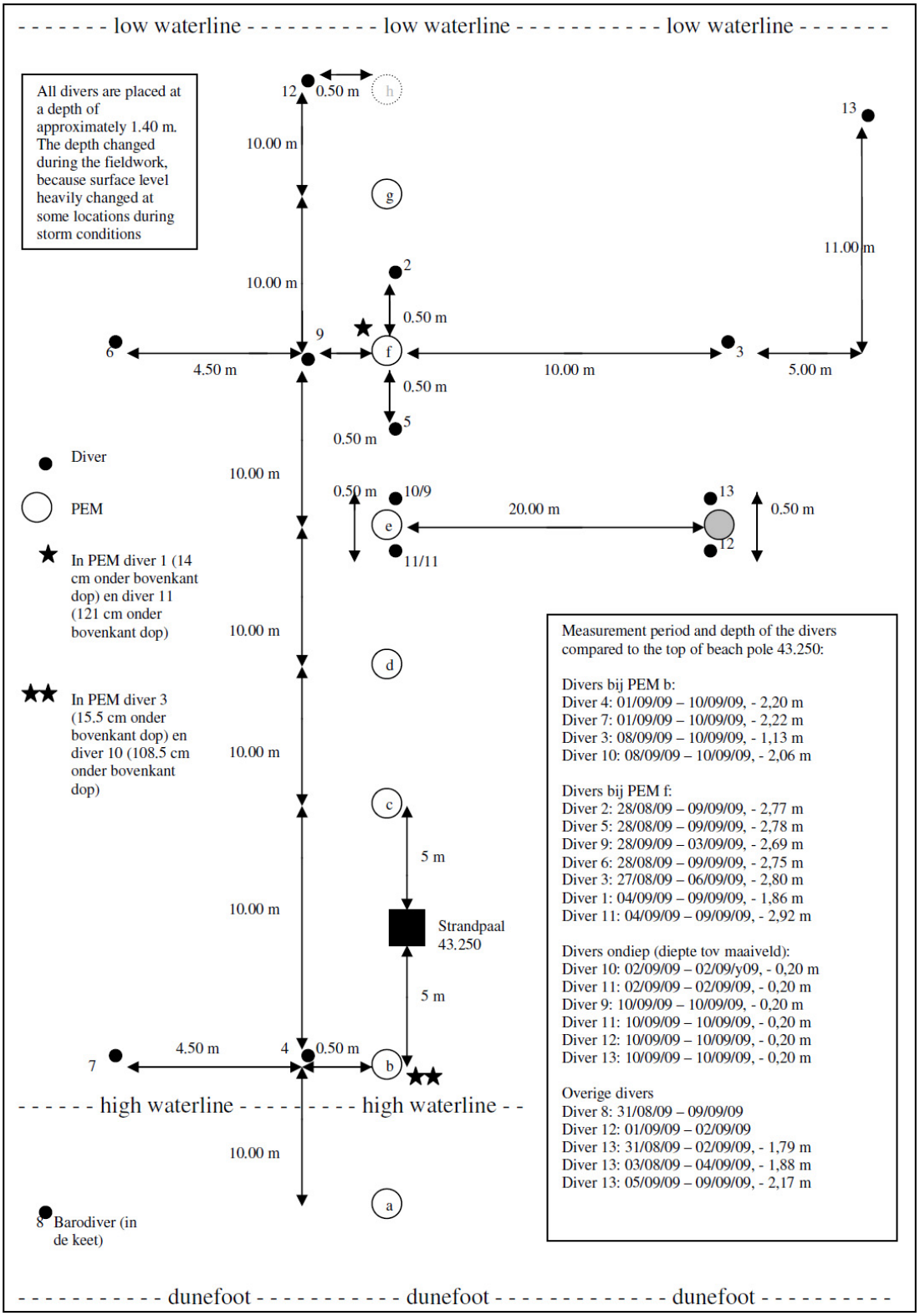

Figure F-2 A scientific study of Ecobeach in The Netherlands [79]

F.2 PEM Project near Hvide Sande

Stn	No. 1	2	3	4	5	6	7	8	9	10	11	12
4011800	X	X	X	X	X	X	X	X	X	X	X	
4011900	X	X	X	X	X	X	X	X	X	X	X	X
4012000	X	X	X	X	X	X	X	X	X	X	X	X
4012100	X	X	X	X	X	X	X	X	X	X	X	
4012200	X	X	X	X	X	X	X	X	X	X	X	
4012300	X	X	X	X	X	X	X	X	X	X	X	X
4012400	X	X	X	X	X	X	X	X	X	X	X	
4012500	X	X	X	X	X	X	X	X	X	X	X	
4012600	X	X	X	X	X	X	X	X	X	X	X	
4012700	X	X	X	X	X	X	X	X	X	X		
4014500	X	X	X	X	X	X	X	X				
4014600	X	X	X	X	X	X	X					
4014700	X	X	X	X	X	X	X					
4014800	X	X	X	X	X	X	X	X				
4014900	X	X	X	X	X	X	X	X				
4015000	X	X	X	X	X	X	X					
4015100	X	X	X	X	X	X	X	X				
4015300	X	X	X	X	X	X	X					
4015400	X	X	X	X	X	X	X					
4015500	X	X	X	X	X	X	X					
4015600	X	X	X	X	X	X	X	X				
4015700	X	X	X	X	X	X	X	X				
4015800	X	X	X	X	X	X	X	X				
4015900	X	X	X	X	X	X	X	X	X			
4016000	X	X	X	X	X	X	X	X	X			
4016100	X	X	X	X	X	X	X	X	X			
4016200	X	X	X	X	X	X	X	X	X	X	X	
4016300	X	X	X	X	X	X	X	X	X	X	X	
4016400	X	X	X	X	X	X	X	X	X	X	X	
4016500	X	X	X	X	X	X	X	X	X	X	X	
4016600	X	X	X	X	X	X	X	X	X	X	X	
4016700	X	X	X	X	X	X	X	X	X	X	X	
4016800	X	X	X	X	X	X	X	X	X	X	X	
4016900	X	X	X	X	X	X	X	X	X	X	X	
4017000	X	X	X	X	X	X	X	X	X	X	X	
4017100	X	X	X	X	X	X	X	X	X	X	X	
4017200	X	X	X	X	X	X	X	X	X	X	X	
4017300	X	X	X	X	X	X	X	X	X	X	X	
4017400	X	X	X	X	X	X	X	X	X	X	X	
4017500	X	X	X	X	X	X	X	X	X	X	X	
4017600	X	X	X	X	X	X	X	X	X	X	X	
4017700	X	X	X	X	X	X	X	X	X	X	X	
4017800	X	X	X	X	X	X	X	X	X	X	X	
4017900	X	X	X	X	X	X	X	X	X	X	X	
4018000	X	X	X	X	X	X	X	X	X	X	X	
4018100	X	X	X	X	X	X	X	X	X	X	X	
4018200	X	X	X	X	X	X	X	X	X	X		
4018300	X	X	X	X	X	X	X	X	X	X		
4018400	X	X	X	X	X	X	X	X	X	X	X	
4018500	X	X	X	X	X	X	X	X	X	X		
4018600	X	X	X	X	X	X	X	X	X	X		
4018700	X	X	X	X	X	X	X	X	X			
4018800	X	X	X	X	X	X	X	X	X			
4018900	X	X	X	X	X	X	X	X	X			
4019000	X	X	X	X	X	X	X	X	X			
4019100	X	X	X	X	X	X	X	X	X			
4019200	X	X	X	X	X	X	X	X	X			

PEM modules Skodbjerge

X PEM modules 28 jan 2005
X ADDITIONAL 28 MAR 2005
X ADDITIONAL 06 MAY 2005
X ADDITIONAL 05 AUG 2005
X ADDITIONAL 20 OCT 2005
X ADDITIONAL 21 FEB 2006

Figure F-3 Installation layout of the drainage tube system at Hvide Sande

Holmsland Klit – water level in beach measured with DIVER

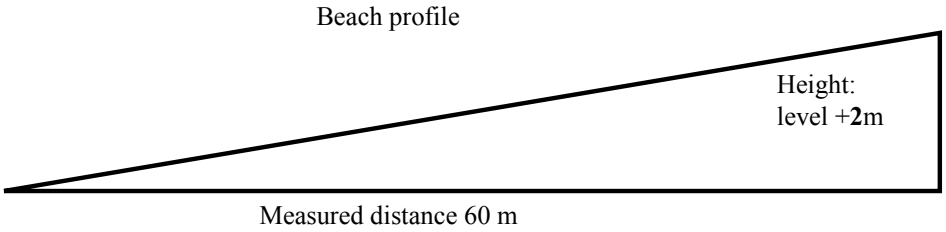

Installation in the beach

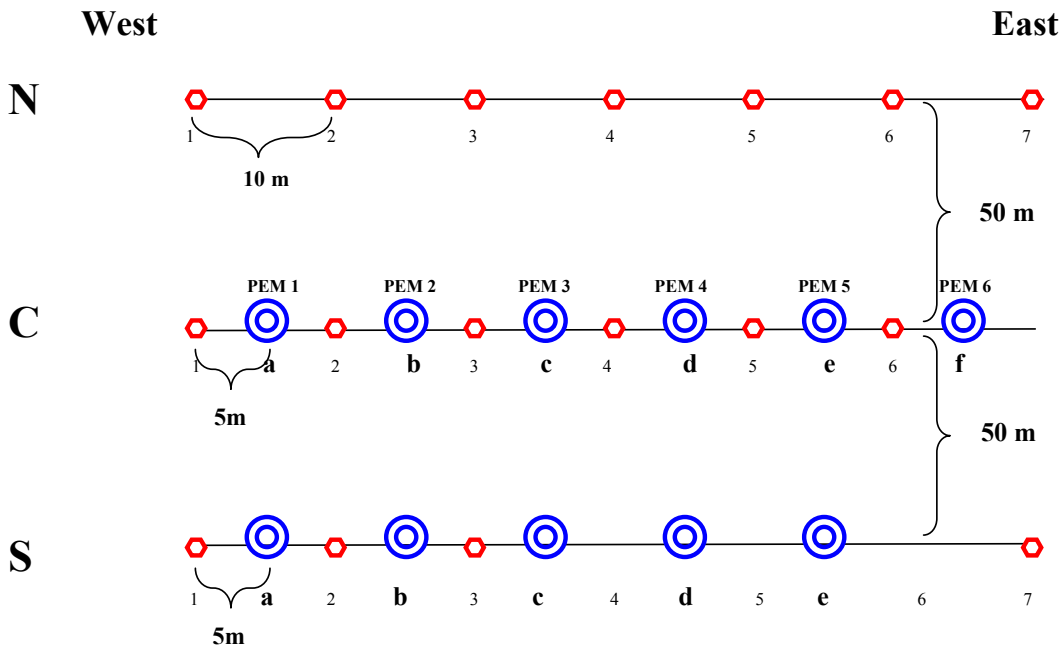

Well with a plastic tube with sensor (Diver) to record water level in the beach

PEM module with sensor (Diver)

N Station 11000 (ch 402100)

Figure F-4 Field test done by SIC an KDI at PEM 2 near Hvide Sande

Appendix G. Historical data of the Dutch geology

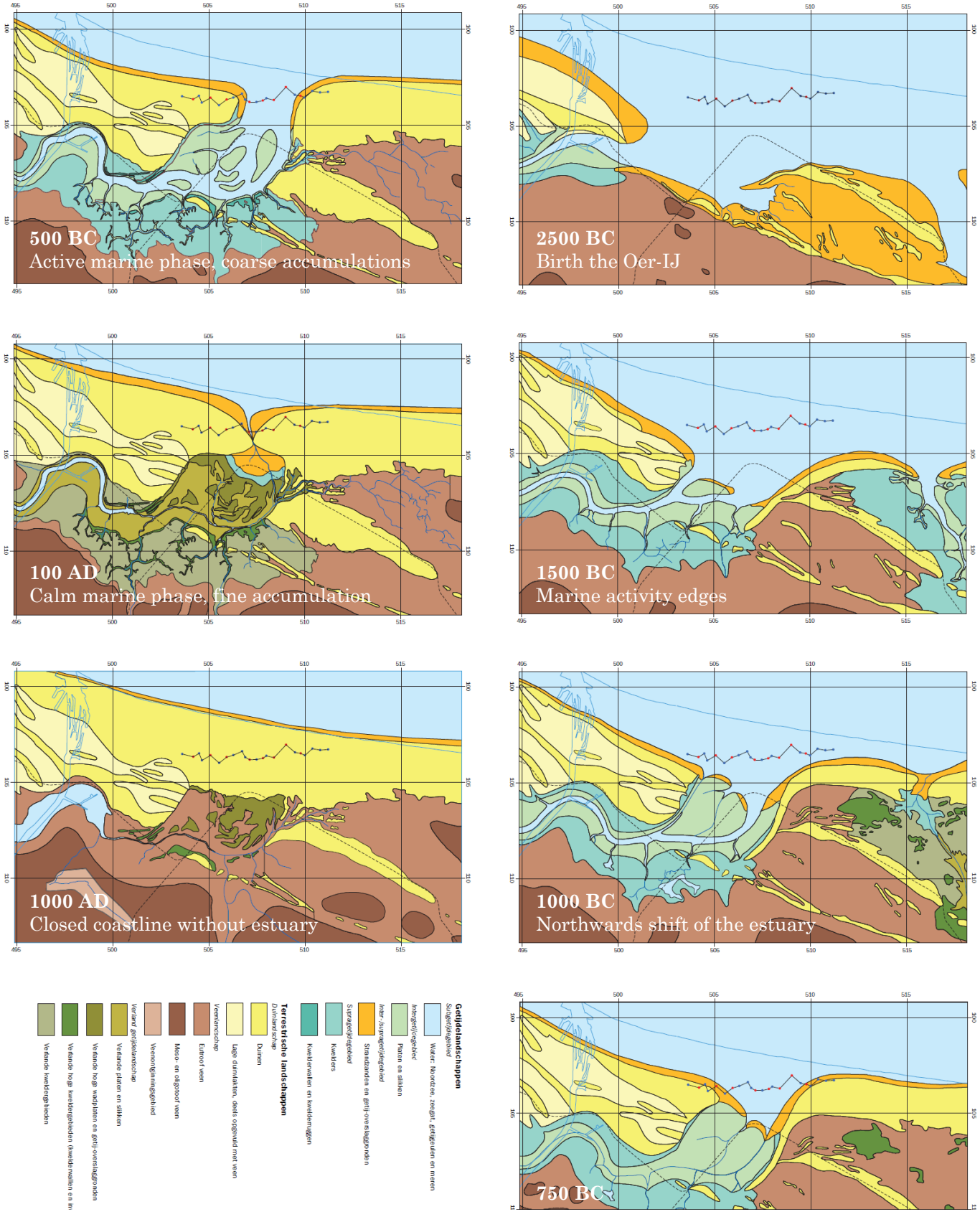

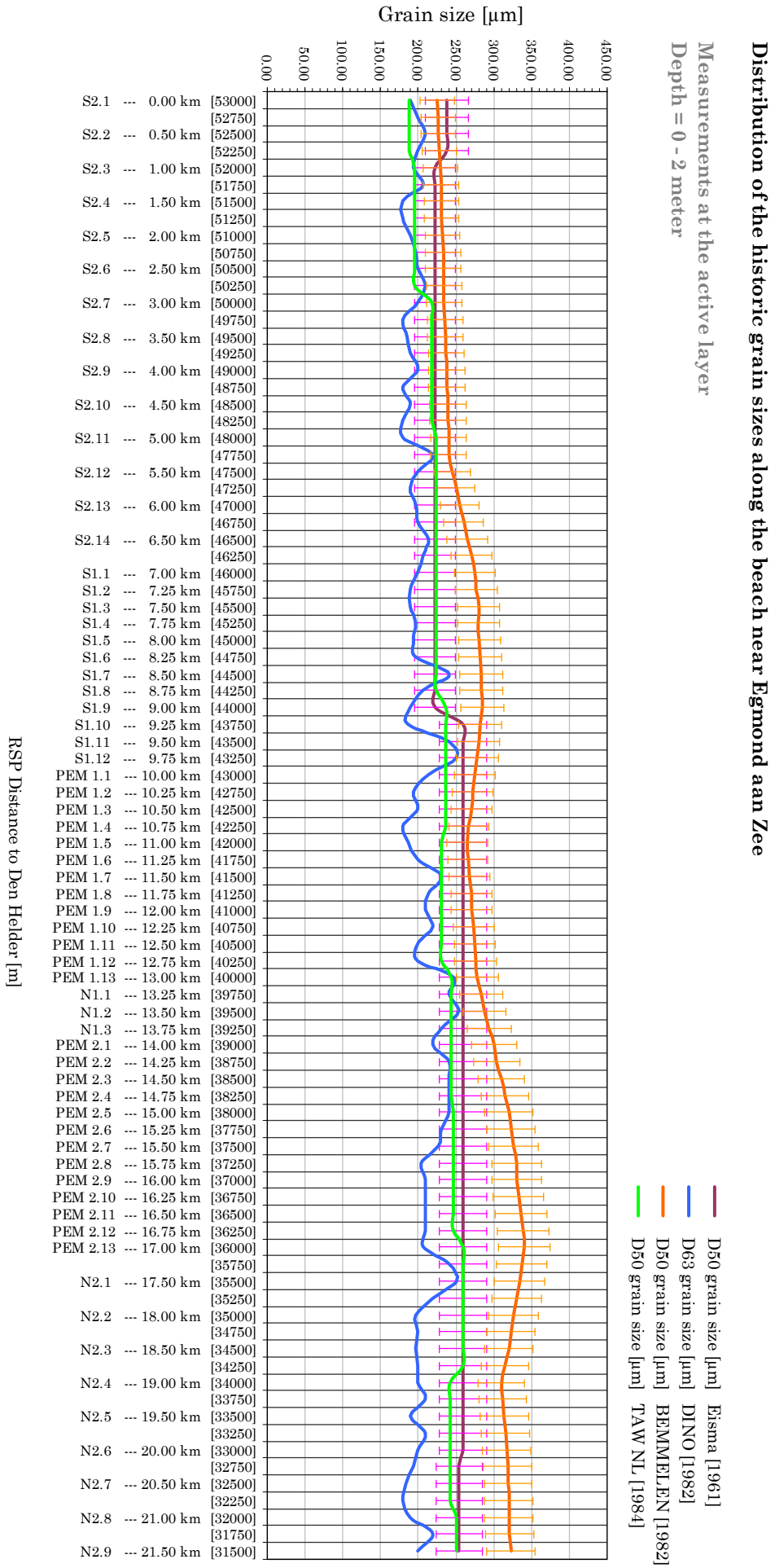
Distribution of the historic grain sizes along the beach near Egmond aan Zee
Measurements at the active layer
Depth = 0 - 2 meter
Grain size [µm]
0.00
50.00
100.00
150.00
200.00
250.00
300.00
350.00
400.00
450.00
RSP Distance to Den Helder [m]
S2.1 --- 0.00 km [53000]
[52750]
S2.2 --- 0.50 km [52500]
[52250]
S2.3 --- 1.00 km [52000]
[51750]
S2.4 --- 1.50 km [51500]
[51250]
S2.5 --- 2.00 km [51000]
[50750]
S2.6 --- 2.50 km [50500]
[50250]
S2.7 --- 3.00 km [50000]
[49750]
S2.8 --- 3.50 km [49500]
[49250]
S2.9 --- 4.00 km [49000]
[48750]
S2.10 --- 4.50 km [48500]
[48250]
S2.11 --- 5.00 km [48000]
[47750]
S2.12 --- 5.50 km [47500]
[47250]
S2.13 --- 6.00 km [47000]
[46750]
S2.14 --- 6.50 km [46500]
[46250]
S1.1 --- 7.00 km [46000]
S1.2 --- 7.25 km [45750]
S1.3 --- 7.50 km [45500]
S1.4 --- 7.75 km [45250]
S1.5 --- 8.00 km [45000]
S1.6 --- 8.25 km [44750]
S1.7 --- 8.50 km [44500]
S1.8 --- 8.75 km [44250]
S1.9 --- 9.00 km [44000]
S1.10 --- 9.25 km [43750]
S1.11 --- 9.50 km [43500]
S1.12 --- 9.75 km [43250]
PEM 1.1 --- 10.00 km [43000]
PEM 1.2 --- 10.25 km [42750]
PEM 1.3 --- 10.50 km [42500]
PEM 1.4 --- 10.75 km [42250]
PEM 1.5 --- 11.00 km [42000]
PEM 1.6 --- 11.25 km [41750]
PEM 1.7 --- 11.50 km [41500]
PEM 1.8 --- 11.75 km [41250]
PEM 1.9 --- 12.00 km [41000]
PEM 1.10 --- 12.25 km [40750]
PEM 1.11 --- 12.50 km [40500]
PEM 1.12 --- 12.75 km [40250]
PEM 1.13 --- 13.00 km [40000]
N1.1 --- 13.25 km [39750]
N1.2 --- 13.50 km [39500]
N1.3 --- 13.75 km [39250]
PEM 2.1 --- 14.00 km [39000]
PEM 2.2 --- 14.25 km [38750]
PEM 2.3 --- 14.50 km [38500]
PEM 2.4 --- 14.75 km [38250]
PEM 2.5 --- 15.00 km [38000]
PEM 2.6 --- 15.25 km [37750]
PEM 2.7 --- 15.50 km [37500]
PEM 2.8 --- 15.75 km [37250]
PEM 2.9 --- 16.00 km [37000]
PEM 2.10 --- 16.25 km [36750]
PEM 2.11 --- 16.50 km [36500]
PEM 2.12 --- 16.75 km [36250]
PEM 2.13 --- 17.00 km [36000]
[35750]
N2.1 --- 17.50 km [35500]
[35250]
N2.2 --- 18.00 km [35000]
[34750]
N2.3 --- 18.50 km [34500]
[34250]
N2.4 --- 19.00 km [34000]
[33750]
N2.5 --- 19.50 km [33500]
[33250]
N2.6 --- 20.00 km [33000]
[32750]
N2.7 --- 20.50 km [32500]
[32250]
N2.8 --- 21.00 km [32000]
[31750]
N2.9 --- 21.50 km [31500]
D50 grain size [µm] Eisma [1961]
D63 grain size [µm] DINO [1982]
D50 grain size [µm] BEMMELEN [1982]
D50 grain size [µm] TAW NL [1984]

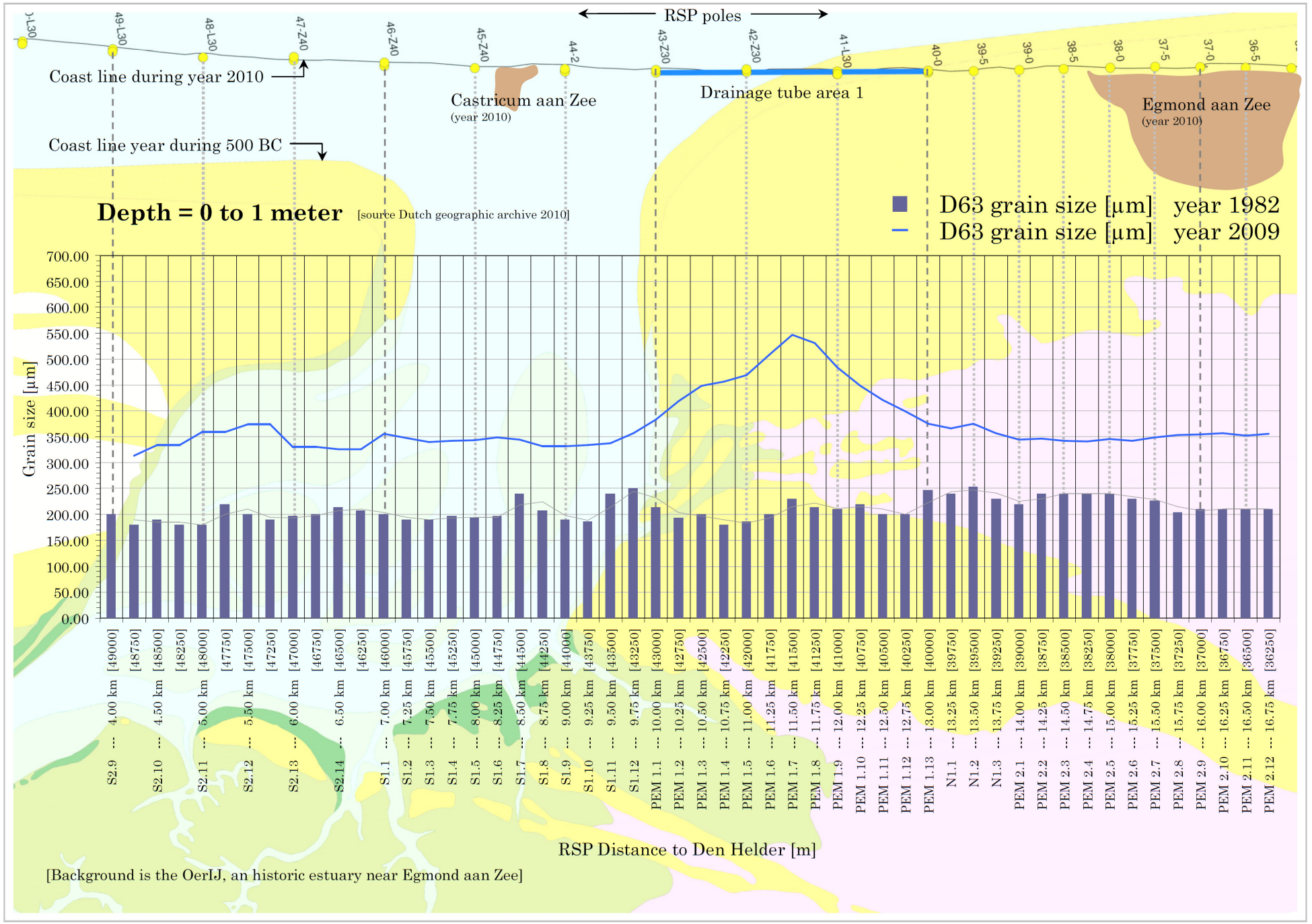
RSP poles
Coast line during year 2010
Coast line year during 500 BC
Castricum aan Zee
(year 2010)
Drainage tube area 1
Egmond aan Zee
(year 2010)
Depth = 0 to 1 meter
[source Dutch geographic archive 2010]
D63 grain size [µm] year 1982
D63 grain size [µm] year 2009
Grain size [µm]
RSP Distance to Den Helder [m]
[Background is the OerIJ, an historic estuary near Egmond aan Zee]

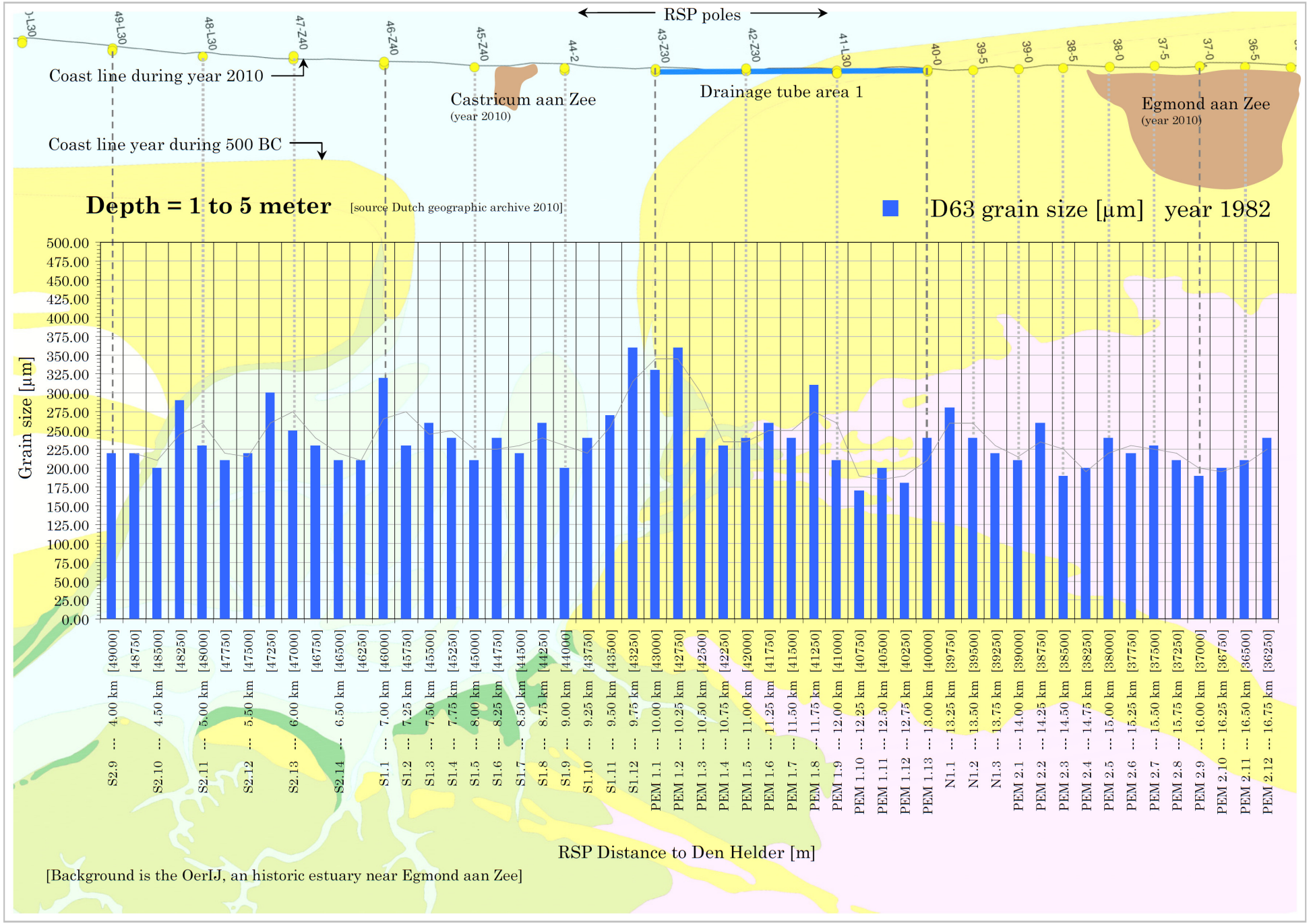
RSP poles
Coast line during year 2010
Coast line year during 500 BC
Castricum aan Zee
(year 2010)
Drainage tube area 1
Egmond aan Zee
(year 2010)
Depth = 1 to 5 meter
[source Dutch geographic archive 2010]
D63 grain size [µm] year 1982
Grain size [µm]
RSP Distance to Den Helder [m]
[Background is the OerIJ, an historic estuary near Egmond aan Zee]

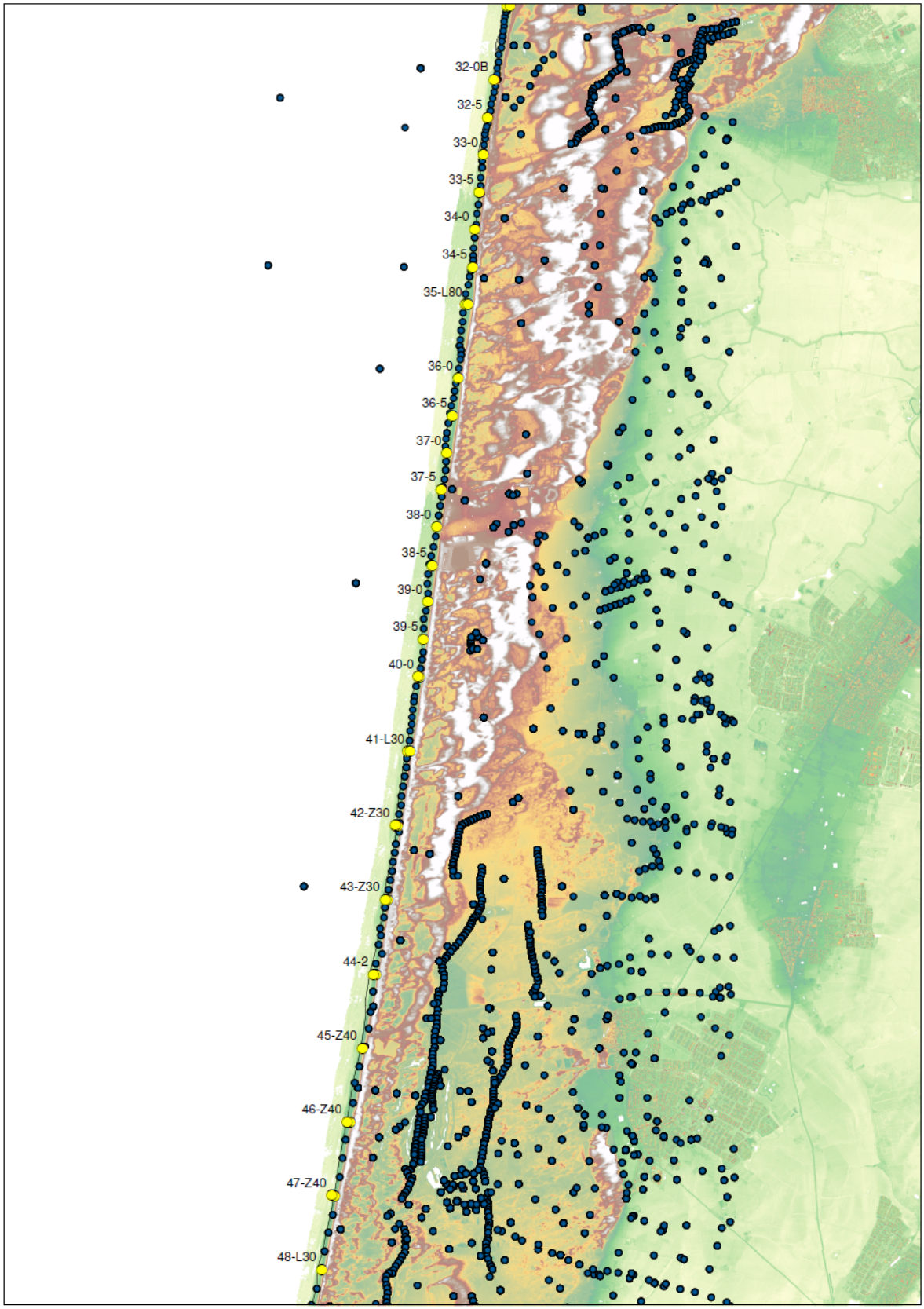

Figure G-5 Overview of measurement locations data Dutch geographic archive 2010

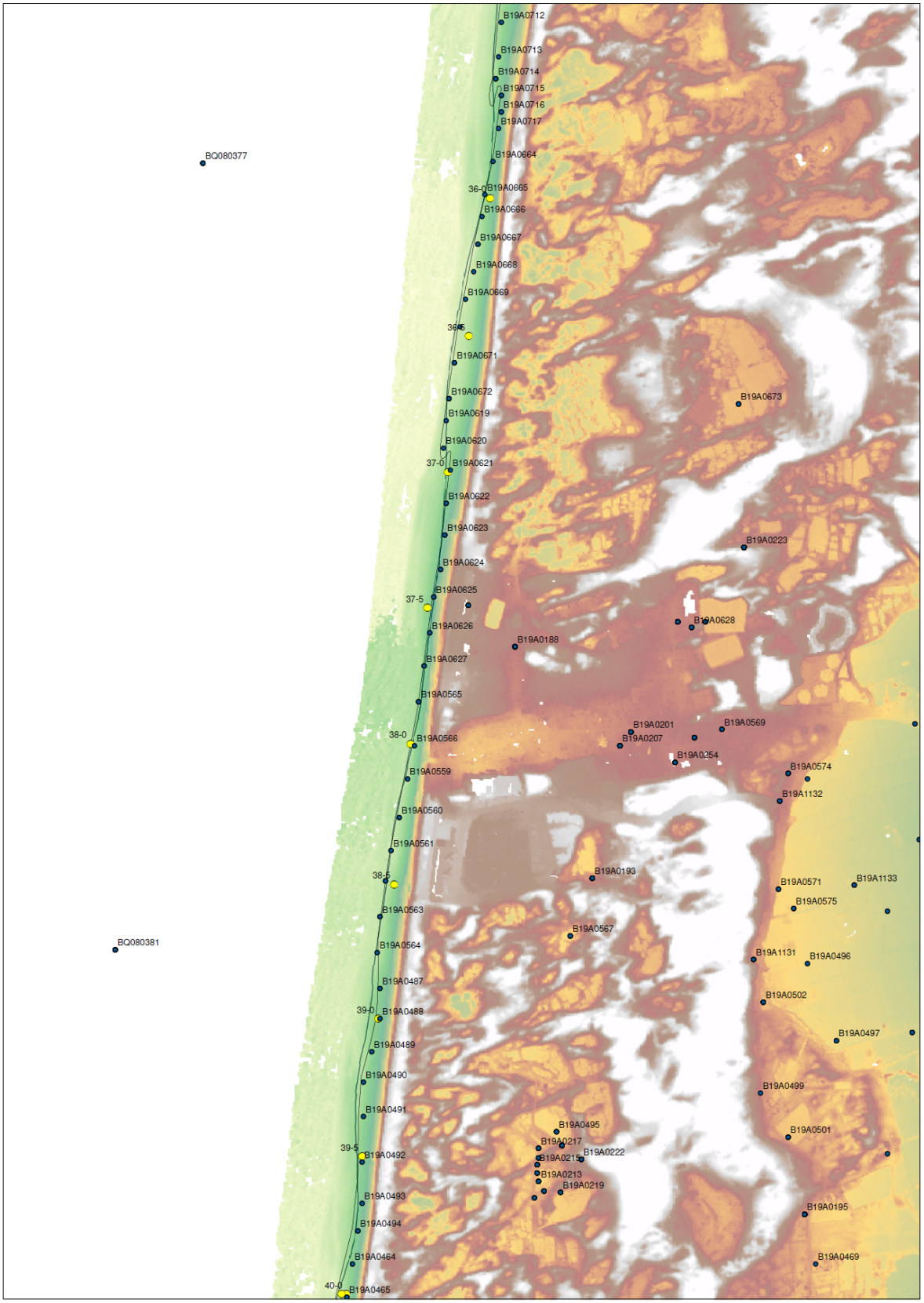

Figure G-6 Measurements done north of drainage tube area 1 [30]

Figure G-7 Measurements done at drainage tube area 1 [30]

Appendix H. Beach nourishments

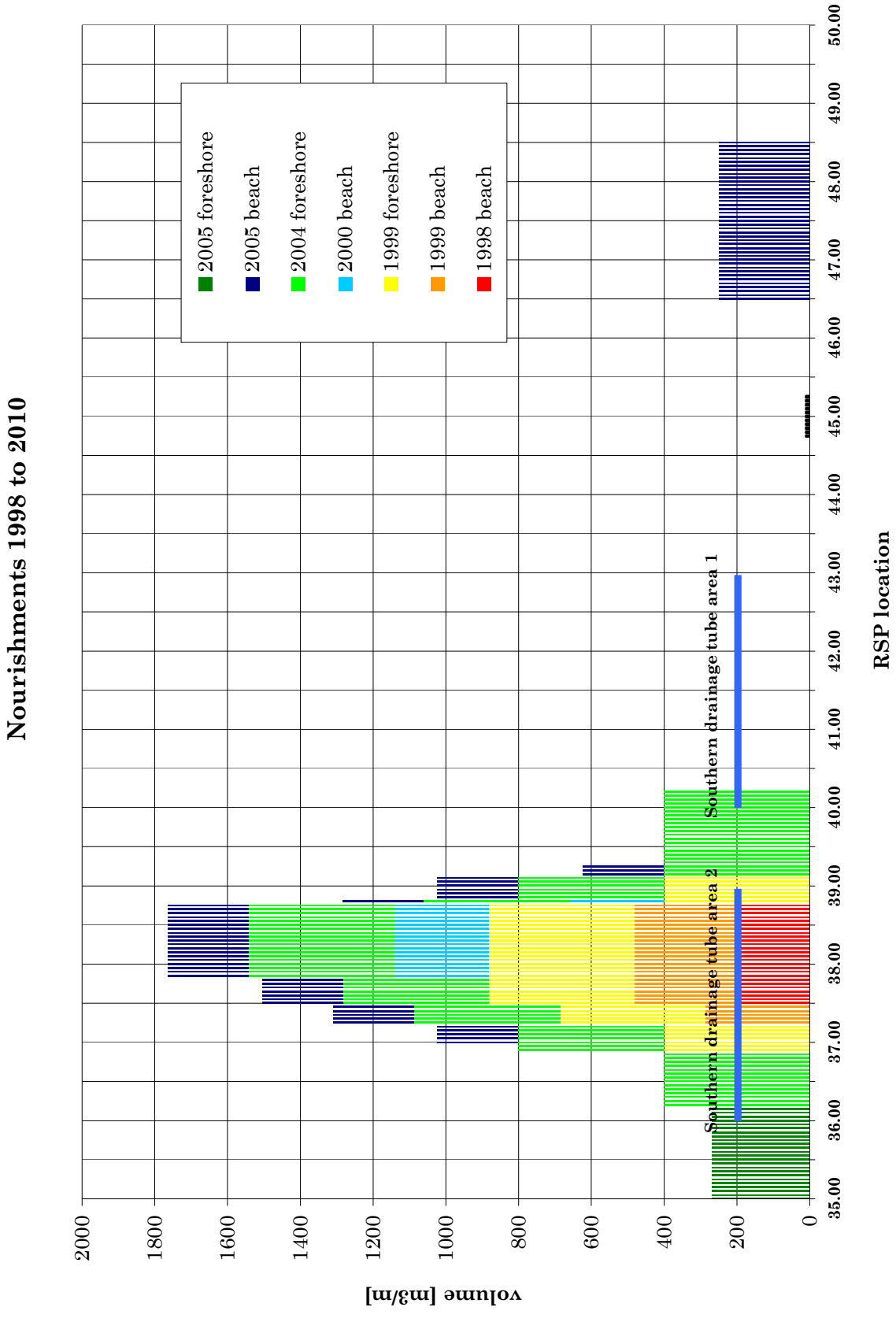

Volumes (m^3)

	Årgab					Havrvig			Skodbjerge	
	dumping at dune foot	beach nourishment	beach scraping	foreshore nourishment	bar nourishment	beach nourishment	beach scraping	foreshore nourishment	beach nourishment	beach scraping
1977	158.007									
1978	48.817			34.959						
1979	57.813			29.014						
1980	54.383			17.005						
1981	87.100									
1982	95.342									
1983	84.656									
1984	89.002		21.726							
1985	119.288		17.704	18.491						
1986	85.816		21.604	29.927						
1987	97.542		9.384	25.900						
1988	173.960		750	44.864						26.997
1989	165.361			41.336			4.410			21.182
1990	187.306			7.100			4.418			21.222
1991	177.766			1.318			4.084			24.422
1992	197.907			3.855		21.099			115.669	
1993	82.333	208.099		2.955		152.115	108.904			81.128
1994	60.602	148.455	13.395	1.591		214.945	51.288		82.345	25.123
1995	35.528	184.655	23.848	33.136			58.969			
1996	18.288	395.811		1.973		185.946	11.131			79.873
1997	12.534	187.718	19.001	2.618			36.565			42.875
1998	36.095	504.742		382		326.358	43.637			57.680
1999	17.480	388.036				228.020	8.010	200.255	154.110	41.624
2000	60.256	519.733		10.800		218.080	13.075			56.060
2001	14.342	429.572					4.634			60.900
2002		628.317					12.540			17.188
2003	28.706	527.925			2.632		20.239			42.907
2004		94.800	11.443		600.041		3.951			15.061
2005		192.400			200.419					
2006		145.884			505.105					
2007		180.000			300.130					
Total	2.246.230	4.736.147	138.855	307.224	1.608.327	1.346.563	385.855	200.255	352.124	614.242

Figure H-2 Beach nourishments done at Hvide Sande

Appendix I. Beach profiles at Egmond aan Zee

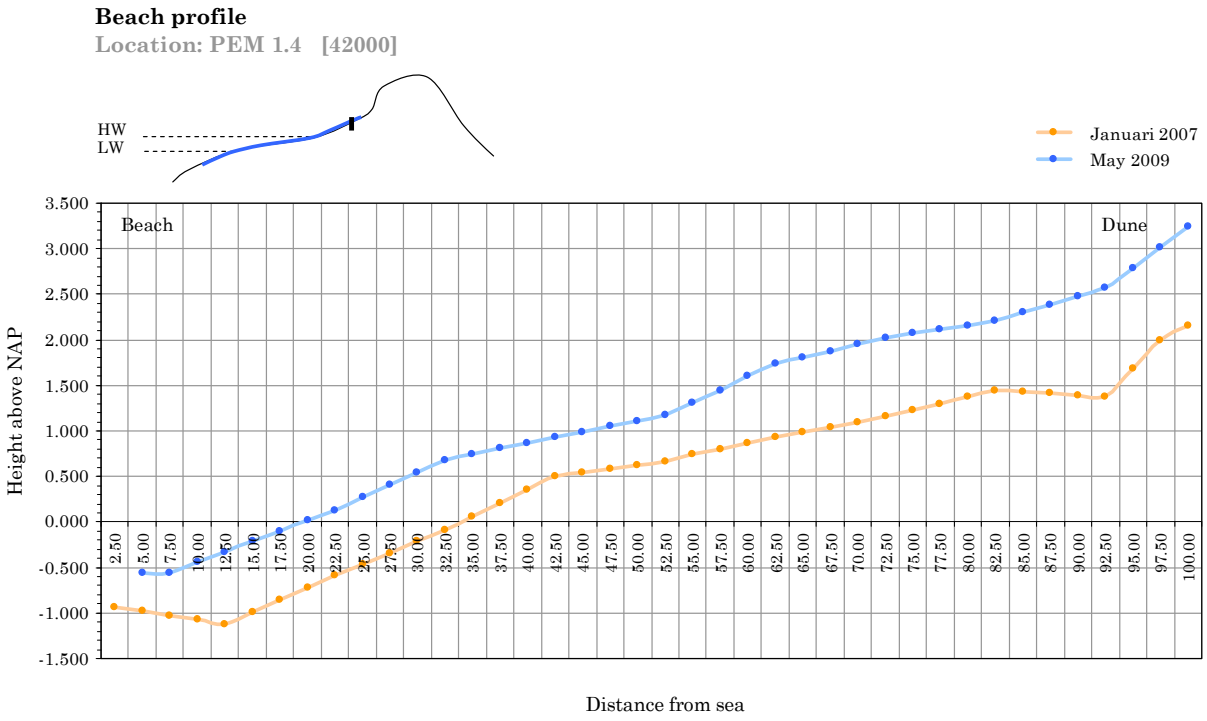

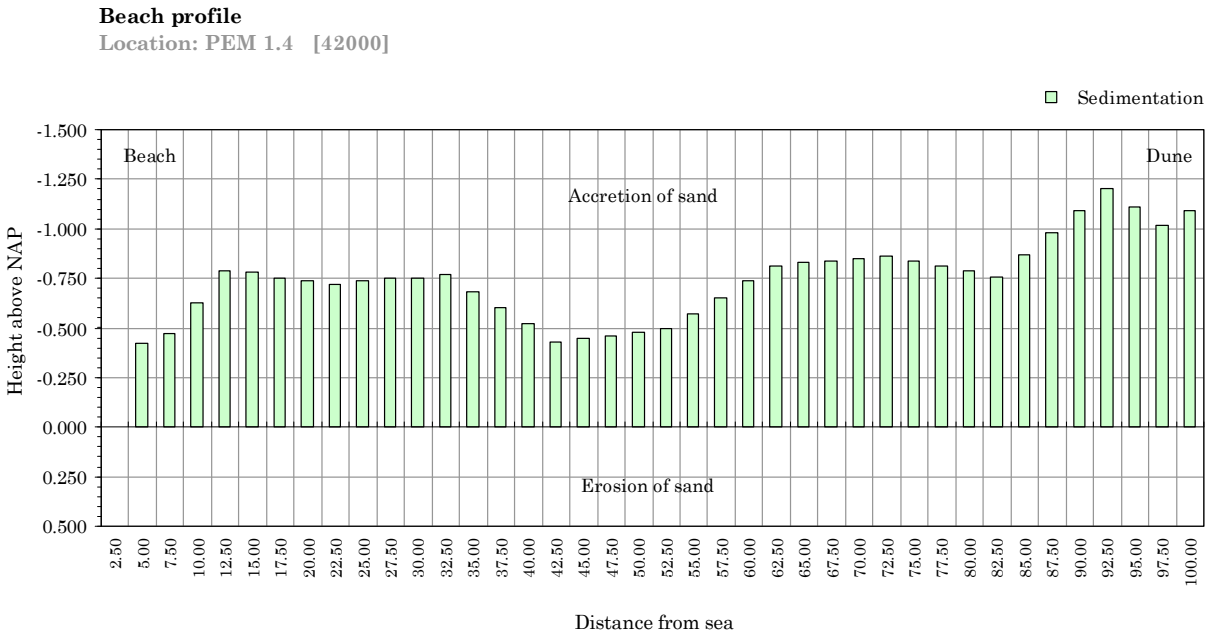

Figure I-1 Beach profiles at the southern part of drainage tube area 1 near Egmond aan Zee

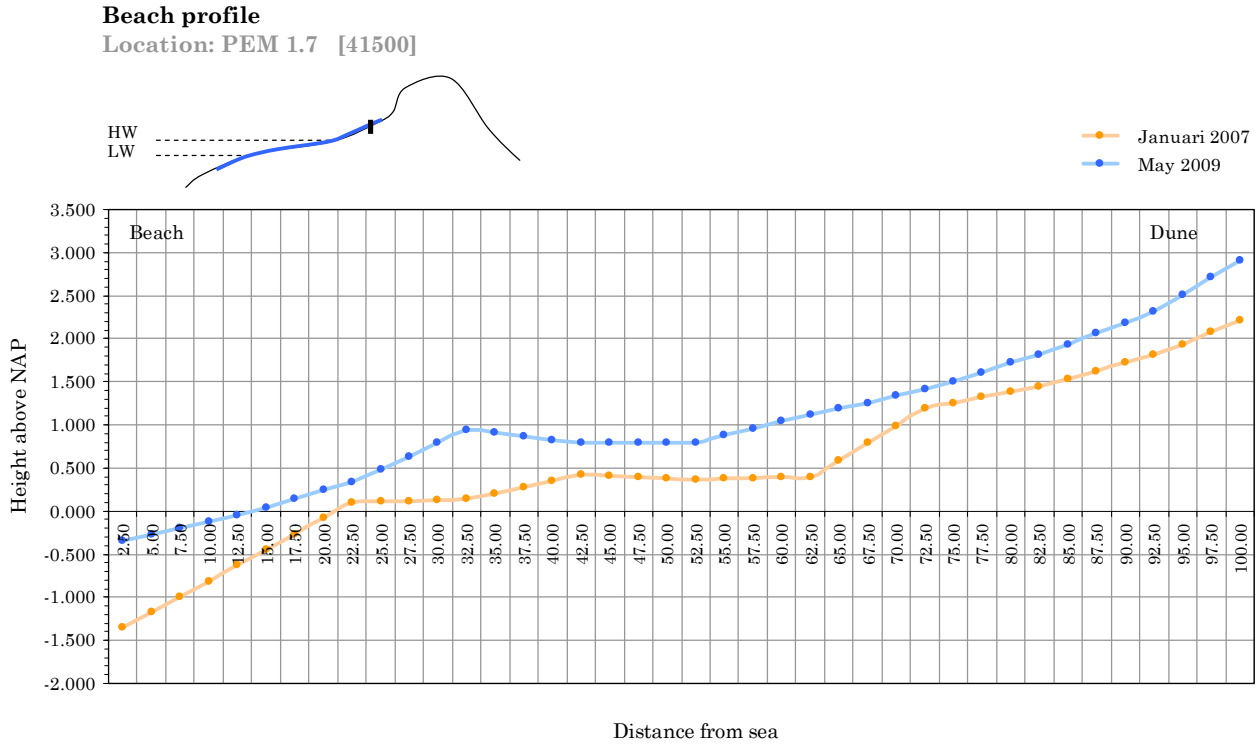

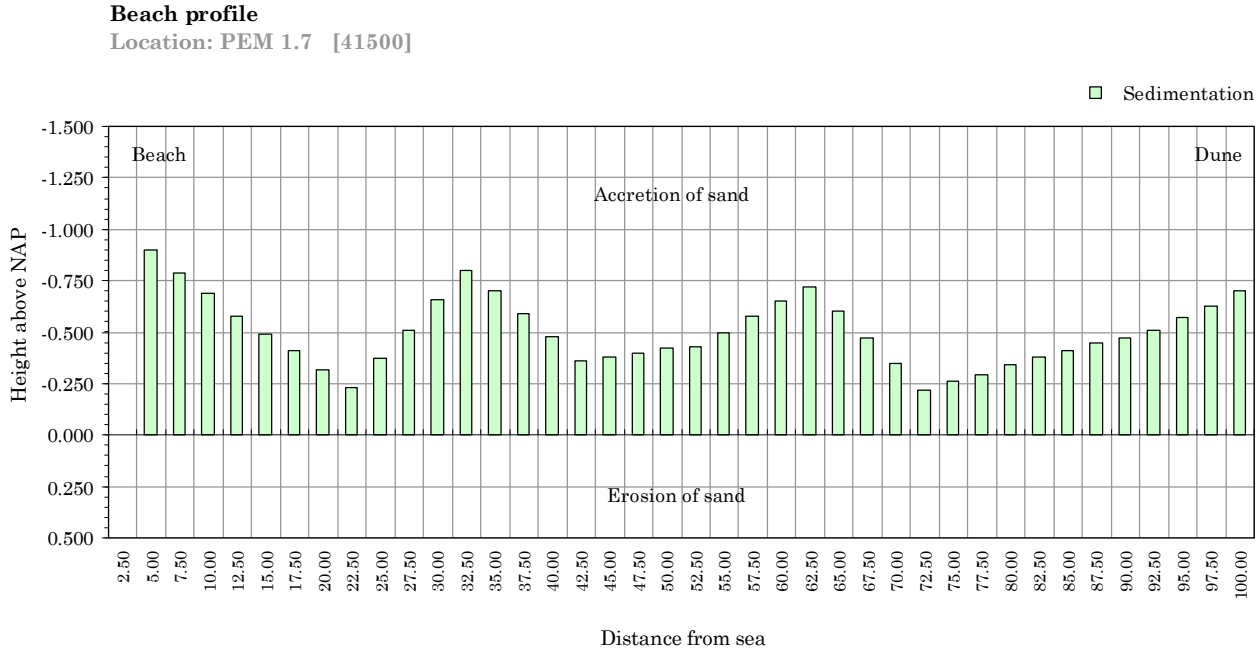

Figure I-2 Beach profiles at the centre part of drainage tube area 1 near Egmond aan Zee

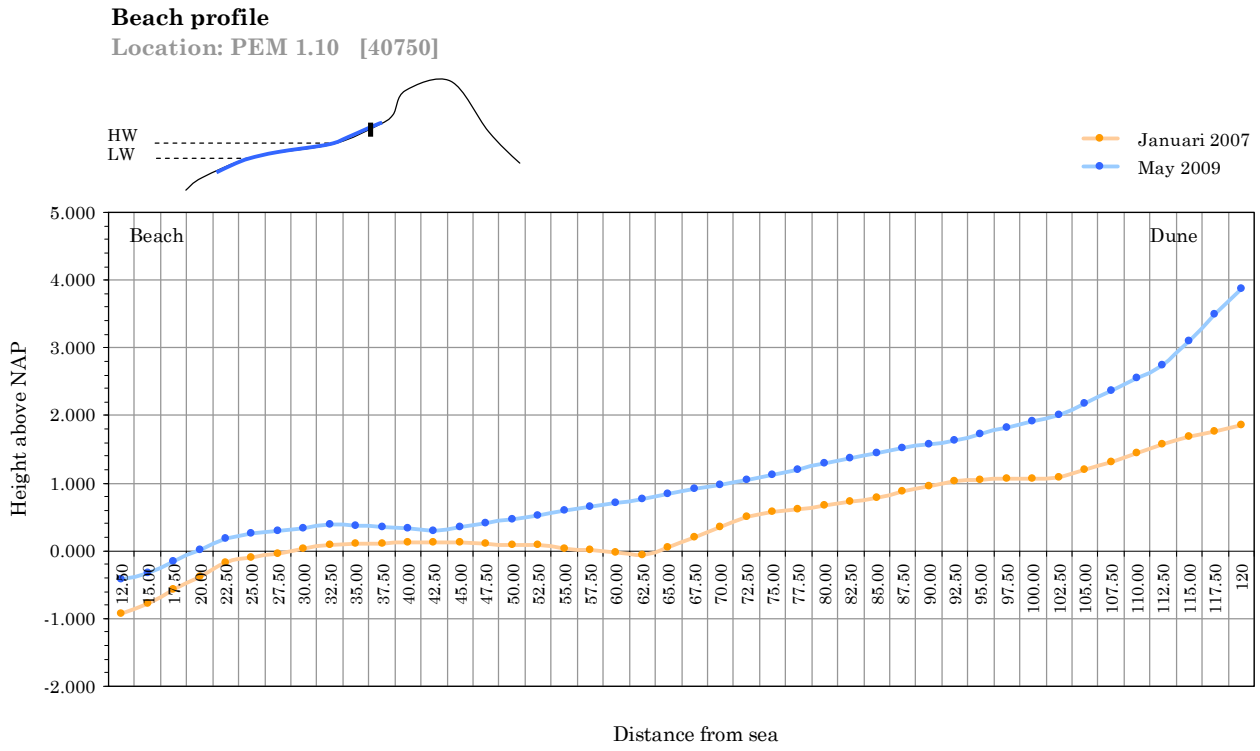

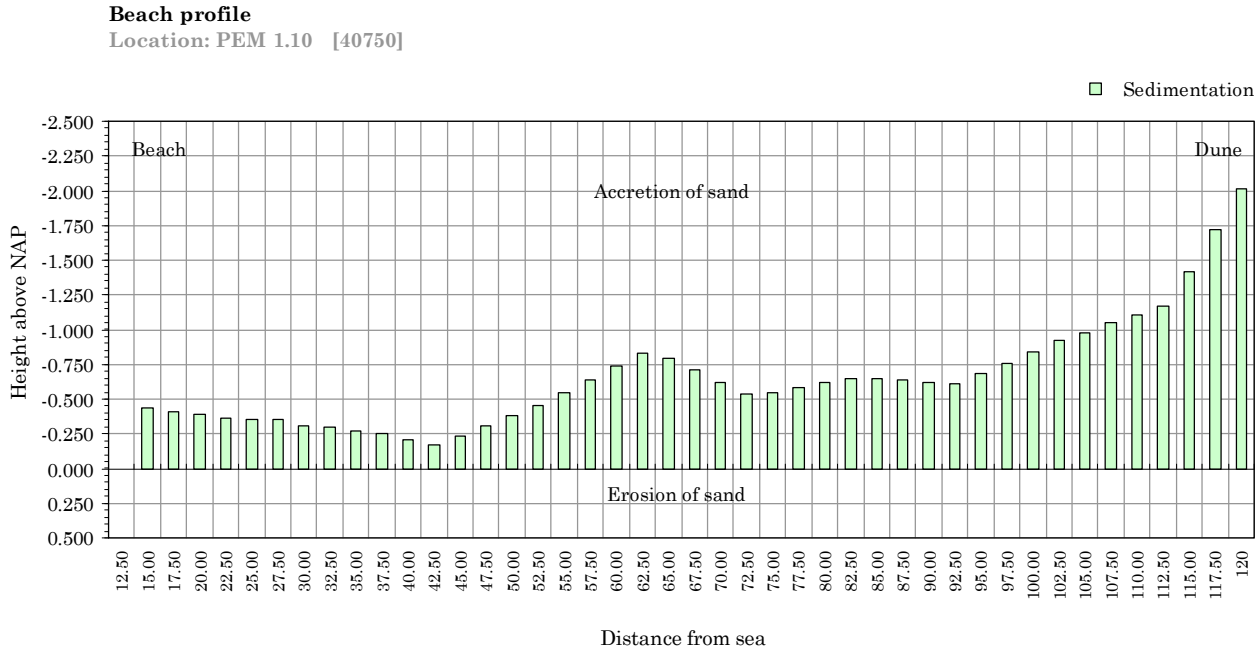

Figure I-3 Beach profiles at the northern part of drainage tube area 1 near Egmond aan Zee

Appendix J. Hydrodynamic conditions

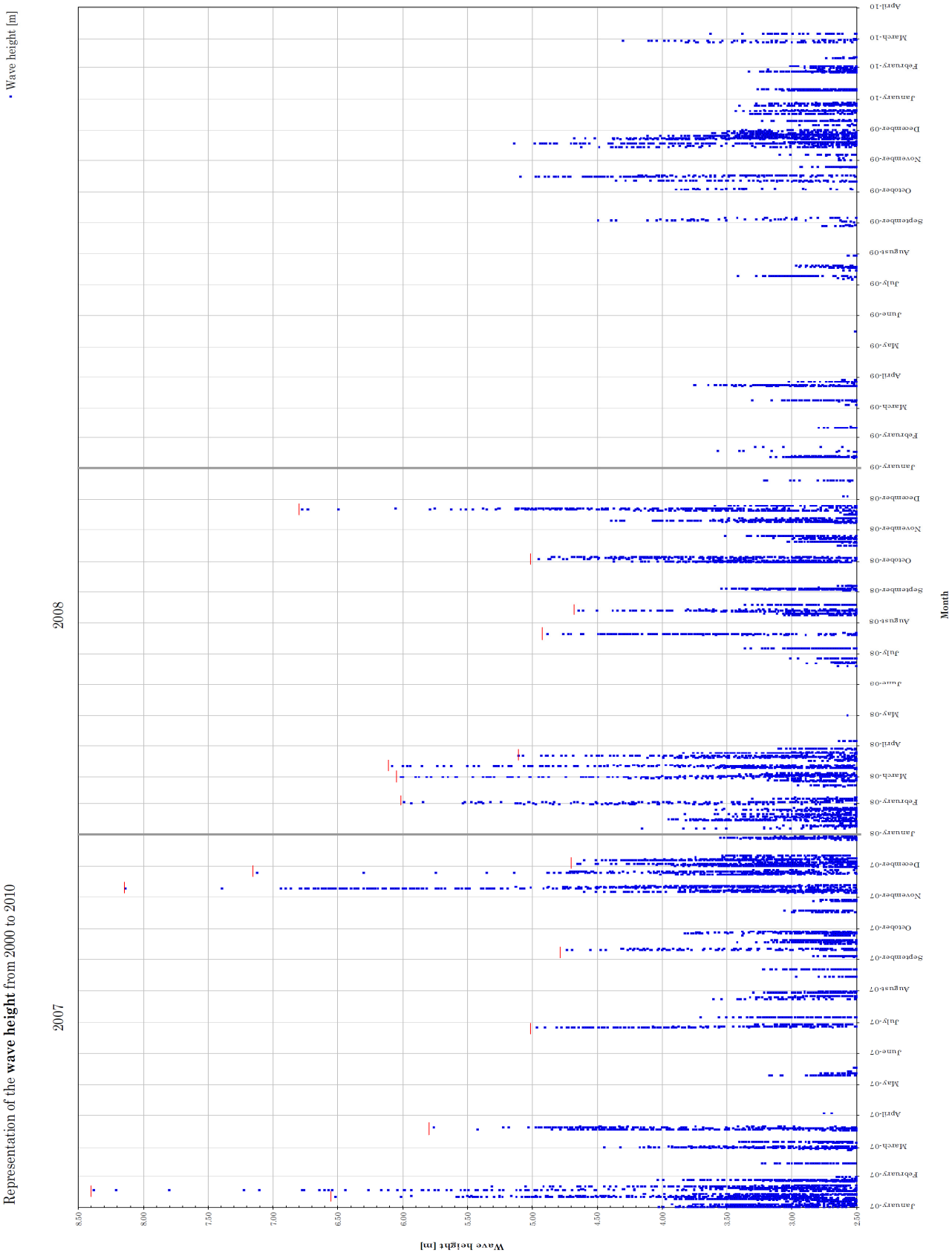

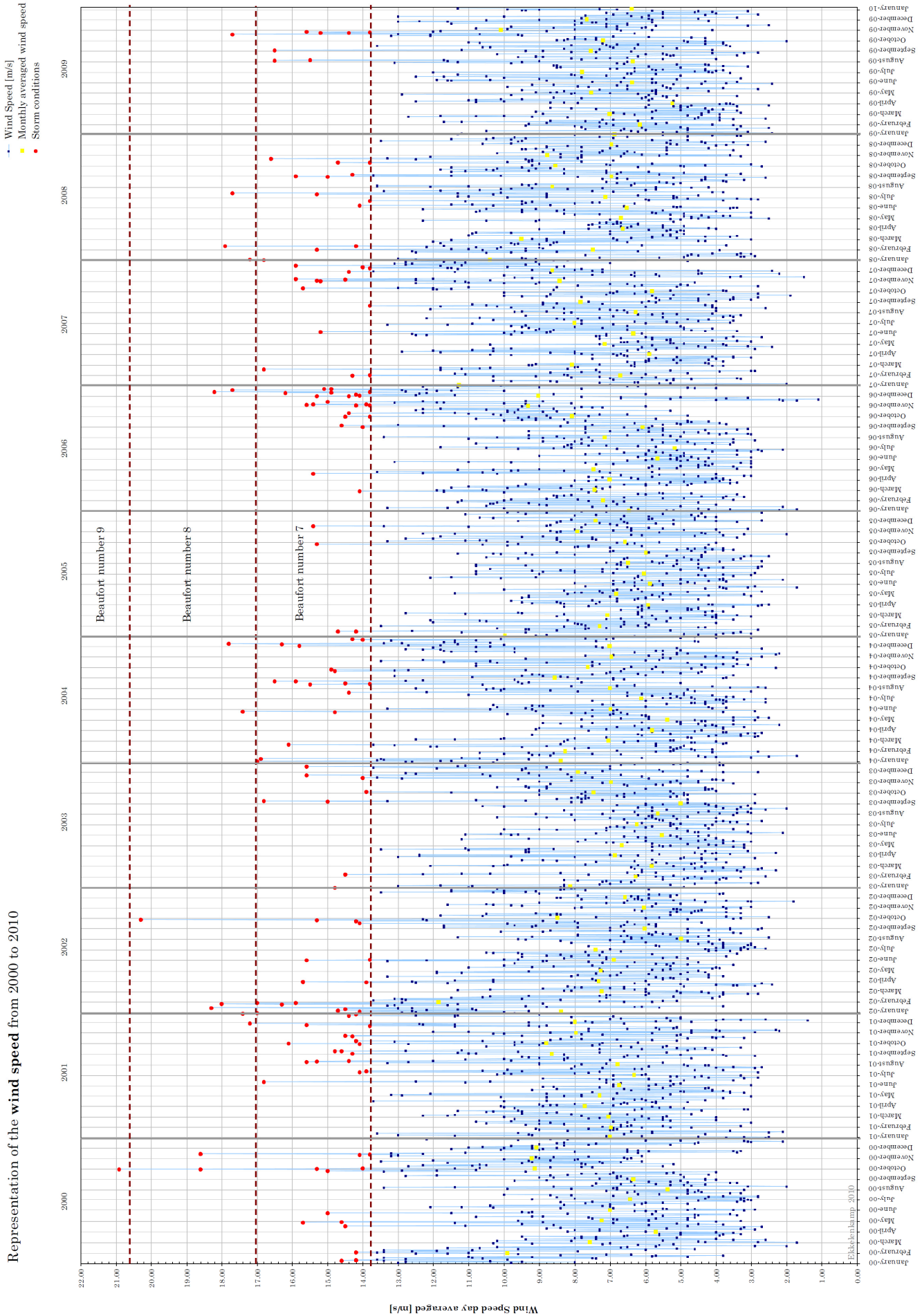
Representation of the **wind speed** from 2000 to 2010
Wind Speed [m/s]
Monthly averaged wind speed
Storm conditions
Beaufort number 9
Beaufort number 8
Beaufort number 7
Wind Speed day averaged [m/s]
Month
Ekkelenkamp 2010

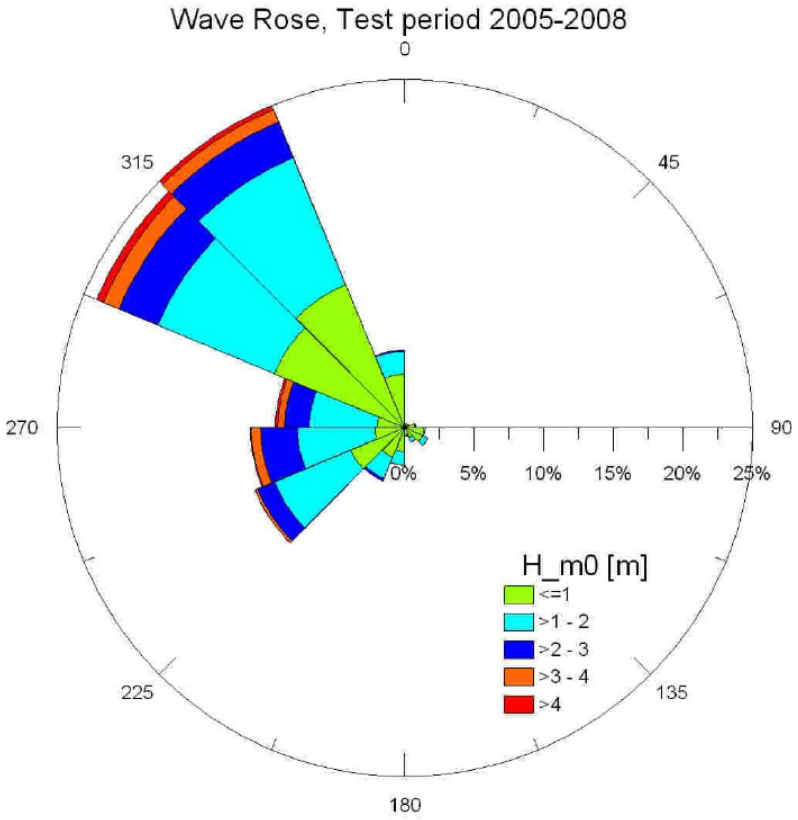

Figure J-3 Wave heights at the beach near Hvide Sande

Hvide Sande (HVIDSDE)
Statistieken gebaseerd op waarnemingen van 7/1999 - 1/2011 dagelijks van 7u tot 7pm lokale tijd.

Maand van het jaar	Jan	Feb	Mrt	Apr	Mei	Jun	Jul	Aug	Sep	Oct	Nov	Dec	Som
	01	02	03	04	05	06	07	08	09	10	11	12	1-12
Overheersende windrichting													
Wind waarschijnlijkheid > = 4 Beaufort (%)	73	66	69	54	64	67	63	56	69	70	70	62	**65**
gemiddelde Windsnelheid (Knots)	15	14	14	12	14	14	14	13	15	15	15	14	**14**
gemiddelde luchttemperatuur (°C)	4	3	5	10	15	18	20	19	17	12	8	5	**11**
Selecteer maand (Help)	Jan	Feb	Mrt	Apr	Mei	Jun	Jul	Aug	Sep	Oct	Nov	Dec	Jaar

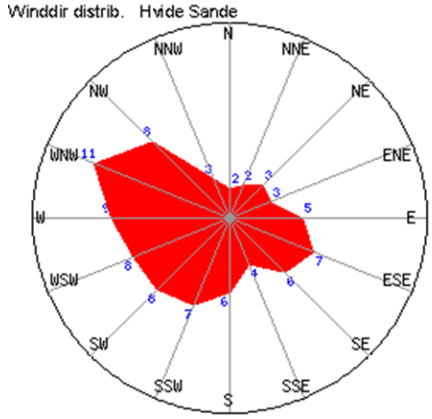

Windrichting

Figure J-4 Wind speeds at the beach near Hvide Sande

Appendix K. Calculations of the bottom friction

Calculation D50=302mu, D50=400mu and D50=417, D50=700

$D50 := 0.00030$
$D50 := 0.00040$
$D50 := 0.00041$
$D50 := 0.00070$

0.00030
0.00040
0.00041
0.00070

$g := 9.81$

9.81

$T := 6$

6

$H := 1.7$
$H := 2.2$

1.7
1.7
2.2
2.2

$h := 2$

2

$\lambda := 57$
$\lambda := 56$

57
57
56
56

$\kappa := 0.4$

0.4

$\upsilon := 1.33 \cdot 10^{-6}$

0.00000133000000

$\omega := \frac{2 \cdot 3.1416}{T}$

1.04720000

$$k := \frac{2 \cdot 3.14}{\lambda}$$

0.110175438

0.110175438

0.112142857

0.112142857

$u0 := 1$

$u0 := 1.5$

1

1

1.5

1.5

$\rho := 100$

100

$\rho s := 265$

265

$$\Delta := \frac{\rho s - \rho}{\rho}$$

$$\frac{33}{20}$$

$$a0 := \frac{u0 \cdot T}{2 \cdot 3.1416}$$

0.954927425

0.954927425

1.432391138

1.432391138

$s := 2.65$

2.65

$r := 0.047$

$r := 0.054$

$r := 0.069$

$r := 0.118$

0.047

0.054

0.069

0.118

$$D\theta := \frac{D50 \cdot \sqrt{(s-1) \cdot g \cdot D50}}{4 \cdot \upsilon}$$

3.968946620

6.049992420

6.439748788

14.00592845

$$fw := \exp\left(-5.977 + 5.213 \cdot \left(\frac{a0}{r}\right)^{-0.194}\right)$$

0.0467283265
0.0506564341
0.0461348303
0.0629674100

$$f25 := \exp\left(-5.977 + 5.213 \cdot \left(\frac{2.5 \cdot D50}{A}\right)^{0.194}\right)$$

0.00934468842
0.0100530958
0.00915249675
0.0104822763

$$u\theta := \sqrt{\frac{1}{2} \cdot fw \cdot u0^2}$$

0.152853404
0.159148412
0.227819411
0.266154722

$$\theta 25 := \frac{\frac{1}{2} \cdot f25 \cdot \rho \cdot (A \cdot \omega)^2}{\rho \cdot (s - 1) \cdot g \cdot D50}$$

0.955817406
0.776348798
1.52546799
1.04077568

Appendix L. Coordinates of the tubes and field research

Table L-1 Sediment samples at Egmond aan Zee

Measurement	North	East
S2.1	522903	43446
S2.2	522930	43479
S2.3	522956	43491
S2.4	522979	43501
S2.5	523002	43518
S2.6	523026	43530
S2.7	523049	43541
S2.8	523068	43549
S2.9	523095	43559
S2.10	523118	43567
S2.11	523143	43576
S2.12	523166	43583
S2.13	523192	43591
S2.14	523218	43597
S1.1	523248	43611
S1.2	523261	43612
S1.3	523274	43612
S1.4	523287	43613
S1.5	523299	43615
S1.6	523310	43617
S1.7	523322	43626
S1.8	523336	43630
S1.9	523347	43633
S1.10	523360	43637
S1.11	523373	43638
S1.12	523385	43638
PEM1.1	523424	43640
PEM1.2	523436	43650
PEM1.3	523448	43660
PEM1.4	523468	43666
PEM1.5	523481	43665
PEM1.6	523495	43668
PEM1.7	523508	43673
PEM1.8	523521	43675
PEM1.9	523534	43681
PEM1.10	523548	43684
PEM1.11	523561	43690
PEM1.12	523575	43688

PEM1.13	523589	43657
N1.1	523601	43693
N1.2	523615	43696
N1.3	523629	43699
PEM2.1	523642	43702
PEM2.2	523656	43705
PEM2.3	523669	43707
PEM2.4	523682	43709
PEM2.5	523696	43712
PEM2.6	523709	43712
PEM2.7	523723	43715
PEM2.8	523736	43718
PEM2.9	523749	43741
PEM2.10	523762	43732
PEM2.11	523776	43727
PEM2.12	523789	43730
PEM2.13	523803	43739
N2.1	523830	43739
N2.2	523856	43746
N2.3	523883	43749
N2.4	523910	43751
N2.5	523937	43757
N2.6	523964	43763
N2.7	523998	43768
N2.8	524017	43775
N2.9	524047	43782

Table L-2 Sediment samples at Hvide Sande

Measurement	North	East
S2.1	554545	81049
S2.2	554572	81056
S2.3	554600	81060
S2.4	554627	81063
S2.5	554052	81059
S2.6	554681	81059
S2.7	554709	81057
S2.8	554736	81056
S2.9	554763	81054
S2.10	554789	81049
S2.11	554816	81045
S2.12	554843	81040
S2.13	554870	81034
S2.14	554896	81027
S2.15	554923	81019
S2.16	554949	81009
S2.17	554976	81001
S2.18	555002	80992
S2.19	555029	80984
S2.20	555056	80978

S2.21	555082	80974
S2.22	555110	80969
S1.1	551348	80962
S1.2	555150	80959
S1.3	555163	80954
S1.4	555176	80948
S1.5	555190	80944
S1.6	555202	80941
PEM1.1	555220	80912
PEM1.2	555230	80936
PEM1.3	555243	80934
PEM1.4	555257	80932
PEM1.5	555283	80928
M1.1	555297	80926
M1.2	555310	80925
M1.3	555323	80924
M1.4	555337	80923
M1.5	555351	80921
M1.6	555364	80920
PEM2.1	555378	80919
PEM2.2	555391	80918
PEM2.3	555405	80916
PEM2.4	555418	80914
PEM2.5	555431	80912
PEM2.6	555450	80909
PEM2.7	555458	80905
PEM2.8	555472	80902
PEM2.9	555490	80898
PEM2.10	555498	80894
PEM2.11	555511	80891
PEM2.12	555525	80887
PEM2.13	555538	80884
PEM2.14	555551	80881
PEM2.15	555565	80877
PEM2.16	555578	80875
PEM2.17	555592	80872
PEM2.18	555605	80872
PEM2.19	555618	80841
N1.1	555645	80865
N1.2	555672	80858
N1.3	555699	80849
N2.1	555725	80826
N2.2	555752	80832
N2.3	555780	80823
N2.4	555804	80809
N2.5	555831	80799
N2.6	555858	80792
N2.7	555884	80782
N2.8	555910	80767
N2.9	555936	80748
N2.10	555961	80731
N2.11	555955	80704

Appendix M. Details of the theoretical backgrounds

M.1 Shear stress velocity

The sediment transport formulae, which are analytically described in this study, contain parameters which depend strongly on the sedimentology. These transport formulae are Bijker (1971), Bailard (1966) and Van Rijn (1989). The parameters are the grain diameter (D_{50}), the ripples (μ), the friction factor (f_{cw}), the bottom shear stress (τ_b), the settling velocity (w_s) and the shear stress velocity (u_*). Eventually these parameters define the beach morphology. The shear stress velocity follows from the velocity distribution which is strongly affected by the bed properties. A typical vertical distribution at a rough bed can be characterised by a sub-bottom and a main flow. The nominal bed is chosen at a level z=0. Below this level, the bed is collision dominated. Above the nominal bed, the region is characterised by both collisions and turbulence [60]. The bedload layer (the granular-fluid region) below the nominal theoretical bed has very high sediment concentrations. Here, the inter-granular resistance is predominant. The outer region, of only pure suspended sediment, has much lower concentration values. Here, convective and diffusive processes are acting. The contact load layer forms the transition zone between the inner and outer layer.

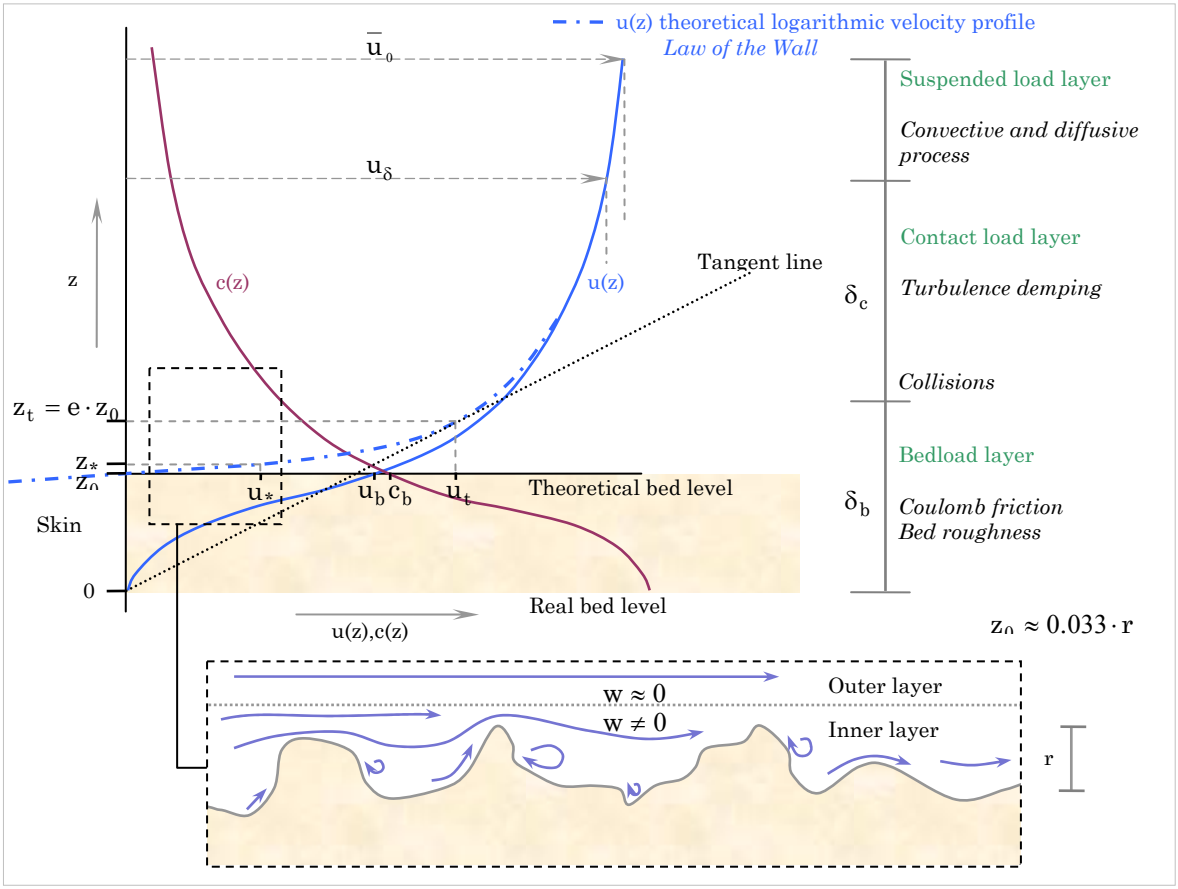

Figure M-1 Velocity and concentration distributions and boundary layer for a stationary current

M.2 Kozenzy-Carman permeability formula

One of the most comprehensive formula, quite useful in determining the beach permeability, is suggested by Kozeny-Carman (Carman 1937 en Kozeny 1927). Their formula contains the porosity in combination with the grain shape. The permeability formula adds the dependence on the grain shape by the angularity factor 'f'. The permeability equals;

$$k = \frac{\eta_{10}}{\eta_t} \cdot \frac{1}{f} \cdot 0.0417 \cdot \frac{e^3}{(1+e)} \cdot D_{50}{}^2 \cdot \exp\left(-\tfrac{1}{8} \cdot \ln^2 \cdot \frac{D_{85}}{D_{15}} \right) \quad [m/s] \qquad \text{Eq.M-1}$$

η_{10} = dynamic viscosity at 10 ^{0}C = 1.3 mPas η_{20} = 1.0 mPas η_{30} = 0.8 mPas

f = angularity factor f=1.10 (rounded) f=1.25 (subrounded) f=1.40(angular)

D_{50}, D_{85}, D_{15} = grain diameters e = void ratio = 0.25 to 0.50, often 0.40

M.3 Empirical relations of friction in oscillatory flows

Kajiura (1968) and Jonsson (1980) suggest upper limits of $f_w = 0.25$ and $f_w = 0.30$. In the past, many experimental data is been collected. This is based on data from Riedel (1972), Kemp and Simons (1982), Sleath (1987) and Jensen (1989).

Nielsen (1998) suggests a correction of the equation to give a better data fit. The adjusted formula becomes;

$$f_w = \exp\left[5.5 \cdot \left(\frac{r}{A} \right)^{0.2} - 6.3 \right] \qquad \text{Eq.M-2}$$

With:
r = bed roughness value
A = orbital amplitude of fluid

M.4 The increase of backwash friction

There are different types of measurement techniques used which are fully dependant on the way the fit the model in case of linear improvements.

The increase of the backwash friction coefficient can be caused by different processes, which can be affected by the sedimentology of the bed surface [74, 79, 76, 75, 81, 68];

1. The influence of pressure gradients. The shape of the uprush flow can be very different from the backwash flow. This will cause varying pressure gradients during each phase of the flow. Uprush is generally assumed to have a steep-faced front with little depth variation immediately behind.
2. The influence of the internal boundary layer structure to uprush and backwash flows. This could raise or lower the friction factor. Shear stresses increase for accelerating flows and decrease for decelerating flow for a detailed explanation). This effect is larger for acceleration flows [75].
3. Hydraulic jumps during backwash could increase the bed shear stress.

4. Infiltration and exfiltration into or out the beach will affect the bed shear stress. Beach permeability would allow vertical fluid exchange trough the beach altering bed shear stresses. The beach permeability is strongly related to the grain sizes (sedimentology) and the saturation level (groundwater and capillary fringe). The influence of the beach porosity is described in section. A coarse beach (bed grain sizes) will mainly affect the backrush friction factor and eventually the net transport volume [24].

The right sediment transport rate can be achieved by incorporating the fact that the bed shear stress becomes larger when it coincides with a pressure gradient from a steep front like a saw tooth wave [74].

M.5 The friction factor

Different bedforms, like ripples, may develop by changing grain sizes. Ripples will also have an effect on the friction. Small ripples appear more often for fine sediments. So, for low current velocities, these ripples have a bigger impact on the friction. The opposite holds for the sensitivity of the friction to small orbital velocities. With increasing grain sizes the latter becomes more important [25]. If the orbital velocity increases, this effect becomes less dominant. Thus, the total friction factor is very sensitive to grain size and current/wave velocities. To visualise this, the dependence on both features is shown the figures below.

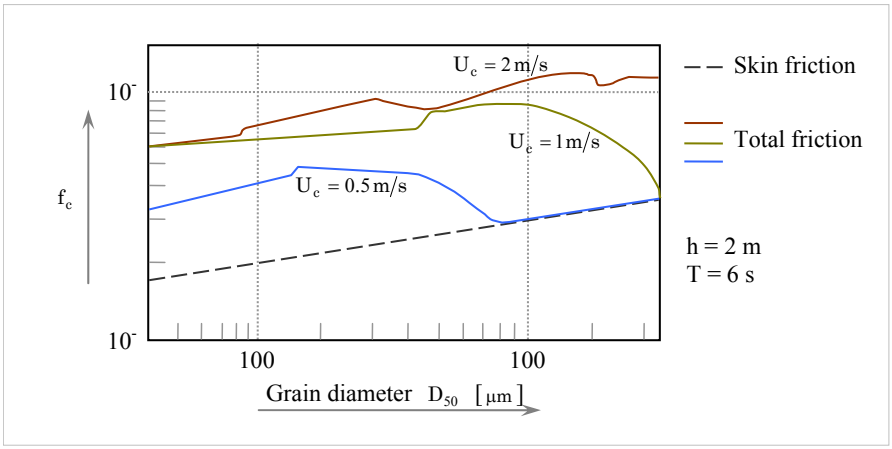

Figure M-2 Skin and total friction due to a current velocity [24]

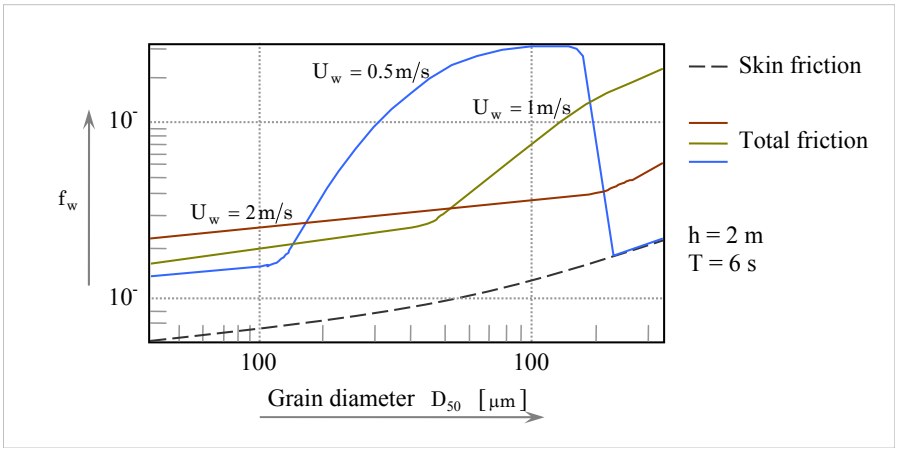

Figure M-3 Skin and total friction due to a wave velocity [24]

The skin friction is basically determined by the grain properties of the bed. Striking is that a higher current velocity results in larger friction term, while the opposite holds for slow flows. At the swash zone wave motions are governing. The impact of larger grain sizes on the wave friction term is significant. The reason is that ripples appear more often [25].

The bottom friction forms the basic ingredient for the bed shear stress τ_b. The moving water interacts mainly with the bottom sediment trough this stress. Almost every sediment transport formula includes the shear stress. Ripples and other bed forms make the water motion within the boundary layer very complex.

M.6 The effect of friction on the swash

The uprush is assumed to be a sheet flow. The near bed velocity profile depends on the friction. The near bed velocity follows from the logarithmic profile based on the quadratic stress law formulation. The backwash is more laminar and depends more on the bed properties. Therefore the friction factor during backwash will fluctuate over the tidal cycle [81]. This effect enlarges with changing grain sizes.

As the friction term is very important in the sediment transport model through the bottom shear stress, it is essential to determine the friction factor and it's behaviour during uprush and backwash. To illustrate the effect of the friction term on the uprush and backwash, a plot of the equations, is shown in the figure below. The sediment transport during swash can be up to two orders of magnitude greater than surf zone sediment transport [81]. This means that an effect on the sedimentology of the intertidal beach by the drainage tubes, may affect the sediment transport extensively. The change of the water depth is taken 0.05m for both uprush and backwash with a beach slope of $\beta = 0.100$.

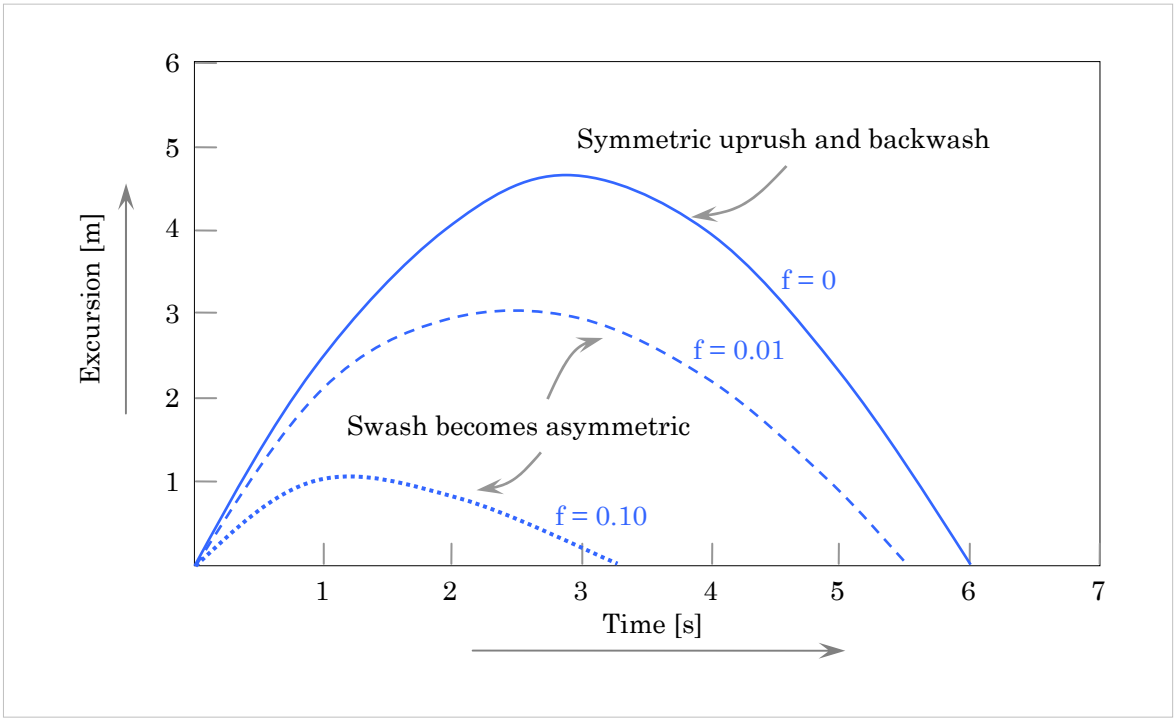

Figure M-4 Effect of friction on the excursion with constant beach slope [79]

The space-time trajectory in the inviscid case (f=0) is perfectly symmetric in time. If the friction coefficient increases to a value of 0.01 or 0.10, the trajectory becomes more asymmetrical. As a consequence of this the swash duration is reduced considerably (50% with f=0.10, from 6s to 3s). Also the maximum excursion distance is reduced significantly by 80% (from 4.5m to 0.9m). Swash asymmetry resulting from an increased friction coefficient is suggested to be an important factor for beach change [79].

The maximum excursion also depends on the beach slope, when β is not taken as a constant (see figure below). For shallow slopes (1:50) with an increased friction factor (from f=0 to f=0.10), the maximum excursion distance becomes 10 times smaller (from 22 m to 2,2 m).

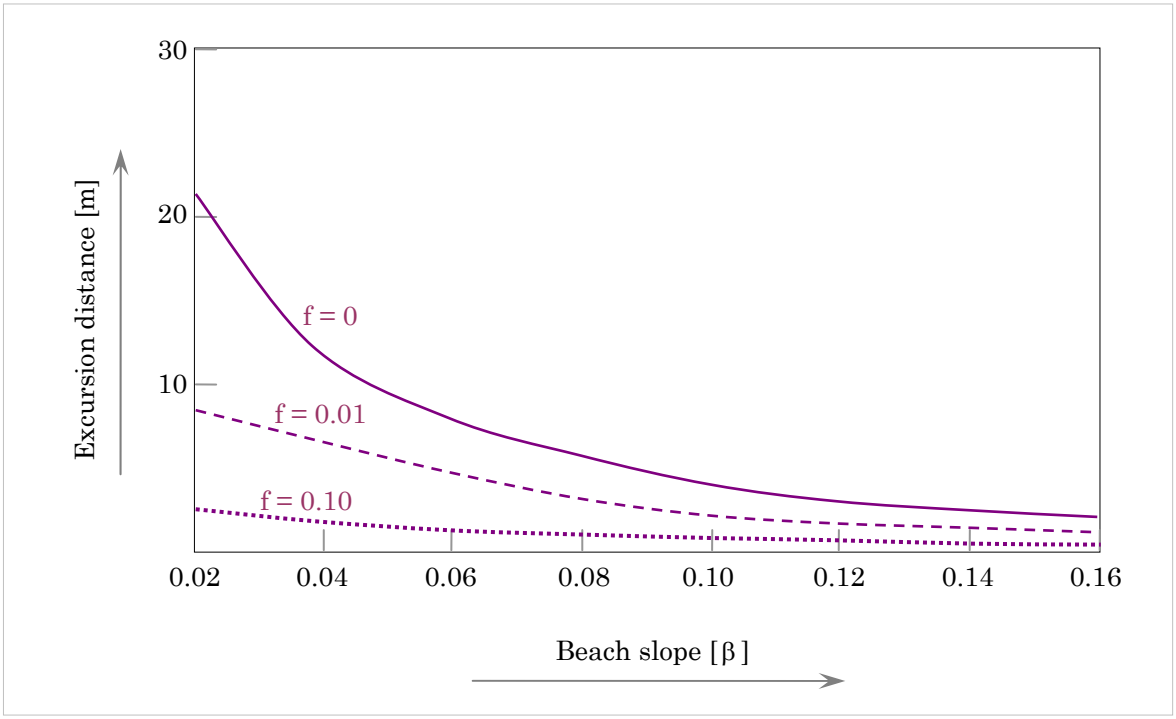

Figure M-5 Effect of friction on the excursion with varying beach slope [79]

An increase of the grain size initiates a steeper slope (see section 4.2.2) and an increase of the friction term. Both features will result in a decreased excursion distance. This effect can be significant. Particularly in the case of the Egmond aan Zee beach (slope of 1:30 – 1:40, section 4.2.1) the influence is larger than for steeper beaches with slopes of 1:10 – 1:20 like Hvide Sande. This has to do with the relatively small run-up distance by gravity forces. Therefore, it is clear that the effect of the friction (grain properties) may be more important on more shallow sloping beaches.

In addition to the friction for swash flows which is generally assumed to be only a function of the grain roughness some other mechanisms are acting. It would be unwise to ignore these effects. There are four mechanisms which may resist the swash flow on a sandy beach [81];

- Skin friction resistance by individual sand grains
- Roughness created by any bed irregularities like ripples
- Resistance attributed to any appreciable sediment load carried by the fluid
- Altered bed shear stresses due to infiltration

The total resistance should be given as some combination of these four mechanisms. Examples which occur at natural beaches are hydraulic jumps [68]. These are often cause by ripples. Also the amount of suspended sediment (sediment loads) may be important to the resistance. These aspects are related to the grain properties of the bed. The concentration as well as the formation of ripples depend on the grain size.

M.7 Shields for infiltration and exfiltration

Nielsen (1997) suggests that the relative importance of these opposing effects depends on the initiation of motion. He gives a revised Shields Parameter that includes the effects of infiltration and exfiltration;

$$\theta_{rev} = \frac{u_*^2 \cdot \left(1 - 16 \cdot \frac{w}{u_*}\right)}{g \cdot D_{50} \cdot \left(S - 1 - \beta \cdot \frac{w}{K}\right)} \qquad \text{Eq.M-3}$$

With:
θ_{rev} = Shields parameter for infiltration and exfiltration effects
u_* = shear stress velocity
w = vertical seepage velocity
D_{50} = mediane grain diameter of the sediment
S = relative density = 2.65 for sand
K = hydraulic conductivity
β = constant which denotes particle in the bed (=1) and above (=0.40)

M.8 Drag coefficients for nonspherical grains

Dietrich (1982) developed an expression which includes the affect of shape and roundness on the settling velocity. Three different drag coefficients are available;

$$C_D = \frac{1}{3} \cdot \left(0.794 + \sqrt{0.630 + 73.696 \cdot \left(\frac{w_s \cdot D_{50}}{\nu}\right)}\right)^2 \quad \text{(spheres)} \qquad \text{Eq.M-4}$$

$$C_D = \frac{1}{3} \cdot \left(0.890 + \sqrt{0.792 + 79.584 \cdot \left(\frac{w_s \cdot D_{50}}{\nu}\right)}\right)^2 \quad \text{(well rounded particles)} \qquad \text{Eq.M-5}$$

$$C_D = \frac{1}{3} \cdot \left(0.954 + \sqrt{0.910 + 81.936 \cdot \left(\frac{w_s \cdot D_{50}}{\nu}\right)}\right)^2 \quad \text{(naturally rounded particles)} \qquad \text{Eq.M-6}$$

$$C_D = \frac{1}{3} \cdot \left(0.995 + \sqrt{0.990 + 83.376 \cdot \left(\frac{w_s \cdot D_{50}}{\nu}\right)}\right)^2 \quad \text{(crushed sediments)} \qquad \text{Eq.M-7}$$

M.9 Effects of a changed bedform

The type of bedform is strongly related to the flow strength at the time. One way to characterise the bedform is by using the grain roughness Shields parameter $\theta_{2.5}$. This parameter differs from the normal Shields parameter θ because the loose sand on flat beds may offer considerably more resistance to the flow [74]. Following the expression of Nielsen in Table 4-7, the grain roughness of the bed is related to the mean grain diameter by $k_n=2.5D_{50}$. The roughness Shields parameter depends on the grain roughness friction factor and the orbital wave motion.

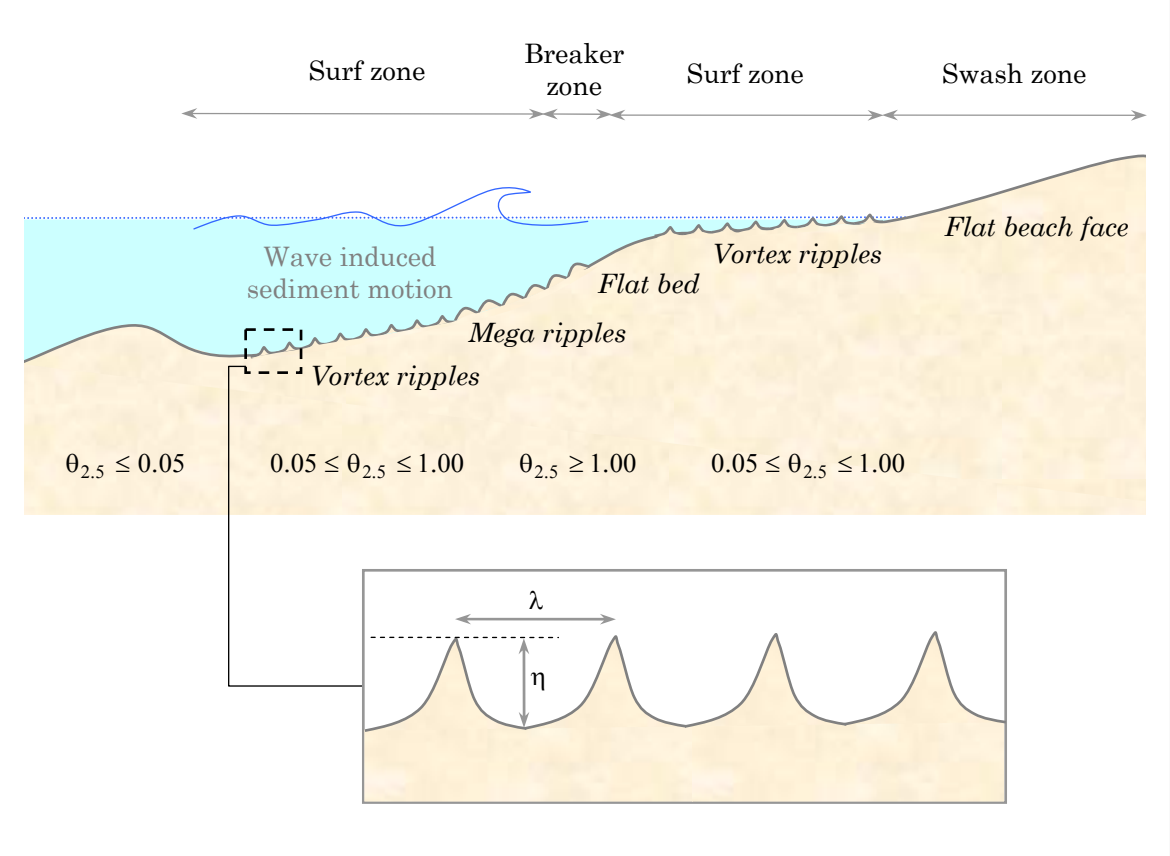

Figure M-6 Bedforms at the nearshore and foreshore [73]

If the flow is weak, the sediment motion will not affect the bed. The bedforms will be dominated by relict bedforms from previous events [73]. For these area's $\theta_{2.5} \le 0.05$. Under flows of intermediate strength, the bed will become more active. There exists a new equilibrium with the flow conditions. Here, $0.05 \le \theta_{2.5} \le 1.00$. For an almost symmetrical oscillatory flow the bed will be covered by long crested vortex ripples. Theses bedforms occur seaward of the breaker zone and the just before the swash zone, where waves have reformed after breaking. Breaking waves create more turbulent flows which give the bed irregular shapes (often rounded crests). These forms are called mega ripples. Here, complicated instabilities cause vortex shedding. Under such flow conditions, $\theta_{2.5} \ge 1.00$, vortex ripples cannot exist [74].

The grain roughness Shields' parameter is defined by;

$$\theta_{2.5} = \frac{\frac{1}{2} \cdot f_{2.5} \cdot \rho \cdot (A \cdot \omega)^2}{\rho \cdot (s-1) \cdot g \cdot D_{50}} = \frac{1}{2} \cdot f_{2.5} \cdot \psi \qquad \text{Eq.6-8}$$

M.10 Sediment transport

Most sediment transport research is done at the region offshore of the intertidal beach area. The sediment transport formulas focus on the development of both analytical and numerical methods which are often concentrated on sand sized sediment [104]. The beach morphology is usually modelled iteratively with each iteration involving three main steps. First, the main flow pattern is calculated on the basis of the incoming waves and the existing topography (second input element in Figure 4-1). Secondly, the local sediment transport rates are calculated from the flow pattern and sedimentology. Thirdly, the rates of morphological change are calculated from local sediment transport rates [73]. This last step involves the implementation of small-scale features like cusps, breaker bars, rip channels and sand waves and large-scale adaptations of shoreline forms like beach plains, headlands, bays, tombolos, spits and forelands [85]. This study restricts itself to the second step where the sedimentology is coupled to the flow dynamics and basic sediment transport formulae. The sensitivity of these formulae to the sediment grain size can be significantly. A distinction is made between longshore and cross-shore sediment transport. The latter has more influence on the transport and accretion of the beach.

The grain properties and hydrodynamic boundary conditions determine the bed and suspended load models. The wave propagation model is based on the time averaged wave energy balance, the dissipation of surface rollers in breaking waves and the mean water level set-up. [17]. The velocity and concentration profile are generated by these equations.

The sedimentology of the intertidal beach area influences the bottom friction (see section 4.3.2). The dissipation of wave energy depends on the amplitude of the wave orbital velocity near the bottom and on the bottom friction.

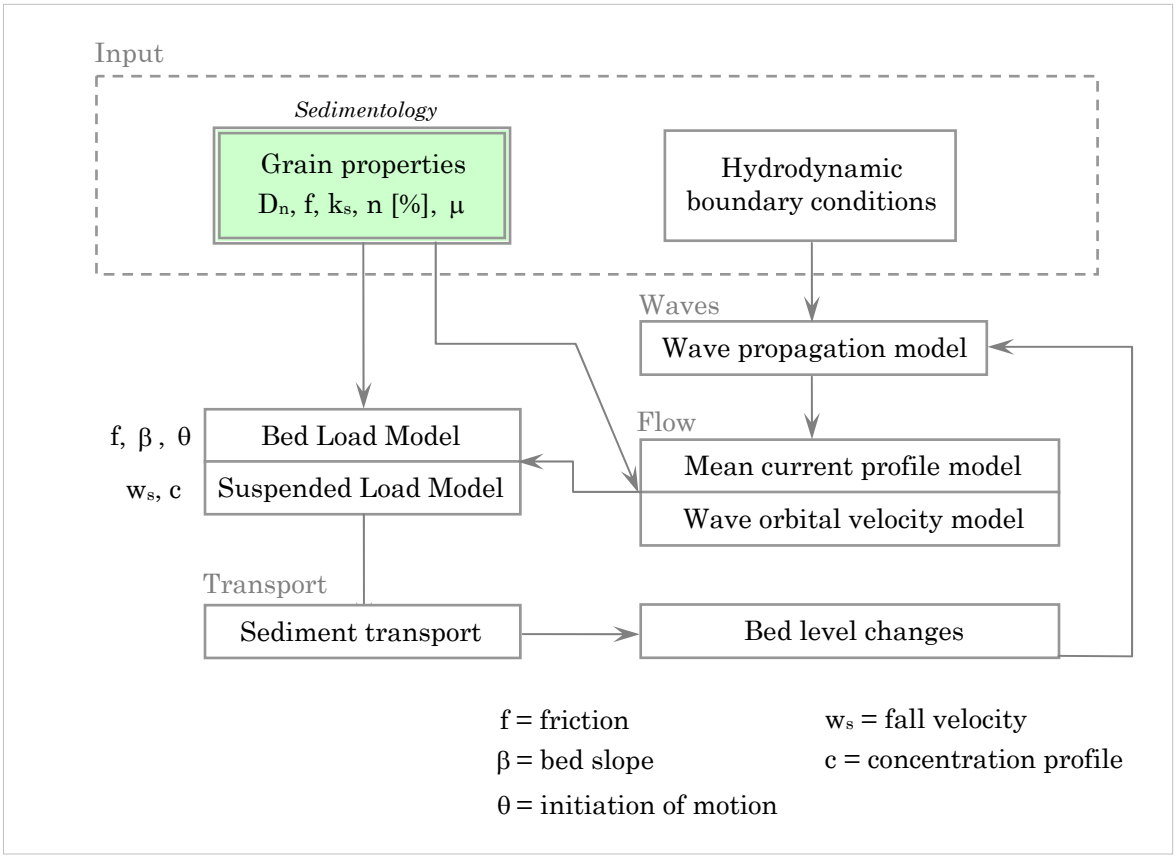

Figure M-7 Overview of the UNIBEST-TC model

The wave energy is balanced by the dissipation of wave breaking and friction.

$$\text{Energy} = \frac{\delta}{\delta x}\left(E \cdot C_g \cdot \cos\theta\right) = -D_w - D_f \qquad \text{Eq.6-9}$$

With:

E = wave energy

C_g = wave group velocity

θ = angle of incidence waves

D_w = dissipation by wave breaking

$D_f = \frac{f \cdot \rho}{\sqrt{\pi}} \cdot u_{orb}^3$ = dissipation due to bottom friction

The amount of wave dissipation follows from the bottom friction factor which can be chosen from 0.001 to 0.100. As described in section 4.2.3 and 4.3.2, this factor is influenced by the bed forms (i.e. ripple height). The factor can have a significant influence on the wave height predictions, particularly nearshore [103].

Appendix N. Tables and graphs from literature

Site	Geomorphology			Hydrodynamics		Data set		Migration (m/day)[a]	
	Setting	Sediment	Slope[b]	Tides (m)	Waves	Region	Resolution	Onshore	Offshore
Daily to Weekly time scales									
Duck, NC, USA	Ocean	180 μm	1:80	1.0–1.3	Sea, swell	Single bar	1–2 per day	12, 29	53, 34
Duck, NC, USA	Ocean	180 μm	1:80	1.0–1.3	Sea, swell	Single bar	1–6 per day		*29* **50**
Duck, NC, USA	Ocean	180 μm	1:80	1.0–1.3	Sea, swell	Inner bar	1–2 per month	0.5	3.9
Duck, NC, USA	Ocean	180 μm	1:80	1.0–1.3	Sea, swell	Inner bar	2 per month	*1.4* **8.7**	*2.6* **18**
Duck, NC, USA	Ocean	180 μm	1:80	1.0–1.3	Sea, swell	Outer bar	2 per month	*0.6* **6.1**	*1.1* **15.2**
Duck, NC, USA	Ocean	180 μm	1:80	1.0–1.3	Sea, swell	Inner bar	8 per day	0–10	0–24
Nags Head, NC, USA	Ocean	250 μm	1:30	≈1	Sea, swell	Sub–intertidal	1 per day	29	
Magdalen Island, Canada	Encl. sea	Medium sand	1:100	0.7	Sea	Sub–intertidal	3–4 per week	0.83–10 *7.5*	
Ventura coast, CA, USA	Ocean	Medium sand		≈2	Sea, swell	Sub–intertidal	1 per day	8.9–30.5	
Black Sea, Bulgaria	Encl. sea	400 μm	1:60		Sea	Single bar	1 per day	4	21.6
Naka North, Japan	Ocean	760 μm	1:90	1.0	Sea, swell	Sub–intertidal	1–2 per week	2.3–11.5	
Naka South, Japan	Ocean	260 μm	1:90	1.0	Sea, swell	Sub–intertidal	1–2 per week	1.2–5.0	
Egmond, Netherlands	Sea	150–200 μm	1:120	1.3–1.7	Sea	Inner bar	3 per week	0.8–12.4 *3.6*	4.1–4.3 *4.2*
Monthly time scales									
Duck, NC, USA	Ocean	180 μm	1:80	1.0–1.3	Sea, swell	Inner bar	24 per year[c]	0–1.0	0–1.0
Duck, NC, USA	Ocean	180 μm	1:80	1.0–1.3	Sea, swell	Outer bar	24 per year[c]	0–1.0	0–1.2
Yearly time scales									
Duck, NC, USA	Ocean	180 μm	1:80	1.0–1.3	Sea, swell	Inner bar	24 per year		0.11–0.14[d]
Duck, NC, USA	Ocean	180 μm	1:80	1.0–1.3	Sea, swell	Outer bar	24 per year		0.33–0.41[d]
Wanganui, New Zealand	Sea	160–200 μm	1:120	0.8–2.4	Sea, swell	Subtidal	4–12 per year		0.30–0.55[d]
Hasaki, Japan	Ocean	180 μm	1:125	1.4	Sea, swell	Subtidal	5 per week		0.49[d]
Terschelling, Netherlands	Sea	150–160 μm	1:220	1.2–2.8	Sea	Middle bar	1 per year		0.11–0.16
Terschelling, Netherlands	Sea	150–160 μm	1:220	1.2–2.8	Sea	Outer bar	1 per year		0.33–0.38
Egmond, Netherlands	Sea	150–200 μm	1:120	1.3–1.7	Sea	Subtidal	1–10 per year		0.04–0.08[d]
Katwijk, Netherlands	Sea	150–200 μm	1:150	1.4–1.8	Sea	Subtidal	2–11 per year		0.14–0.16[d]

[a] Maximum rates are in bold, mean rates are in italic.
[b] Mean slope of the nearshore area, preferably of the bar region only.
[c] Migration rates determined from monthly averages.
[d] Migration rates are determined from linear regression to bar position time series.
[e] In Dutch, summary of the results can be found in Van Rijn (1998).

Figure N-1 Observed bar migration rates and bar specifications [34]

	Offshore migration (m/day)			Onshore migration (m/day)		
	Weekly	Seasonal	Inter-annual	Weekly	Seasonal	Inter-annual
Outer bar						
Mean	1.57	0.16	0.07	1.21	0.11	0.00
St. dev.	1.80	0.09	0.05	1.27	0.07	0.00
Max.	10.12	0.53	0.15	6.73	0.53	0.00
Inner bar						
Mean	1.17	0.09	0.04	1.04	0.05	0.00
St. dev.	1.34	0.07	0.02	1.13	0.04	0.00
Max.	9.98	0.39	0.08	7.48	0.29	0.01

Figure N-2 Statistics cross-shore bar migration rates [34]

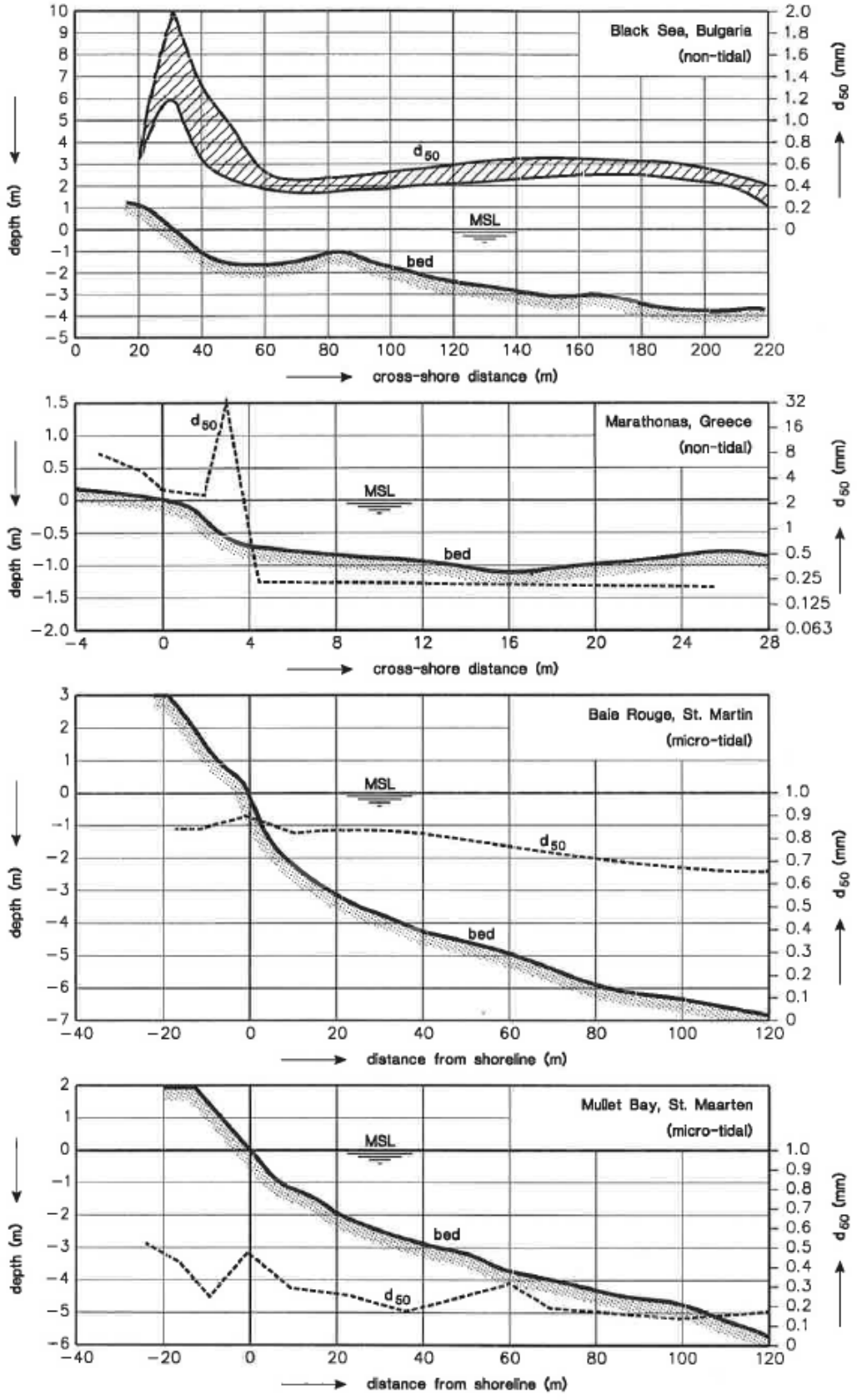

Figure N-3 Sediment sorting in cross-shore direction at several beaches [85]

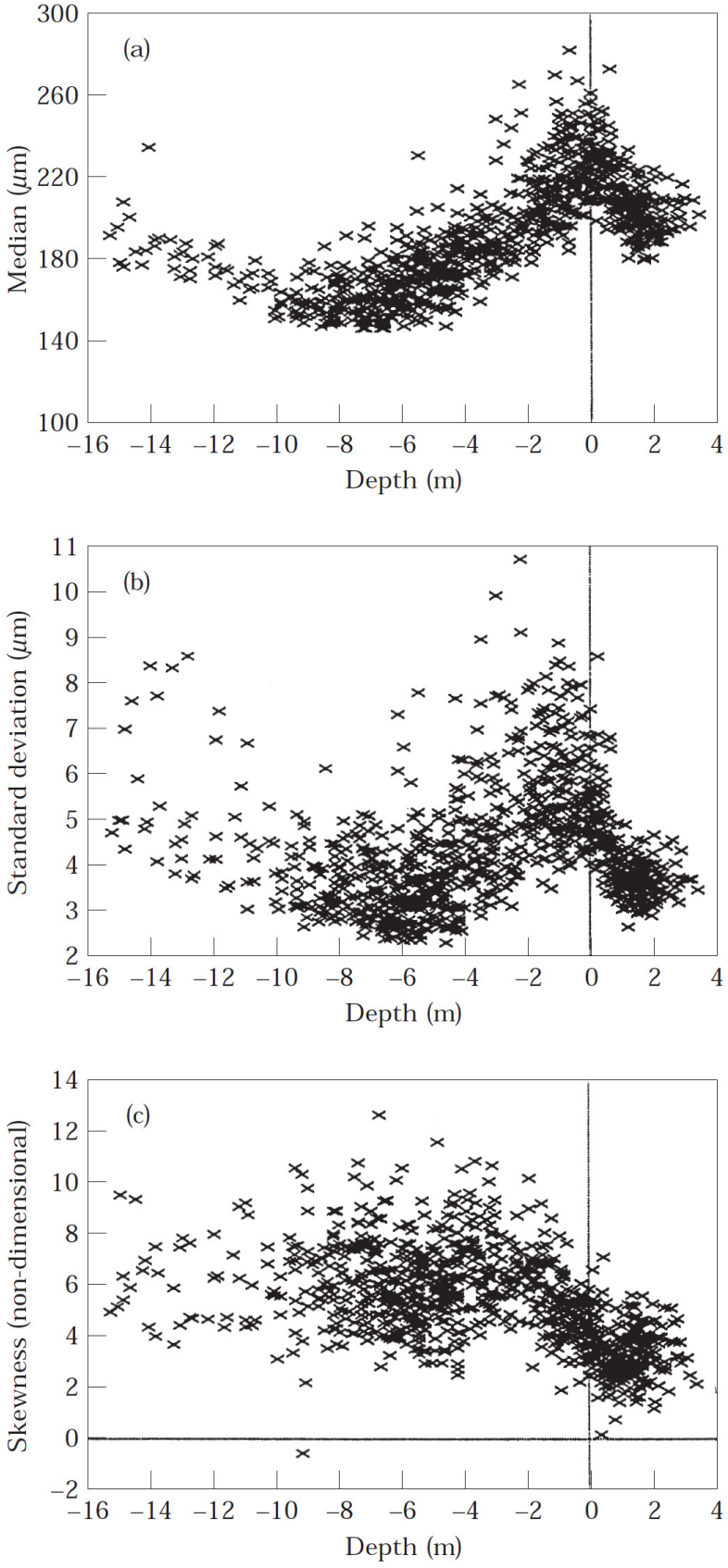

Figure N-4 Variations of textural parameters versus depth at the beach of Terschelling, NL

Grain size		Descriptive terminology			
phi	mm/μm	Udden (1914) and Wentworth (1922)	Friedman and Sanders (1978)	GRADISTAT program	
			Very large boulders		
−11	2048 mm		Large boulders	Very large	
−10	1024		Medium boulders	Large	
−9	512	Cobbles	Small boulders	Medium	Boulders
−8	256		Large cobbles	Small	
−7	128		Small cobbles	Very small	
−6	64		Very coarse pebbles	Very coarse	
−5	32		Coarse pebbles	Coarse	
−4	16	Pebbles	Medium pebbles	Medium	Gravel
−3	8		Fine pebbles	Fine	
−2	4	Granules	Very fine pebbles	Very fine	
−1	2	Very coarse sand	Very coarse sand	Very coarse	
0	1	Coarse sand	Coarse sand	Coarse	
1	500 μm	Medium sand	Medium sand	Medium	Sand
2	250	Fine sand	Fine sand	Fine	
3	125	Very fine sand	Very fine sand	Very fine	
4	63		Very coarse silt	Very coarse	
5	31		Coarse silt	Coarse	
6	16	Silt	Medium silt	Medium	Silt
7	8		Fine silt	Fine	
8	4		Very fine silt	Very fine	
9	2	Clay	Clay	Clay	

Figure N-5 Descriptive terminology of grain sizes

Shape parameter	Description	Comment
Circularity/ form factor	$(4 * \pi *)/(\text{Perimeter}^2)$	Area and perimeter estimation differs
Roundness	$(4 * A)/(\pi * L^2_{\text{Major}})$	Major axis = Feret
Compactness	$(\text{SQRT}[(4 * A)/\pi])/L_{\text{Major}}$	Major axis = Feret
Aspect Ratio	$L_{\text{Major}}/L_{\text{Minor}}$	Major axis = Feret Minor axis = Breadth
Solidity	A/ConvexArea	Area estimation differs
Convexity	ConvexPerimeter/ Perimeter	Perimeter estimation differs
RFactor	ConvexHull/ (Feret * π)	Parameter only measured in Particle Plus8
ModRatio	$(2 * R_I)$/Feret	Parameter only measured in Particle Plus8
Rectang	Area/ (Feret * Breadth)	Parameter only measured in Particle Plus8

Figure N-6 Definition of shape parameters

Formula	Range	Reference	Notes
$\frac{4A}{\pi(L)^2}$	0 to 1	Pentland (1927)	Ratio of the area of the grain to the area of a circle with diameter equal to the longest diameter of the grain. Pentland called this 'roundness'
$\frac{4\pi A}{P^2}$	0 to 1	Cox (1927)	Ratio of the area of the grain to the area of a circle with the same perimeter. Cox called this 'roundness'
$\frac{4A}{\pi(D_c)^2}$	0 to 1	Tickell (1931)	Ratio of the area of the grain to the area of the smallest circumscribing circle. Tickell called this 'roundness'
$\frac{c}{C} = \sqrt{\frac{4\pi A}{P^2}}$	0 to 1	Wadell (1933)	Ratio of the perimeter of a circle with the same area as the grain to the actual perimeter of the grain. Square root of Cox's (1927) formula
$\frac{d_c}{D_c} = \sqrt{\frac{4A}{\pi(D_c)^2}}$	0 to 1	Wadell (1935)	Ratio of the diameter of a circle with the same area as the grain to the diameter of the smallest circumscribing circle. Formula also given in Wadell (1933) but in a different form
$\sqrt{\frac{D_i}{D_c}}$	0 to 1	Riley (1941)	Square root of the ratio of the diameter of the largest inscribed circle to the diameter of the smallest circumscribing circle. Riley called this the 'inscribed circle sphericity'
$\frac{P^2}{A}$	4π to ∞	Janoo (1998)	General ratio of perimeter to area

Figure N-7 Commonly used circularity factors [16]

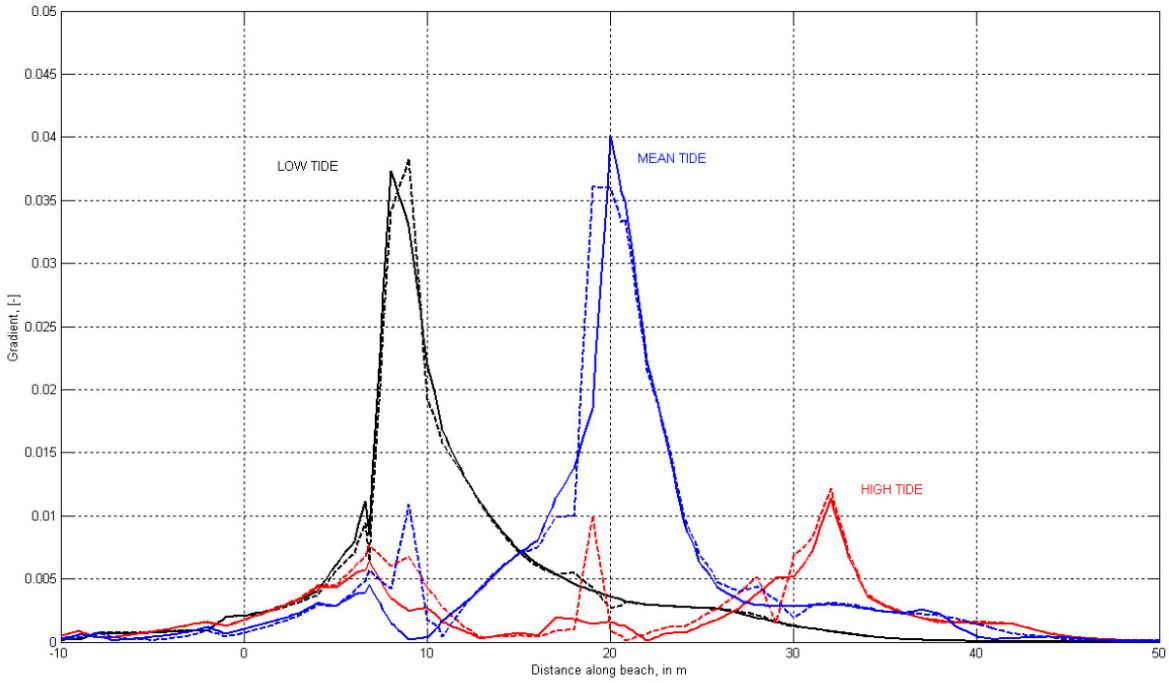

Figure N-8 Hydraulic gradient with (solid) and without (dashed) drainage tube]